SYNTHESIS AND CHARACTERIZATION OF MULTINUCLEAR/ SUPRA-MOLECULAR COMPLEXES OF PLATINUM GROUP METALS WITH CHALCOGEN LIGANDS

By

K. V. Vivekananda

(CHEM01200904015)

BHABHA ATOMIC RESEARCH CENTRE

A thesis submitted to the

Board of Studies in Chemical Sciences

In partial fulfillment of requirements

For the degree of

DOCTOR OF PHILOSOPHY

of

HOMI BHABHA NATIONAL INSTITUTE

July 2016

Homi Bhabha National Institute

Recommendations of the Viva Voce Board

As members of the Viva Voce Board, we certify that we have read the dissertation prepared by **Mr. K. V. Vivekananda** entitled **"Synthesis and characterization of multinuclear/supra-molecular complexes of platinum group metals with chalcogen ligands"** and recommend that it may be accepted as fulfilling the dissertation requirement for the Degree of Doctor of Philosophy.

D Das.

Chairman: Prof. D. Das Date:22.07.2016

Guide: Prof. V. K. Jain Date:22.07.2016

Dey

Co-guide: Dr. Sandip Dey Date:22.07.2016

Member: Prof. S. Kannan Date:22.07.2016

Member: Prof. S. K. Ghosh Date: 22.07.2106

External Examiner: Prof. C. P. Rao Date:22.07.2016

Final approval and acceptance of this thesis is contingent upon the candidate's submission of the final copies of the thesis to HBNI.

I hereby certify that I have read this thesis prepared under my direction and recommend that it may be accepted as fulfilling the thesis requirement.

Date: 22.07.2016
Place: Mumbai

Guide

STATEMENT BY AUTHOR

This dissertation has been submitted in partial fulfilment of requirements for an advanced degree at Homi Bhabha National Institute (HBNI) and is deposited in the Library to be made available to borrowers under rules of the HBNI.

Brief quotations from this dissertation are allowable without special permission, provided that accurate acknowledgement of source is made. Requests for permission for extended quotation from or reproduction of this manuscript in whole or in part may be granted by the Competent Authority of HBNI when in his or her judgment the proposed use of the material is in the interests of scholarship. In all other instances, however, permission must be obtained from the author.

Vivekananda. K. V

(K. V. Vivekananda)

DECLARATION

I, hereby declare that the investigations presented in this Thesis has been carried out by me. The work is original and has not been submitted earlier in whole or part for a degree / diploma to this or any other Institution / University.

Vivekananda. K.V

(K.V. Vivekananda)

Dedicated to...

My beloved Mother

and loving Sister

Acknowledgements

First and foremost I wish to thank my advisor, Professor V. K. Jain. It has been an honour to be his 25th and last Ph. D. student. He has been supportive since the days I began working in the lab. I appreciate all his contributions of time and ideas to make my Ph. D. experience productive and stimulating. I remember he used to say something like "you have to work 25 hrs a day!!" to encourage me to stay in the lab. The joy, enthusiasm and patience he has for research was contagious and motivational for me, even during tough times in the Ph. D. pursuit. He has been an inspiration on how to make things 'perfect', 'ordered' and 'disciplined', which made me to handle the scientific problems and organizing the vast scientific data in a systematic way. Without his guidance and persistent help this dissertation would not have been possible.

Similar, profound gratitude goes to Dr. Sandip Dey, who has been a truly dedicated mentor. I am particularly indebted to him for his constant faith, moral support and freedom in my lab work. His technical and editorial advices have taught me innumerable lessons and insights on the workings of academic research in general.

It is hard to overstate my gratitude to my Ph. D. doctoral committee members. Valuable suggestions and advice from Drs. D. Das, S. Kannan and S. K. Ghosh have helped me in keeping my progress on schedule. I would like to thank Dr. B. N. Jagtap, Director, Chemistry Group and Ex Directors of the Group Drs. T. Mukherjee and S. Sarkar for their encouragement and constant support to work in Chemistry Division.

My heartfelt thanks to our seniors Drs. Liladhar, Kedarnath, Prasad for their constant support in laboratories and in their engrossing scientific discussions. I would like to thank all other senior fellow students Drs. Ninad, Ananda, Prabhu, Rakesh, Rohit, Mr. Siddhartha, Mr. Adish Tyagi and Mr. Pravin for keeping the lab environment lively and obliging.

I owe a lot to Mr. Amey Wadawale and Dr. N. Bhuvanesh for single crystal X-ray diffraction support and providing the structural data for the compounds reported in the thesis. I am thankful to Dr. Dilip K. Maithy for extending theoretical support for few of the compounds. I feel very happy to express my deep sense of gratitude to Mr. Kamal Chaudhary, Mr. Manoj Pal, Mr. Suresh Chopade, Mrs. Nisha Kushwah, Mrs. Alpa Shah, Mr. P. B. Sonawane and Mr. Gopal for putting their valuable time in recording NMR spectra, elemental analyses and other lab related activities.

It is also a privilege to acknowledge Chemistry Division Office staff for assisting in official work; I would like to offer my sincere thanks to Santosh, Yogesh, Vinayak from Ch.D, for maintaining the lab clean and tidy.

Another staunch supporter and fan was a special sister of eleven years, Suji. Her love, support and belief in me were a treasure. Thank you, pretty girl, for motivating me to keep reaching for excellence. Thank you for everything that you are, and everything you will become. My special thanks to Anu who has played the part of friend, confidant, conscience...what not!!! Thank you for being persistent & encouraging, for believing in me and for the many precious memories along the way.

At any rate, I have finished, but not alone, and am elated... Special mentions go to my M.Sc friends & supporters especially Siree, Ummi, Suddhu, Kirru, Raghu, & Seetu (BBS group) who have been through a lot!!! I'll never forget the many wonderful lunches and fun activities we've done together. There *are many more that I could name, but the list would be absurdly long. Hence, I take this opportunity to offer my sincere thanks to those "Good Samaritans" who at some point of time have been of some help.*

I am eternally grateful to my training school batchmates Avishek, Vasundhara, Suman Rana, Shagufta, Jerina, Shikha and Debashree for being persistent and encouraging over the years and for giving me many precious memories along the way. Special thanks to some of them who used to constantly ask me "are you done yet?" and for their affectionate encouragement and support. Most importantly I am indebted to my friends cum roommates Dilip, Suresh, Ahmed, Yusuf, GM, Venkatesh, Khaisar, Kamal, Rajamoorthy and Abdulla who have helped me stay sane through these difficult years. Their support and care helped me overcome setbacks and stay focused on my research. I greatly value their friendship and deeply appreciate their belief in me. I am also grateful to Trombay friends Somu, Srinivas, Shithal, Tapas, Ganga Babu and Satish for rendering their continuous support during the writing of this thesis. I would like to extend my thanks to many family friends Goutam and Mousami, GM and Suma, Yusuf and Jesna, Naresh and Vani and Satish and Anusha for an indulging festival atmosphere. Lastly, I wish to sincerely thank my (batch+bench+lab+room)mate Dilip, a source of great emotional support, and the best "fun stuff" organizer. Your company and friendship during this time will never be forgotten.

I would never forget all the chats and beautiful moments I shared with some of my junior friends and labmates Praveen, Kamal, Anitha and Samatha. Special thanks to the younger students Somu and Ramya G Nair, you were always there with a word of encouragement or listening ear. You knew it would be sometimes a bumpy road, but encouraged and supported me along the way in stressful and difficult moments.

Most importantly, none of this would have been possible without the love and patience of my family. Thank you for encouraging me in all of my pursuits and inspiring me to follow my dreams. I am especially grateful to my mother, sister, brother-in-law and uncle, who supported me emotionally and financially. Thank you for teaching me that my job in life was to learn, to be happy, and to know and understand myself; only then could I know and understand others. Special thanks to the newest additions to my sister's family, the two naughty kids Spoorthy and Kruthi for relieving me from depression during stressful moments. Dad you were often in my thoughts on this journey – you are missed. Finally thanks to the God, the Almighty, for his showers of blessings throughout my research work to complete it successfully.

I keep a softcopy of my dissertation with me and I read the acknowledgments section often. Yes, I've almost memorized it by now, but reading it again always brings back a flood of happy, sad, and funny memories.

Sometimes, you need that.

Vivekananda K. V.

Abbreviations

PPh$_3$ = triphenylphosphine

dppm = bis(diphenylphosphino)methane

dppe = 1,2-bis(diphenylphosphino)ethane

dppp = 1,3-bis(diphenylphosphino)propane

E = sulfur, selenium, tellurium

X = halogen

OTf = triflate

Ph = phenyl

py = pyridyl

Epy = pyridine-4-chalcogenolate

H$_2$mba = mercaptobenzoic acid

SCCs = supramolecular coordination complexes

Publications

Journal papers

1. Syntheses of Pd(II)/Pt(II) complexes with non-chelating 4-pyridylselenolate ligand ranging from mononuclear to macrocyclic structures and their utility as catalysts in Suzuki C–C coupling reaction
   K. V. Vivekananda, S. Dey, A. Wadawale, N. Bhuvanesh, V. K. Jain,
   Dalton Trans., *42* (2013) 14158-14167.

2. Supramolecular 3-/4-mercaptobenzoic acid complexes of palladium(II) and platinum(II) stabilized by hydrogen bonding
   K. V. Vivekananda, S. Dey, A. Wadawale, N. Bhuvanesh, and V. K. Jain,
   Eur. J. Inorg. Chem., (2014) 2153-2161.

3. Supramolecular macrocyclic Pd(II) and Pt(II) squares and rectangles with aryldithiolate ligands and their unprecedented catalytic activity in Suzuki C–C coupling reaction
   K. V. Vivekananda, S. Dey, D. K. Maity, N. Bhuvanesh and V. K. Jain, *Inorg. Chem*., 54 (2015) 10153–10162.

4. Molecular architecture and self assembly of hemilabile organoselenium/ tellurium complexes of palladium and platinum
   K. V. Vivekananda, S. Dey, N. Bhuvanesh and V. K. Jain
   (manuscript under preparation).

5. Synthesis and characterization of unprecedented formation of Pt/Pd complexes with 4-pyridyltellurolate ligand
   K. V. Vivekananda, S. Dey, A. Wadawale, N. Bhuvanesh, V. K. Jain
   (manuscript under preparation).

Conferences/Symposia

1. Syntheses of Pt(II) complexes with non-chelating 4-pyridylselenolate ligand ranging from mononuclear to supramolecular structures.
   K. V. Vivekananda, S. Dey, V. K. Jain and N. Bhuvanesh
   "4th DAE-BRNS Interdisciplinary Symposium on Materials Chemistry" during 11th–15th December 2012, held at Bhabha Atomic Research Centre, Mumbai.

2. Palladium (II) and platinum (II) complexes with 4-pyridylselenolate ligand
   K. V. Vivekananda, S. Dey, V. K. Jain and N. Bhuvanesh
   "7th CRSI-RSC Symposium in Chemistry and 15th CRSI National Symposium in Chemistry" during January 31st - February 3rd 2013, held at Banaras Hindu University, Varanasi.

3. Supramolecular assemblies of palladium(II) and platinum(II) complexes with 3-/4-mercaptobenzoic acid *via* hydrogen bonding
K. V. Vivekananda, S. Dey, A. Wadawale, N. Bhuvanesh and V. K. Jain
"5th DAE-BRNS Interdisciplinary Symposium on Materials Chemistry" during 9th-13th December 2014, held at Bhabha Atomic Research Centre, Mumbai.

Table of Contents

Title **Page No.**

Synopsis

Chapter 1: Introduction

Chapter 2: Experimental

Chapter 3: Results and Discussion

Synopsis

Homi Bhabha National Institute

Ph. D. PROGRAMME

1. **Name of the Student:** Mr. K. V. Vivekananda
2. **Name of the Constituent Institution:** Bhabha Atomic Research Centre
3. **Enrolment No. :** CHEM01200904015
4. **Title of the Thesis:** **"Synthesis and characterization of multinuclear/ supra-molecular complexes of platinum group metals with chalcogen ligands".**
5. **Board of Studies:** Chemical Sciences, HBNI

Synopsis

Among transition elements, palladium and platinum have played an important role in the development of coordination [1] and organometallic [2] chemistry. The notable developments have been recognition of cis- and trans isomerism, trans effect, isolation of the first transition metal organometallic compound (e.g., Ziese's salt in 1827 and $[Me_3PtI]_4$ in 1907), cyclometalated palladium compounds, metallocycloalkanes, etc. Both metals form a myriad of complexes with a wide variety of ligands from Groups IV- VII [3, 4]. Their complexes find applications in diverse areas, like homogeneous catalysis [5], biology (as anti tumor drugs) [6] and materials science [7]. Of late, dendrimers and supra-molecular assemblies have been designed by selecting suitable ligand systems.

The chemistry of these metals with chalcogen ligands has been pursued for over several decades and has been dominated by sulfur ligands [8]. The chemistry with heavier chalcogen ligands (Se or Te) has gained momentum only during the past two decades or so and in several instances unprecedented products have been isolated and structurally characterized [9]. Although organochalcogen ligands, in the absence of auxiliary donor groups, afford polymeric complexes, their use in stabilizing supra-molecular assemblies has been scanty.

The present thesis aims to design and synthesize multinuclear/ supra-molecular Pd/Pt complexes based on internally functionalized non-chelating chalcogen (S, Se, Te) ligands. Non-covalent and weak interactions like hydrogen bonding have been utilized to stabilize these structures. The thesis is divided into four chapters, *viz.*, introduction, experimental, results and discussion and summary and conclusions, followed by references.

Chapter 1: Introduction

This chapter deals with the general introduction to the coordination chemistry of palladium and platinum complexes with organochalcogenolate ligands with an emphasis on formation of self-assembled macrocycles. A short note on various types of organometallic reactions, e.g., oxidative addition reaction, exchange reaction, cyclometallation reactions, *etc.* are discussed. Applications of palladium chalcogenolate complexes in catalytic reactions are covered and also a brief discussion on biological activity is included. Coverage on the complex chemistry of chalcogen ligands (S, Se, Te) is described which is followed by the scope of the present work. Relevant literature references are provided in bibliography at the end of the thesis.

Chapter 2: Experimental

In this chapter, materials and methods used during the present study are described followed by details on analytical and instrumental techniques, viz. elemental analysis, IR, UV-visible, NMR (^{1}H, ^{13}C, ^{19}F, ^{31}P, ^{77}Se, ^{125}Te, ^{195}Pt) and single crystal X-ray diffraction analyses. Synthesis of various chalcogen ligands, and palladium and platinum precursors used in the present work is described. Synthesis of new palladium and platinum complexes is presented in five sub-sections.

Chapter 3: Results and discussion

Chapter **3** deals with the results obtained during the present investigation and include discussion on these findings. All the complexes have been characterized by elemental analysis, multinuclear NMR (^{1}H, ^{13}C{^{1}H}, ^{31}P{^{1}H}, ^{19}F{^{1}H}, ^{77}Se{^{1}H}, ^{125}Te{^{1}H} and ^{195}Pt{^{1}H}) spectroscopy. Techniques like IR, UV-vis absorption, mass spectrometry and cyclic voltammetery were also employed for few complexes. Molecular structures of several complexes have been established unambiguously by single crystal X-ray diffraction analyses. This chapter is sub divided into five sections.

The section **3.1** deals with the chemistry of palladium and platinum complexes of non-chelating bidentate ligands like 4-pyridylchalcogenolate. The oxidative addition of bis(4-pyridyl)diselenide to $Pt(PPh_3)_4$ yielded exclusively *trans*-$[Pt(4\text{-}SeC_5H_4N)_2(PPh_3)_2]$. Treatment of two eqv. of $Na(4\text{-}SeC_5H_4N)$, prepared by reductive cleavage of Se–Se bond of 4,4'-py_2Se_2 by $NaBH_4$ in methanol, with *cis*-$[PtCl_2(PR_3)_2]$ ($PR_3 = PPh_3, PEt_3$) afforded similar products, *trans*-$[Pt(4\text{-}SeC_5H_4N)_2(PPh_3)_2]$ and *trans*-$[Pt(4\text{-}SeC_5H_4N)_2(PEt_3)_2]$ (Scheme 1). The reactions of *cis*-$[MCl_2(P^\frown P)]$ and $[M_2Cl_2(\mu\text{-}Cl)_2(PR_3)_2]$ with two eqv. of $Na(4\text{-}SeC_5H_4N)$ yielded *cis*-[M(4-

$SeC_5H_4N)_2(P^{\cap}P)]$ ($M/P^{\cap}P$ = Pd/dppe, Pt/dppm and Pt/dppp) and $[MCl(4\text{-}SeC_5H_4N)(PR_3)]_n$, respectively. The complex *trans*-$[PtCl(4\text{-}SeC_5H_4N)(PEt_3)_2]$ can be prepared by redistribution reaction between *trans*-$[Pt(4\text{-}SeC_5H_4N)_2(PEt_3)_2]$ and *cis*-$[PtCl_2(PEt_3)_2]$.

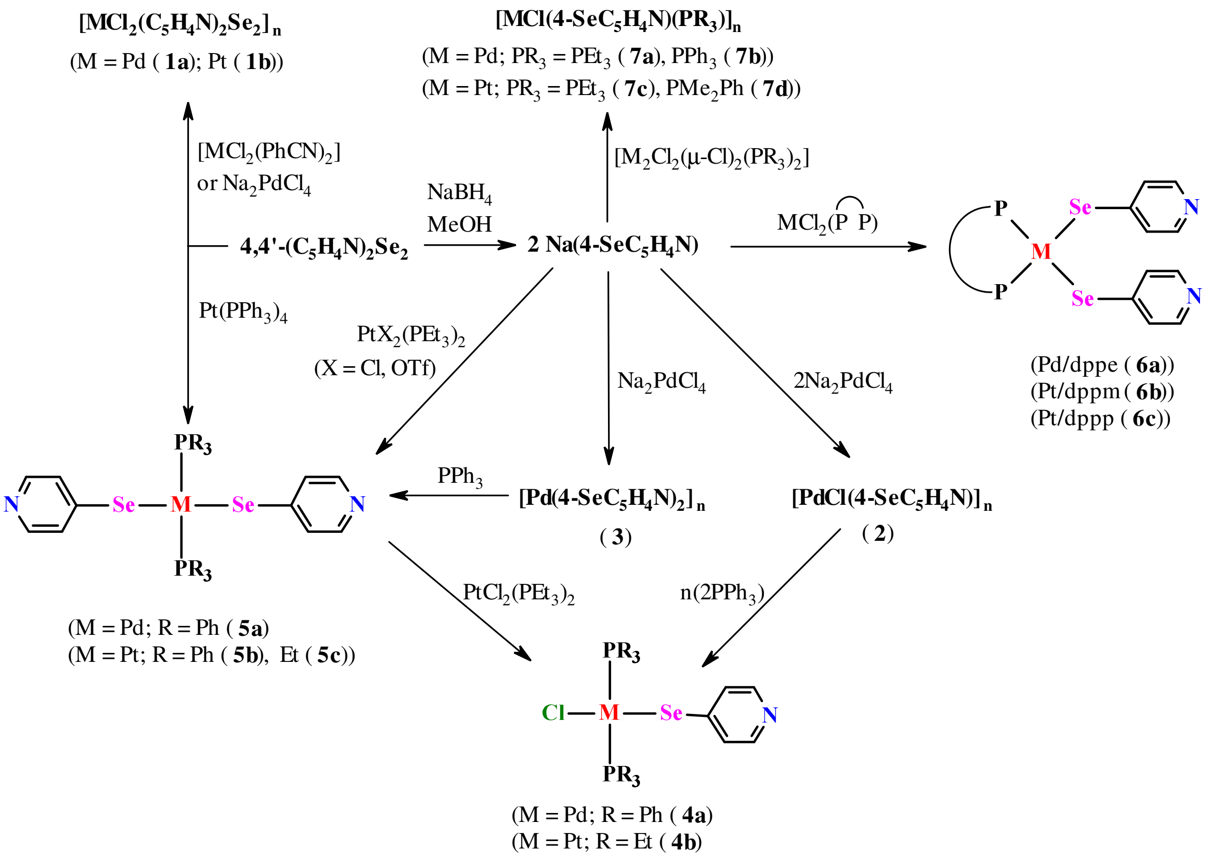

Scheme 1

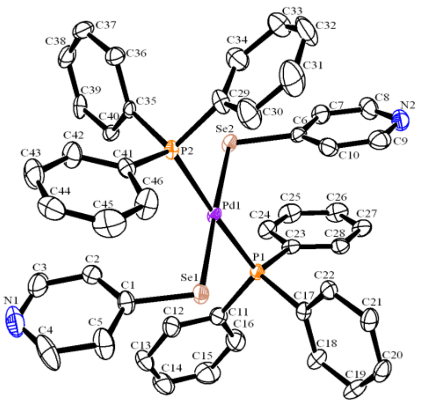

Fig 1. Molecular structure of $[Pd(SeC_5H_4N)_2(PPh_3)_2]$

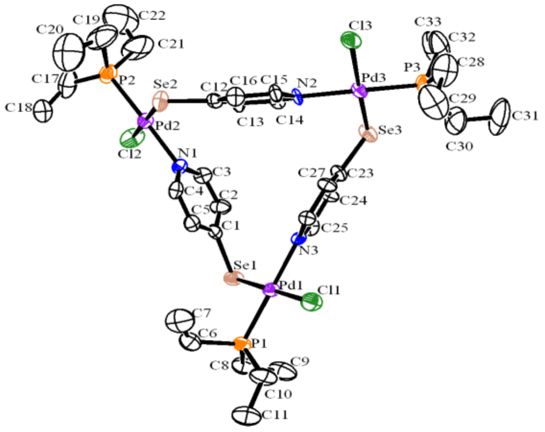

Fig 2. Molecular structure of $[PdCl(SeC_5H_4N)_2(PEt_3)]_3$

Molecular structures of a number of complexes were established by single crystal X-ray diffraction analyses (Figs. 1, 2). The catalytic activity of *trans*-[PdCl(4-SeC$_5$H$_4$N)(PPh$_3$)$_2$] and [PdCl(4-SeC$_5$H$_4$N)(PPh$_3$)]$_n$ in Suzuki C–C cross coupling reaction was investigated.

The section **3.2** deals with the preparation and characterization of Pd(II)/Pt(II) complexes with 3-/4-H$_2$mba (mba = mercaptobenzoic acid) (Scheme 2) ligand possessing both coordinating thiolate group and a carboxylic acid group in non-chelating position which may serve as a versatile binding motif for the formation of hydrogen-bonded supra-molecules.

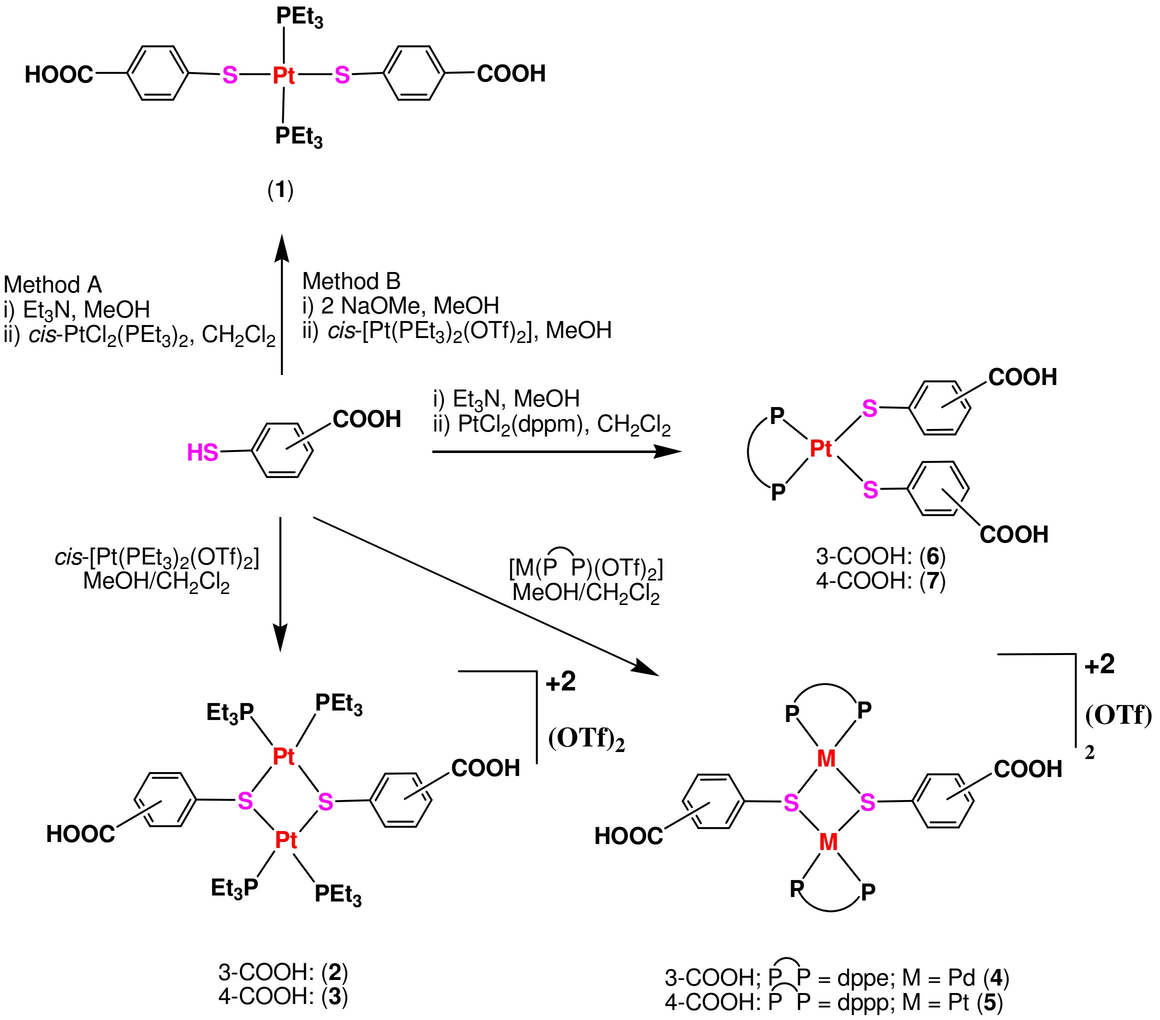

Scheme 2

Addition of 3-/4-mercaptobenzoic acid to *cis*-$[\mathrm{Pt(PEt_3)_2(OTf)_2}]$ and *cis*-$[\mathrm{M(P^{\cap}P)_2\ (OTf)_2}]$ gave self-assembled complexes *cis*-$[\mathrm{Pt(\mu\text{-}SC_6H_4COOH\text{-}n)(PEt_3)_2}]_2\mathrm{(OTf)_2}$ (n = 3, 4) (Fig. 3) and $[\mathrm{M(\mu\text{-}SC_6H_4COOH\text{-}n)(P^{\cap}P)_2}]_2\mathrm{(OTf)_2}$ (M /n /$\mathrm{P^{\cap}P}$ = Pd/ 3/ dppe, Pd/ 4/ dppe, Pt/ 4/ dppp) (Fig. 4), respectively. Treatment of *cis*-$[\mathrm{PtCl_2(P^{\cap}P)}]$ with 3-/4-mercaptobenzoic acids in the presence of triethylamine yielded mononuclear complexes $[\mathrm{Pt\{SC_6H_4COOH\text{-}n\}_2(P^{\cap}P)}]$ {$\mathrm{P^{\cap}P}$ = dppm, $\mathrm{(PR_3)_2}$; R = Et, Ph; n = 3, 4}. One of the above mentioned mononuclear complexes can also be obtained from the reaction of *cis*-$[\mathrm{Pt(PEt_3)_2(OTf)_2}$with 4-mercaptobenzoic acid (4-$\mathrm{H_2}$mba) in the presence of sodium methoxide.

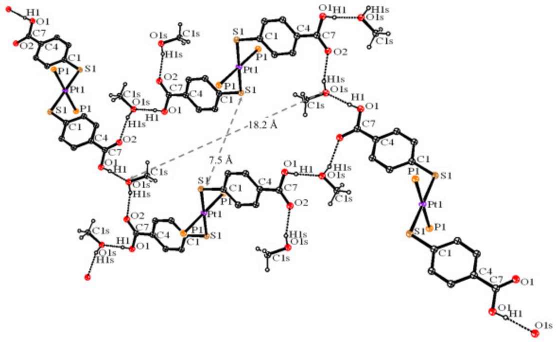

Fig 3. Molecular structure of $[\mathrm{Pt(SC_6H_4COOH\text{-}4)_2(PEt_3)_2}]\cdot\mathrm{(MeOH)_2}$

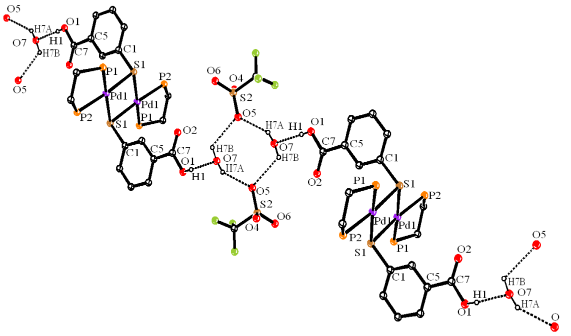

Fig 4. Molecular structure of $[\mathrm{Pd(SC_6H_4COOH\text{-}3)_2(dppe)}]_2\mathrm{(OTf)_2}\cdot\mathrm{(H_2O)_2}$

The section **3.3** describes the synthesis of rigid Pd(II) and Pt(II)-based macrocyclic tetranuclear rectangles and octanuclear squares derived from 1,4-aryl dithiolates (Scheme 3). Addition of 1,4-benezenedithiol and 4,4′-biphenyldithiol to $\mathrm{M(OTf)_2}$ (M = *cis*-$[\mathrm{Pt(PEt_3)_2}]^{2+}$ or *cis*-$[\mathrm{Pd(dppe)}]^{2+}$) gave self-assembled tetranuclear complexes $[\mathrm{M_2\{S(C_6H_4)_nS\}}]_2\mathrm{(OTf)_4}$ (n = 1, 2) (Figs. 5, 6). The same reaction of 1,4-benezenedimethanethiol yielded octanuclear supramolecular coordination complexes (SCC) $[\mathrm{M_2\{SCH_2C_6H_4CH_2S\}}]_4\mathrm{(OTf)_8}$. The palladium complexes showed excellent catalytic activity in Suzuki C–C cross coupling reactions with high turnover numbers (2 × 10^7), even with low catalyst loading.

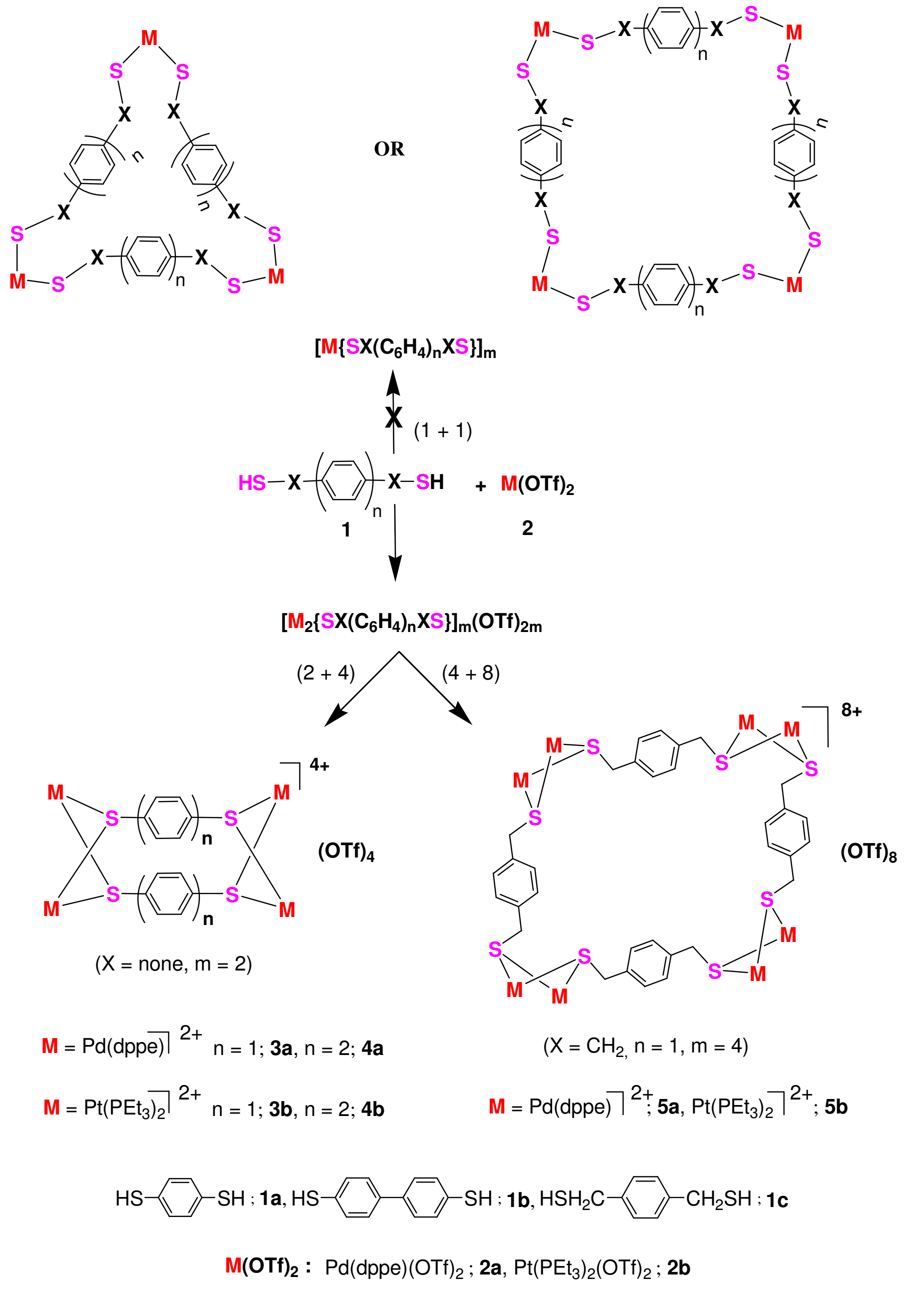

Scheme 3

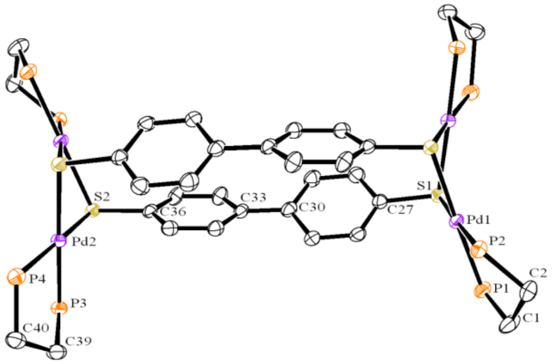

Fig 5. Molecular structure of $[Pd_2(dppe)_2(S(C_{12}H_8)S)]_2(OTf)_4$

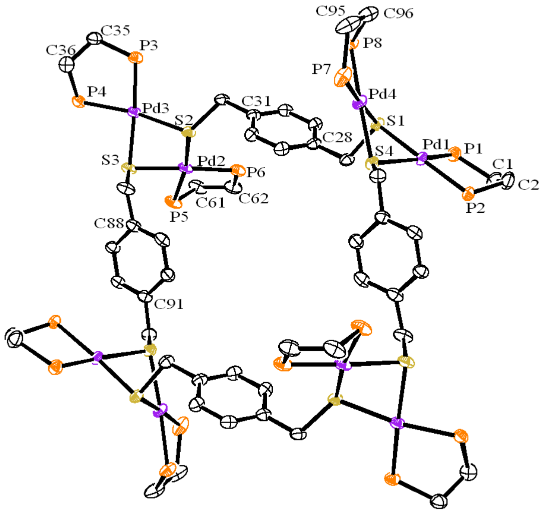

Fig 6. Molecular structure of $[Pd_2(dppe)_2(SCH_2(C_6H_4)CH_2)S)]_4(OTf)_8$

The section **3.4** covers the synthesis of coordination directed self-assembled Pd(II)/Pt(II) metallacycles. Simple addition reactions of $M(P^{\cap}P)(OTf)_2$ ($P^{\cap}P = (PEt_3)_2$, dppe) with 4,4'-py_2Se_2 in 1:1 ratio gave highly symmetrical self-assembled binuclear complexes of the form $[M(P^{\cap}P)(py_2Se_2)]_2(OTf)_4$ (Scheme 4). When 4,4'–py_2Te_2 was employed as nucleophilic tecton in the reaction with *cis*-$Pt(PEt_3)_2(OTf)_2$, $[Pt(PEt_3)_2(py_2Te_2)]_2(OTf)_4$ was formed whereas the reaction with $Pd(dppe)(OTf)_2$ under similar conditions gave a trinuclear telluride-bridged Pd(II) complex. The molecular structures of the complexes (Figs. 7, 8) have been established by single crystal X-ray diffraction analyses.

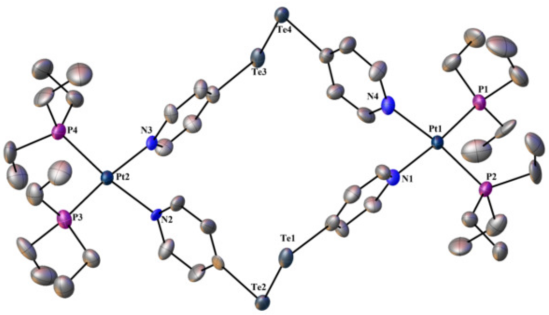

Fig 7. Molecular structure of $[Pt(PEt_3)_2(py_2Te_2)]_2(OTf)_4]$

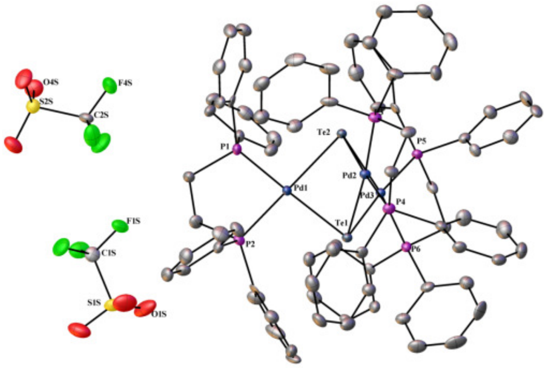

Fig 8. Molecular structure of $[Pd_3(\mu\text{-}Te)_2(dppe)_3](OTf)_2$

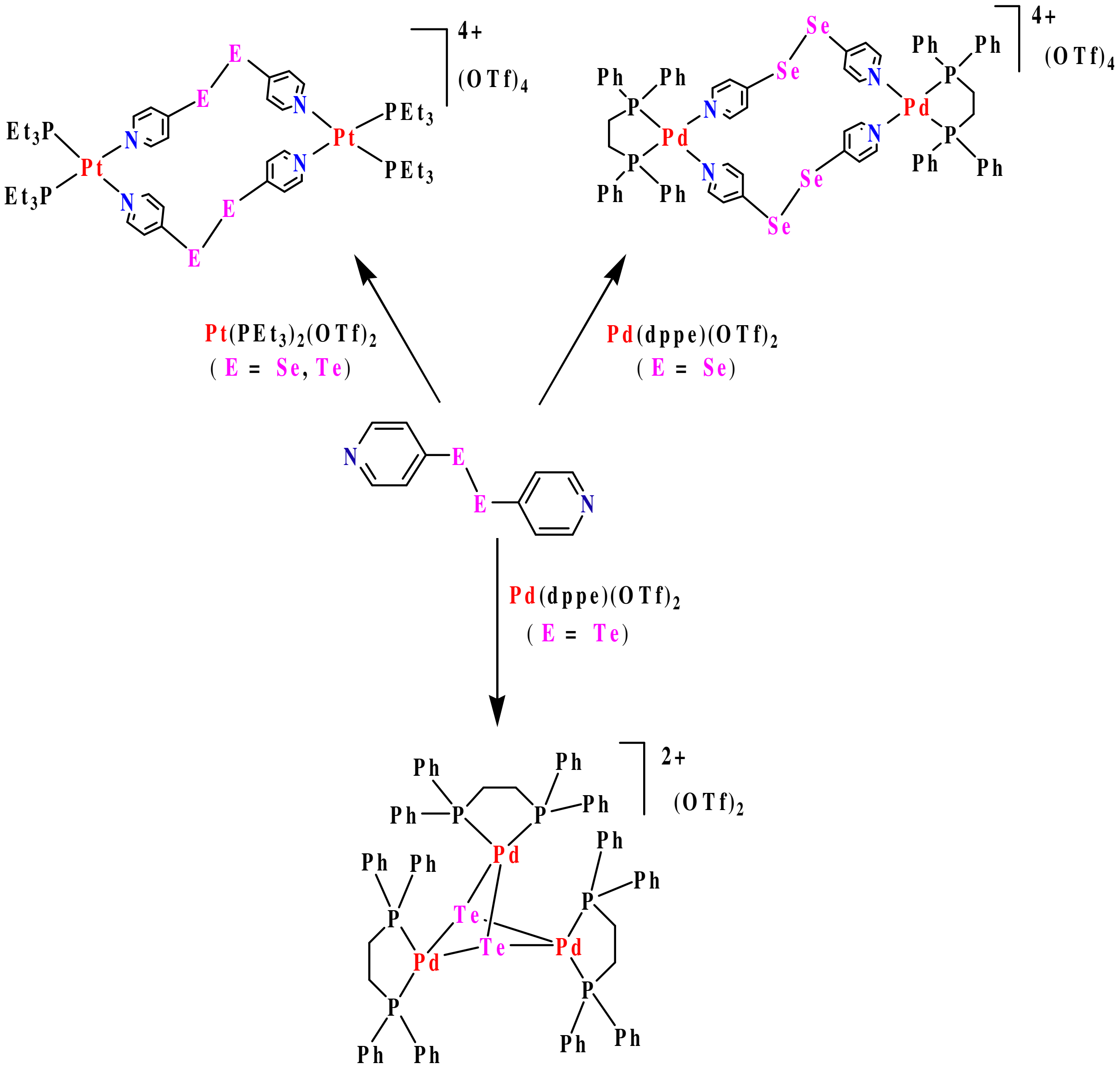

Scheme 4

The section **3.5** describes the reactions of 4-telluropyridine with Pt(II)/Pd(II) precursors. Substitution reactions between [MCl$_2$(dppe)] (M = Pd, Pt) and NaTepy, prepared by reductive cleavage of Te–Te bond in 4,4'–py$_2$Te$_2$ by NaBH$_4$ in methanol gave expected mononuclear bis complexes whereas in the case of MCl$_2$(dppm) (M = Pt, Pd) serendipitous products such as [Pt{PPh$_2$C(TeC$_5$H$_4$N)PPh$_2$}$_2$], [Pd$_4$(μ$_3$-Te)$_2$(μ$_2$-Tepy)$_2$(Tepy)$_2$(dppm)$_2$] have been isolated, respectively in good yields. Reaction conditions, palladium precursors (nature of the chelating phosphine), chalocogen atom played an important role in the formation of these unusual products. On the other hand, hemilabile ambidentate ligand moiety 4-pyridyl selenolate was employed *in situ* reaction with M(P$^\frown$P)Cl$_2$ and NaBPh$_4$, in order to make use of both hard nitrogen atom and soft selenium atom in bonding. In this case self-recognition and self-selection lead to the formation of essentially a single product [Pt$_2$(dppe)$_2$(Se$^\frown$N)(N$^\frown$Se)](BPh$_4$)$_2$ in high yield (84 %). Reaction of [PdCl$_2$(py$_2$Te$_2$)]$_n$ with one equivalent of PPh$_3$ was monitored by NMR spectroscopy which indicated the formation of telluride-bridged binuclear complex *cis*-[Pd$_2$Cl$_2$(PPh$_3$)$_2$(TeC$_5$H$_4$N)$_2$] together with an unidentified product in solution.

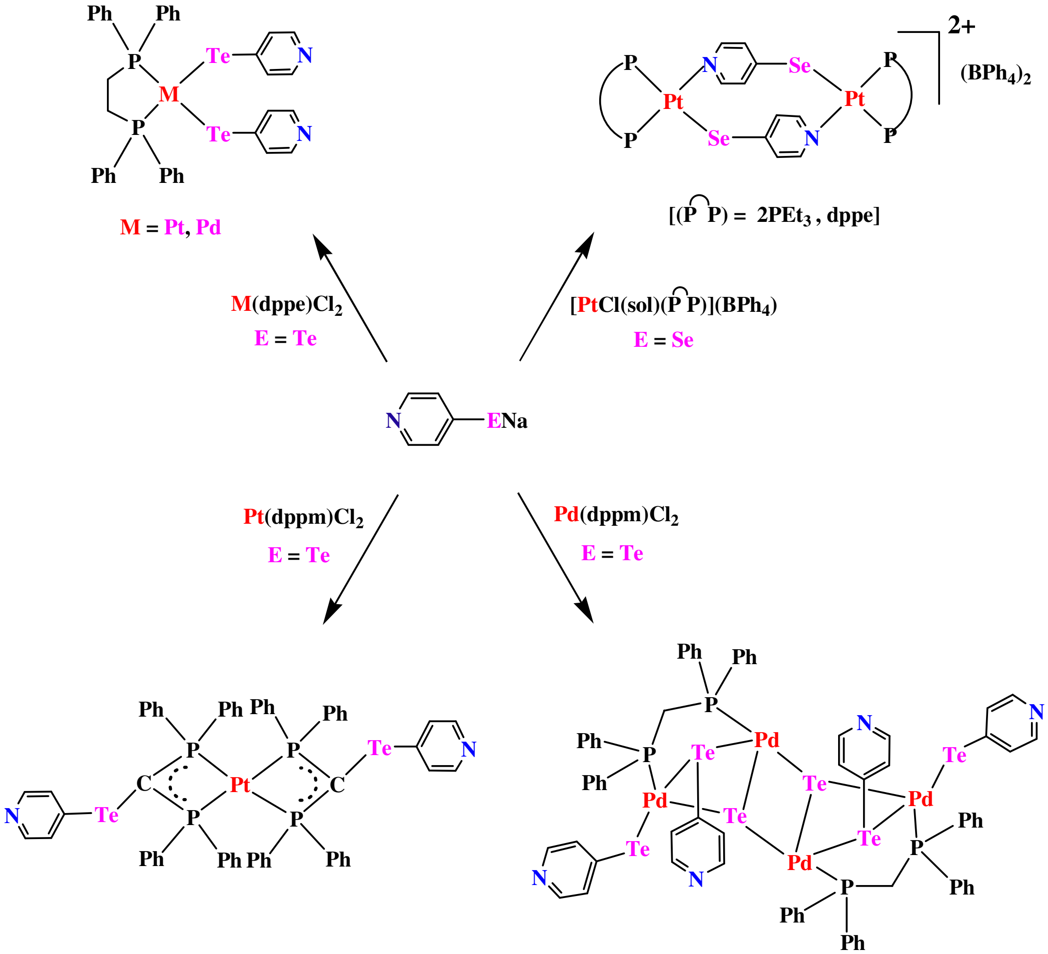

Scheme 5

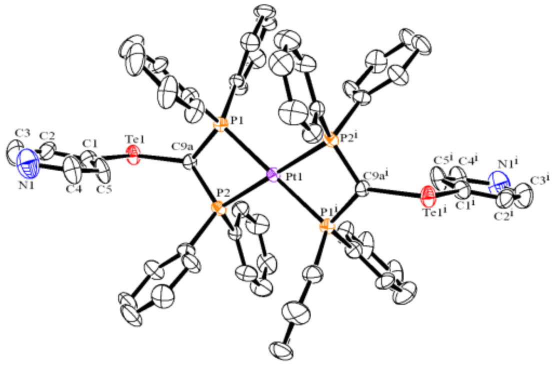

Fig 9. Molecular structure of $[Pt\{PPh_2C(TeC_5H_4N)PPh_2\}_2]$

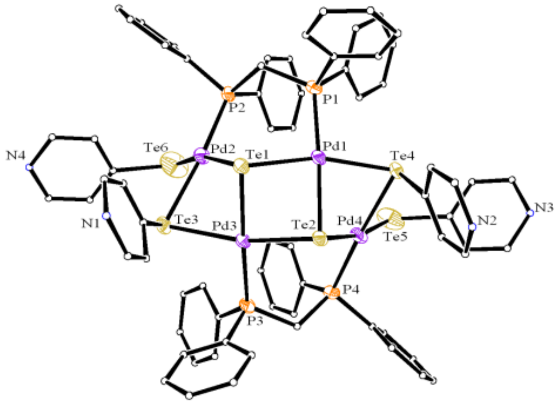

Fig 10. Molecular structure of $[Pd_4(\mu_3\text{-}Te)_2(\mu_2\text{-}Tepy)_2(Tepy)_2(dppm)_2]$

Chapter 4: Summary and conclusions

This chapter gives summary and conclusions of the present investigation. Diverse binding modes of 4-pyridylselenolate ligand has a promising potential in constructing multinuclear complexes which may exhibit dynamic behavior in solution depending on the nature of metal atom and also other auxiliary ligands. Aryldithiol ligands while holding the Pt/Pd metals through bridging mode facilitate stabilizing rigid unique supra-molecular coordination complexes. The excellent catalytic application of palladium complexes with both 4-pyridylselenolate and aryldithiol ligands have been demonstrated in Suzuki C–C cross coupling reactions. Directional intermolecular hydrogen bonding has been exploited to form a supra-molecular assembly of square-planar building blocks containing two carboxylic acid groups in the case of 3-/4-mercaptobenzoic acid as ligand by varying the phosphine as co-ligands and reaction conditions. The reactivity of tellurium ligands is markedly different from those of sulfur/ selenium lignads yielding unexpected and interesting products.

References

[1] *Comprehensive Coordination Chemistry-II*, vol. 6 (2004).

[2] *Comprehensive Organometallic Chemistry-III*, vol. 8 (2007).

[3] V. K. Jain and L. Jain, *Coord. Chem. Rev.*, 249 (2005) 3075.

[4] V. K. Jain and L. Jain, *Coord. Chem. Rev.*, 254 (2010) 2848.

[5] J. Magano and J. R. Dunetz, *Chem. Rev.*, 111 (2011) 2177.

[6] N. J. Wheate, S. Walker, G. E. Craig and R. Oun, *Dalton Trans.*, 39 (2010) 8113.

[7] S. Dey and V. K. Jain, *Platinum Met. Rev.*, 48 (2004) 16.

[8] B. J. Blower and J. R. Dilworth, *Coord. Chem. Rev.*, 76 (1987) 121.

[9] V. K. Jain and R. S. Chauhan, *Coord. Chem., Rev.*, 306 (2016) 270.

A part of the work reported in this thesis has already been published. This was done to secure priority of work in the field. The details are as follow:

Journal papers

1. Syntheses of Pd(II)/Pt(II) complexes with non-chelating 4-pyridylselenolate ligand ranging from mononuclear to macrocyclic structures and their utility as catalysts in Suzuki C–C coupling reaction

   K. V. Vivekananda, S. Dey, A. Wadawale, N. Bhuvanesh, V. K. Jain,

   Dalton Trans., *42* (2013) 14158-14167.

2. Supramolecular 3-/4-mercaptobenzoic acid complexes of palladium(II) and platinum(II) stabilized by hydrogen bonding

   K. V. Vivekananda, S. Dey, A. Wadawale, N. Bhuvanesh, and V. K. Jain,

   Eur. J. Inorg. Chem., (2014) 2153-2161.

3. Supramolecular macrocyclic Pd(II) and Pt(II) squares and rectangles with aryldithiolate ligands and their unprecedented catalytic activity in Suzuki C–C coupling reaction

   K. V. Vivekananda, S. Dey, N. Bhuvanesh and V. K. Jain, *Inorg. Chem.* (*under revision*).

4. Molecular architecture and self assembly of hemilabile organoselenium/ tellurium complexes of palladium and platinum

   K. V. Vivekananda, S. Dey, N. Bhuvanesh and V. K. Jain (manuscript under preparation).

5. Synthesis and characterization of unprecedented formation of Pt/Pd complexes with 4-pyridyltellurolate ligand

   K. V. Vivekananda, S. Dey, A. Wadawale, N. Bhuvanesh, V. K. Jain (manuscript under preparation).

Conferences/Symposia

1. Syntheses of Pt(II) complexes with non-chelating 4-pyridylselenolate ligand ranging from mononuclear to supramolecular structures.

   K. V. Vivekananda, S. Dey, V. K. Jain and N. Bhuvanesh

   "4th DAE-BRNS Interdisciplinary Symposium on Materials Chemistry" during 11th–15th December 2012, held at Bhabha Atomic Research Centre, Mumbai.

2. Palladium (II) and platinum (II) complexes with 4-pyridylselenolate ligand

   K. V. Vivekananda, S. Dey, V. K. Jain and N. Bhuvanesh

   "7th CRSI-RSC Symposium in Chemistry and 15th CRSI National Symposium in Chemistry" during January 31st - February 3rd 2013, held at Banaras Hindu University, Varanasi.

3. Supramolecular assemblies of palladium(II) and platinum(II) complexes with 3-/4-mercaptobenzoic acid *via* hydrogen bonding

K. V. Vivekananda, S. Dey, A. Wadawale, N. Bhuvanesh and V. K. Jain

"5th DAE-BRNS Interdisciplinary Symposium on Materials Chemistry" during 9th-13th December 2014, held at Bhabha Atomic Research Centre, Mumbai.

Vivekananda. K.V

Signature of Student

Date: 04-08-2015

Doctoral Committee

S. No.	Name	Designation	Signature	Date
1.	**Prof. D. Das**	**Chairman**	D.Das.	04/8/2015
2.	**Prof. V. K. Jain**	**Guide & Convener**		4/8/2015
3.	**Dr. S. Kannan**	**Member**		4.8-15
4.	**Dr. S. K. Ghosh**	**Member**		4-8·15
5.	**Dr. Sandip Dey**	**Co-Guide**		04.08.15

Chapter 1

Introduction

1.1 General introduction

The platinum group metals (PGMs) are six transitional elements from Groups 8 (ruthenium and osmium), 9 (rhodium and iridium) and 10 (palladium and platinum) of the periodic table. These six metals have similar physical and chemical properties and tend to occur together in nature with abundance in the earth's crust ~0.01 ppm. The single largest application of PGMs is in catalysis. Platinum was discovered by a Spanish scientist Antonio de Ulloa in 1735 and was first described in 1748 as a new metal of Columbian origin, although its existence was encountered for a few centuries earlier than its actual discovery. Palladium, named after an asteroid Pallas (from Greek "Pallas' means goddess of wisdom) was discovered by a British chemist W.H. Wollaston in 1803. Both the elements are lustrous silvery-white metals which are malleable, ductile and are resistant to corrosion. Some physical properties of palladium and platinum are given in Table 1.

Both the metals show variable oxidation states, *viz.* 0, +1, +2, +3 and +4; the +2 being the most common oxidation state [1]. Complexes in zero oxidation state are stabilized by strong σ-donor as well as π-acceptor ligands, such as carbonyls, isocyanide, cyanide, acetylide, nitric oxide and also by σ-donors such as phosphine, phosphite and arsine. These complexes exhibit geometries ranging from linear (e.g., $[Pt(PPh_3)_2]$) to tetrahedral (e.g., $[Pt(PPh_3)_4]$). The chemistry of palladium and platinum complexes in +1 and +3 oxidation states has not been much explored until the late 20th century. In general, complexes in +1 and +3 oxidation states are diamagnetic due to the formation of metal-metal bonds. The chemistry of palladium(I) [2] and platinum(I) [3] complexes has been reviewed. The chemistry in +3 oxidation state has received much attention only during the past two decades [4-9]. Although these complexes are isolated as dimeric species, the first monomeric, paramagnetic blue colour complex, $[NBu_4][Pt(C_6Cl_5)_4]$, was reported by Uson, et. al. [10]. The organoplatinum(IV) complexes have been known for more than a century, $[PtMe_3I]_4$ being the first organometallic compound reported in 1907 [11]. Unlike organoplatinum(IV).

Table 1. Some physical properties of palladium and platinum

Properties	Palladium	Platinum
Atomic number/ atomic weight	46/106.4	78/195.08
Ground state electronic configuration	$[Kr]4d^{10}5s^{0}$	$[Xe]5d^{9}6s^{1}$
Abundance in earth's crust (by weight) (ppm)	0.015	0.01
Melting point (°C)	1554.9	1768.3
Boiling point (°C)	2963	3825
Lattice structure	*fcc*	*fcc*
Density (g cm^{-3})	12.02	21.45
Pauling's electro negativity	2.2	2.2
Radius (Å): Atomic	1.375	1.387
M(0) Covalent	1.39	1.36
M(II) Covalent	1.28	1.29
Ionic (II)	0.86	0.80
Ionization potentials (eV)		
$M^{\circ}\rightarrow M^{+}$; $M\rightarrow M^{+2}$	8.33; 27.75	9.0; 27.56
$M^{\circ}\rightarrow M^{+3}$; $M\rightarrow M^{+4}$	60.67; 109.47	56.06; 97.16
$M^{+}\rightarrow M^{+2}$; $M^{+2}\rightarrow M^{+3}$	19.42; 32.92	18.56; 28.50
$M^{+3}\rightarrow M^{+4}$; $M^{+4}\rightarrow M^{+5}$	48.80; 66.00	41.10; 55.00
Oxidation potential (eV)		
$M^{\circ} \rightleftarrows M^{2+} + 2e$	−0.92	−1.2
$M^{II} \rightleftarrows M^{4+} + 2e$	−1.26	−0.77
Naturally occurring isotopes	^{102}Pd (1.0, 0)	^{190}Pt (0.01, 0)
(% abundance, spin (I))	^{104}Pd (11.1, 0)	^{192}Pt (0.8, 0)
	^{105}Pd (22.2, 5/2)	^{194}Pt (32.9, 0)
	^{106}Pd (27.3, 0)	^{195}Pt (33.8, 1/2)
	^{108}Pd (26.5, 0)	^{196}Pt (25.3, 0)
	^{110}Pd (11.7, 0)	^{198}Pt (7.2, 0)

complexes, organopalladium(IV) compounds are less prevalent [12, 13] because of the fact that the sum of the first four ionisation potentials of palladium (109.5 eV) are greater than that of platinum (97.2 eV). Only platinum shows +5 (e.g., PtF_5) and +6 (e.g., PtF_6) oxidation states, but these complexes are highly unstable. Stereochemistry of palladium and platinum complexes adopted in different oxidation states is given in Table 2.

Table 2: Stereochemistry of palladium and platinum complexes in various oxidation states and coordination numbers (C. N.) of the metal ion

Oxidation state	C. N.	Geometry	Examples
0	2	Linear	$[Pt(PPh_3)_2]$, $K_2[Pd(C{=}CR)_2]$
	3	Trigonal planar	$[Pd(PPh_3)_3]$, $[Pt(SO_2)(PCy_3)_2]$
		Distorted planar	$[PtX(PPh_3)_2]$ ($X = O_2$, C_2H_4, CS_2)
	4	Tetrahedral	$[Pt(PF_3)_4]$, $[Pt(CO)(PPh_3)_3]$
I	4	Square planar	$[M_2X_2(\mu\text{-dppm})_2]$
	5	Trigonal bipyramidal	$[Pt_3(SnCl_3)_2(C_8H_{12})_3]$
II	3	T-shaped	$[Pd(Br)(Ph)(P^tBu_3)]$
	4	Tetrahedral	$[Pd(EDM)_2]I_2$ (EDM = N, N′ ethylene dimorpholine)
	4	Square planar	All authenticated four coordinated complexes
	5	Trigonal bipyramidal	$[Pt(SnCl_3)_5]^{3-}$, $[Pd(QAs)I]^+$ $[Pd(Me_4[14]aneP_4]Br_2\cdot 6H_2O$,
		Square pyramidal	$[PtMeCl(AsMe_3)_2(CF_3C{\equiv}CCF_3)]$ $[Pt(Me_4[14]aneP_4]Br_2\cdot 4H_2O$
		Distorted square-pyramid	$[Pd(triphos)Cl]^+$
	6	Octahedral	$[Pd(diars)_2I_2]$
III	4	Square planar	$[Pd_2\{(C_6H_4PPh_2)\}_2(2\text{-}Spy)_2]Cl_2]$
	6	Octahedral	$K_2[Pt_2(SO_4)_4(H_2O)_2]$
IV	6	Octahedral	$[PtL_6]^{2-}$; L = X, SCN; $[PtMe_3I]_4$
	8	Piano-stool	$[Pt(\eta^5\text{-}C_5H_5)Me_3]$
V	6	Octahedral	$[PtF_6]^-$
VI	6	Octahedral	$[PtF_6]$

1.2 A brief coverage on palladium and platinum complexes

The chemistry of palladium and platinum complexes has been described in several books, monographs and review articles [14]. Both the metal ions fall in the category of class 'b' (soft metal ions) as per Chatt's concept [15] and 'soft' acid according to Pearson's theory [16]. Thus their chemistry is not only limited to soft bases like phosphorous and sulfur but is also extended to hard ligands like nitrogen and oxygen. The chemistry of palladium and platinum is similar, except that the reactivity of palladium is higher by more than a million times than platinum. Several examples of *cis-trans* isomerization are known in case of Pt(II) complexes due to their kinetic inertness over Pd(II). At the same time palladium compounds offer a balance between thermodynamic and kinetic labiality enabling product selectivity and specificity during the reactions. Square planar complexes of the type MA_2B_2 or MA_2BC exhibit *cis-trans* isomerism. Palladium(II) complexes generally form only one isomer since they are labile enough to yield only thermodynamically stable isomer whereas both the isomers can be isolated for platinum. The *trans* isomer is thermodynamically more stable due to increase in entropy.

There are several pathways by which one ligand is replaced by another in a square planar complex, that include ligand substitution, ligand addition, insertion reactions and oxidative addition followed by reductive elimination [17]. Ligand substitution reactions of square planar platinum(II) complexes occur stereospecifically. From purely steric considerations, the geometry of the transition state is expected to be approximately trigonal bipyramidal, since this arrangement minimizes the mutual repulsions of the five ligands. Rate of these substitution reactions is primarily affected by the nature of entering and leaving groups, and also by the nature of the other ligands in the complex (*trans* effect) [18, 19]. The *trans* effect is defined as the rate of substitution of an atom or molecule linked to central atom is determined by the nature of substituent at the opposite end of diagonal. The approximate order of decreasing trans effect is: CO > CN^- > C_2H_4 > PR_3 > H^- > CH_3^- > $SC(NH_2)_2$ > $C_6H_5^-$ > NO_2^- > I^- > SCN^- > Br^-> Cl^- > py > NH_3 > OH^- > H_2O.

Oxidative addition reactions with square planar d^8 metal complexes are of special interest as it is one of the key steps in homogenous catalysis. Gonzales, et. al. have presented a possible mechanism of an oxidative addition reaction of diaryl dichalcogenides to platinum(0) and palladium(0) precursors (Scheme 1) [20].

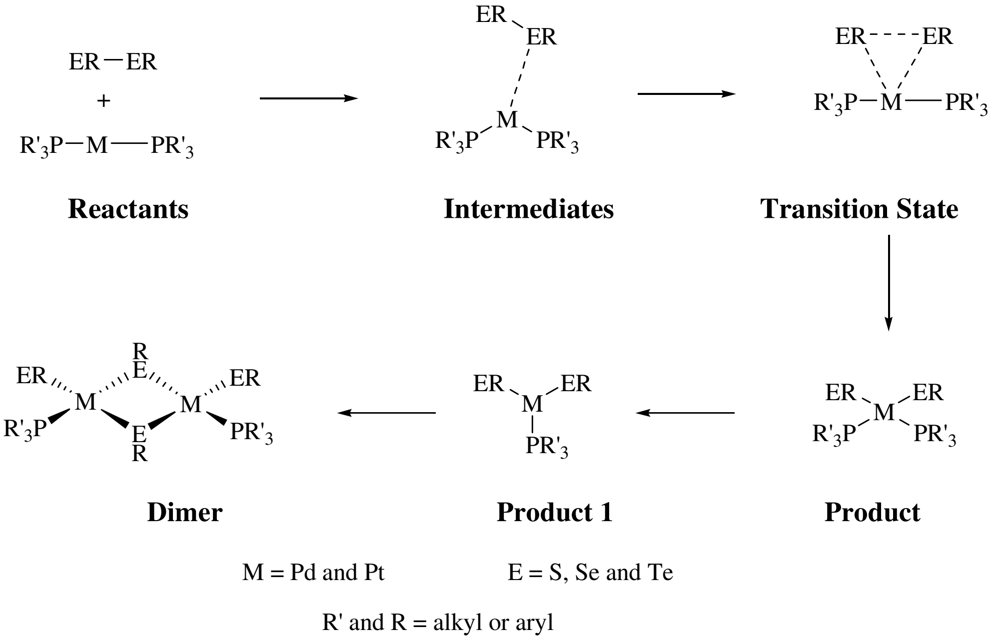

Scheme 1: Mechanistic path of an oxidative addition reaction

Palladium and platinum form a myriad of classical and organometallic complexes with a variety of ligands containing Groups14-17 donor atoms. Complexes with phosphine ligands, due to their relevance in homogeneous catalysis, and chalcogen in particular sulfur containing ligands, due to rich structural diversity, have been extensively investigated. Thus a brief coverage on these ligand systems is presented here.

1.3 Phosphine and chalcogenide as ligands

Tertiary phosphines (PR_3), represent an important family of ligands which have played a pivotal role in the development of transition metal complexes catalyzed organic transformations. The electronic and steric properties of phosphine ligands can be altered in a systematic and predictable manner over a wide range by changing the organic substituent (R). They are usually strong σ-donor ligands and weak π-acceptors. This effect can be increased with electron-donating groups in the R, while electron with-drawing groups in R favour the π-acceptor back bonding. Effects of phosphine ligands on reactions of metal complexes have been rationalized in terms of electronic effects [21] as well as steric effects in terms of stability of complexes [22]. Various parameters responsible for the reactivity of phosphine ligands are cone angle, bite angle, etc.

The steric effect of phosphine has been quantified by Tolmann. It is given by a parameter called *Cone Angle* (θ) (Figure 1) that measures the angle at the metal formed by the monodentate PR_3 ligand binding to a metal [23]. One unique feature of the phosphine ligand is that it allows convenient change of electronic effect without undergoing much change in its steric effects. For example, PBu_3 and $P(O^{i}Pr)_3$ have similar steric effects but vary in their electronic effects. The converse is also true as the steric effect can be easily changed without undergoing much change in the electronic effect. For example, PMe_3 and $P(o\text{-tolyl})_3$ have similar electronic effect but differ in their steric effects. The concept of cone angle is of practical importance in homogeneous catalysis because the size of the ligand affects the reactivity of the attached metal centre. Cone angle for monodentate phosphine ligands can be extended to di-phosphines and is defined as the average cone angle as measured for the two substituents and the angle between the M-P bond and the bisector of the P-M-P angle [24]. Various studies correlate ligand cone angle with single crystal X-ray diffraction technique [25, 26] and $^{1}J(^{195}Pt–^{31}P)$ coupling constants in NMR spectroscopy [27].

It has been reported that tri-*tert*-butylphosphine, with a cone angle of 182° [28] undergoes facile cyclometalation through C–H bond activation on treatment with $[PtCl_2(PhCN)_2]$ to a yield four-membered cyclometalated complex, $[Pt(\mu\text{-}C1)\{Bu^t_2PC(Me_2)CH_2\}]_2$ [29].

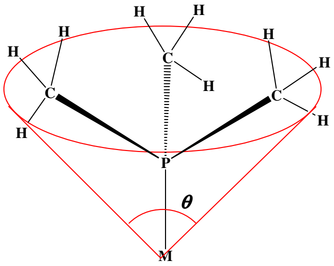

Figure 1. Tolman's cone angle for monodentate phosphine ligands

The ligand bite angle (β_n) is defined as the chelation angle determined by ligand backbone constraints. Diphosphine ligands offer control over regio- and stereo-selectivity in many catalytic reactions. Effect of bite angle of diphosphine ligands in catalytic reactions can be clubbed into two groups, viz., steric bite angle effect and electronic bite angle effect [30, 31].

Chalcogen Chemistry

Chemistry of platinum group metal chalcogenolates has been one of the active areas of research due to their wide structural diversity [32, 33] and relevance in catalysis [34-36]. Their potential application as single-source molecular precursors for metal chalcogenides [37-39] has further accelerated work on these complexes. The metal chalcogenides tend to form covalent, often low-dimensional structures. The greater covalence of the metal-chalcogen interactions reduces the relative charge on the metal ion. The chemistry of thio ligand is well explored while the chemistry of higher analogs, selenium and tellurium complexes have gained momentum only during the past decade or so. Metal chalcogenolates, in general, are isolated as non-volatile, insoluble or sparingly soluble oligomeric species.

There are different types of chacogen ligands which have been used for the preparation of numerous palladium and platinum complexes and are briefly given below:

Hydrochalcogenide (H_2E, REH, HE^-)

Hydrochalcogenide as ligands have hardly been employed to prepare palladium and platinum complexes because they react with metal ions to precipitate metal chalcogenides [40, 41]. The chemistry of hydrochalcogenides has been reviewed [42, 43].

Chalcogenides (E^{2-}, E_n^{2-})

The E^{2-} in general acts as a bridging ligand with an increasing order of S < Se <<Te to behave as a bridging ligand. The two sets of electron lone pair would be available easily for further reaction and thus resulting in the formation of clusters or polymers. The basicity of the lone pairs on the chalcogen atoms in 'Pt_2E_2' (E = S or Se) fragment can be compared with bidendate thioethers, which enabled them to behave as bidendate metallo ligand. Thus a variety of palladium and platinum coordination complexes have been prepared and characterized [44-47]. Unlike oxo- and sulfido- bridged complexes, heavier chalcogenido-bridged complexes have a planar four-membered M_2E_2 ring [48, 49].

Chalcogenolates (RE^-)

Jain *et al.* have reviewed the chemistry of palladium and platinum complexes with chalcogen ligands [50-53]. Chemistry of palladium and platinum complexes derived from two different classes of internally functionalized chalcogen ligands, *viz.* N,N-dimethylaminoalkylchalcogenolate [54-60] and 2-pyridylchalcogenolate [40, 61-65] is well explored.

Organometallic complexes, $[M_2R_2(\mu\text{-}ER')_2(PR_3)_2]$, can be conveniently prepared by treatment of $[M_2R_2(\mu\text{-}Cl)_2(PR_3)_2]$ with NaER′. The mixed bridged complexes, $[M_2R_2(\mu\text{-}Cl)(\mu\text{-}ER')(PR_3)_2]$ have been isolated by redistribution reaction between $[M_2Cl_2(\mu\text{-}ER')_2(PR_3)_2]$ and $[MCl_2(\mu\text{-}Cl)_2(PR_3)_2]$ (Scheme 2) which is believed to proceed *via* a tetranuclear intermediate

[66]. Asymmetric complexes of organo-chalcogenide-bridge having general formula, $[L_2M(\mu\text{-}ER')_2M'X_2]$ have also been reported [67]. They are prepared by the treatment of mononuclear complex $M(ER')_2L_2$ (ER' = SPh, SC_6H_5, SePh, TePh, L_2 = dppe, dppm, 2 PPh_3) with $PdCl_2(RCN)_2$ (R = Me or Ph) [68] or $M'(C_6H_5)_2(THF)_2$ (M′ = Pd or Pt) [67].

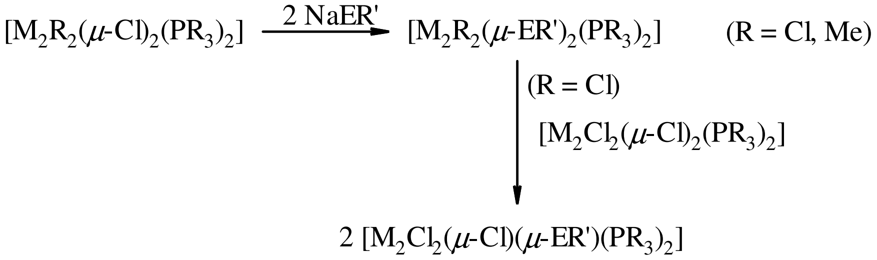

Scheme 2

Mononuclear chalcogenolato complexes play a significant role as building blocks for polynuclear palladium complexes. It has been suggested [69] that they are formed from mononuclear complexes by successive condensation reactions. This kind of structural relationships were initially suggested for the formation on hexanuclear complex, $[Pd_6Te_6(PEt_3)_8]$ involving a dinuclear intermediate $[Pd_2Te_4(PEt_3)_4]$ [70]. The complexes $[Pd_6Te_4(TeR)_2(PPh_3)_6]$ (R = Ph, C_4H_3S), containing the same framework as $[Pd_6Te_6(PEt_3)_8]$, have been isolated by oxidative addition of R_2E_2 to $[Pd(PPh_3)_4]$.

Chalcogenoethers

Monodentate, chelating bi-/ tri-dentate and hybrid chalcogenoethers incorporating N, O, S hetero donor atoms have been used for the synthesis of metal complexes. A number of reviews pertaining to specific aspects of the chemistry of these compounds have been published [71-76]. The metal complexes are usually isolated in a single step reaction between metal halides with the free ligand in an appropriate solvent. The metal complexes are usually obtained by stirring either an aqueous solution of metal salts with a chalcogenoether or a solution of a metal complex containing labile ligands such organonitriles, olefins, etc. with a chalcogenoether in an organic solvent. Organochalcogeno ether-based binuclear palladium and platinum complexes of general formula, $[M_2X_4(R_2E)_2]$ (M = Pd or Pt; E = S, Se, Te) are prepared in several ways [77-79] and the one involving reaction of $MCl_2(R_2E)_2$ with Na_2MX_4 in ethanol is commonly employed. Dimeric thioether complexes, $[M_2Y_2(\mu\text{-}X)_2(R_2E)_2)]$ [80, 81], $[Pd_2Me_2(\mu\text{-}X)_2(SMe_2)_2]$ [82-84] and $[Pt_2Me_4(\mu\text{-}SMe_2)_2]$ [85,86] are versatile precursors for the synthesis of a variety of complexes. Thioethers have a greater π-acceptor capacity than nitrogen donor ligands such as pyridine, but rather less than PR_3 or AsR_3. Inversion at pyrimidyl chalcogen atom in several metal complexes has been investigated by NMR spectroscopy and in general it is a facile process [76]. The barrier of inversion increases with increasing size of the chalcogen atom and follows the order Te > Se > S [76]. Inversion barrier in platinum complexes is higher than those in the corresponding palladium complexes. Chalcogenoether complexes undergo a variety of reactions; and to name a few are, Te-C bond cleavage, transmetalation and cyclometalation reactions.

Diorgano dichalcogenides

Diorganodichalcogenides are important precursors in coordination chemistry [87] because of their implication to different fields of research. They undergo oxidative addition reactions with Pt(0)/Pd(0) precursors to yield a variety of mono-/ bi-nuclear complexes respectively (E = S, Se) [88-91]. Similar trend has been noticed in the oxidative addition reaction between $M(PPh_3)_4$ and dipyridyl ditellurides (scheme 3) [62-64]. In general tellurium derivatives are more reactive and in several cases yield Te–C bond cleaved tellurido-bridged trinuclear complexes, $[M_3(\mu\text{-}Te)_2(P^\frown P)_3]^{2+}$ formation of which is more pronounced with dppp ligand [63, 64, 92] and with more basic pyrimidyl group [92].

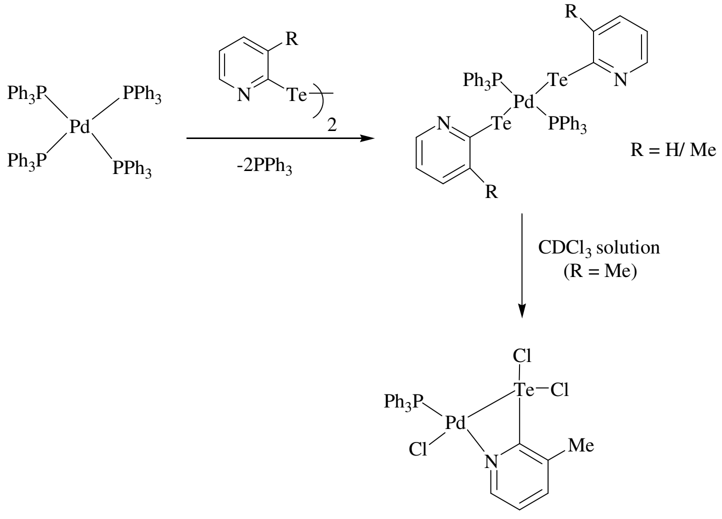

Scheme 3

1.4 Supra-molecular Chemistry

The modern concept of supra-molecular chemistry was introduced by Jean-Marie Lehn in the year 1978, which he defined as "…chemistry of molecular assemblies and of the inter-molecular bond" [93]. Traditionally, phrases such as "chemistry beyond the molecule," "the chemistry of the non-covalent bond," and "non-molecular chemistry" were also used to describe the field. In the broad sense, supra-molecules are aggregates in which a number of components come together either spontaneously, or by design to form a larger entity with properties derived from its components. These aggregates can be of the host-guest type in which one molecule encapsulates the other, or they can involve mutually in a self-assembly. The molecular complexes thus formed are usually held together in several ways such as hydrogen bonding, ion pairing, π-acid to π-base interactions, metal-to-ligand binding, van der Waals attractive forces, solvent reorganizing, and partially made and broken covalent bonds.

Self-assembly is a spontaneous association of two or more moieties under equilibrium condition into stable, structurally well defined aggregates through covalent or non- covalent interactions [94, 95]. Metal directed self–assembly of Supra-molecular architectures, such as

2D triangles, squares (Scheme 4) rectangles and other polygons, polyhedra and 3D cages are the main targets for use as cavity materials [96].

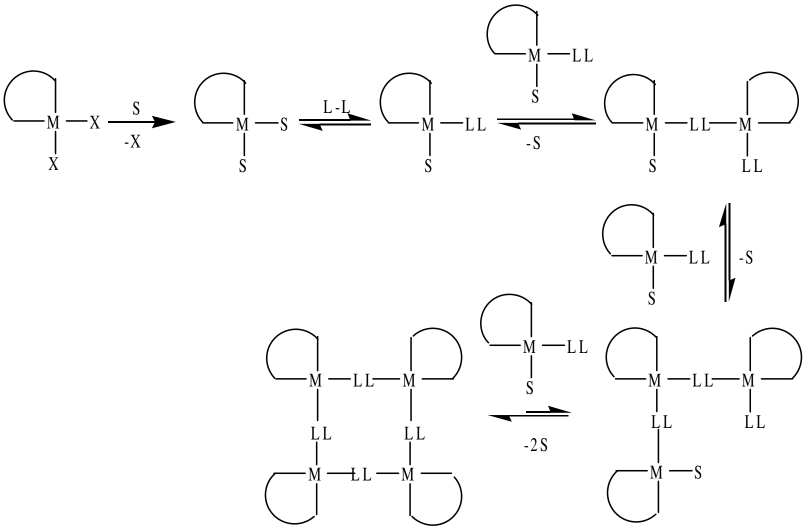

Scheme 4. Proposed mechanism of molecular square formation (where M = square planar / octahedral metal; X = labile counter ion; S = coordinating solvent molecule; LL= bidentate ligand).

The use of weak interactions in Supra-molecular arrays is important for two reasons: (i) the weak forces holding the molecules together incorporate a large degree of flexibility into molecules which allows conformational changes that are often necessary for a function, and (ii) the large number of weaker interactions allow greater specificity through annealing processes which ultimately form the most thermodynamically favourable structure. Several approaches have been developed for self-assembly of discrete multinuclear species [97]. A few of them are briefly discussed here.

The Directional-bonding approach

This emerging methodology was used to construct macrocycles in the shape of selected polygons by rationally designing organic ligands and metal-containing precursors to occupy the edges and vertices of the target shape. This design approach is sometimes referred to as "edge-directed self-assembly". Typically, the metals are introduced into these structures with directing or blocking ligands that only make coordination sites available to incoming ligands with an appropriate angle to form the desired shape. For example, a binuclear macrocycle can be assembled by using a metal complex with a 60° angle between the coordinatively labile sites and a rigid ligand with a 120° twist. This same metal complex can be used to construct a molecular triangle by using a linear ligand system (Scheme 5) [95]. For instance, there are two complementary ways to construct a molecular square, *viz.* (i) by using a metal starting material with a 90° angle between the coordination sites and a rigid linear ligand and (ii) by utilizing a metal complex with a 180° geometry and a ligand system with a 90° turn. Since either the ligand or metal used in this approach has a directing influence, the term "directional-bonding approach" is more descriptive (Scheme 6) [98].

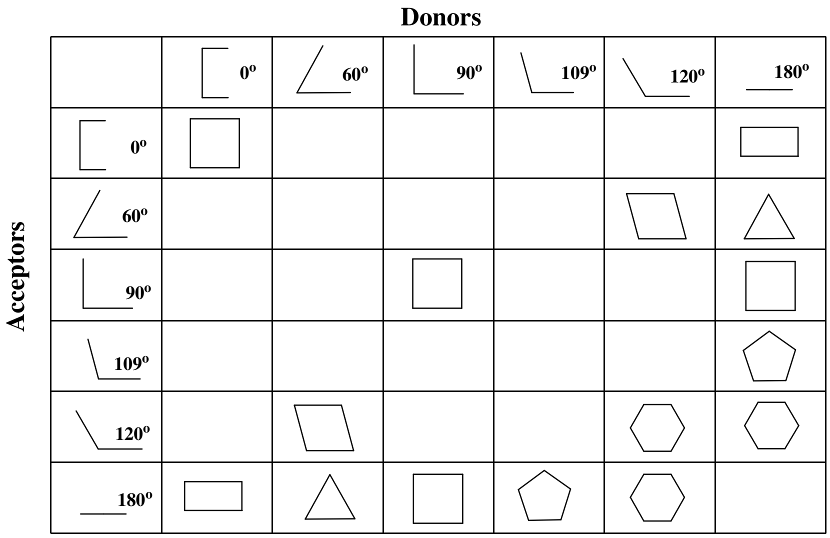

Scheme 5. A representation of ditopic building blocks to generate a suite of 2D convex polygons via self-assembly

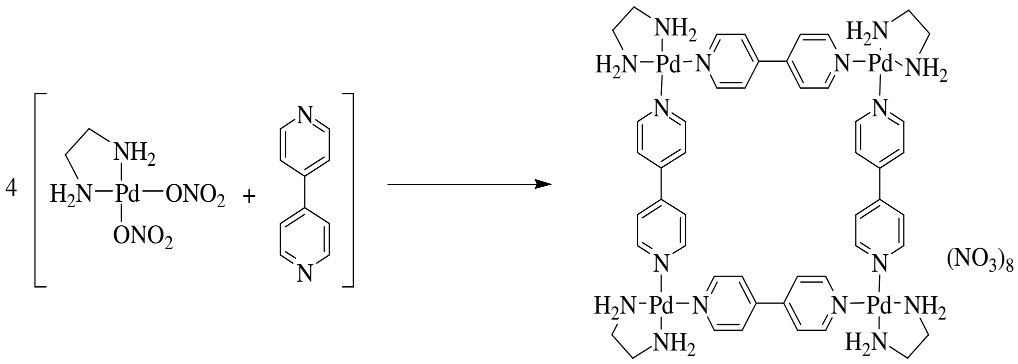

Scheme 6. M_4L_4 square can be interpreted as the combination of linear and 90^o components using a directional bonding approach.

Symmetry-interaction approach

This methodology relies on concepts from edge directed self-assembly [53, 99]. The coordination vectors that are critical to defining the angularity and directionality of molecular building blocks remain an important parameter when designing ligands for symmetry-interaction self-assembly. In this strategy, multi-branched chelating ligands are generally used in conjunction with sources of transition or main group metals which are free of strongly coordinating ligands. With this combination of starting materials, the formation of a given Supra-molecular shape is driven by inherent symmetry of the coordination sites available on the metal centre. The metal/ ligand combinations must be chosen carefully in order to maintain coordinative lability. Finally, the symmetry interactions with which one must contend (e.g., metal geometry, ligand orientation, and ligand-ligand steric interactions) when designing a Supra-molecular assembly utilizing this method (Scheme 7) [53].

Weak link approach

The weak-link synthetic strategy for two- and three-dimensional structures offers the ability to prepare Supra-molecular architectures from flexible ligands and transition metal starting materials free of directing ligands to yield structures with coordination sites that are available for further chemistry. This approach was developed by Mirkin and co-workers, utilizing hemilabile ligands [100, 101] such that the initial Supra-molecular coordination complexes (SCCs) formed can undergo post-self-assembly modifications to access new structures [102]. It is important to note that this approach is conceptually different from the directional-bonding and symmetry-interaction approaches and yields structures that are not accessible by other approaches. The reactions used in the weak-link approach are under kinetic rather than thermodynamic control.

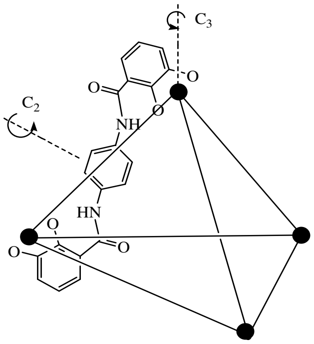

Scheme 7. M_4L_6 tetrahedra constructed by designing C_2 symmetric ligands with proper angle between coordination vectors

Supra-molecular Catalysis

The interface between Supra-molecular chemistry and transition metal catalysis has received surprisingly little attention. The first efforts to integrate transition metal catalysis and Supra-molecular encapsulation were published by Breslow and Overman in 1970 [103] using cyclodextrins as the Supra-molecular host. The design and construction of large molecules with well defined cavities opens the possibilities of host-guest and inclusion chemistry and, therefore, the ultimate goal of selective substrate activation and catalysis. There are several examples in the recent literature where the internal cavity of covalently linked Supra-molecular structures has been exploited to arrange reactants and stabilize reactive intermediates involved in organic transformations [104, 105]. Supra-molecular coordination complexes have been used by Fujita and co-workers to facilitate a metal mediated catalytic transformation [106]. A Supra-molecular nanoreactor has been constructed by employing phthalocyanine- bridged β-cyclodextrins as host and the carboxylated porphyrin as amphiphilic guest by using extremely strong non- covalent complexation interactions. This hollow tubular structure has been utilized for Suzuki C-C coupling reactions [107].

1.5 Applications of palladium and platinum complexes

Homogenous catalysis

Among all the PGM based homogenous catalysis, perhaps the palladium catalysed cross-coupling made vast impact in practical terms since the early 1970s [108, 109]. The transformations in a homogenous carbon-carbon cross-coupling allow the substitution of an aryl, vinyl and alkyl halide/pseudohalide by a nucleophile in the presence of a transition-metal catalyst. Most commonly, these reactions involve the formation of a carbon–carbon bond utilizing a range of different carbon nucleophiles, such as, aryl, vinyl and alkyl derivatives of magnesium (Kumada–Corriu) [110, 111], boron (Suzuki–Miyaura) [112, 113], zinc (Negishi) [114, 115], silicon (Hiyama) [116], tin (Stille) [117]. The field of cross-coupling has been broadened to include carbon–heteroatom bond forming reactions; the most important of these involve the construction of C–N [118], C–O [119] and C–S bonds [120]. Famous representatives among them are the Heck however, because of the absence of a transmetallation step. The coupling reactions which were recognized by a Nobel Prize in Chemistry 2010 are shown in Scheme 8.

The coupling of aryl halides with organoboronic acids is one of the most important palladium-catalyzed cross-coupling reactions usually referred as Suzuki coupling, first described in 1979 by Akira Suzuki. The most commonly used catalyst is $Pd(PPh_3)_4$, but several other palladium complexes have been developed for this catalytic reaction including Pd(II) pre-catalysts that are reduced to the active Pd(0) *in situ*. Typically, the mechanism of cross-coupling of an electrophile (R–X) and the nucleophile ($R'B(OR'')_2$) takes place *via* a three-step mechanism (Scheme 9), (i) oxidative addition of $L_2Pd(0)$ to $L_2RPd(II)X$, (ii) transmetalation of R′ from boron to Pd, forming $L_2RPd(II)R'$, and (iii) reductive elimination of R–R′, converting Pd(II) to Pd(0).

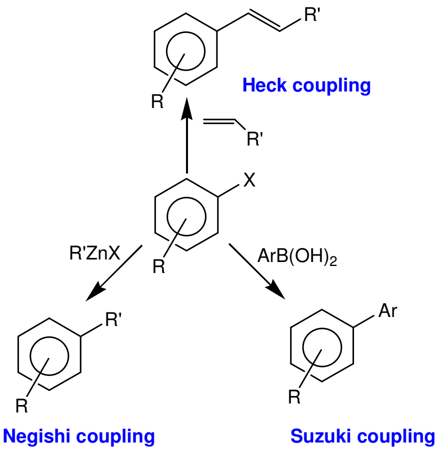

Scheme 8: C-C coupling reactions

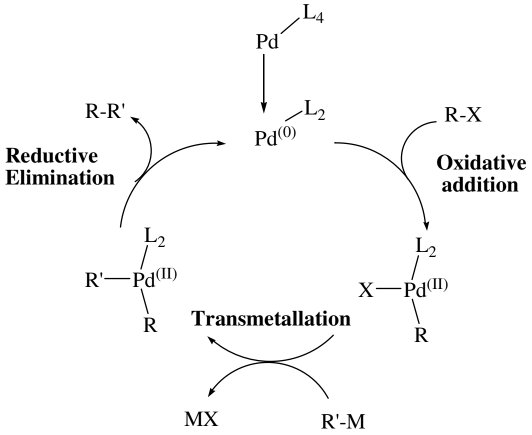

Scheme 9

Molecular precursors for metal and metal chalcogenide nano-particles

A variety of organometallic palladium and platinum complexes, such as [Pd(allyl)acac], [$PdMe_2(PEt_3)_2$], [M(allyl)Cp] (M = Pd or Pt; Cp = cyclopentadienyl), [$Pt(hfac)_2$] (hfac = hexafluoroacetylacetonate), [$PtMe_3Cp$] have been successfully used for deposition of thin films and nanocrystals [121-123].

Platinum group metal chalcogenides have relevance in catalysis and materials science. Several of these chalcogenides occur in nature as minerals, for instance, braggite ($PdPt_3S_4$), luberoite (Pt_5Se_4) and Pt_6AgTe_4. The binary compounds of palladium and platinum show a higher diversity and binary phases and can be classified as MX (PdS, PdSe PdTe, PtSe, PtTe); Pd_3X (X = S, Se, Te); Pd_4X (X = S, Se, Te); MX_2 (PdS_2, $PdSe_2$, $PdTe_2$, PtS_2, $PtSe_2$, $PtTe_2$), etc.

Jain's group has studied synthesis and structural chemistry of oragnochalcogenolate-based single source precursors for preparing metal chalcogenides [124, 125]. They have reported the synthesis of metal chalcogenides by thermal decomposition of metal benzyl selenolates, 2-(diethylamino)ethaneselenolates, monoselenocarboxylates, 2-(methoxycarbonyl)ethylselenolates, 3-(diethylamino)propylselenolates. The facile cleavage of Pd–allyl bond in the allylpalladium chalcogenolate complexes has been exploited for deposition of palladium chalcogenides. Solvothermal decomposition of [$Pd(SeCOAr)_2(PR_3)_2$] and [$Pd(OAc)(ECH_2CH_2CH_2NMe_2)]_2$ (E = S, Se, Te) yields palladium chalcogenides nanoparticles (e.g., Pd_7Te_3, $Pd_{17}Se_{15}$) [126]. Singh and coworkers have synthesized $Pd_{17}Se_{15}$ nanoparticles from a single source precursor [$Pd(L)Cl_2$] {L=1,3-bis(phenylselenyl) propan-2-ol} and grafted onto graphene oxide which show high catalytic activity in C-O coupling between aryl/heteroaryl chlorides/bromides and phenol at room temperature [127]. Radha and Kulkarni reported a single step synthesis of palladium sulfide (Pd_4S) films as well as nano-patterns by heating a drop coated palladium octane thiolate solution on a glass substrate in H_2

atmosphere at 250°C. The obtained Pd_4S conducts like a metal, but unlike Pd, is impermeable to H_2 [39].

Anticancer Drugs

Investigation of the potential of platinum complexes as anti-tumour agents came into light in the earlier 1960's by Rosenberg, when he found *in-situ* formation of *cis*-diamminedichloroplatinum (*cis*-$[PtCl_2(NH_3)_2]$) and *cis*-diamminetetrachloroplatinum (*cis*-$[PtCl_4(NH_3)_2]$) [128] as highly potent agents that could inhibit the cell division. Since then extensive work on design and development of several platinum complexes has been undertaken. These efforts have led to development of new platinum based drugs shown in Scheme 10. The extensive investigations on design of such complexes have led to the following general features in the active molecules [129].

- The compound should have two amine groups with cis geometry, as those with trans geometries are inactive.
- It is necessary, although not sufficient, for the compound to have two leaving groups that are cis with respect to one another. Leaving groups are those groups on the molecule that are the most easily lost.
- The ease with which the leaving groups are able to be lost affects the activity and the toxicity of the compound. It is preferable for the leaving groups to be only moderately easy to remove.
- The compound should be neutral.
- Compounds with fewer alkyl substituents on the amine ligands had greater activity.
- Each amine ligand should possess at least one proton.

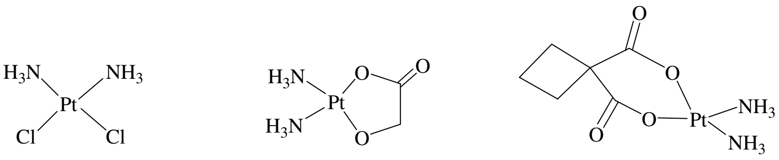

cis-platin Nedaplatin Carboplatin

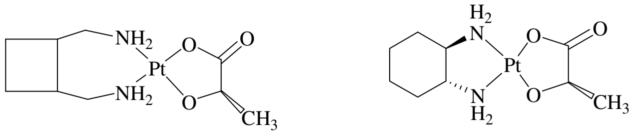

Lobaplatin Oxaliplatin

Scheme 10: Anticancer platinum based drugs

Luminescent properties

Luminescent platinum complexes have attractive chemical and photophysical properties such as high stability, emission in the visible region, high emission quantum yields and long excited state lifetimes [130]. The square-planar geometry of d^8 transition metal complexes, such as platinum(II), leads to a high tendency towards stacking, through establishment of ground-state intermolecular non-covalent weak metal...metal and/or ligand–ligand interactions through the π-electron cloud of the aromatic rings. It has been reported that in organic or aqueous media, luminescent Pt(II) complexes are able to form homo [131] and hetero-metallic [132-134], Supra-molecular architectures and superstructures such as nano-wires [135] nano-sheets, nano-wheels, nano-tubes [136] liquid crystals [137], etc.

Owing to good photoluminescence property of Pt_2 complexes, the luminescence studies of platinum-chalcogen complexes has also attracted considerable interest. Yam and co-workers [138] have synthesized binuclear platinum complex, $[Pt_2(\mu\text{-}S)_2(dppy)_4]$. Compared to $[PtCl_2(dppy)_2]$, $[Pt_2(\mu\text{-}S)_2(dppy)_4]$ has an additional good σ-donating sulfido moiety, which may lead to ligand-to-metal charge transfer (LMCT) character from the newly emergent low-energy emitting state.

1.6 Scope of the work

The above discussion on palladium and platinum chemistry clearly indicates that there are several areas which offer new opportunities for further investigations. Coordination /transition metal driven self-assembly represent a powerful synthetic methodology for the synthesis of multinuclear systems with well-defined architectures. So it is proposed to synthesize multinuclear/Supra-molecular complexes of platinum group metals. The ligands with Group 15 donor atoms have been widely used to construct the above types of molecules, whereas it is almost unexplored with chalcogen ligands. The bridging ability and additional lone pair of electrons on chalcogen atom are very promising features to construct large assemblies. The non-chelating bidentate ligands such as 4-pyridyl chalcogenolate offer several bonding possibilities. Ligands containing both the COOH group and a soft donor atom like sulfur have not so far been employed in the design of Supra-molecular assemblies. In this regard mercaptobenzoic acids have been chosen to design hydrogen–bonded supramolecules. The metal-sulfur linkage, being a stronger bond, can be exploited to construct rigid structures. In order to assess the suitability of palladium complexes as homogenous catalyst in C–C coupling reaction, the activity of some of these complexes has been examined in Suzuki coupling reactions.

The emphasis has been to understand and synthesize various palladium and platinum Supra-molecular complexes with chalcogen ligands. All the complexes have been characterized by elemental analyses, IR, NMR (^{1}H, ^{13}C, ^{31}P, ^{77}Se, ^{125}Te, ^{195}Pt), UV-Vis, mass spectrometry. In several cases structures have been established unambiguously by single crystal diffraction analyses. For the sake of convenience and clarity the present work is sub-divided as follows:

- Chemistry of 4-pyridylselenolate complexes of palladium and platinum and their catalytic activity in Suzuki C-C coupling reaction.

- Chemistry of 3-/4-mercaptobenzoic acid complexes of palladium(II) and platinum(II) stabilized by hydrogen bonding.
- Chemistry of aryldithiolate ligands of palladium and platiunm and their unprecedented catalytic activity in Suzuki C-C coupling reaction.
- Chemistry of nitrogen bonded hemilabile organoselenium/tellurium complexes of palladium and platinum.
- Chemistry of 4-pyridyltellurolate complexes of palladium and platinum.

Chapter 2

Experimental

2.1 Materials and methods

Glassware with inter-changeable standard conical ground joints were used throughout this investigation. Special type of glasswares like Schlenk flasks, two-necked flasks and three-way stopcocks with appropriate joints were used for synthesis and storage of moisture and air sensitive compounds. All the glass-wares were immersed overnight in an alkali bath [5% NaOH in ethanol-water (1:1 v/v) mixture], washed thoroughly with soap and water followed by rinsing with acetone and dried in an oven at 120-130 °C for at least 6 h. Before using, hot apparatus were kept in desiccators filled with silica gel for cooling. Filtration assemblies with G-2/G-3 sintered discs were used for filtering precipitates. Celite was used for filtration of solvent extracts. Vacuum pump was used to evaporate/ concentrate solvents under reduced pressure. Various methods such as cooling, and evaporation, etc. were employed for growing crystals of the complexes.

All solvents and reagents were of A. R. grade and were dried, purified by standard procedures [139]. Hexane (67-68 °C), benzene (78 °C) and toluene (110 °C) were dried by refluxing them on sodium with benzophenone followed by distillation in an inert atmosphere. Diethyl ether (36 °C) and tetrahydrofuran (65-67 °C) were dried initially over $CaCl_2$ followed by distillation over anhydrous P_2O_5, and further dried by refluxing over sodium metal using benzophenone as an indicator. Dichloromethane (38 °C) was dried over calcium chloride followed by decantation and distillation. Methanol (65 °C) was refluxed over magnesium methoxide (prepared from magnesium turnings and methanol in the presence of catalytic amount of iodine) for 4 h and distilled. Iodomethane (43 °C) was freshly distilled prior to the preparation of Grignard reagent. 4-Bromopyridine hydrochloride, 1-(4-pyridyl)pyridinium chloride hydrochloride, 4-Mercaptobenzoic acid (4-H_2mba), 3-mercaptobenzoic acid (3-H_2mba), 1,4-

benezenedithiol, 4,4′-biphenyldithiol, 1,4-benezenedimethanethiol, silver triflate (AgOTf), aryl boronic acids, aryl halides and other reagents were used as purchased from commercial sources without any further purification.

2.2 Experimental techniques

Melting points were determined in glass capillary tubes sealed at one end and are uncorrected. Microanalyses (C, H, N and S) were carried out on Thermo Fischer Flash EA-1112 CHNS instrument. The IR spectra were recorded as KBr wafer on a Jasco FT-IR 6100 spectrometer in the range of 4000-400 cm^{-1} with a resolution of 5 cm^{-1}. Electronic absorption spectra were recorded in CH_2Cl_2, MeOH, and acetone on a UV-vis Jasco V-630 double beam spectrophotometer using quartz cuvettes with path length of 1 cm. The spectra were recorded in a wavelength range of 200-800 nm with a resolution of ~1 nm. The molar extinction coefficient (ε) was calculated using Beer-Lambert law expressed by thefollowing equation (Eq. 1).

$$\varepsilon = \frac{O.D.}{c\,.\,I} \qquad ...(1)$$

O.D. = Absorbance determined experimentally

c = concentration of the solution

I = thickness of the absorbing medium (in the present study 1 cm)

The ^1H, $^{13}C\{^1H\}$, $^{31}P\{^1H\}$, $^{77}Se\{^1H\}$, $^{125}Te\{^1H\}$, $^{195}Pt\{^1H\}$ NMR spectra were recorded on Bruker Avance II-300 MHz and Bruker Avance III-400 MHz NMR spectrometers operating at 300/ 400.13, 75.47/ 100.61, 121/ 161.97, 57.24/ 76.33, 94.86/ 126.24 MHz, respectively in thin walled 5 nm NMR tubes. Chemical shifts are relative to internal chloroform peak ($\delta = 7.26$ ppm for ^1H and $\delta = 77.0$ ppm for ^{13}C), external 85% H_3PO_4 for $^{31}P\{^1H\}$, Na_2PtCl_6 in D_2O for

$^{195}Pt\{^1H\}$, external Me_2Se for $^{77}Se\{^1H\}$ (secondary reference Ph_2Se_2 in $CDCl_3$, δ 463 ppm) and Me_2Te for $^{125}Te\{^1H\}$ (secondary reference Ph_2Te_2 in C_6D_6, δ 421 ppm). A 90° pulse was used in every case.

Mass spectra were recorded on a Waters Q-TOF micro (YA-105) time of flight mass spectrometer. Cyclic voltammetry was performed on PGSTAT 20 Eco Chemie instrument. The voltammograms were recorded using a three electrode configuration with a platinum pseudo reference electrode (square foil 8 x 8 mm; electrode potential: 0.12 V vs. Ag/AgCl (saturated)), platinum wire coated with platinum black as a counter electrode and polished glassy carbon electrode (diameter = 5 mm) as a working electrode. Solutions of the complexes were prepared in CH_3CN/ 0.05 M Me_4NPF_6, cycling between –2.5 and 1.5 V. Concentrations of the samples were maintained in the range 0.25-1.0 mM.

The single crystal X-ray structural analyses of a number of complexes were carried out on BRUKER GADDS using Cu sealed X-ray tube (K_α = 1.5418 Å) radiation / BRUKER APEX 2 using Mo Kα radiation or Rigaku AFC7S diffractometer using graphite monochromated Mo Kα (λ = 0.71069 Å) radiation [140]. The crystals were directly mounted on the diffractometer after examining the quality of crystal under a polarizing microscope. Most of the structures were solved using direct methods using SHELX-97 [141, 142] and refined by full matrix least square method [143] on F^2 using data correction for absorption effects using empirical procedures [144]. All non-hydrogen atoms were refined anisotropically and hydrogen atoms were placed in their geometrically idealized positions with coordinate and thermal parameters riding on host atoms. The molecular structures were drawn using ORTEP [145-147]. Crystallographic and refinement details are given in Tables 3 - 11.

Table 3. Crystallographic and structure refinement data for Pd/Pt (II) 4-pyridylselenolate complexes

Compound	$[PdCl(SeC_5H_4N\text{-}4)(PPh_3)_2]\cdot$acetone	$[PtCl(SeC_5H_4N\text{-}4)(PEt_3)_2]$	$[Pd(SeC_5H_4N\text{-}4)_2(PPh_3)_2]$	$[Pt(SeC_5H_4N\text{-}4)_2(PEt_3)_2]$
Chemical formula	$C_{44}H_{40}ClNOP_2PdSe$	$C_{17}H_{34}ClNP_2PtSe$	$C_{46}H_{38}N_2P_2PdSe_2$	$C_{22}H_{38}N_2P_2PtSe_2$
Formula weight	881.52	623.89	945.04	745.49
Crystal Size (mm^3)	0.12 × 0.06 × 0.03	0.42 × 0.31 × 0.25	0.50 × 0.43 × 0.16	0.43 × 0.41 × 0.24
Diffractometer	BRUKER GADDS	BRUKER APEX 2	BRUKER APEX 2	BRUKER APEX 2
T/K	110(2)	110(2)	110(2)	110(2)
λ/Å	1.54178	0.71073	0.71073	0.71073
Crystal system	Monoclinic	Monoclinic	Monoclinic	Orthorhombic
Space group	$P2_1/n$	$P2_1/n$	$P2_1$	$Pca2_1$
a/Å	10.4301(3)	14.4320(6)	10.1330(11)	19.975(3)
b/Å	16.8918(6)	10.6073(5)	12.8723(14)	9.0763(15)
c/Å	43.8939(14)	15.4103(7)	15.0542(16)	14.380(2)
$\alpha/^o$	90	90	90	90
$\beta/^0$	93.019(2)	105.0360(10)	91.1260	90
$\gamma/^0$	90	90	90	90
V/Å^3	7722.6(4)	2278.31(18)	1963.2(4)	2607.1(7)
ρ_{calc}, g cm^{-3}	1.516	1.819	1.599	1.899
Z	8	4	2	4
μ/mm^{-1}	6.646	8.014	2.444	8.309
Reflections collected	135477	47227	30774	27666
Data/restraints/parameters	11447 / 0 / 923	5237 / 2 / 222	8936 / 1 / 479	5919 / 15 / 262
Final R1,*w*R2 indices	R1 = 0.0382, wR2 = 0.0863	R1 = 0.0162, wR2 = 0.0396	R1 = 0.0440, wR2 = 0.1128	R1 = 0.0238, wR2 = 0.0499
R_1, wR_2 (all data)	R1 = 0.0511, wR2 = 0.0894	R1 = 0.0177, wR2 = 0.0405	R1 = 0.0485, wR2 = 0.1162	R1 = 0.0281, wR2 = 0.0511
Largest diff.peak & hole [eÅ^{-3}]	0.408 and -0.822	0.675 and -0.985	3.155 and -0.849	1.445 and -1.015

Table 4. Crystallographic and structure refinement data for Pd/Pt (II) 4-pyridylselenolate complexes

Compound	$[Pd(SeC_5H_4N\text{-}4)_2(dppe)]\cdot 2H_2O$	$[Pt(SeC_5H_4N\text{-}4)_2(dppp)]\cdot 0.5H_2O$	$[PdCl(SeC_5H_4N\text{-}4)(PPh_3)]_2$
Chemical formula	$C_{36}H_{36}N_2O_2P_2PdSe_2$	$C_{37}H_{35}N_2O_{0.5}P_2PtSe_2$	$C_{46}H_{38}Cl_2N_2P_2Pd_2Se_2$
Formula weight	854.93	930.62	1122.34
Crystal Size (mm^3)	0.13 × 0.08 × 0.03	0.06 × 0.05 × 0.03	0.25 × 0.18 × 0.12
Diffractometer	BRUKER GADDS	BRUKER GADDS	BRUKER APEX 2
T/K	110(2)	110(2)	110(2)
λ/Å	1.54178	1.54178	0.71073
Crystal system	Monoclinic	Triclinic	Monoclinic
Space group	$P2_1/c$	P-1	$P2_1/n$
a/Å	15.7931(8)	10.5487(12)	10.1799(12)
b/Å	10.5303(5)	10.7006(13)	14.6690(17)
c/Å	21.2888(11)	14.9796(16)	14.8568(17)
$\alpha/^o$	90	91.771(9)	90
$\beta/^0$	105.650(3)	94.027(9)	93.4050
$\gamma/^0$	90	95.391(9)	90
V/Å^3	3409.2(3)	1678.0(3)	2214.6(4)
ρ_{calc}, g cm^{-3}	1.666	1.842	1.683
Z	4	2	2
μ/mm^{-1}	7.999	11.443	2.683
Reflections collected	9607	9931	24421
Data/restraints/parameters	5063 / 0 / 406	9942 / 0 / 407	5068 / 0 / 253
Final R1,*w*R2 indices	0.0347, 0.0828	0.0373, 0.1104	0.0178, 0.0437
R_1, wR_2 (all data)	0.0446, 0.0848	0.0423, 0.1151	0.0193, 0.0443
Largest diff.peak & hole [eÅ $^{-3}$]	1.067 and -0.774	1.065 and -1.036	0.492 and -0.445

Table 5. Crystallographic and structure refinement data for trinuclear palladium and platinum 4-pyridylselenolate complexes

Compound	$[PdCl(SeC_5H_4N\text{-}4)(PEt_3)]_3$	$[PtCl(SeC_5H_4N\text{-}4)(PEt_3)]_3 \bullet CHCl_3$
Chemical formula	$C_{33}H_{57}Cl_3N_3P_3Pd_3Se_3$	$C_{34}H_{58}Cl_6N_3P_3Pt_3Se_3$
Formula weight	1251.16	1636.59
Crystal Size (mm^3)	0.25 × 0.20 × 0.10	0.30 × 0.15 × 0.15
Diffractometer	RIGAKU AFC7S	RIGAKU AFC7S
T/K	298 (2)	298 (2)
λ/Å	0.71069	0.71069
Crystal system	Monoclinic	Monoclinic
Space group	$P2_1/n$	$P2_1/a$
a/Å	14.2500(12)	14.501(3)
b/Å	13.984(6)	24.574(3)
c/Å	24.400(5)	14.763(4)
$\alpha/^o$	90	90
$\beta/^0$	105.330(13)	102.72(2)
$\gamma/^0$	90	90
$V/Å^3$	4689(2)	5131.7(18)
ρ_{calc}, g cm^{-3}	1.772	2.026
Z	4	4
μ/mm^{-1}	3.766	10.567
Reflections collected	14523	14086
Data/restraints/parameters	10760/20/410	11757/63/363
Final R1,*w*R2 indices	0.0745, 0.1409	0.0696, 0.1331
R_1, wR_2 (all data)	0.1803, 0.3474	0.2161, 0.3843
Largest diff.peak & hole [$eÅ^{-3}$]	1.032 & -0.886	1.000, -1.247

Table 6. Crystallographic and structure refinement data for mononuclear mercaptobenzoic acid complexes of platinum.

Compound	$[Pt(SC_6H_4COOH\text{-}4)_2(PEt_3)_2]\cdot H_2O$	$[Pt(SC_6H_4COOH\text{-}4)_2(PEt_3)_2]\cdot(MeOH)_2$	$[Pt(SC_6H_4COOH\text{-}4)_2(PPh_3)_2]$
Chemical formula	$C_{26}H_{42}O_5P_2PtS_2$	$C_{28}H_{48}O_6P_2PtS_2$	$C_{50}H_{40}O_4P_2PtS_2$
Formula weight	753.73	801.81	1025.97
Crystal Size (mm^3)	0.20 X 0.20 X 0.10	0.10 X 0.10 X 0.05	0.08 X 0.03 X 0.02
Diffractometer	RIGAKU AFC7S	RIGAKU AFC7S	BRUKER GADDS
T/K	298	298	110.15
λ/Å	0.71069	0.71069	1.54178
Crystal system	Triclinic	Monoclinic	Triclinic
Space group	P-1	P $2_1/c$	P-1
a/Å	7.694(7)	12.675(4)	10.8776(4)
b/Å	8.820(6)	10.199(4)	18.0407(6)
c/Å	13.924(6)	14.263(4)	24.6712(9)
$\alpha/^o$	89.42(5)	90	81.901(2)
$\beta/^0$	83.80(4)	113.13(2)	83.211(2)
$\gamma/^0$	78.41(4)	90	84.888(2)
$V/Å^3$	920.2(11)	1707.7(10)	4746.6(3)
μ_{calc}, g cm^{-3}	1.360	1.559	1.436
Z	1	2	4
μ/mm^{-1}	4.040	4.360	7.318
Reflections collected	5150	4702	74601
Data/restraints/parameters	4211/0/173	3925/0/184	13777/67/1053
Final R1,*w*R2 indices	0.0796, 0.1700	0.0511, 0.0861	0.0518, 0.1271
R_1, wR_2 (all data)	0.2223, 0.2580	0.1107, 0.1596	0.0643, 0.1330
Largest diff.peak & hole [eÅ $^{-3}$]	1.365 and -2.204	1.184 and -1.767	2.955 and -1.438

Table 7. Crystallographic and structure refinement data for dinuclear mercaptobenzoic acid complexes of palladium and platinum.

Compound	$[Pt(SC_6H_4COOH\text{-}3)(PEt_3)_2]_2$ $(OTf)_2$	$[Pt(SC_6H_4COOH\text{-}4)(PEt_3)_2]_2$ $(OTf)_2\cdot(H_2O)_2$	$[Pd(SC_6H_4COOH\text{-}3)(dppe)]_2$ $.(OTf)_2\cdot(H_2O)_2$
Chemical formula	$C_{20}H_{36}F_3O_5P_2PtS_2$	$C_{40}H_{74}F_6O_{12}P_4Pt_2S_4$	$C_{68}H_{62}F_6O_{12}P_4Pd_2S_4$
Formula weight	733.63	1503.29	1650.10
Crystal Size (mm^3)	0.06 X 0.04 X 0.03	0.18 X 0.05 X 0.04	0.30 x 0.15 x 0.15
Diffractometer	BRUKER GADDS	BRUKER APEX 2	RIGAKU AFC7S
T/K	110(2)	110(2)	298
λ/Å	1.54178	0.71073	0.71069
Crystal system	Triclinic	Triclinic	Triclinic
Space group	P-1	P-1	P-1
a/Å	11.4772(19)	11.117(4)	11.175(3)
b/Å	11.5470(18)	15.396(5)	12.647(4)
c/Å	12.838(2)	17.488(6)	13.273(6)
$\alpha/^o$	65.338(8)	83.270(4)	79.42(3)
$\beta/^0$	73.374(8)	77.901(4)	70.60(3)
$\gamma/^0$	74.230(8)	71.860(4)	85.66(3)
V/Å^3	1458.7(4)	2776.9(16)	1739.1(11)
ρ_{calc}, g cm^{-3}	1.670	1.798	1.576
Z	2	2	1
μ/mm^{-1}	11.783	5.371	0.805
Reflections collected	22063	37046	9570
Data/restraints/parameters	4081 / 35 / 298	12542 / 250 / 690	7965/18/432
Final R1,*w*R2 indices	0.0370, 0.0950	0.0257, 0.0546	0.0760, 0.2043
R_1, wR_2 (all data)	0.0419, 0.0979	0.0318, 0.0570	0.1757, 0.2565
Largest diff.peak & hole [eÅ $^{-3}$]	1.477 and -1.572	1.258 and -0.998	1.355 and -1.476

Table 8. Crystallographic and structure refinement data for palladium complexes

Compound	$[Pd_2(SC_6H_4S)(dppe)_2]_2(OTf)_4 \cdot 0.36CH_2Cl_2$	$[Pd_2(SC_{12}H_8S)(dppe)_2]_2(OTf)_4$	$[Pd_2(SCH_2C_6H_4CH_2S)(dppe)_2]_4(OTf)_8 \cdot (CH_3COCH_3)_2$	$[Pt_2(SC_6H_4S)(PEt_3)_4]_2(OTf)_4 \cdot (CH_2Cl_2)_2$
Chemical formula	$C_{120}H_{104}F_{12}O_{12}P_8Pd_4S_8$ $.0.36CH_2Cl_2$	$C_{132}H_{112}F_{12}O_{12}P_8Pd_4S_8$	$C_{250}H_{236}F_{12}O_{14}P_{16}Pd_8S_{12}$	$C_{66}H_{136}Cl_8F_6O_6P_8Pt_4S_6$
Formula weight	2926.61	3048.05	5423.81	2643.83
Crystal Size (mm^3)	0.21 x 0.17 x 0.03	0.26 x 0.26 x 0.15	0.48 x 0.14 x 0.08	0.50 x 0.20 x 0.10
Diffractometer	BRUKER APEX 2	BRUKER APEX 2	BRUKER APEX 2	Rigaku AFC7S
T/K	110.15	110.15	110.15	298
λ/Å	0.71073	0.71073	0.71073	0.71069
Crystal system	Triclinic	Triclinic	Triclinic	Triclinic
Space group	P-1	P-1	P-1	P-1
a/Å	13.145(2)	14.619(3)	17.2155(16)	12.323(4)
b/Å	14.789(3)	14.797(3)	21.975(2)	13.000(6)
c/Å	16.778(3)	18.150(3)	22.457(2)	18.163(8)
α/°	79.21(5)	92.291(2)	61.808(10)	73.35(4)
β/°	85.46(4)	113.233(2)	71.330(10)	83.01(3)
γ/°	70.71(4)	91.287(2)	68.640(2)	88.12(4)
V/Å^3	3023.6(10)	3601.6(11)	6859.3(11)	2766.9(19)
ρ_{calc}, g cm^{-3}	1.607	1.405	1.313	1.587
Z	1	1	1	1
μ/mm^{-1}	0.924	0.766	0.757	5.509
Reflections collected	34721	40761	127933	3812
Data/restraints/parameters	13475/0/766	16120/516/939	31331/0/1407	3489/0/209
Final R1,*w*R2 indices	0.0270, 0.0600	0.0466, 0.1257	0.0533, 0.1143	0.0768, 0.2243
R_1, wR_1 (all data)	0.0338, 0.0639	0.0579, 0.1359	0.0724, 0.1256	0.0944, 0.2130
Largest diff.peak & hole [eÅ]$^{-3}$	0.666 and – 0.516	3.049 and –1.179	2.138 and –1.690	1.953 & –2.708

Table 9. Crystallographic and structure refinement data for palladium and platinum complexes

Compound	$[Pd_3(\mu\text{-}Te)_2(dppe)_3)](OTf)_2$	$[Pt\{(C_5H_4N\text{-}4,4)_2Te_2\}(PEt_3)_2]_2(OTf)_4.3.75H_2O$
Chemical formula	$C_{80}H_{72}F_6O_6P_6Pd_3S_2Te_2$	$C_{48}H_{83.50}F_{12}N_4O_{15.75}P_4Pt_2S_4Te_4$
Formula weight	2067.71	2349.39
Crystal Size (mm^3)	0.13 × 0.05 × 0.02	0.13 X 0.06 X 0.05
Diffractometer	BRUKER GADDS	BRUKER APEX 2
T/K	110	150(2)
λ/Å	1.54178	0.71073
Crystal system	Orthorhombic	Monoclinic
Space group	P*bca*	P2
a/Å	22.6715(9)	9.437(2)
b/Å	18.0553(7)	34.224(7)
c/Å	38.3415(16)	12.002(3)
$\alpha/^{o}$	90	90
$\beta/^{0}$	90	93.226(3)
$\gamma/^{0}$	90	90
V/Å^3	15694.7(11)	3870.0(14)
ρ_{calc}, g cm^{-3}	1.750	2.016
Z	8	2
μ/mm^{-1}	13.450	5.365
Reflections collected	95758	45300
Data/restraints/parameters	11873 / 0 / 946	17475/1/867
Final R1,*w*R2 indices	0.0407, 0.0936	0.0541, 0.1113
R_1, wR_2 (all data)	0.0536, 0.0999	0.0653, 0.1176
Largest diff. peak & hole [eÅ^{-3}]	1.000 and -1.154	1.813 and -1.181

Table 10. Crystallographic and structure refinement data for palladium and platinum 4-pyridyl selenolate complexes

Compound	$[Pt(SeC_5H_4N\text{-}4)(dppe)]_2(BPh_4)_2 .4CH_2Cl_2$	$[Pt(SeC_5H_4N\text{-}4)(PEt_3)_2]_2(BPh_4)_2$
Chemical formula	$C_{114}H_{104}B_2Cl_8N_2P_4Pt_2Se_2$	$C_{82}H_{108}B_2N_2P_4Pt_2Se_2$
Formula weight	2479.19	1815.3
Crystal Size (mm^3)	0.16 × 0.14 × 0.06	0.05 × 0.05 × 0.05
Diffractometer	BRUKER APEX 2	RIGAKU AFC7S
T/K	150.15	298(2)
λ/Å	0.71073	0.71069
Crystal system	Triclinic	Monoclinic
Space group	P-1	C_2/m
a/Å	11.5598(19)	22.000(5)
b/Å	15.143(2)	18.012(4)
c/Å	15.801(3)	10.9961(18)
$\alpha/^o$	86.121(2)	90
$\beta/^0$	72.408(2)	109.450(17)
$\gamma/^0$	84.689(2)	90
V/Å^3	2622.9(7)	4108.7(15)
ρ_{calc}, g cm^{-3}	1.570	1.467
Z	1	2
μ/mm^{-1}	3.672	4.406
Reflections collected	48285	4763
Data/restraints/parameters	11872 / 7 / 602	4763 / 0 / 149
Final R1,*w*R2 indices	0.0365, 0.0745	0.0560, 0.1324
R_1, wR_2 (all data)	0.0503, 0.0819	0.3094, 0.1324
Largest diff. peak & hole [eÅ $^{-3}$]	2.113 and -2.661	1.018 and -2.322

Table 11. Crystallographic and structure refinement data for palladium and platinum tellurolate complexes

Compound	$[Pd(TeC_5H_4N\text{-}4)_2(dppe)]$	$[Pt(TeC_5H_4N\text{-}4)_2(dppe)]$	$[Pt\{PPh_2C(TeC_5H_4N\text{-}4)PPh_2\}_2]$	$[Pd_2(\mu\text{-}Te)(\mu\text{-}TeC_5H_4N\text{-}4)(TeC_5H_4N\text{-}4)(dppm)]_2$	$[PdCl\,(TeC_5H_4N\text{-}4)_2(PPh_3)]_2$
Chemical formula	$C_{36}H_{32}N_2P_2PdTe_2$	$C_{36}H_{32}N_2P_2PdTe_2$	$C_{60}H_{48}N_2P_4PtTe_2$	$C_{70}H_{60}N_4P_4Pd_4Te_6$	$C_{48.68}H_{43.37}Cl_{7.37}N_2P_2Pd_2Te_2$
Formula weight	916.17	1004.86	1371.17	2272.30	1447.54
Crystal Size (mm^3)	0.15 × 0.05 × 0.02	-	0.20 × 0.10 × 0.05	0.30 × 0.15 × 0.05	0.08 × 0.06 × 0.02
Diffractometer	RIGAKU AFC7S	RIGAKU AFC7S	RIGAKU AFC7S	RIGAKU AFC7S	BRUKER GADDS
T/K	298(2)	293(2)	298(2)	298(2)	110(2)
λ/Å	0.71069	0.71069	0.71069	0.71069	1.54178
Crystal system	Monoclinic	Monoclinic	Monoclinic	Triclinic	Monoclinic
Space group	C_2/c	C_2/c	C_2/c	P-1	P 21/n 1
a/Å	33.748(5)	33.927(15)	22.800(4)	13.808(3)	17.3108(6)
b/Å	9.4115(14)	9.3843(18)	13.403(3)	17.782(5)	16.1040(6)
c/Å	22.785(4)	22.798(8)	23.477(8)	18.461(5)	19.9246(8)
$\alpha/^o$	90	90	90	84.02(2)	90
$\beta/^0$	99.580(2)	100.04(3)	121.48(2)	72.93(2)	108.131(3)
$\gamma/^0$	90	90	90	84.14(2)	90
V/Å^3	7136.1(19)	7147(4)	6118(3)	4297.4(19)	5278.6(4)
ρ_{calc}, g cm^{-3}	1.706	1.868	1.489	1.756	1.821
Z	8	8	4	2	4
μ/mm^{-1}	2.239	5.643	3.368	2.930	18.329
Reflections collected	8186	10944	7020	19826	116877
Data/restraints/parameters	8186 / 0 / 389	8189/ 48/ 388	7020 / 0 / 253	19826 / 432 / 649	7865 / 93 / 602
Final R1,*w*R2 indices	0.1082, 0.2674	0.0999, 0.2054	0.0660, 0.1602	0.1106, 0.2816	0.0668, 0.1523
R_1, wR_2 (all data)	0.3007, 0.3404	0.3402, 0.3064	0.1612, 0.1878	0.3628, 0.4099	0.0752, 0.1579
Largest diff.peak & hole [eÅ^{-3}]	2.995 and -2.159	3.378 and -3.876	1.168 and -1.338	1.730 and -2.680	2.464 and -1.158

2.3 Catalysis

In a typical experiment, a two-necked round bottomed flak under a nitrogen atmosphere was charged with dioxane (3 ml), aryl halide (1.0 mmol), arylboronic acid (1.3 mmol), aqueous base (2.0 mmol, 1 mL) and a catalyst (0.1 mol%). The reactants were refluxed with stirring for a specified time. After cooling the reaction mixture to room temperature, the contents were diluted with water (10 ml), neutralized with dil. HCl and extracted with hexane (3 × 15 mL). The whole organic extract was washed with water (2 × 15 mL), brine (2 × 10 mL), dried over anhydrous Na_2SO_4, filtered and the solvent was removed under reduced pressure. The products were characterized by ^1H and $^{13}C\{^1H\}$ NMR spectra. In case of any contamination with other impurities, the product was chromatographed on a silica gel column to give the pure product.

2.4 Syntheses of ligands and metal precursors

2.4.1 Synthesis of ligands

4, 4'-Dipyridyldiselenide [$Se_2(C_5H_4N\text{-}4,4')_2$]

i) To an ethoxy ethanol solution (500 mL) of Na_2Se_2 [prepared by reduction of selenium (20 g, 253 mmol) with $NaBH_4$ (11.5 g, 304 mmol) over a period of 1 h] was added dropwise an aqueous solution (50 mL) of 1-(4-pyridyl)pyridinium chloride hydrochloride (57.3 g, 250 mmol) and the reaction mixture was stirred for 15 h at room temperature. The solution was concentrated to 100 mL and aq. Na_2CO_3 (75 g, 707 mmol) was added and stirred for 0.5 h. The reaction solution was shaken with toluene and the aqueous layer was filtered and kept for aerial oxidation for two days. The yellowish brown solid that formed was separated and extracted with THF and concentrated. To this, toluene was added and kept for recrystallization at –5 °C. A yellowish orange solid was dissolved in chloroform, filtered through Celite and kept at –5 °C to yield yellow crystals of the title compound in 42% yield [148]. M.p.113 ^{o}C. Anal. Calcd for $C_{10}H_8N_2Se_2$: C, 38.24; H, 2.57; N, 8.92%; Found: C, 38.27; H, 2.46; N, 9.12%. ^1H NMR ($CDCl_3$) δ: 7.47 (d, $^3J_{HH}$ = 4.5 Hz, 4H, 3,5-H); 8.42 (d, $^3J_{HH}$ = 4.5 Hz, 4H, 2,6-H) ppm.$^{13}C\{^1H\}$ NMR ($CDCl_3$) δ: 124.2 (s, C-3), 140.9 (s, C-4), 150.1 (s, C-2) ppm. $^{77}Se\{^1H\}$ NMR ($CDCl_3$) δ: 409 (s)ppm. ESI-MS m/z (ion, relative intensity): 317 ($[M+H]^+$, 100), 237 ($[M+H+Se]^+$, 15).

4, 4'-Dipyridylselenide [$Se(C_5H_4N\text{-}4,4')_2$]

To a suspension of selenium powder (1.015 g, 27.03 mmol) in water (100 ml), sodium borohydride ($NaBH_4$) (1.02 g, 12.85 mmol) was added at 5-10 °C with constant stirring. To the obtained colorless solution of NaHSe, ethanolic solution of 4-bromopyridine (4.99 g, 25.7 mmol) was added dropwise with stirring and was refluxed for 4 hrs, where upon a pale yellow precipitate formed. After cooling, the reaction mixture was extracted with hexane (3 x

50 ml) and the organic part was dried over anhydrous sodium sulphate, which was finally concentrated to give pale yellow needle like crystals of 4, 4'-dipyridylselinide (0.84 g, 28 %). M.p. 63 °C. Anal. Calcd. for $C_{10}H_8N_2Se$: C, 51.08; H, 3.43; N, 11.91; Found: C, 51.48; H, 3.34; N, 4.2 %. ^1H NMR ($CDCl_3$) δ: 7.32 (d, $^3J_{HH}$ = 4.5 Hz, 4H, 3,5-H), 8.47 (d, $^3J_{HH}$ = 6.0 Hz, 4H, 2,6-H); $^{13}C\{^1H\}$ NMR ($CDCl_3$) δ: 127.0 (s, C-3), 140.2 (s, C-4), 150.2 (s, C-2); $^{77}Se\{^1H\}$ NMR ($CDCl_3$) δ: 430 (s) ppm.

4, 4'-Dipyridylditelluride [$Te_2(C_5H_4N\text{-}4,4')_2$]

(a) 4-Bromopyridine (7.32 g, 46.3 mmol) was added drop wise to a vigorously stirred mixture of isopropylmagnesium chloride (5.0 g, 48.6 mmol) in THF. After stirring for 2h at room temperature the mixture was cooled in an ice bath and tellurium powder (6.18 g, 48.6 mmol) was added. After all the tellurium had dissolved, stirring was stopped and dilute nitric acid (~1M, 40 mL) was added slowly. The mixture was extracted with ethylacetate (4 × 150 ml) and the organic layer was dried over anhydrous sodium sulfate. The solvent was removed under vacuum and the residue was purified by silica gel column chromatography with hexane/ethyl acetate (5:1) as eluent. After TLC assessment, the solvents were evaporated under vaccum to give a reddish brown powder. The latter was thoroughly washed with hot hexane (3 × 10 mL) so as to remove any monotelluride. The residue was recrystallized from methanol as reddish-brown needles (1.7 g, 18% yield).

(b) Since the yield of 4,4'-py_2Te_2 from the above method was rather poor another method described in literature was attempted after modification [149]. To a clear colorless solution of NaTeH [prepared by reduction of tellurium (4.91g, 38.5 mmol) in refluxing alkaline ethanol (NaOH, 1.54 g, 38.5 mmol in 500 mL EtOH) by $NaBH_4$ (9.6 g, 254 mmol) for 1 hr] ethanolic solution of 4-pyBr.HCl (15.0 g, 77.12 mmol) was added and the contents were refluxed with stirring for 30 hrs. The contents were transferred into a beaker for areal oxidation followed by addition of an aqueous solution of $K_3Fe(CN)_6$. The product was extracted with chloroform (3 × 100 mL), the combined extracts were dried over anhydrous sodium sulfate for 1 hr. The solution was filtered and dried under vaccum. The residue was washed thoroughly with hot hexane (3 × 20 mL) and recrystallized from methanol (yield 2.0 g, 25% based on tellurium).

The title compound prepared from the above two methods showed identical m. p. and NMR spectra. M.p.121^{o}C (dec). Anal. Calcd for $C_{10}H_8N_2Te_2$: C, 29.20; H, 1.96; N, 6.81 %; Found: C, 28.33; H, 1.47; N, 0.00 %. ^{1}H NMR (acetone-d_6) δ: 7.82 (dd, 1.6, 4.4 Hz, 4H), 8.28 (dd, 1.6, 4.4 Hz, 4H)ppm. ^{13}C{^{1}H} NMR (acetone-d_6) δ: 118.4 (Te-C), 130.8, 148.9 ppm. ^{125}Te{^{1}H} NMR (acetone-d_6) δ: 370 (s).

2.4.2 Synthesis of metal precursors

$Na_2[PdCl_4]$ [150], $K_2[PtCl_4]$ [151] and other phosphine complexes were prepared according to literature methods.

[MCl$_2$(P$^\frown$P)]

Complexes were prepared according to reported literature methods [152]. To an aqueous solution of Na_2PdCl_4 (0.89 g, 2.3 mmol) was added a solution of dppm (0.90 g, 2.3 mmol) in methanol and stirred for 3 h whereupon an off-white precipitate was formed. The precipitate was filtered, washed thoroughly with water and cold acetone followed by diethyl ether and dried under reduced pressure. Similar procedure was employed for other phosphines, viz. dppe and dppp. Similarly, [$PtCl_2$(dppm)] was prepared by adding a solution of dppm (0.31 g, 0.81 mmol) in methanol to an aqueous solution of K_2PtCl_4 (0.34 g, 0.82 mmol), and stirred for 3 h whereupon a white precipitate was obtained. The precipitate was filtered, washed successively with water and ether and dried under vacuum. Similarly $PtCl_2$(dppe) and $PtCl_2$(dppp) were prepared. Pertinent data are summarized in Table 12.

[Pt(PPh$_3$)$_4$]

To an aqueous ethanolic reaction mixture of $K_2[PtCl_4]$ (450 mg, 11 mmole) and PPh_3 (1.42 g, 54 mmole), an aqueous solution of $NaBH_4$ (123 mg, 32 mmole) was added with stirring which continued for 3h at room temperature whereupon a yellow precipitate formed. The latter was filtered, washed thoroughly with ethanol, cold water and warm ethanol to yield a yellow powder of $[Pt(PPh_3)_4]$ [153].

Table 12. Physical, analytical and NMR data of various platinum(II) and palladium(II) phosphine precursors

Complex	Recrystallization Solvent (% Yield)	Color	m.p. (^{o}C)	% Analysis Found (calcd.)		$^{31}P\{^{1}H\}$NMR in $CDCl_3$ δ[^{1}J(Pt-P) in Hz]
				C	H	
[$PtCl_2(PPh_3)_2$]	Chloroform (72)	White	310	54.69 (54.69)	3.80 (3.82)	14.4 [^{1}J(Pt-P) = 3678]
[$PtCl_2$(dppm)]	Chloroform (78)	White	330	45.88 (46.17)	3.32 (3.41)	–64.4 [^{1}J(Pt-P) = 3087]
[$PtCl_2$(dppe)]	Chloroform (82)	White	290	47.09 (47.00)	3.64 (3.64)	41.3 [^{1}J(Pt-P) = 3605]
[$PtCl_2$(dppp)]	Chloroform (60)	Pale flesh	230	48.00 (47.80)	3.78 (3.86)	–5.6 [^{1}J(Pt-P) = 3420]
[$PdCl_2(PPh_3)_2$]	Chloroform (69)	Yellow	270	61.60 (61.60)	4.54 (4.31)	23.1
[$PdCl_2$(dppm)]	Chloroform (63)	Cream	340	53.41 (53.46)	3.95 (3.95)	–54.2
[$PdCl_2$(dppe)]	Chloroform (90)	Pale buff	360	54.21 (54.24)	4.07 (4.20)	64.2
[$PdCl_2$(dppp)]	Chloroform (58)	White	>360	54.89 (54.99)	4.32 (4.44)	11.5

2.5 Synthesis of 4-pyridylselenolate complexes of palladium and platinum

[PdCl$_2${4,4'-(C$_5$H$_4$N)$_2$Se$_2$}]

(i) A methanolic solution (8 mL) of Na$_2$PdCl$_4$ (236 mg, 0.802 mmol) was added to a methanolic solution (10 mL) of 4,4'-(C$_5$H$_4$N)$_2$Se$_2$ (252 mg, 0.802 mmol) with stirring which continued for 5 h at room temperature. The yellow suspension was filtered through a G3 assembly and washed thoroughly with water, acetone and diethyl ether and dried under vaccum to yield [PdCl$_2${4,4'-(C$_5$H$_4$N)$_2$Se$_2$}] (324 mg, 0.659 mmol, 82%).

(ii) A dichloromethane solution (8 mL) of [PdCl$_2$(PhCN)$_2$] (122 mg, 0.318 mmol) was added to a dichloromethane solution (10 mL) of 4,4'-(C$_5$H$_4$N)$_2$Se$_2$ (108 mg, 0.344 mmol) with stirring which continued for 4 h whereupon a yellow suspension formed. The latter was filtered through a G3 assembly and washed thoroughly with methanol, acetone, and diethyl ether and dried (66 mg, 0.133 mmol, 42%).

Similarly the platinum analog, [PtCl$_2${4,4'-(C$_5$H$_4$N)$_2$Se$_2$}] was prepared by using [PtCl$_2$(PhCN)$_2$] and 4,4'-(C$_5$H$_4$N)$_2$Se$_2$ in 68% yield.

[Pd(SeC$_5$H$_4$N-4)$_2$]$_n$

A methanolic solution (10 mL) of Na$_2$PdCl$_4$ (360 mg, 1.224 mmol) was added to a freshly prepared methanolic solution (15 mL) of Na(SeC$_5$H$_4$N-4) (prepared from 4,4'-(C$_5$H$_4$N)$_2$Se$_2$ (398 mg, 1.267 mmol) and NaBH$_4$ (98 mg, 2.58 mmol)) with stirring which continued for 4 h at RT whereupon a dark brown precipitate formed. The latter was filtered through a G3 assembly and washed with water, acetone and diethyl ether and dried in *vacuo* (460 mg, 1.094 mmol, 89%).

$[PdCl(SeC_5H_4N\text{-}4)]_n$

Prepared similar to the above from Na_2PdCl_4 (428 mg, 1.455 mmol) and $Na(SeC_5H_4N\text{-}4)$ (prepared from $4,4'\text{-}(C_5H_4N)_2Se_2$ (229 mg, 0.729 mmol) and $NaBH_4$ (56 mg, 1.475 mmol)) in 1:1 ratio in methanol and isolated as a dark brown powder (380 mg, 1.271 mmol, 88%).

***trans*-$[PdCl(SeC_5H_4N\text{-}4)(PPh_3)_2]$**

A dichloromethane solution (10 mL) of PPh_3 (1.02 g, 3.89 mmol) was added to a dichloromethane suspension (15 mL) of $[PdCl(SeC_5H_4N\text{-}4)]_n$ (573 mg, 1.920 mmol) with stirring which continued for 6 h at room temperature. The solvent was evaporated *in vacuo*, the pink residue was washed with diethyl ether, extracted with acetone (3 × 5 mL) and filtered. The filtrate was reduced to a minimum volume of (5 mL), to yield pink crystals of the title complex (671 mg, 0.081 mmol, 43%).

***trans*-$[PtCl(SeC_5H_4N\text{-}4)(PEt_3)_2]$**

To a $CDCl_3$ solution (0.5 mL) of $[Pt(SeC_5H_4N\text{-}4)_2(PEt_3)_2]$ (30 mg, 0.04 mmol) was added $PtCl_2(PEt_3)_2$ (20 mg, 0.04 mmol) in an NMR tube and the formation of *trans*-$[PtCl(SeC_5H_4N\text{-}4)(PEt_3)_2]$ was monitored by ^{31}P NMR spectroscopy The redistribution reaction took 5 days for completion. The contents of the NMR tube were transferred into a flask and the solvent was evaporated *in vacuo*, the yellow residue was washed with hexane and diethyl ether and recrystallized from a CH_2Cl_2/ hexane mixture to yield pale yellow crystals of the title complex (15 mg, 0.024 mmol, 30%). A small amount ~5% of $PtCl_2(PEt_3)_2$ and $[Pt(SeC_5H_4N\text{-}4)_2(PEt_3)_2]$ existed in solution (by ^{31}P and ^{195}Pt NMR) even after 20 days of monitoring the reaction.

***trans*-[Pd(SeC_5H_4N-4)$_2$(PPh_3)$_2$]**

To an acetone (10 mL) suspension of [Pd(SeC_5H_4N-4)$_2$]$_n$ (50 mg, 0.119 mmol) PPh_3 (63 mg, 0.240 mmol) was added with stirring. The whole was stirred at RT for 4 h whereupon a brownish red solution formed which was dried *in vacuo*. The residue was washed with hexane and recrystallized from an acetone/hexane mixture to yield the title complex (38 mg, 0.04 mmol, 34%).

***trans*-[Pt(SeC_5H_4N-4)$_2$(PPh_3)$_2$]**

(i) To a stirred dichloromethane solution of [Pt(PPh_3)$_4$] (330 mg, 0.265 mmol) was added a solution (8 mL) of 4,4'-(C_5H_4N)$_2Se_2$ (84 mg, 0.267 mmol) dropwise and further stirred for 3 h. The solvent was evaporated *in vacuo*, the yellow residue was washed with hexane and diethyl ether, extracted with dichloromethane (3 × 5 mL) and filtered. The filtrate was reduced (5 mL) which on cooling gave yellow crystals of the title complex (98 mg, 0.095 mmol, 36%).

(ii) A dichloromethane solution (8 mL) of [$PtCl_2$(PPh_3)$_2$] (78 mg, 0.099 mmol) was added to a freshly prepared methanolic solution (15 mL) of Na(SeC_5H_4N-4) (prepared from 4,4'-(C_5H_4N)$_2Se_2$ (32 mg, 0.102 mmol) and $NaBH_4$ (8 mg, 0.210 mmol)) with stirring. The yellow solution was stirred for 4 h at room temperature. The solvents were evaporated *in vacuo*, the yellow residue was washed with hexane and diethyl ether, extracted with dichloromethane (3 × 5 mL) and filtered. The filtrate was concentrated to 5 mL which on cooling afforded yellow crystals of the title complex (88 mg, 0.085 mmol, 86%) and the NMR data are consistent with the sample prepared from (i) above. However, the sample was contaminated by ~5% impurities (δ ^{31}P 21.7 and 17.9 ppm).

***trans*-[Pt(SeC_5H_4N-4)$_2$(PEt_3)$_2$]**

Prepared similar to the above method (ii) employing [$PtCl_2(PEt_3)_2$] (150 mg, 0.299 mmol) and (15 mL) of Na(SeC_5H_4N-4) (from 4,4'-(C_5H_4N)$_2$$Se_2$ (97 mg, 0.308 mmol) and $NaBH_4$ (25 mg, 0.658 mmol)) as a pale yellow crystalline solid (186 mg, 0.249 mmol, 83%); (ii) A similar reaction between *cis*-[Pt(OTf)$_2$(PEt_3)$_2$] and Na(SeC_5H_4N-4) as starting material gave *trans*-[Pt(SeC_5H_4N-4)$_2$(PEt_3)$_2$] in 41% yield.

[Pd(SeC_5H_4N-4)$_2$(dppe)]

A dichloromethane solution (8 mL) of [$PdCl_2$(dppe)] (124 mg, 0.215 mmol) was added to a methanolic solution (15 mL) of Na(SeC_5H_4N-4) (from 4,4'-(C_5H_4N)$_2$$Se_2$ (70 mg, 0.222 mmol) and $NaBH_4$ (18 mg, 0.474 mmol) with stirring. After 5 hours of stirring, solvents were evaporated *in vaccuo* and the residue was extracted with dichloromethane (3 × 7 mL) and the extract was passed through a florisil column. The solvent was evaporated *in vacuo*, the residue was washed with hexane (2 mL) and recrystallized from an acetone/ hexane mixture to yield yellow crystals of [Pd(SeC_5H_4N-4)$_2$(dppe)] (136 mg, 0.166 mmol, 77%). The complexes [Pt(SeC_5H_4N-4)$_2$(dppm)] and [Pt(SeC_5H_4N-4)$_2$(dppp)] were analogously prepared with 41% and 85% yields, respectively.

[PdCl(SeC_5H_4N-4)(PEt_3)]$_n$

A dichloromethane solution (8 mL) of [Pd_2Cl_2(μ-Cl)$_2$(PEt_3)$_2$] (96 mg, 0.162 mmol) was added to a stirred methanolic solution (15 mL) of Na(SeC_5H_4N-4) (prepared from 4,4'-(C_5H_4N)$_2$$Se_2$ (53 mg, 0.169 mmol) and $NaBH_4$ (13 mg, 0.342 mmol)). After 5 h of stirring, solvents were evaporated *in vacuo* and the residue was extracted with dichloromethane and passed through a florisil column. The solvent was evaporated *in vacuo,* the residue was washed with hexane and recrystallized from a CH_2Cl_2/ hexane mixture (122 mg, 0.097 mmol, 93%). The complexes [PdCl(SeC$_5$H$_4$N-4)(PPh$_3$)]$_n$, PtCl(SeC$_5$H$_4$N-4)(PEt$_3$)]$_n$ and [PtCl(SeC$_5$H$_4$N-4)(PMe$_2$Ph)]$_n$ were prepared similarly with 55%, 77%, 42% yields, respectively. Pertinent data are given in Table 13.

Table 13. Physical and analytical data of palladium and platinum 4-pyridylselenolate complexes

Complex	Recrystallization solvent	m.p. (°C)	% Analysis Found (Calcd.)		
			C	H	N
[PdCl$_2${4,4'-(C$_5$H$_4$N)$_2$Se$_2$}]	-	> 230	24.40	1.84	5.51
			(24.44)	(1.64)	(5.70)
[PtCl$_2${4,4'-(C$_5$H$_4$N)$_2$Se$_2$}]	-	> 230	21.54	1.33	4.59
			(20.71)	(1.39)	(4.83)
[Pd(SeC$_5$H$_4$N-4)$_2$]$_n$	-	> 230	27.92	2.12	6.46
			(28.56)	(1.92)	(6.66)
[PdCl(SeC$_5$H$_4$N-4)]$_n$	-	> 230	19.83	1.16	4.48
			(20.09)	(1.35)	(4.69)
trans-[PdCl(SeC$_5$H$_4$N-4)(PPh$_3$)$_2$]	Acetone	143	60.35	4.36	1.50
			(59.80)	(4.16)	(1.70)
trans-[PtCl(SeC$_5$H$_4$N-4)(PEt$_3$)$_2$]	Dichloromethane-	175	31.59	4.18	2.04
	Hexane		(32.72)	(5.49)	(2.24)
trans-[Pd(SeC$_5$H$_4$N-4)$_2$(PPh$_3$)$_2$]	Acetone-Hexane	150	57.82	3.86	2.76
			(58.46)	(4.05)	(2.96)
trans-[Pt(SeC$_5$H$_4$N-4)$_2$(PPh$_3$)$_2$]	Dichloromethane	212	53.57	3.81	2.91
			(53.45)	(3.71)	(2.71)
trans-[Pt(SeC$_5$H$_4$N-4)$_2$(PEt$_3$)$_2$]	Dichloromethane	157	34.95	5.34	3.55
			(35.44)	(5.14)	(3.76)
[Pd(SeC$_5$H$_4$N-4)$_2$(dppe)]	Acetone-Hexane	157	52.02	4.28	3.62
			(52.80)	(3.94)	(3.42)
[Pt(SeC$_5$H$_4$N-4)$_2$(dppm)]	Acetone-Hexane	155	46.43	3.20	3.18
			(47.04)	(3.38)	(3.13)
[Pt(SeC$_5$H$_4$N-4)$_2$(dppp)]	Acetone-Hexane	160	48.03	3.72	2.96
			(48.22)	(3.72)	(3.04)
[PdCl(SeC$_5$H$_4$N-4)(PEt$_3$)]$_n$	Dichloromethane-	200	31.82	4.78	3.18
	Hexane		(31.68)	(4.59)	(3.36)
[PdCl(SeC$_5$H$_4$N-4)(PPh$_3$)]$_n$	Acetone-Hexane	191	48.72	3.38	2.40
			(49.22)	(3.41)	(2.50)
[PtCl(SeC$_5$H$_4$N-4)(PEt$_3$)]$_n$	Dichloromethane-	215	26.52	3.60	2.57
	Hexane		(26.12)	(3.79)	(2.77)
[PtCl(SeC$_5$H$_4$N-4)(PMe$_2$Ph)]$_n$	Dichloromethane-	187	30.30	3.09	2.87
	Hexane		(29.70)	(2.88)	(2.66)

2.6 Synthesis of 3-/4-mercaptobenzoic acid complexes of palladium and platinum

$[Pt(SC_6H_4COOH\text{-}4)_2(PEt_3)_2]$

(i) To a stirred methanolic solution (8 mL) of 4-H_2mba (42 mg, 0.274 mmol) methanolic NaOMe (1.1 mL, 0.548 mmol), a dichloromethane solution (8 mL) of $[Pt(PEt_3)_2(OTf)_2]$ (80 mg, 0.110 mmol) was added whereupon a yellow solution formed which was stirred for 14 h. The solvent was evaporated *in vacuo*, the yellow residue was washed with hexane and diethylether and extracted with methanol (2 × 5 mL). The volume of the solution was reduced to 5 mL, few drops of diethylether were added to yield pale yellow crystals of $[Pt(SC_6H_4COOH\text{-}4)_2(PEt_3)_2]$ (58 mg, 0.072 mmol, 65%).

(ii) To a methanolic solution (6 mL) of 4-H_2mba (51 mg, 0.329 mmol) and triethylamine (0.1 mL) was added a dichloromethane solution (8 mL) of $[Pt(PEt_3)_2Cl_2]$ (75 mg, 0.150 mmol). The yellow solution was stirred for 4 h. The solvent was evaporated *in vacuo*, the yellow residue was thoroughly washed with water and extracted with methanol (2 × 4 mL). The volume of the extract was minimized to 2 mL, few drops of diethylether was added to yield pale yellow crystals of $[Pt(SC_6H_4COOH\text{-}4)_2(PEt_3)_2]$ (78 mg, 0.097 mmol, 68%). The data matches with the data of the compound prepared above (i).

$[Pt(SC_6H_4COOH\text{-}3)(PEt_3)_2]_2(OTf)_2$

To a dichloromethane solution (8 mL) of $[Pt(PEt_3)_2(OTf)_2]$ (77 mg, 0.105 mmol), a solution of 3-H_2mba (34.0 mg, 0.220 mmol) in dichloromethane (10 mL) was added with stirring. Colourless solution was stirred for 14 h at room temperature. The solvent was evaporated *in vacuo* and the yellow residue was washed with ether and extracted with acetone (2 × 4 mL). The volume of the extract was minimized to 2 mL, few drops of hexane were added to yield off-white crystals of $[Pt(SC_6H_4COOH\text{-}3)(PEt_3)_2]_2(OTf)_2$ (Yield 128 mg, 0.087 mmol, 83%).

Similarly the complexes $[Pt(SC_6H_4COOH\text{-}4)(PEt_3)_2]_2\cdot(OTf)_2$, $[Pd(SC_6H_4COOH\text{-}3)(dppe)]_2(OTf)_2$, $[Pd(SC_6H_4COOH\text{-}4)(dppe)]_2(OTf)_2$ and $[Pt(SC_6H_4COOH\text{-}4)(dppp)]_2(OTf)_2$ were prepared analogously with 81, 71, 76 and 58%, respectively.

$[Pt(SC_6H_4COOH\text{-}4)_2(PPh_3)_2]$

Prepared similar to $[Pt(SC_6H_4COOH\text{-}4)_2(PEt_3)_2]$ as described in method (ii) under refluxing condition using $PtCl_2(PPh_3)_2$ as precursor to yield yellow crystals of the title complex (85 mg, 0.073 mmol, 79%).

$[Pt(SC_6H_4COOH\text{-}3)_2(dppm)]$

Prepared similar to $[Pt(SC_6H_4COOH\text{-}4)_2(PEt_3)_2]$ as described in method (ii) under refluxing condition using $PtCl_2(dppm)$ as precursor to yield dark yellow crystals of the title complex (198 mg, 0.193 mmol, 50%).

$[Pt(SC_6H_4COOH\text{-}4)_2(dppm)]$

Prepared similar to $[Pt(SC_6H_4COOH\text{-}4)_2(PEt_3)_2]$ as described in method (ii) under refluxing condition using $PtCl_2(dppm)$ as precursor to yield dark yellow crystals of title complex (163 mg, 0.159 mmol, 35%). Pertinent data are given in Table 14.

Table 14. Physical and analytical data of mercaptobenzoic acid complexes of palladium and platinum

Complex	Recrystallization solvent	m.p. (°C)	% Analysis Found (Calcd.) C	H	S
$[Pt(SC_6H_4COOH\text{-}4)_2(PEt_3)_2]$	Methanol-Ether	> 230 (dec)	39.87 (40.36)	5.52 (5.73)	8.11 (8.29)
$[Pt(SC_6H_4COOH\text{-}3)(PEt_3)_2]_2(OTf)_2$	Acetone-Hexane	> 230 (dec)	32.21 (32.74)	4.62 (4.81)	8.12 (8.74)
$[Pt(SC_6H_4COOH\text{-}4)(PEt_3)_2]_2.(OTf)_2$	Methanol-Ether	> 230 (dec)	31.81 (31.96)	4.76 (4.96)	8.23 (8.53)
$[Pd(SC_6H_4COOH\text{-}3)(dppe)]_2(OTf)_2$	Methanol-Ether	> 230 (dec)	48.14 (48.71)	3.25 (3.49)	8.34 (8.54)
$[Pd(SC_6H_4COOH\text{-}4)(dppe)]_2(OTf)_2$	Methanol-Ether	> 230 (dec)	48.80 (49.49)	3.56 (3.79)	7.60 (7.77)
$[Pt(SC_6H_4COOH\text{-}4)(dppp)]_2(OTf)_2$	Methanol-Ether	> 230 (dec)	47.23 (46.21)	3.77 (3.43)	7.13 (7.05)
$[Pt(SC_6H_4COOH\text{-}4)_2(PPh_3)_2]$	Methanol-Ether	> 230 (dec)	57.79 (57.80)	4.15 (4.85)	3.73 (5.51)
$[Pt(SC_6H_4COOH\text{-}3)_2(dppm)]$	Methanol-Ether	> 230 (dec)	53.25 (52.81)	4.81 (4.73)	5.86 (6.27)
$[Pt(SC_6H_4COOH\text{-}4)_2(dppm)]$	Methanol-Ether	> 230 (dec)	52.20 (52.81)	4.46 (4.73)	5.96 (6.27)

2.7 Synthesis of aryldithiolate complexes of palladium and platinum

$[Pd_2(S(C_6H_4)S)(dppe)_2]_2(OTf)_4$

To a methanolic solution (10 mL) of HSC_6H_4SH (6.7 mg, 0.047 mmol), added $[Pd(dppe)(OTf)_2]$ (75.6 mg, 0.094 mmol) in methanol (7 mL). The wine red solution was stirred for 6 h. The solvent was evaporated in vaccuo, the red residue was washed with ether and hexane and extracted with dichloromethane (5 mL). Few drops of hexane were added to yield orange crystals of the title complex (49.6 mg, 0.017 mmol, 72%).

$[Pd_2(S(C_{12}H_8)S)(dppe)_2]_2(OTf)_4$

Prepared similar to $[Pd_2(S(C_6H_4)S)(dppe)_2]_2(OTf)_4$ using $[Pd(dppe)(OTf)_2]$ (80.1 mg, 0.10 mmol) and $HSC_{12}H_8SH$ (11 mg, 0.05 mmol) and recrystallized from dichloromethane-hexane mixture to yield orange crystals of $[Pd_2(S(C_{12}H_8)S)(dppe)_2]_2(OTf)_4$ (51 mg, 0.017 mmol, 67%).

$[Pd_2(SCH_2(C_6H_4)CH_2S)(dppe)_2]_4(OTf)_8$

Prepared similar to $[Pd_2(S(C_{12}H_8)S)(dppe)_2]_2(OTf)_4$, using $[Pd(dppe)(OTf)_2]$ (76.1 mg, 0.095 mmol) and $HSCH_2C_6H_4CH_2SH$ (8.1 mg, 0.048 mmol) and recrystallized from acetone-hexane mixture to yield yellow crystals of $[Pd_2(SCH_2(C_6H_4)CH_2S)(dppe)_2]_4(OTf)_8$ (36.6 mg, 0.007 mmol, 52%).

$[Pt_2(S(C_6H_4)S)(PEt_3)_4]_2(OTf)_4$

To a methanolic solution (10 mL) of $[Pt(PEt_3)_2(OTf)_2]$ (70.5 mg, 0.097 mmol), added methanolic solution (7 mL) of HSC_6H_4SH (7.0 mg, 0.049 mmol) yellow solution was stirred for 8 h. The solvent was evaporated *in vaccuo*, the residue was washed with hexane and ether and extracted with dichloromethane (5 mL). Few drops of hexane were added to yield pale yellow crystals of $[Pt_2(S(C_6H_4)S)(PEt_3)_4]_2(OTf)_4$ (52.0 mg, 0.020 mmol, 83%).

$[Pt_2(S(C_{12}H_8)S)(PEt_3)_4]_2(OTf)_4$

Prepared similar to $[Pt_2(S(C_6H_4)S)(PEt_3)_4]_2(OTf)_4$, using $[Pt(PEt_3)_2(OTf)_2]$ (72.3 mg, 0.099 mmol) and $HSC_{12}H_8SH$ (11 mg, 0.05 mmol) and recrystallized from dichloromethane-hexane mixture to yield the title complex as a pale yellow solid (45 mg, 0.016 mmol, 66%).

$[Pt_2(S(CH_2C_6H_4CH_2)S)(PEt_3)_4]_4(OTf)_8$

Prepared similar to $[Pt_2(S(C_6H_4)S)(PEt_3)_4]_2(OTf)_4$, using $[Pt(PEt_3)_2(OTf)_2]$ (66.0 mg, 0.09 mmol) and $HSCH_2C_6H_4CH_2SH$ (7.8 mg, 0.046 mmol) and recrystallized from acetone-hexane mixture to yield the title complex as a colorless solid (38.5 mg, 0.007 mmol, 64%). Pertinent data are given in Table 15.

Table 15. Physical and analytical data of palladium and platinum arylthiolate complexes

Complex	Recrystallization solvent	m.p. (°C)	% Analysis Found (Calcd.) C	H	S
$[Pd_2(S(C_6H_4)S)(dppe)_2]_2(OTf)_4$	Dichloromethane-Hexane	> 230	49.72 (49.77)	3.53 (3.62)	9.46 (8.86)
$[Pd_2(S(C_{12}H_8)S)(dppe)_2]_2(OTf)_4$	Dichloromethane-Hexane	188	51.60 (52.01)	3.52 (3.70)	8.94 (8.42)
$[Pd_2(SCH_2(C_6H_4)CH_2S)(dppe)_2]_4(OTf)_8$	Acetone-Hexane	> 230	50.06 (50.45)	3.63 (3.82)	8.77 (8.69)
$[Pt_2(S(C_6H_4)S)(PEt_3)_4]_2(OTf)_4$	Dichloromethane-Hexane	210	30.08 (29.54)	4.78 (4.96)	9.72 (9.86)
$[Pt_2(S(C_{12}H_8)S)(PEt_3)_4]_2(OTf)_4$	Dichloromethane-Hexane	> 230	33.60 (33.14)	4.90 (4.98)	9.40 (9.31)
$[Pt_2(S(CH_2C_6H_4CH_2)S)(PEt_3)_4]_4(OTf)_8$	Acetone-Hexane	141	31.23 (30.72)	5.08 (5.16)	10.25 (9.65)

2.8 Synthesis of palladium and platinum complexes of hybrid nitrogen and organoselenium/tellurium donor ligands

[Pt {(4,4'-$C_5H_4N)_2Se_2$}($PEt_3)_2]_2(OTf)_4$

To a methanolic solution (10 mL) of [Pt($PEt_3)_2(OTf)_2$] (71.8 mg, 0.098 mmol) a solution (7 mL) of (4,4'-$C_5H_4N)_2Se_2$ (30.9 mg, 0.098 mmol) was added with stirring which continued for 5 h at room temperature. The solvent was evaporated *in vaccuo,* the pale yellow residue was washed with diethylether and hexane and the residue was extracted with methanol (5 mL) and recrystallized by diffusing slowly dry diethylether to yield pale yellow crystals of the title complex (95 mg, 93% yield).

[Pt{(4,4'-$C_5H_4N)_2Te_2$}($PEt_3)_2]_2(OTf)_4$

This was prepared similar to [Pt{(4,4'-$C_5H_4N)_2Te_2$}($PEt_3)_2]_2(OTf)_4$ using [Pt($PEt_3)_2(OTf)_2$] (54 mg, 0.074 mmol), and (4,4'-$C_5H_4N)_2Te_2$ (30.5 mg, 0.074 mmol) in methanol and recrystallized from methanol-diethylether mixture at -5 ^oC as a yellow crystalline solid (66 mg, 78% yield).

[Pd{(4,4'-$C_5H_4N)_2Se_2$}(dppe)$]_2(OTf)_4$

This was prepared in a similar mannaer to [Pt{(4,4'-$C_5H_4N)_2Se_2$}($PEt_3)_2]_2(OTf)_4$ by using [Pd(dppe)($OTf)_2$] (54.3 mg, 0.068 mmol) and 4,4'-py_2Se_2 (21.2 mg, 0.067 mmol) in methanol and recrystallized from methanol-diethyl ether mixture to give a pale yellow powder (60 mg, 80% yield).

[Pd_3(μ-Te$)_2$(dppe$)_3$)]($OTf)_2$

A reaction between [Pd(dppe)($OTf)_2$] (39.1 mg, 0.049 mmol) and (4,4'-$C_5H_4N)_2Te_2$ (20.3 mg, 0.049 mmol) in methanol for 4 hrs at room temperature afforded the title complexes as orange-red crystals (28 mg, 84% yield). Pertinent data are given in Table 16.

Table 16. Physical and analytical data of palladium and platinum nitrogen bonded complexes.

Complex	Recrystallization solvent	m.p. (°C)	% Analysis Found (Calcd.)	
			C	H
$[Pt\{(4,4'-C_5H_4N)_2Se_2\}(PEt_3)_2]_2(OTf)_4$	Methanol-Ether	143	26.98 (27.62)	3.80 (3.67)
$[Pt\{(4,4'-C_5H_4N)_2Te_2\}(PEt_3)_2]_2(OTf)_4$	Methanol-Ether	138	23.83 (25.26)	2.84 (3.36)
$[Pd\{(4,4'-C_5H_4N)_2Se_2\}(dppe)]_2(OTf)_4$	Methanol-Ether	218	40.77 (40.86)	2.94 (2.89)
$[Pd_3(\mu-Te)_2(dppe)_3)](OTf)_2$	Dichloromethane-Hexane	172	45.94 (46.47)	3.34 (3.51)

2.9 Synthesis of 4-pyridyltellurolate complexes of palladium and platinum

[Pd(TeC$_5$H$_4$N-4)$_2$(dppe)]

A dichloromethane suspension (8 mL) of [PdCl$_2$(dppe)] (155 mg, 0.27 mmol) was added to a methanolic solution (10 mL) of Na(TeC$_5$H$_4$N-4) (prepared from 4,4′-(C$_5$H$_4$N)$_2$Te$_2$ (111 mg, 0.27 mmol) and NaBH$_4$ (20.4 mg, 0.54 mmol) with stirring at room temperature. After 5 hours of stirring, solvents were evaporated *in vacuo* and the residue was extracted with dichloromethane (3 × 5 mL) and the combined extracts were passed through a Florisil column. The solvent was evaporated *in vacuo*, the residue was washed with hexane (2 mL) and recrystallized from an acetone–hexane mixture to give dark purple crystals of the title complex (192 mg, 78% yield).

[Pt(TeC$_5$H$_4$N-4)$_2$(dppe)]

This was prepared similar to the above using [PtCl$_2$(dppe)] (113 mg, 0.17 mmol) and 4,4′-(C$_5$H$_4$N)$_2$Te$_2$ (70 mg, 0.17 mmol) and NaBH$_4$ (13 mg, 0.34 mmol) and recrystallized from dichloromethane-hexane as yellow crystals (130 mg, 76% yield).

[Pt{PPh$_2$C(TeC$_5$H$_4$N-4)PPh$_2$}$_2$]

To a methanolic solution of NaTepy (prepared from (4,4'-C$_5$H$_4$N)$_2$Te$_2$ (56 mg, 0.14 mmol) and NaBH$_4$ (11 mg, 0.29 mmol in 8 mL methanol) a suspension of PtCl$_2$(dppm) (87 mg, 0.13 mmol) in methanol was added with stirring which continued for 5 hrs at room temperature. The solvent was evaporated under vaccum and the residue was extracted with dichloromethane which was concentrated in vaccum and recrystallized from dichloromethane-hexane to give brown crystals (52 mg, 57% yield).

$[Pd_2(\mu\text{-}Te)(\mu\text{-}TeC_5H_4N\text{-}4)(TeC_5H_4N\text{-}4)(dppm)]_2$

Reaction similar to the above using $[PdCl_2(dppm)]$ (110 mg, 0.20 mmol) and NaTepy (from $(4,4'\text{-}C_5H_4N)_2Te_2$ (81 mg, 0.20 mmol), $NaBH_4$ (15 mg, 0.40 mmol) in methanol was carried out. Product was extracted from dichloromethane and recrystallized from dichloromethane–hexane-diethylether mixture as black cubic crystals (84 mg, 76% yield).

$[Pt(SeC_5H_4N\text{-}4)(dppe)]_2(BPh_4)_2$

To a dichloromethane suspension (8 mL) of $[PtCl_2(dppe)]$ (150 mg, 0.23 mmol), $NaBPh_4$ (77.3 mg, 0.23 mmol) was added with stirring. To this suspension a methanolic solution (10 mL) of $Na(SeC_5H_4N\text{-}4)$ (from $4,4'\text{-}(C_5H_4N)_2Se_2$ (36 mg, 0.115 mmol) and $NaBH_4$ (9.1 mg, 0.24 mmol) was added at room temperature with stirring which continued for 5 hours. The solvents were evaporated *in vacuo* and the residue was extracted with dichloromethane (3 × 5 mL). The combined extracts were passed through a Florisil column. The solvent was evaporated *in vacuo*, the residue was washed with hexane (2 mL) and recrystallized from dichloromethane–hexane mixture to afford yellow crystals of the title complex (174 mg, 71% yield).

$[Pt(SeC_5H_4N\text{-}4)(PEt_3)_2]_2(BPh_4)_2$

This was prepared similar to the above using $[PtCl_2(PEt_3)_2]$ (120 mg, 0.24 mmol), $NaBPh_4$ (81.7 mg, 0.24 mmol), $4,4'\text{-}(C_5H_4N)_2Se_2$ (37.5 mg, 0.12 mmol) and $NaBH_4$ (9.1 mg, 0.24 mmol), in dichloromethane and methanol. Product was extracted from dichloromethane recrystallized from dichloromethane-hexane mixture as yellow crystals (120 mg, 55%). Pertinent data are given in Table 17.

Table 17. Physical and analytical data of palladium and platinum tellurolate complexes

Complex	Recrystallization solvent	m.p. (°C)	% Analysis Found (Calcd.)	
			C	H
$[Pd(TeC_5H_4N\text{-}4)_2(dppe)]$	Acetone-Hexane	162	47.71 (47.19)	3.55 (3.52)
$[Pt(TeC_5H_4N\text{-}4)_2(dppe)]$	Dichloromethane-Hexane	168	43.73 (43.03)	3.25 (3.21)
$[Pt\{PPh_2C(TeC_5H_4N\text{-}4)PPh_2\}_2]$	Dichloromethane-Hexane	174	50.57 (52.56)	3.50 (3.53)
$[Pd_2(\mu\text{-}Te)(\mu\text{-}TeC_5H_4N\text{-}4)(TeC_5H_4N\text{-}4)(dppm)]_2$	Dichloromethane-Hexane	--	- (37.00)	- (2.66)
$[Pt(SeC_5H_4N\text{-}4)(dppe)]_2(BPh_4)_2$	Dichloromethane-Hexane	187	61.62 (61.75)	4.04 (4.52)
$[Pt(SeC_5H_4N\text{-}4)(PEt_3)_2]_2(BPh_4)_2$	Dichloromethane-Hexane	172	53.29 (54.25)	5.77 (6.00)

Chapter 3

Results and Discussion

Chemistry of 4-pyridylselenolate complexes of palladium and platinum

Palladium and platinum(II) complexes based on hemilabile ligands containing chalcogen atom and nitrogen donor are of particular interest due to their extensive applications in homogeneous catalysis [154-158] and as versatile molecular precursors for metal chalcogenide nanomaterials [50, 159]. The chemistry of palladium and platinum complexes derived from two different classes of hemilabile ligands, *viz.* N,N-dimethylaminoalkylchalcogenolate [54, 57] and 2-pyridyl chalcogenolate [50, 62, 64] has been investigated during the past decade in Jain's group. Although, the chemistry of 2-pyridylchalcogenolate ligands is well documented [40, 50, 65], the corresponding 4-isomer i.e., 4-pyridyl chalcogenolate (**I**) is hardly explored [50] with some attention given to only thiolate derivatives. The 4-pyridylthiolate has been employed for construction of macrocycles [160, 161], heteronuclear supra-molecular assemblies [162, 163] and also pincer complexes [164]. These ligands offer several bonding possibilities with a metal ion as the two donor atoms (chalcogen and nitrogen) are inaccessible to the same metal unlike in the case of 2-pyridyl chalcogenolate [50] which is having completely different reactivity. Stang and co-workers have explored the chemistry of 4,4-dipyridyl disulfides for the synthesis of supra-molecular architectures [165]. The chemistry of the higher homologue, i.e., 4-pyridylselenolate, though known for quite some time, has been hardly investigated. Thus 4-pyridylselenolate complexes of palladium(II) and platinum(II) have been studied and their catalytic activity has been explored.

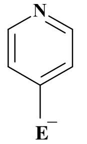

I E = S, Se, Te

The synthesis of 4-pyridylselenolate complexes of palladium and platinum is depicted in **Scheme 11**. Reactions of Na_2PdCl_4 or $MCl_2(PhCN)_2$ with 4,4'-dipyridyldeselenide gave yellow colored insoluble products of composition $[MCl_2\{Se_2(C_5H_4N)_2\}]$. It is worth noting that such reactions with 2,2'-dipyridyldichalcogenides or diaryldichalcogenides yield complexes (when M = Pd) of composition, $[PdCl(EAr)]_n$ (E = S, Se, Te; Ar = aryl or 2-pyridyl) [61, 166, 167]. In the present case the pyridyl nitrogen coordinates to the metal atom making the diselenide linkage inaccessible for oxidative addition to the metal center. The complexes of composition, $[PdCl(SeC_5H_4N\text{-}4)]_n$ could be isolated by the reaction between Na_2PdCl_4 and $NaSeC_5H_4N\text{-}4$ in 1:1 molar ratio. This reaction in 1:2 molar ratio afforded a homoleptic selenolate complex, $[Pd(SeC_5H_4N\text{-}4)_2]_n$. The ^{13}C NMR spectrum of the latter displayed two sets of resonances for the pyridyl ring as has been reported for the hexanuclear homoleptic selenolates, $[Pd(SeR)_2]_6$ [168]. However, the ^{77}Se NMR spectrum exhibited only a single resonance.

Treatment of $[PdCl(SeC_5H_4N\text{-}4)]_n$ with PPh_3 in acetone gave $[PdCl(SeC_5H_4N\text{-}4)(PPh_3)_2]$, which was isolated as the *trans* isomer after recrystallization (see later, X-ray crystallography). The ^{31}P NMR spectrum displayed a single resonance at δ 23.6 ppm indicative of *trans* configuration. The spectrum also showed resonances due to free PPh_3 and $[PdCl(SeC_5H_4N\text{-}4)(PPh_3)]_n$ (total integration ~ 10%) indicating dissociation of the complex in solution. Similarly, the corresponding thiolate derivative $[PdCl(SC_5H_4N\text{-}4)(PPh_3)_2]$ tends to exist in an equilibrium with PPh_3 and a trinuclear complex, $[PdCl(SC_5H_4N\text{-}4)(PPh_3)]_3$ in solution. A redistribution reaction between $[Pt(SeC_5H_4N\text{-}4)_2(PEt_3)_2]$ and $[PtCl_2(PEt_3)_2]$ in $CDCl_3$ proceeded slowly to give $[PtCl(SeC_5H_4N\text{-}4)(PEt_3)_2]$. About ~ 5% starting material existed in solution even after 20 days as revealed by ^{31}P and ^{195}Pt NMR spectral data.

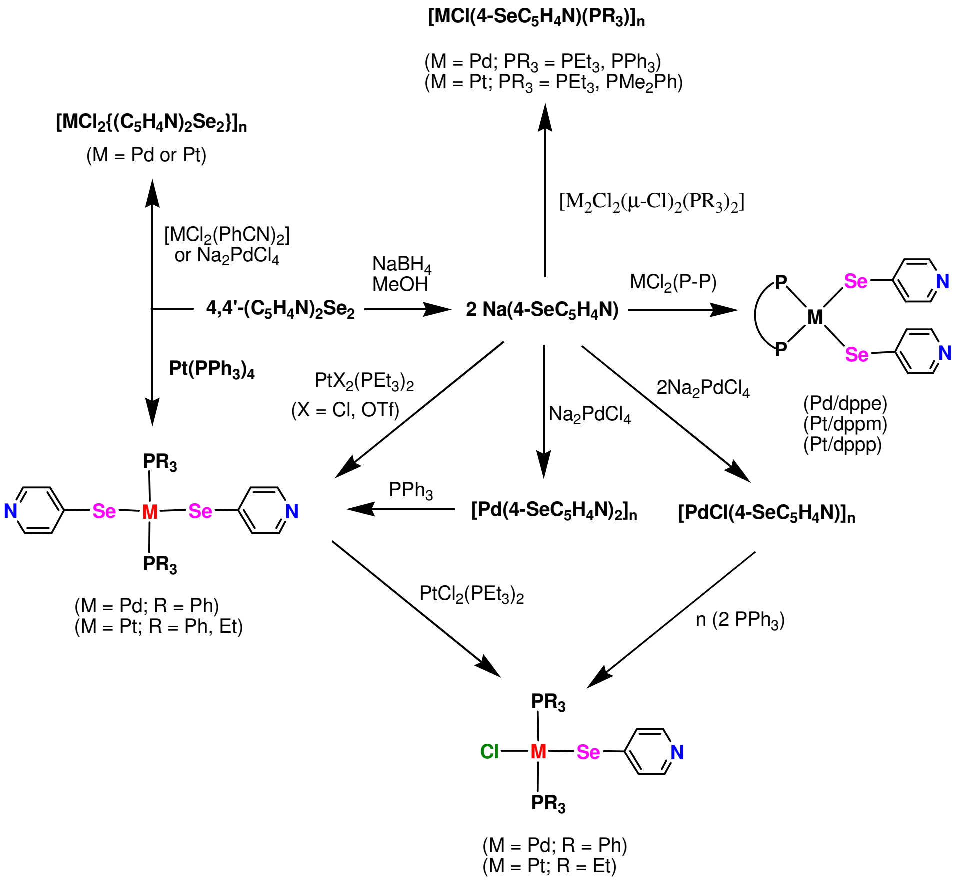

Scheme 11. Syntheses of 4-pyridylselenolate complexes of palladium and platinum

The reaction of $[Pd(SeC_5H_4N\text{-}4)_2]_n$ with PPh_3 in acetone afforded a brown crystalline solid, $[Pd(SeC_5H_4N\text{-}4)_2(PPh_3)_2]$. Alternatively $[Pd(SeC_5H_4N\text{-}4)_2(PPh_3)_2]$ could be obtained by the reaction of $[PdCl_2(PPh_3)_2]$ with 2-equivalents of $NaSeC_5H_4N\text{-}4$ in a benzene-methanol mixture. Similarly reactions of $PtCl_2(PR_3)_2$ with two equivalents of $NaSeC_5H_4N$ yielded *trans*-$[Pt(SeC_5H_4N\text{-}4)_2(PPh_3)_2]$ and *trans*-$[Pt(SeC_5H_4N\text{-}4)_2(PEt_3)_2]$. Oxidative addition of 4,4'-$(C_5H_4N)_2Se_2$ to $Pt(PPh_3)_4$ yielded *trans*-$[Pt(SeC_5H_4N\text{-}4)_2(PPh_3)_2]$. The magnitude of ^1J(Pt-P) for *trans*-$[Pt(SeC_5H_4N\text{-}4)_2(PPh_3)_2]$ and *trans*-$[Pt(SeC_5H_4N\text{-}4)_2(PEt_3)_2]$ is in accordance with the *trans* configuration of the complex and is further confirmed by the X-ray structural analysis of *trans*-$[Pt(SeC_5H_4N\text{-}4)_2(PEt_3)_2]$. The ^{195}Pt NMR spectra of *trans*-$[Pt(SeC_5H_4N\text{-}4)_2(PPh_3)_2]$ and *trans*-[Pt(SeC_5H_4N-4)$_2$(PEt_3)$_2$] exhibit a triplet at ~ −5000 ppm due to coupling with two chemically equivalent phosphorus nuclei (Table 18).

The reactions of MCl_2(P$^\frown$P) [M/P$^\frown$P = Pd/dppe; Pt/dppm; Pt/dppp)] with two equivalents of $NaSeC_5H_4N$-4 gave *cis*-[M(SeC_5H_4N-4)$_2$(P$^\frown$P)]. The ^{31}P NMR spectra exhibited single resonances in the expected regions; the resonances for platinum complexes were flanked by ^{195}Pt satellites. The ^{77}Se NMR spectra showed a doublet at ~ 240 ppm due to coupling with *trans* phosphorus nucleus; the *cis*-Se-P couplings being much smaller and hence could not be resolved. The ^{195}Pt NMR spectra exhibit a triplet due to coupling with two phosphorus nuclei [169].

Reactions of [M_2Cl_2(μ-Cl)$_2$(PR_3)$_2$] (R = PEt_3, PPh_3, PMe_2Ph) with two equivalents of $NaSeC_5H_4N$-4 gave complexes of composition [MCl(SeC_5H_4N-4)(PR_3)]$_n$ which were isolated as trimer/dimer containing bridging selenolate ligands. The ^{31}P, ^{77}Se and ^{195}Pt NMR spectra (Figures 2 and 3; Table 18) of [PdCl(SeC_5H_4N-4)(PEt_3)]$_n$, [PtCl(SeC_5H_4N-4)(PEt_3)]$_n$ and [PtCl(SeC_5H_4N-4)(PMe_2Ph)]$_n$ showed single resonances in solution but [PdCl(SeC_5H_4N-4)(PPh_3)]$_n$ exhibit two such resonances. One is attributed to a trinuclear species while the other to the dimer. The ^{77}Se NMR spectrum of [PdCl(SeC_5H_4N-4)(PPh_3)]$_n$ displayed three resonances one singlet at 390 ppm attributable to the trimer and two doublets at -91 and -104 ppm with ^{2}J(Se-P) = ~ 145 Hz (Figure 4). The latter are due to coupling with *trans* phosphine to bridging selenolate ligand (Scheme 12). Both di- and trimeric forms could be separated and structurally characterized.

The absorption spectra of the complexes in CH_2Cl_2 solution were characterized by a weak band in the visible region. The distinct violet colored Pd complex, trans-[PdCl(SeC_5H_4N-4)(PPh_3)$_2$] exhibited a broad, well-separated but relatively weak band at 517 nm whereas the yellow Pt complex, [PtCl(SeC_5H_4N-4)(PEt_3)]$_n$ showed a similar band at comparatively higher energy at about 403 nm. This long-wavelength weak band has been observed in selenolate/ tellurolate complexes [MCl(E$^\frown$N)(PR$_3$)] (M = Pd, Pt; E$^\frown$N = 2-C$_5$H$_4$N [20], ECH$_2$CH$_2$NMe$_2$ [54, 55]). The distinct color in these complexes has been attributed to the low-energy electronic transition from ligand (Se or Te)-to-ligand (PR$_3$) charge transfer transitions (LLCT).

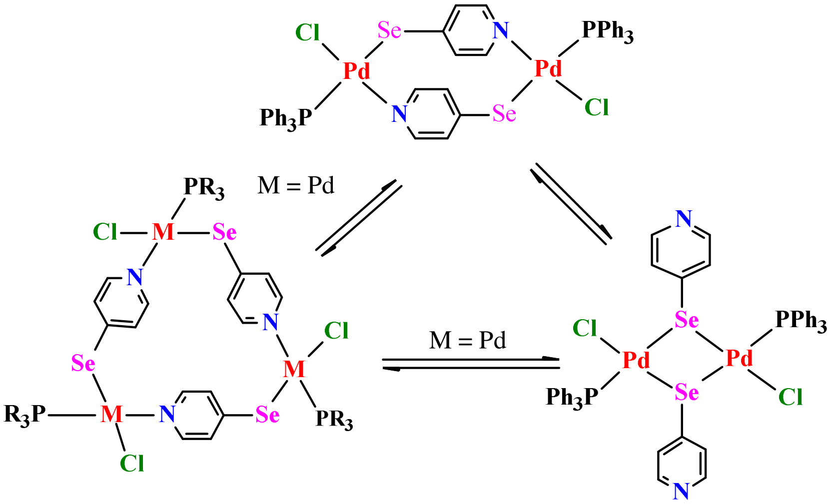

(M = Pd; PR$_3$ = PEt$_3$, PPh$_3$)
(M = Pt; PR$_3$ = PEt$_3$, PMe$_2$Ph)

Scheme 12 Possible isomers of complex [MCl(SeC$_5$H$_4$N-4)(PR$_3$)]$_n$

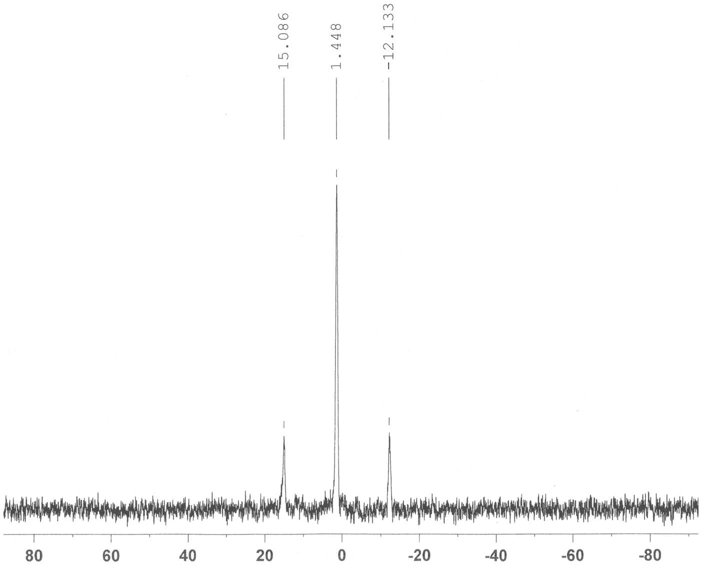

Figure 2. ^{31}P{^{1}H} NMR spectra of [PtCl(SeC$_5$H$_4$N-4)(PEt$_3$)]$_n$ in CDCl$_3$

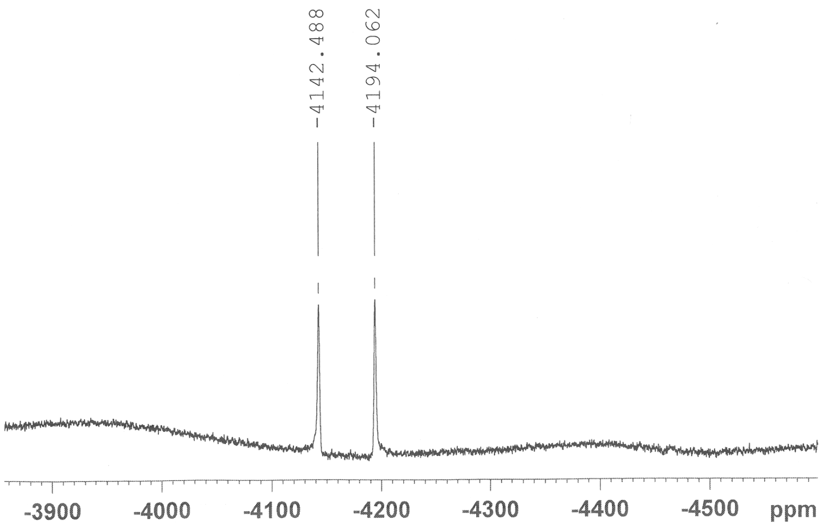

Figure 3. $^{195}Pt\{^1H\}$ NMR spectra of $[PtCl(SeC_5H_4N\text{-}4)(PEt_3)]_n$ in $CDCl_3$

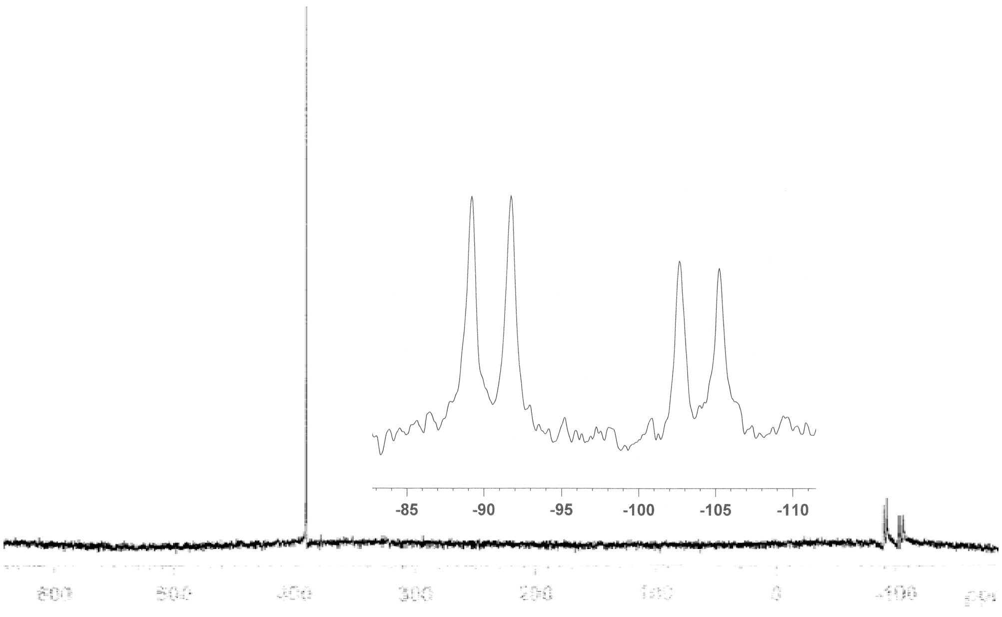

Figure 4. $^{77}Se\{^1H\}$ NMR spectrum of $[PdCl(SeC_5H_4N\text{-}4)(PPh_3)]_n$ in $CDCl_3$

Table 18. Spectroscopic data for 4-pyridylselenolate complexes of palladium and platinum

Complex	UV-Vis (CH_2Cl_2) λ_{max} in nm (ε in M^{-1} cm^{-1})	^1H NMR data in (δ ppm)	$^{31}P\{^1H\}$ NMR data in (δ ppm)	$^{77}Se\{^1H\}$ NMR data in (δ ppm)	^{195}Pt $\{^1H\}$ NMR data in (δ ppm)
$[Pd(SeC_5H_4N\text{-}4)_2]_n$[a]	–	7.96, 7.80, 7.62, 7.48 (each br, s)	-	287 (s)	-
trans-$[PdCl(SeC_5H_4N\text{-}4)(PPh_3)_2]$	276(17211), 343(14080), 378(11322), 517(449)	7.80-7.50 (m, 14H, *o*-H, Ph and 2,6-H, py), 7.50-7.25 (m, 18H, *m/p*-H, Ph), 6.94 (d, $^3J_{HH}$ = 5.1 Hz, 2H, 3,5-H, py)	23.6	278	-
trans-$[PtCl(SeC_5H_4N\text{-}4)(PEt_3)_2]$[b]	-	7.98 (br s, 4H, 2,6-H, py), 7.58 (br s, 4H, 3,5-H, py); 2.35-1.80 (m, 12H, PCH_2), 1.40-0.90 (m, 18H, PCH_2CH_3)	11.1 (s, $^1J_{Pt\text{-}P}$ = 2401 Hz)	111 (s, $^2J_{Pt\text{-}Se}$ = 90 Hz)	–4594 (t, $^1J_{Pt\text{-}P}$ = 2407 Hz)
trans-$[Pd(SeC_5H_4N\text{-}4)_2(PPh_3)_2]$[a]	–	-	27.1 (s)	-	-
trans-$[Pt(SeC_5H_4N\text{-}4)_2(PPh_3)_2]$	-	7.66 (d, $^3J_{HH}$ = 5.7 Hz, 4H, 2,6-H, py), 7.64-7.53 (m, 12H, *o/p*-Ph), 7.38-7.18 (m, 18H, *m/p*-Ph), 6.87 (d, $^3J_{HH}$ = 5.7 Hz, 4H, 3,5-H, py)	19.5 (s, $^1J_{Pt\text{-}P}$ = 2695 Hz)	-	–5035 (t, $^1J_{Pt\text{-}P}$ = 2680 Hz)
trans-$[Pt(SeC_5H_4N\text{-}4)_2(PEt_3)_2]$	-	8.07 (d, $^3J_{HH}$ = 4.5 Hz, 4H, 2,6-H, py), 7.54 (d, $^3J_{HH}$ = 4.2 Hz, 4H, 3,5-H, py), 2.03 (br, 12H, PCH_2), 1.11-0.96 (m, 18H, PCH_2CH_3)	7.1 (s, $^1J_{Pt\text{-}P}$ = 2384 Hz)	106 (s, $^1J_{Pt\text{-}Se}$ = 81 Hz)	–4996 (t, $^1J_{Pt\text{-}P}$ = 2379 Hz)

$[Pd(SeC_5H_4N\text{-}4)_2(dppe)]$	328 (3800), 409 (1000)	7.87 (d, $^3J_{HH}$ = 5.4 Hz, 4H, 2-H, 2py), 7.67 (m, 8H, *o*-Ph), 7.50 (m, 4H, *p*-Ph), 7.42 (m, 8H, *m*-Ph), 7.15 (d, $^3J_{HH}$ = 5.7 Hz, 4H, 3py), 2.30 (d, $^2J_{PH}$ = 21.6 Hz, 4H, PCH_2)	55.2 (s)	235 (d, $^2J_{SeP}$ = 90 Hz)	
$[Pt(SeC_5H_4N\text{-}4)_2(dppm)]$	–	7.68 (d, $^3J_{HH}$ = 4.2 Hz, 4H, 2-H, 2py), 7.58 (m, 8H, *o*-Ph), 7.47 (m, 4H, *p*-Ph), 7.38 (m, 8H, *m*-Ph), 7.22 (d, $^3J_{HH}$ = 4.2 Hz, 4H, 3py), 4.41 (t, $^2J_{P\text{-}H}$ = 11 Hz, $^3J_{Pt\text{-}H}$ = 50 Hz, PCH_2–)	–52.5 (s, $^1J_{Pt\text{-}P}$ = 2540 Hz)	236, 235 (d, $^2J_{P\text{-}Se}$ = 45 Hz)	–4314 (t, $^1J_{Pt\text{-}P}$ = 2542 Hz)
$[Pt(SeC_5H_4N\text{-}4)_2(dppp)]$	–	7.75 (d, $^3J_{HH}$ = 4.8 Hz, 4H, 2,6-H, py), 7.65 (br, Ph), 7.75-7.25 (m, 12H, Ph), 7.09 (d, $^3J_{HH}$ = 4.5 Hz, 4H, 3,5-H, py), 2.75- 2.36 (br, 4H, PCH_2–), 2.15-1.90 (br, 2H, –CH_2–)	–4.2 (s, $^1J_{Pt\text{-}P}$ = 2798 Hz)	249 (d, $^2J_{P\text{-}Se}$ = 46 Hz)	–4894 (t, $^1J_{P\text{-}Pt}$ = 2819 Hz)
$[PdCl(SeC_5H_4N\text{-}4)(PEt_3)]_n$	259(17230), 331(12794), 362(10864), 451(949)	8.26 (dd, $^3J_{HH}$ = 6.3 Hz, $^4J_{PH}$ = 2.7 Hz, 2H, 2-H, py), 7.30 (d, $^3J_{HH}$ = 5.4 Hz, 2H, 3-H, py), 2.02 (dq, J(d) = 10.5 Hz, J(q) = 7.5 Hz, PCH_2), 1.19 (dt, J(d) = 17.4 Hz, J(t) = 7.8 Hz, PCH_2CH_3)	31.4 (s)	324 (s)	–

$[PdCl(SeC_5H_4N\text{-}4)(PPh_3)]_n$	–	8.23 (m, 2H, 2,6-H, py), 7.80-7.60 (m, 6H, *o*-H, Ph), 7.53-7.25 (m, 9H, *m/p*-Ph),7.10 (m, 2H, 3,5-H, py)	29.8 (s), 29.2 (s br)	390 (s), −91 (d, $^2J_{Se\text{-}P}$ = 145 Hz), −104 (d, $^2J_{Se\text{-}P}$ = 149 Hz)	–
$[PtCl(SeC_5H_4N\text{-}4)(PEt_3)]_n$	265(26008), 343(67099), 403(sh)	8.20 (br, 2H, 2,6-H, py), 7.39 (d, $^3J_{HH}$ = 5.4 Hz, 2H, 3,5-H, py), 1.99 (dq , J(d) = 9.9 Hz, J(q) = 7.2 Hz, PCH_2), 1.54 (dt, J(d) = 17.1 Hz, J(t) = 7.5 Hz, PCH_2CH_3)	1.4 (s, $^1J_{Pt\text{-}P}$ = 3307 Hz)	278 (s, $^1J_{Pt\text{-}Se}$ = 91 Hz)	–4168 (d, $^1J_{Pt\text{-}P}$ = 3335 Hz)
$[PtCl(SeC_5H_4N\text{-}4)(PMe_2Ph)]_n$	–	8.14 (br s, 2H, 2,6-H, py), 7.73 (br s, 2H, Ph), 7.43 (br s, 3H, m/p-o, Ph), 7.31 (d, ^3J = 5.7 Hz, 2H, 3,5-H, py), 1.94 (d, $^3J_{P\text{-}H}$ = 11 Hz, 6H, PMe_2)	–22.5 (s), ($J_{Pt\text{-}P}$ = 3352 Hz)		

[a] Recorded in acetone-d_6.

[b] A small amount ~5% of $PtCl_2(PEt_3)_2$ and $Pt(SeC_5H_4N\text{-}4)_2(PEt_3)_2$ existed in solution (by ^{31}P and ^{195}Pt NMR) even after 20 days of monitoring the reaction.

Crystallography

Crystal and molecular structures of *trans*-[PdCl(SeC$_5$H$_4$N-4)(PPh$_3$)$_2$], *trans*-[PtCl(SeC$_5$H$_4$N-4)(PEt$_3$)$_2$], *trans*-[Pd(SeC$_5$H$_4$N-4)$_2$(PPh$_3$)$_2$], *trans*-[Pt(SeC$_5$H$_4$N-4)$_2$(PEt$_3$)$_2$], *cis*-[Pd(SeC$_5$H$_4$N-4)$_2$(dppe)], *cis*-[Pt(SeC$_5$H$_4$N-4)$_2$(dppp)], [PdCl(SeC$_5$H$_4$N-4)(PEt$_3$)]$_n$, [PdCl(SeC$_5$H$_4$N-4)(PPh$_3$)]$_n$ and [PtCl(SeC$_5$H$_4$N-4)(PEt$_3$)]$_n$ have been established by single crystal X-ray diffraction analyses. The ORTEP drawings with crystallographic numbering scheme are shown in Figures 5-13, and the selected inter-atomic parameters are given in Tables 19-23. The complex trans-[PdCl(SeC$_5$H$_4$N-4)(PPh$_3$)$_2$] crystallized with a molecule of acetone whereas the complexes [Pd(SeC$_5$H$_4$N-4)$_2$(dppe)] and [Pt(SeC$_5$H$_4$N-4)$_2$(dppp)], were crystallized with molecule(s) of water.

The structures of [PdCl(SeC$_5$H$_4$N-4)(PPh$_3$)$_2$] (Figure 5) and [PtCl(SeC$_5$H$_4$N-4)(PEt$_3$)$_2$] (Figure 6) are isomorphous with nearly similar bond lengths and angles (Table 19). These complexes adopt a *trans* configuration defined by mutually trans disposed two neutral phosphine ligands and two anionic groups (Cl and SeC$_5$H$_4$N). The M–Cl, M–Se and M–P bond distances can be compared with [MCl(SeC$_6$H$_5$)(PPh$_3$)$_2$] (M = Pd [69], Pt [170]). The two M–P distances are dissimilar which is more pronounced in the case of *trans*-[PdCl(SeC$_5$H$_4$N-4)(PPh$_3$)$_2$] (Pd1–P1: 2.3454(12) Å; Pd1–P: 2.3161(12) Å).

The coordination environment around the distorted square planar metal center in the isomorphous [Pd(SeC$_5$H$_4$N-4)$_2$(PPh$_3$)$_2$] (Figure 7) and [Pt(SeC$_5$H$_4$N-4)$_2$(PEt$_3$)$_2$] (Figure 8) is defined by the *trans*-P$_2$Se$_2$ donor atoms. The two selenolate groups adopt an *anti* configuration. The existence of both *syn* and *anti* forms have been reported for *trans*-[Pt(SeC$_6$H$_5$)$_2$(PEt$_3$)$_2$] [91]. The M–Se distances (Table 20) can be compared with those reported for *trans*-[M(SeR′)$_2$(PR$_3$)$_2$] (M/R′/R = Pd/Ph/Bu^n (2.4609(4) Å) [171]; Pt/Ph/Et (2.461(1) Å [91, 172]; Pt/Ph/Bu (2.463(3) Å [91]; Pt/Ph/Ph (2.4525(5), 2.4548(5) Å) [173].

The two acute (~ 85°) and two obtuse (93.08(3)-96.62(3)°) P–M–Se angles can be compared with other phenylselenolate derivatives *trans*-[Pt(SeC_6H_5)$_2$(PR_3)$_2$] [91, 173, 174].

Table 19. Selected interatomic distances [Å] and angles [°] for [PdCl(SeC_5H_4N-4)(PPh_3)$_2$]•acetone and [PtCl(SeC_5H_4N-4)(PEt_3)$_2$]

	[PdCl(SeC_5H_4N-4)(PPh_3)$_2$] ·(acetone)	[PtCl(SeC_5H_4N-4)(PEt_3)$_2$]
M1–P1	2.3454(12)	2.3182 (6)
M1–P2	2.3161(12)	2.3092 (6)
M1–Se1	2.4254(5)	2.4275 (2)
M1–Cl1	2.3462(11)	2.3455 (6)
Se1–C1	1.906 (5)	1.900 (2)
P1–M1–P2	177.48(4)	177.56 (2)
P1–M1–Se1	92.25(3)	92.886 (16)
P1–M1–Cl1	91.35(4)	86.37 (2)
P2–M1–Se1	85.44(3)	88.747 (17)
P2–M1–Cl1	90.94(4)	91.87 (2)
Se1–M1–Cl1	176.29(3)	175.892 (16)

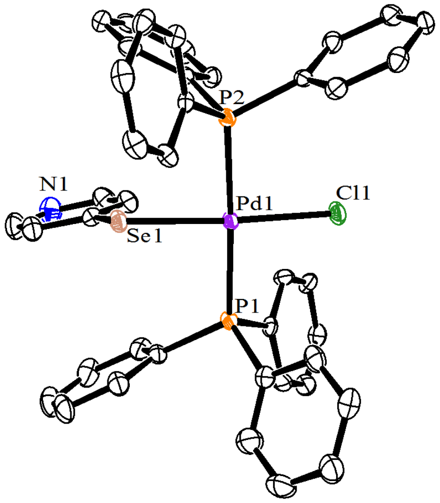

Figure 5. Molecular structure of *trans*-[PdCl(SeC_5H_4N-4)(PPh_3)$_2$]•acetone; ellipsoids drawn at 50% probability (Hydrogen atoms and solvent molecule are omitted for clarity).

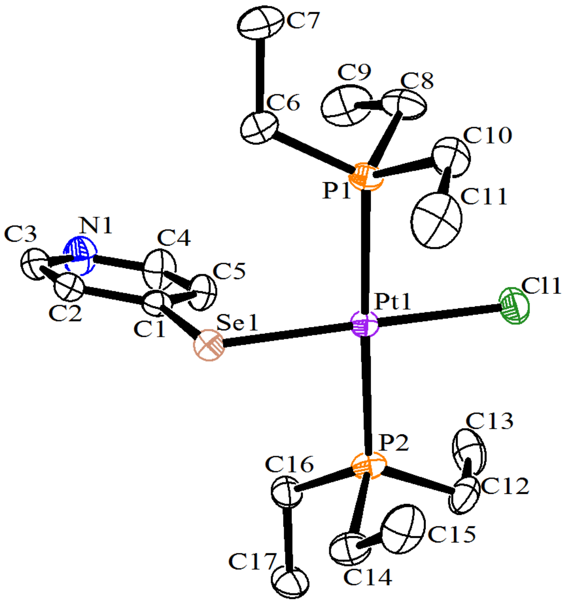

Figure 6. Molecular structure of *trans*-[PtCl(SeC$_5$H$_4$N-4)(PEt$_3$)$_2$]; ellipsoids drawn at 50% probability (Hydrogen atoms are omitted for clarity).

Table 20. Selected interatomic distances [Å] and angles [°] of *trans*-[Pd(SeC$_5$H$_4$N-4)$_2$(PPh$_3$)$_2$] and *trans*-[Pt(SeC$_5$H$_4$N-4)$_2$(PEt$_3$)$_2$]

	[Pd(SeC$_5$H$_4$N-4)$_2$(PPh$_3$)$_2$]	[Pt(SeC$_5$H$_4$N-4)$_2$(PEt$_3$)$_2$]
M1–Se1	2.4521(6)	2.4594(5)
M1–Se2	2.4544(5)	2.4570(5)
M1–P1	2.3395(14)	2.3171(12)
M1–P2	2.3507(15)	2.3178(12)
Se1–C1	1.896(4)	1.896(5)
Se2–C6	1.906(4)	1.897(5)
Se1–M1–Se2	177.99(2)	177.01(2)
Se1–M1–P1	85.25(3)	86.12(30
Se1–M1–P2	96.62(3)	93.37(3)
Se2–M1–P1	93.08(3)	93.79(3)
Se2–M1–P2	85.00(3)	86.87(3)
P1–M1–P2	177.05(4)	177.05(5)

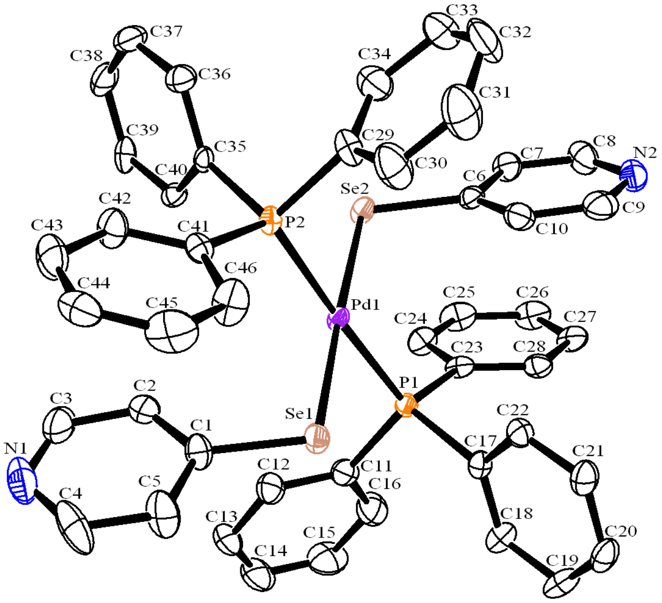

Figure 7. Molecular structure of *trans*-[Pd(SeC_5H_4N-4)$_2$(PPh_3)$_2$]; ellipsoids drawn at 50% probability (Hydrogen atoms are omitted for clarity).

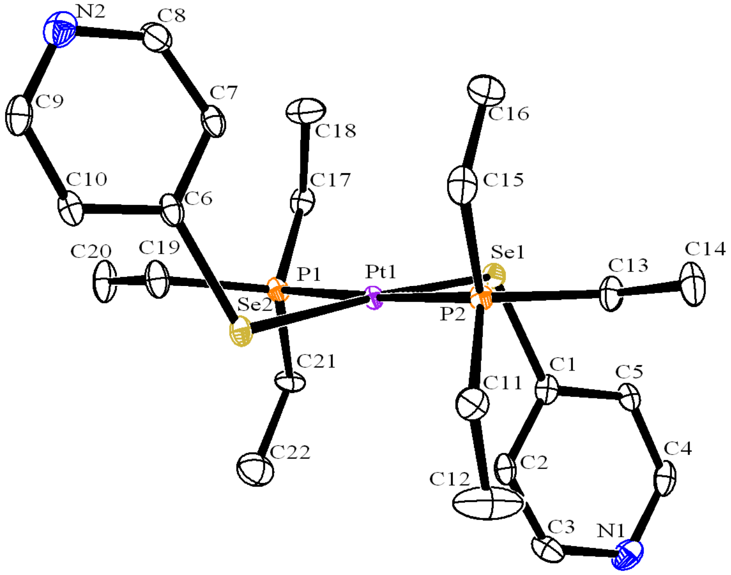

Figure 8. Molecular structure of *trans*-[Pt(SeC_5H_4N-4)$_2$(PEt_3)$_2$] ellipsoids drawn at 50% probability. (Hydrogen atoms are omitted for clarity)

The metal atom in the isostructural complexes, [Pd(SeC_5H_4N-4)$_2$(dppe)] (Figure 9) and [Pt(SeC_5H_4N-4)$_2$(dppp)] (Figure 10) adopts a distorted square planar configuration defined by a *cis*-P_2Se_2 coordination core. The two M–Se and two M–P distances in these complexes are essentially similar (Table 21). These distances in several such complexes are either similar or quite often dissimilar and are primarily governed by the relative orientation of the aryl group of the chalcogenolate ligand [175] For instance, the two M–Se distances in [Pd(SeC_6H_5)$_2$(dppe)] (Pd–Se = 2.444(1), 2.480(1) Å) [176] and [Pt(SeC_5H_4N-2)$_2$(dppe)] (Pt–Se = 2.4335(13); 2.4980(14) Å) [177] are dissimilar. The pyridyl groups in [Pd(SeC_5H_4N-4)$_2$(dppe)] and [Pt(SeC_5H_4N-4)$_2$(dppp)] are *syn* oriented. Both complexes show intermolecular hydrogen bonding with solvated water molecule(s). The two pyridyl nitrogen atoms of [Pd(SeC_5H_4N-4)$_2$(dppe)] from two adjacent molecules are H-bonded *via* two H_2O to form an infinite zig-zag chain. The [Pt(SeC_5H_4N-4)$_2$(dppp)] on the other hand is a discrete molecule as only one pyridyl nitrogen is H-bonded with H_2O.

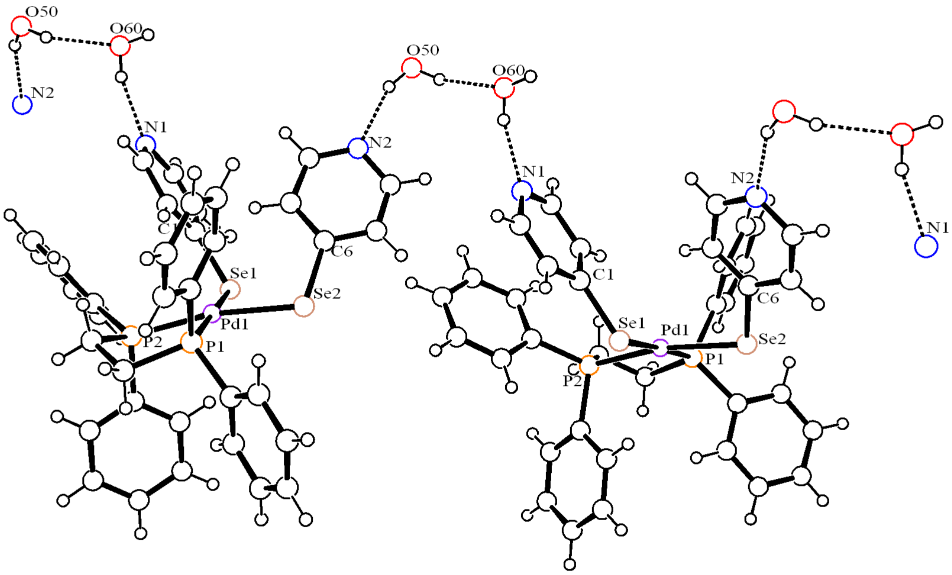

Figure 9. H-bonding in *cis*-[Pd(SeC_5H_4N-4)$_2$(dppe)]·$2H_2O$ ellipsoids drawn at 50% probability.

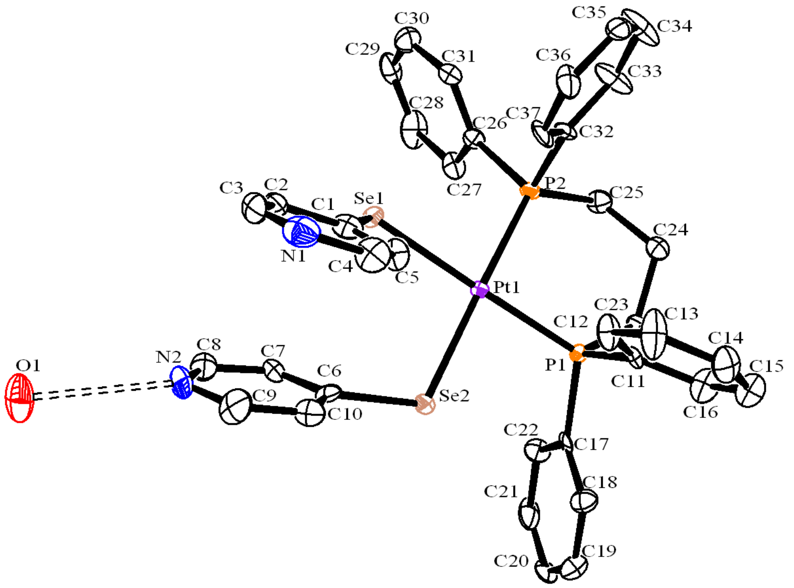

Figure 10. Molecular structure of *cis*-[Pt(SeC_5H_4N-4)$_2$(dppp)]•0.5H_2O; ellipsoids drawn at 50% probability. (Hydrogen atoms are omitted for clarity)

Table 21. Selected interatomic distances [Å] and angles [°] of [Pd(SeC_5H_4N-4)$_2$(dppe)]•2H_2O and [Pt(SeC_5H_4N-4)$_2$(dppp)]•0.5H_2O

	[Pd(SeC_5H_4N-4)$_2$(dppe)]•2H_2O	[Pt(SeC_5H_4N-4)$_2$(dppp)]•0.5H_2O
M1–Se1	2.4750(6)	2.4822(7)
M1–Se2	2.4777(6)	2.4760(7)
M1–P1	2.2691(13)	2.2744(15)
M1–P2	2.2675(12)	2.2656(15)
Se1–C1	1.911(5)	1.875(6)
Se2–C6	1.912(5)	1.925(6)
Se1–M1–Se2	93.34(2)	95.49(2)
Se1–M1–P1	176.59(4)	175.98(4)
Se1–M1–P2	91.96(4)	86.47(4)
Se2–M1–P1	88.91(3)	84.65(4)
Se2–M1–P2	168.93(3)	176.69(4)
P1–M1–P2	85.40(5)	93.58(5)

The complex, $[PdCl(SeC_5H_4N\text{-}4)(PPh_3)]_2$ (Figure 11) is a centrosymmetric dimer with a *sym-trans* configuration as reported for similar other complexes, $[PdCl(\mu\text{-}SeR)(PPh_3)]_2$ (R = Ph [178] CH_2CH_2–COOMe [124]). The molecule comprises of a central planar Pd_2Se_2 rhombus. The two palladium atoms are held together by two bridging selenolate groups. The two pyridyl groups of the bridging selenolate adopt an *anti* configuration. The two Pd–Se distances are distinctly different (Table 22), the one *trans* to the phosphine ligand is longer (~ 2.47 Å) than the one trans to the chloride (~ 2.40 Å), owing to the strong *trans* influence of the phosphine ligand.

Table 22. Selected interatomic distances [Å] and angles [°] of $[PdCl(\mu\text{- }SeC_5H_4N\text{-}4)(PPh_3)]_2$

	$[PdCl(\mu\text{- }SeC_5H_4N\text{-}4)(PPh_3)]_2$
Pd1–Se1	2.4001(3)
Pd1–Se1#	2.4739(3)
Pd1#–Se1	2.4740(3)
Pd1–P1	2.2908(4)
Pd1–Cl1	2.3278(4)
Se1–C1	1.9215(16)
Pd1…Pd1#	3.657
P1–Pd1–Cl1	91.975(15)
P1–Pd1–Se1	95.063(12)
P1–Pd1–Se1#	177.509(12)
Cl1–Pd1–Se1#	90.291(12)
Cl1–Pd1–Se1	171.368(12)
Se1–Pd1–Se1#	82.772(7)
C1–Se1–Pd1	105.97(5)
C1–Se1–Pd1#	100.08(5)
Pd1–Se1–Pd1#	97.227(7)

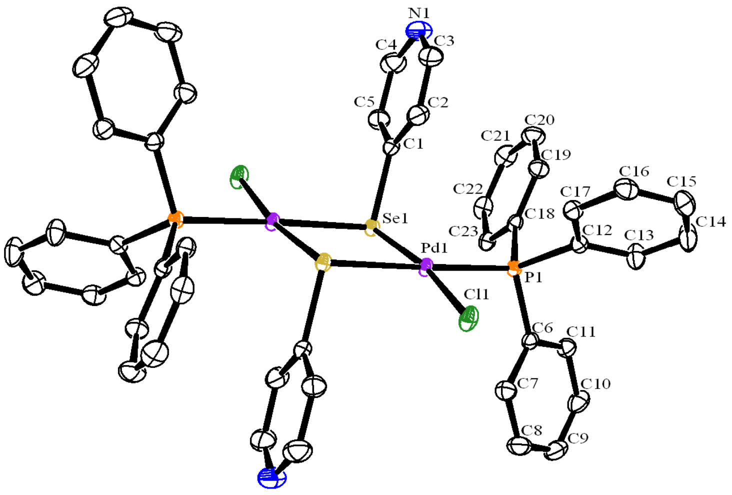

Figure 11. Molecular structure of $[PdCl(SeC_5H_4N\text{-}4)(PPh_3)]_2$; ellipsoids drawn at 50% probability. (Hydrogen atoms are omitted for clarity)

The complexes $[PdCl(SeC_5H_4N\text{-}4)(PEt_3)]_3$ (Figure 12) and $[PtCl(SeC_5H_4N\text{-}4)(PEt_3)]_3$ (Figure 13) are isostructural and represent an interesting example of neutral triangular (nearly equilateral triangle) shaped molecules, although cationic complexes, e.g. $[Pt(PMe_3)_2(pyrazine)]_3^{6+}$, are fairly well documented [53, 179]. The distance between the metal and the pyridyl ring facing the metal atom varies in the range 7.0–7.1 Å (for Pd) and 6.5 –7.0 Å (for Pt) indicating palladium metallacycle is bigger in size than the platinum analog. Both $[PdCl(SeC_5H_4N\text{-}4)(PEt_3)]_n$ and $[PtCl(SeC_5H_4N\text{-}4)(PEt_3)]_n$ are comprised of three distorted square planar palladium atoms which are held together by bridging selenolate groups, *via* Se and N atoms. The coordination environments, defined by PSeNCl set, around each metal atom and inter atomic parameters involving the metal center is similar. The neutral donors (P and N) are *trans* to each other at an angle (N–Pd–P) of ~ 177° (Table 23). The pyridyl ring is almost perpendicular to the metal square plane. The trinuclear complexes in a triangular arrangement are usually held by single bridging atom (O, S, Se, Cl) [38, 53] so as to form a six-membered "M_3X_3" ring adopting different conformations.

Table 23. Selected interatomic distances [Å] and angles [°] of $[MCl(SeC_5H_4N\text{-}4)(PEt_3)]_3$ (M = Pd ; Pt).

	$[PdCl(SeC_5H_4N\text{-}4)(PEt_3)]_3$	$[PtCl(SeC_5H_4N\text{-}4)(PEt_3)]_3\cdot CHCl_3$
M1–Se1	2.4043(18)	2.434(3)
M2–Se2	2.3965(17)	2.426(3)
M3–Se3	2.3921(17)	2.385(3)
M1–Cl1	2.333(4)	2.362(7)
M2–Cl2	2.323(4)	2.353(7)
M3–Cl3	2.339(4)	2.315(7)
M1–P1	2.245(4)	2.181(9)
M2–P2	2.239(5)	2.203(9)
M3–P3	2.226(4)	2.250(9)
M1–N3	2.146(10)	2.080(12)
M2–N1	2.141(11)	2.068(12)
M3–N2	2.140(9)	2.133(12)
P1–M1–Cl1	93.65(14)	90.0(3)
P1–M1–Se1	86.95(11)	93.4(3)
P1–M1–N3	177.0(3)	175.3(5)
Cl1–M1–Se1	178.71(13)	172.3(2)
Cl1–M1–N3	89.0(3)	89.8(5)
N3–M1–Se1	90.4(3)	87.4(4)
P2–M2–Cl2	89.33(16)	87.8(3)
P2–M2–Se2	90.69(13)	94.5(3)
P2–M2–N1	177.8(3)	175.7(6)
Cl2–M2–Se2	179.13(14)	177.5(2)
Cl2–M2–N1	88.5(3)	87.9(5)
N1–M2–Se2	91.5(3)	89.8(5)
P3–M3–Cl3	89.61(16)	92.4(3)
P3–M3–Se3	89.61(13)	92.0(2)
P3–M3–N2	177.6(3)	177.4(5)
Cl3–M3–Se3	172.44(13)	175.4(2)
Cl3–M3–N2	89.3(3)	86.6(5)

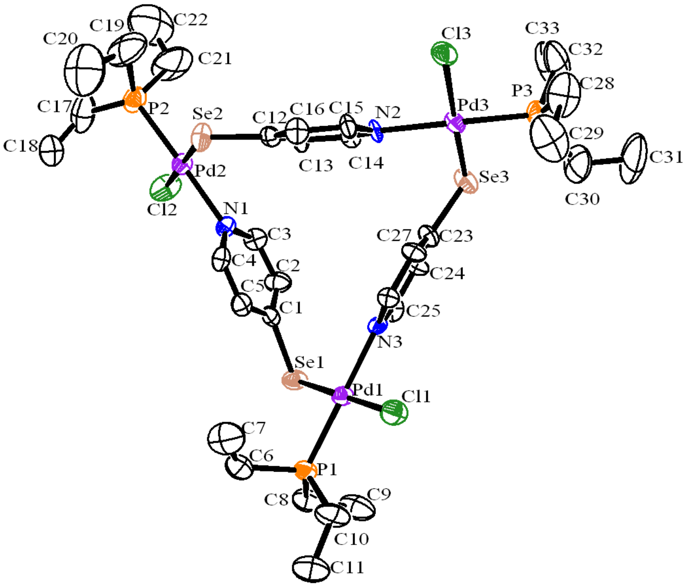

Figure 12. Molecular structure of [PdCl(SeC$_5$H$_4$N-4)(PEt$_3$)]$_3$; ellipsoids drawn at 50% probability. (Hydrogen atoms are omitted for clarity)

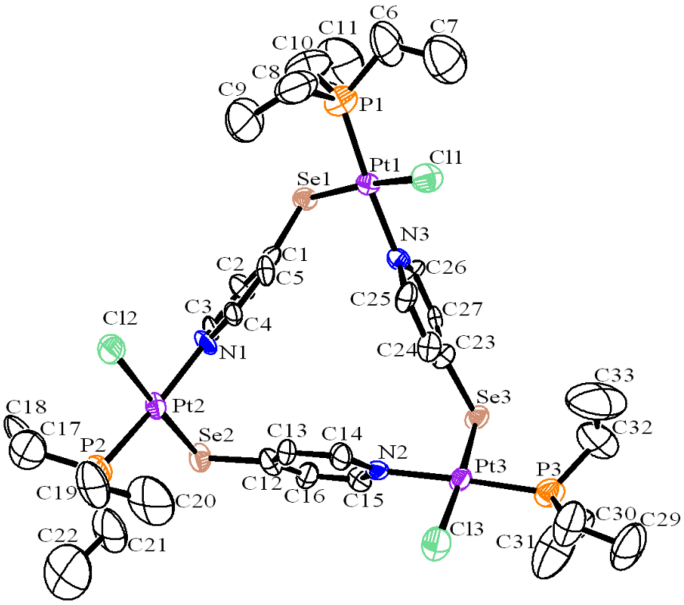

Figure 13. Molecular structure of [PtCl(SeC$_5$H$_4$N-4)(PEt$_3$)]$_3$•CHCl$_3$; ellipsoids drawn at 50% probability. (Hydrogen atoms and solvent molecules are omitted for clarity)

Suzuki C–C Coupling Reaction

The complexes *trans*-[PdCl(SeC$_5$H$_4$N-4)(PPh$_3$)$_2$] and [PdCl(SeC$_5$H$_4$N-4)(PPh$_3$)]$_n$ were examined as catalysts in Suzuki cross-coupling reactions of arylbromide and arylboronic acid to yield biaryls (Table 24). Catalysts are tolerant to various functional groups, such as CHO, NO$_2$, COCH$_3$, etc. Cross-coupling yielded products almost quantitatively when electron deficient arylbromides were used (Table 24, entries 6-7). High yields were also obtained (> 82%) when the catalyst concentration was lowered by ten times in the case of electron-deficient arylbromides (Table 24, entries 9-10). The catalytic activity of monomeric complex *trans*-[PdCl(SeC$_5$H$_4$N-4)(PPh$_3$)$_2$] and trimeric-dimeric complex, [PdCl(SeC$_5$H$_4$N-4)(PPh$_3$)]$_n$ are comparable as both gave similar yields of biaryls under similar reaction conditions. As it is commonly believed that catalytically active species are generally monomeric which indirectly also supports the trimer-dimer-monomer equilibrium of [PdCl(SeC$_5$H$_4$N-4)(PPh$_3$)]$_n$ prior to catalyst initiation [155, 180].

Table 24. Suzuki-Miyaura cross-coupling of aryl bromide with phenylboronic acid.[a]

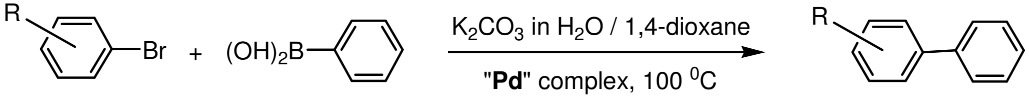

S. No.	R	X	Complex	mol% Pd	Time (hrs)	[b]Yield (%)	TON
1.	4-CH_3	Br	*trans*-[PdCl(SeC_5H_4N-4)(PPh_3)$_2$]	0.1	8	27	270
2.	4-CH_3	Br	*trans*-[PdCl(SeC_5H_4N-4)(PPh_3)$_2$]	0.1	20	39	390
3.	4-CH_3	Br	*trans*-[PdCl(SeC_5H_4N-4)(PPh_3)$_2$]	0.3	8	40	133
4.	4-CH_3	Br	*trans*-[PdCl(SeC_5H_4N-4)(PPh_3)$_2$]	0.5	8	80	160
5.	4-CH_3	Br	[PdCl(SeC_5H_4N-4)(PPh_3)]$_n$	0.1	8	28	280
6.	4-NO_2	Br	*trans*-[PdCl(SeC_5H_4N-4)(PPh_3)$_2$]	0.1	8	91	910
7.	4-NO_2	Br	[PdCl(SeC_5H_4N-4)(PPh_3)]$_n$	0.1	8	97	970
8.	4-NO_2	Br	[PdCl(SeC_5H_4N-4)(PPh_3)]$_n$	0.01	8	62	6200
9.	2-CHO	Br	*trans*-[PdCl(SeC_5H_4N-4)(PPh_3)$_2$]	0.01	6	82	8200
10.	2-CHO	Br	[PdCl(SeC_5H_4N-4)(PPh_3)]$_n$	0.01	6	84	8400
11.	4-$COCH_3$	Br	*trans*-[PdCl(SeC_5H_4N-4)(PPh_3)$_2$]	0.01	12	14	1400
12.	4-$COCH_3$	Br	[PdCl(SeC_5H_4N-4)(PPh_3)]$_n$	0.01	12	29	2900

[a] Reaction conditions: Aryl halide (1.0 mmol), aryl boronic acid (1.3 mmol), K_2CO_3 as base (2 mmol), dioxane (2 mL), H_2O (1 mL).

[b] Isolated yield.

3.2 Chemistry of 3-/4-mercaptobenzoic acid complexes of palladium and platinum

Supra-molecular coordination chemistry has made great strides in the past few decades with the design of ever-increasing families of exotic molecules [95, 181-183]. Three different strategies are generally employed in the design of supra-molecular structures [95, 183], viz., (i) the use of a strong metal-ligand directional bond [95] and flexible hemi-labile ligands [183]; (ii) the use of non-covalent secondary interactions such as π-π stacking, van der Waals and ion-dipole; and (iii) the use of a ligand capable of hydrogen bonding. The latter strategy plays a major role in designing supra-molecular structures [95, 183, 184], widely represented especially by biomolecules in nature. A large number of infinite network of varied dimensions have been generated in organometallic [185, 186] and metallo organic systems based on hydrogen bonding through carboxylic acid group as a supra-molecular connector. When the same –COOH group is present in a ligand possessing another coordination site like N, S donor atoms, predictable assemblies of coordination complexes can be constructed through directional intermolecular interactions.

Mercaptobenzoic acids (H_2 mba) which contain both the –COOH group and a soft donor atom like sulfur have been employed so far in the design of square planar building blocks for the construction of supra-molecular assemblies. Since these are small ligands they can strengthen their coordination with metal ions without any steric hindrance. The 3- and 4-H_2mba (**II** and **III**) posses both a coordinating thiolate and a carboxylic acid group in non-chelating positions [187, 188] stabilize themselves through hydrogen bonding, and serve as a versatile binding motif for the formation of supramolecules. Aurophilic and hydrogen bonding interactions have been thoroughly exploited in supra-molecular gold complexes of 4-H_2mba [187] and 2-H_2mba [189-191].

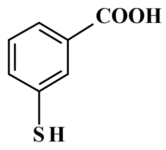

3-H 2 mba

II

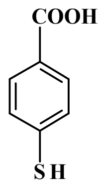

4-H 2 mba

III

Square planar palladium and platinum complexes have been widely used to synthesize supra-molecular architectures. It was considered worthwhile to design supra-molecular assemblies of palladium and platinum containing the 3-/4- H_2mba ligand.

Synthesis of various 3-/4-mercaptobenzoic acid complexes of palladium(II) and platinum(II) is given in Scheme 13. The complex *trans*-$[Pt(SC_6H_4COOH\text{-}4)_2(PEt_3)_2]$ was prepared by two different synthetic routes, viz. (i) reaction of 4-mercaptobenzoic acid (4-H_2mba) with *cis*-$PtCl_2(PEt_3)_2$ in the presence of Et_3N and (ii) treatment of *cis*-$[Pt(PEt_3)_2(OTf)_2]$ with 4-H_2mba in the presence of NaOMe. The *trans*-$[Pt(SC_6H_4COOH\text{-}4)_2(PEt_3)_2]$ existed exclusively in the *trans* form in solution (by NMR) and solid state (X-ray structure, see later). $^{31}P\{^1H\}$ NMR spectrum showed a singlet with ^{195}Pt coupling ($^1J_{Pt\text{-}P}$ = 2484 Hz). The $^{195}Pt\{^1H\}$ NMR spectrum displayed a triplet at –4697 ppm with $^1J(Pt\text{-}P)$ = 2510 Hz.

When the above reaction of 3-/4-H_2mba with $[Pt(PEt_3)_2(OTf)_2]$ or $[M(P^{\cap}P)(OTf)_2]$ either in 1:1 or 2:1 molar ratio was carried out in the absence of any base, binuclear cationic complexes of compositions $[Pt(\mu\text{-}SC_6H_4COOH\text{-}n)(PEt_3)_2]_2(OTf)_2$ (n = 3, 4) and $[M(\mu\text{-}SC_6H_4COOH\text{-}n)(P^{\cap}P)]_2(OTf)_2$ (M/n/$P^{\cap}P$ = Pd/3/dppe, Pd/4/dppe, Pt/4/dppp) were formed exclusively via self-assembly process. Deprotonation of H_2mba with sodium alkoxide and co-ordination of the carboxylate group to the metal centre as in $[R_3Sn(SC_6H_4COO\text{-}4)SnR_3]$ [192] and $[Au(SC_6H_4COOH\text{-}4)(PR_3)]$ [187] has been reported earlier. All the five binuclear complexes ([Pt(SC_6H_4COOH-3)(PEt_3)$_2$]$_2$(OTf)$_2$, [Pt(SC_6H_4COOH-4)(PEt_3)$_2$]$_2$·(OTf)$_2$, [Pd(SC_6H_4COOH-3)(dppe)]$_2$(OTf)$_2$, [Pd(SC_6H_4COOH-4)(dppe)]$_2$(OTf)$_2$ and [Pt(SC_6H_4COOH-4)(dppp)]$_2$(OTf)$_2$) displayed a single sharp peak in their ^{31}P NMR spectra indicating magnetic equivalence of two phosphorus nuclei both in complexes containing monodentate and chelating phosphines. The *cis* orientation of monodentate phosphines is assigned by increased ^{1}J(Pt-P) values 2891 Hz for [Pt(SC_6H_4COOH-3)(PEt_3)$_2$]$_2$(OTf)$_2$ and 2903 Hz for [Pt(SC_6H_4COOH-4)(PEt_3)$_2$]$_2$·(OTf)$_2$ (Figures 14 and 15). The free –COOH group has been identified as singlets at δ ≈166 ppm for [Pt(SC_6H_4COOH-3)(PEt_3)$_2$]$_2$(OTf)$_2$ and [Pt(SC_6H_4COOH-4)(PEt_3)$_2$]$_2$·(OTf)$_2$ in ^{13}C{^{1}H} NMR spectra. A single ^{19}F resonance is observed at δ -81.6 and -80.1 ppm in ^{19}F{^{1}H} NMR spectra of [Pt(SC_6H_4COOH-4)(PEt_3)$_2$]$_2$·(OTf)$_2$ and [Pd(SC_6H_4COOH-4)(dppe)]$_2$(OTf)$_2$, respectively.

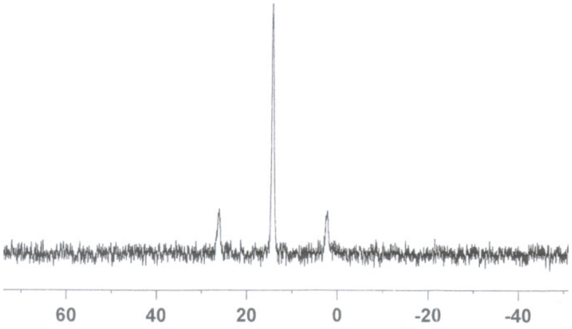

Figure 14. ^{31}P{^{1}H} NMR spectrum of [Pt(SC_6H_4COOH-4)(PEt_3)$_2$]$_2$·(OTf)$_2$ in CH_3OD

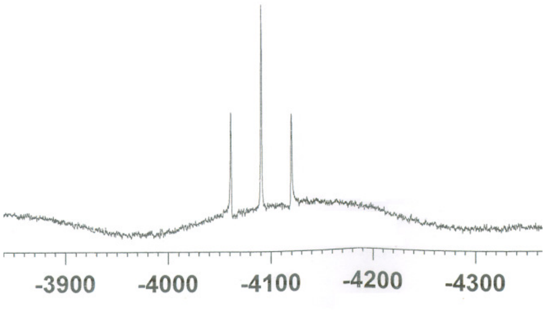

Figure 15. ^{195}Pt{^{1}H} NMR spectrum of of [Pt(SC_6H_4COOH-3)$_2$(dppmin CD_3OD

The reaction of *cis*-$Pt(PEt_3)_2(OTf)_2$ with one equivalent of Na_2(4-mba) yielded three products $[Pt(SC_6H_4COOH\text{-}4)_2(PEt_3)_2]$ and $[Pt(SC_6H_4COOH\text{-}4)(PEt_3)_2]_2\cdot(OTf)_2$ and a complex tentatively assigned as *cis*-$[Pt(SC_6H_4COOH\text{-}4)_2(PEt_3)_2]$ (12.3 ppm, ^1J(Pt-P) = 2887 Hz) in 1:1:0.3 ratio from $^{31}P\{^1H\}$ NMR integration. When the same reaction was carried out with one equivalent of Na_2(4-mba) which was prepared from NaOH instead of NaOMe, the same three products were obtained in 1:1.4:1.2 ratio.

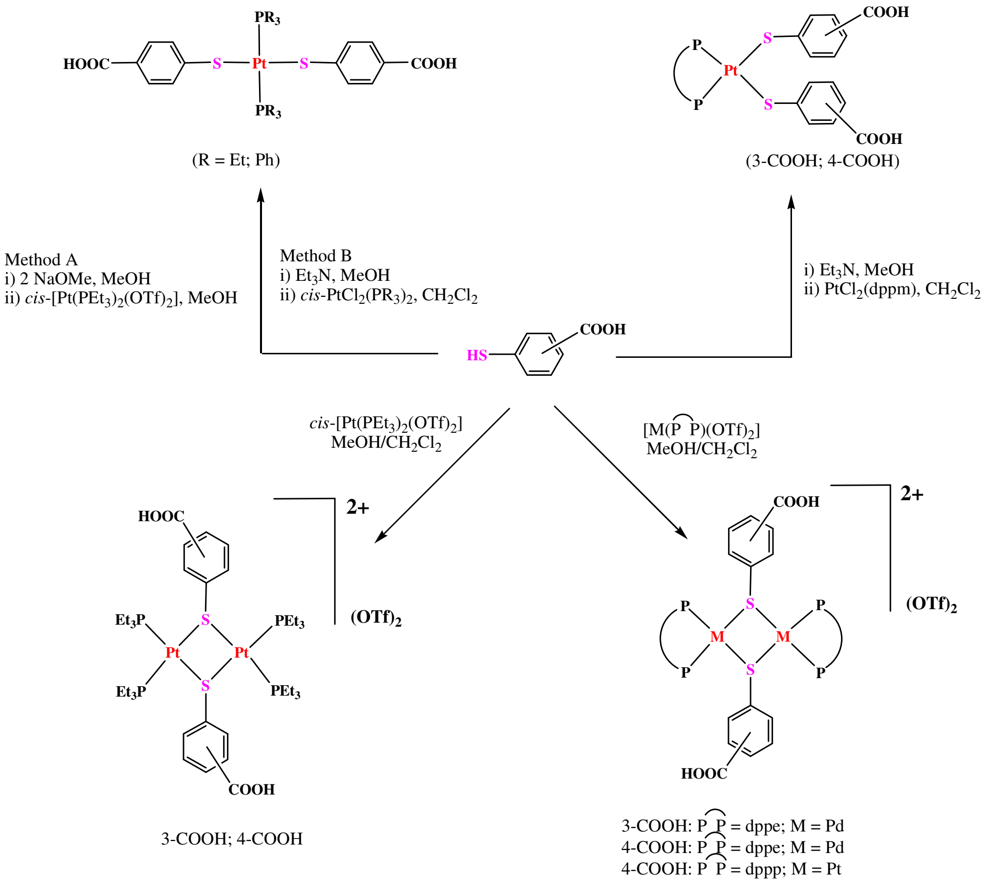

Scheme 13. Synthesis of 3-/4-mercaptobenzoic acid complexes of palladium and platinum

Treatment of $PtCl_2(PPh_3)_2$ and $PtCl_2$(dppm) with H_2mba in 1:2 molar ratio in the presence of triethylamine in refluxing methanol yielded mononuclear complexes, $[Pt(SC_6H_4COOH\text{-}4)_2(PPh_3)_2]$ and *cis*-$[Pt(SC_6H_4COOH\text{-}n)_2(dppm)]$ (n = 3, 4) which are often contaminated with one equivalent of $Et_3N\cdot HCl$. The ^{31}P NMR spectrum of these complexes displayed a single resonance with ^{195}Pt coupling indicative of only one isomeric form in solution. Since both PPh_3 and aryl thiolate groups have similar trans influence [193, 194], the magnitude of $^1J(Pt\text{-}P)$ coupling constants serve little diagnostic purpose in assigning the configuration (*cis* or *trans*) of $[Pt(SC_6H_4COOH\text{-}4)_2(PPh_3)_2]$. The X-ray analysis reveals the *trans* configuration for $[Pt(SC_6H_4COOH\text{-}4)_2(PPh_3)_2]$.

All the complexes are off-white to yellow crystalline stable solids. They are soluble in methanol and acetone but insoluble or sparingly soluble in other common organic solvents such as dichloromethane, chloroform, ether, THF, benzene or toluene. The uv-vis spectra of these complexes in methanol showed strong absorptions in the UV region (Table 25). The mononuclear yellow complex $[Pt(SC_6H_4COOH\text{-}4)_2(PEt_3)_2]$ displayed a relatively low energy broad band at about 341 nm ($\varepsilon \approx 27000\ M^{-1}cm^{-1}$) whereas binuclear off-white complexes $[Pt(SC_6H_4COOH\text{-}3)(PEt_3)_2]_2(OTf)_2$ and $[Pt(SC_6H_4COOH\text{-}4)(PEt_3)_2]_2{\bullet}(OTf)_2$ showed bands at 299 nm ($\varepsilon \approx 24300\ M^{-1}cm^{-1}$) and 294 nm ($\varepsilon \approx 27600\ M^{-1}cm^{-1}$) respectively. These bands may be assigned due to allowed thiolate (HOMO) to phosphine or phosphine mixed with Pt(II) (LUMO) charge transfer transitions. The hypsochromic shift of the band in $[Pt(SC_6H_4COOH\text{-}_3)(PEt_3)_2]_2(OTf)_2$ and $[Pt(SC_6H_4COOH\text{-}4)(PEt_3)_2]_2{\bullet}(OTf)_2$ may be due to changed coordination environment and binding modes of the similar ligands to the Pt(II) center. In the cases of $[Pt(SC_6H_4COOH\text{-}3)(PEt_3)_2]_2(OTf)_2$ and $[Pt(SC_6H_4COOH\text{-}4)(PEt_3)_2]_2{\bullet}(OTf)_2$, binuclear complexes with cis-coordinated ligands, the greater orbital overlap between phosphine with Pt(II) makes stronger back bonding interaction which destabilizes the LUMO. This is also supported by larger $^1J(Pt\text{-}P) \approx 2900$ Hz coupling constants for $[Pt(SC_6H_4COOH\text{-}3)(PEt_3)_2]_2(OTf)_2$ and $[Pt(SC_6H_4COOH\text{-}4)(PEt_3)_2]_2{\bullet}(OTf)_2$ than for $[Pt(SC_6H_4COOH\text{-}4)_2(PEt_3)_2]$ ($^1J(Pt\text{-}P) \approx 2500$ Hz) in ^{31}P NMR spectra. In the visible region the low-energy electronic transition from ligand (Se or Te)-to-ligand (PR_3) charge transfer transitions (LLCT) has been observed by us in complexes $[MCl(E^{\frown}N)(PR_3)]$ (E = Se, Te; $E^{\frown}N$ = 2-/4-EC_5H_4N [61], $ECH_2CH_2NMe_2$[54, 55]).

The IR spectra exhibited sharp υ C=O band at 1672, 1712 and 1699 cm^{-1} for trans-$[Pt(SC_6H_4COOH\text{-}4)_2(PEt_3)_2]$, $[Pt(SC_6H_4COOH\text{-}3)(PEt_3)_2]_2(OTf)_2$ and $[Pt(SC_6H_4COOH\text{-}4)(PEt_3)_2]_2{\bullet}(OTf)_2$ indicating the presence of free -COOH groups. The variation is due to the different mode of association and involvement of solvent and counter-anion in the H-bonding. For example the vibration at higher frequency for C=O group in $[Pt(SC_6H_4COOH\text{-}3)(PEt_3)_2]_2(OTf)_2$ indicates that they are relatively unperturbed compared to the C=O groups in $[Pt(SC_6H_4COOH\text{-}4)_2(PEt_3)_2]$ and $[Pt(SC_6H_4COOH\text{-}4)(PEt_3)_2]_2{\cdot}(OTf)_2$ which is supported by crystal structure in which the C=O groups in $[Pt(SC_6H_4COOH\text{-}3)(PEt_3)_2]_2(OTf)_2$ are not involved in H-bonding.

Molecular Structures

Crystal and molecular structures of $[Pt(SC_6H_4COOH\text{-}4)_2(PEt_3)_2].2MeOH$, $[Pt(SC_6H_4COOH\text{-}4)_2(PEt_3)_2].H_2O$, $[Pt(SC_6H_4COOH\text{-}4)_2(PPh_3)_2]$, $[Pt(SC_6H_4COOH\text{-}3)(PEt_3)_2]_2(OTf)_2$, $[Pt(SC_6H_4COOH\text{-}4)(PEt_3)_2]_2.(OTf)_2$ and $[Pd(SC_6H_4COOH\text{-}3)(dppe)]_2(OTf)_2$ have been established by single crystal X-ray diffraction analyses. The ORTEP drawings with crystallographic numbering scheme are shown in Figures 16-21, and the selected inter-atomic parameters are given in Tables 26-29.

Table 25. Spectroscopic Data for 3-/4-mercaptobenzoic acid complexes of palladium(II) and platinum(II)

Complex	UV-Vis (CH_2Cl_2) λ_{max} in nm (ε in M^{-1} cm^{-1})	^{1}H NMR data in (δ ppm)	$^{13}C\{^{1}H\}$ NMR data in (δ ppm)	$^{31}P\{^{1}H\}$ NMR data in (δ ppm)
$[Pt(SC_6H_4COOH\text{-}4)_2(PEt_3)_2]$[a]	266(16000), 341(27000)	7.65 (d, $^{3}J_{HH}$ = 8.1 Hz, 4H, 2,6-H, Ph), 7.48 (d, $^{3}J_{HH}$ = 7.8 Hz, 4H, 3,5-H, Ph), 1.92 (br m, 12H, PCH_2), 1.05 (m, 18H, PCH_2CH_3)	–	10.6 (s, $^{1}J_{Pt\text{-}P}$ = 2484 Hz)
$[Pt(SC_6H_4COOH\text{-}3)(PEt_3)_2]_2(OTf)_2$[b]	231(89800), 253(83800), 279(45700), 299(24300)	8.86 (s, 2H, 2-H), 8.22 (d, $^{3}J_{HH}$ = 7.2 Hz, 2H, 6-H), 8.00 (d, $^{3}J_{HH}$ = 7.5 Hz, 2H, 4-H), 7.61 (t, $^{3}J_{HH}$ = 7.8 Hz, 2H, 5-H), 1.04 (br m, 36H, PCH_2CH_3), the peak corresponds to PCH_2 merge with the solvent peak at δ 2.05	165.7 (s, -COOH), 137.7 (s, C-2), 136.5 (s, C-6), 133.9 (s, C-1), 132.1 (s, C-3), 130.4, 130.2 (each s, C-5, C-4), 119.3 (q, $^{1}J_{CF}$ = 302 Hz, OTf), 15.4 (m, PCH_2), 7.7 (s, PCH_2CH_3)	16.2 (s, $^{1}J_{Pt\text{-}P}$ = 2891 Hz)
$[Pt(SC_6H_4COOH\text{-}4)(PEt_3)_2]_2(OTf)_2$[a,c]	(47800), 250(47200), 260(44000), 279(36400), 294(sh, 27600)	8.14 (m, 8H, Ph), 1.93 (m, 24H, PCH_2), 1.01 (m, 36H, PCH_2CH_3)	166.8 (s, -COOH), 138.5 (s, C-4), 134.9 (s, C-5), 132.2 (s, C-1), 130.5 (s, C-6), 15.1 (br m, PCH_2), 7.2 (s, PCH_2CH_3), not observed (OTf)	14.2 (s, $^{1}J_{Pt\text{-}P}$ = 2903 Hz)

$[Pd(SC_6H_4COOH\text{-}3)(dppe)]_2(OTf)_2$[a]	–	8.45 (s, 2H, 2-H), 7.68-7.37 (m, 40H, Ph), 6.49 (t, $^3J_{HH}$ = 7.8 Hz, 2H, 5-H), 6.13 (d, $^3J_{HH}$ = 8.4 Hz, 4-H), 2.55 (d, $^2J_{PH}$ = 23.7 Hz, 8H, PCH_2)	–	66.2 (s)
$[Pd(SC_6H_4COOH\text{-}4)(dppe)]_2(OTf)_2$[a]	-	7.61 (t, $^3J_{HH}$ = 7.4 Hz, 8H, p-H, Ph), 7.52 (m, 16H, o-H, Ph), 7.44 (m, 16H, m-H, Ph), 7.19 (d, $^3J_{HH}$ = 8.0 Hz, 4H, 2,6-H), 6.85 (d, $^3J_{HH}$ = 7.6 Hz, 4H, 3,5-H), 2.64 (d, $^2J_{PH}$ = 17.1 Hz, 8H, PCH_2)		65.4 (s)
$[Pt(SC_6H_4COOH\text{-}4)(dppp)]_2(OTf)_2$[b,d]	-	8.03 (s), 7.81 (br t), 7.54 (br m), 7.35 (s), 6.77 (m), 1.27 (s), 1.10 (t)	–	0.1 (s, $^1J_{Pt\text{-}P}$ = 2809 Hz)
$[Pt(SC_6H_4COOH\text{-}4)_2(PPh_3)_2]$[a]	–	7.48 - 7.35 (m, 16H, o-H, Ph; 2,6-H, Ph), 7.32 (t, $^3J_{HH}$ = 7.3 Hz, 6H, p-H, Ph), 7.23 (d, $^3J_{HH}$ = 8.1 Hz, 4H, 3,5-H, Ph), 7.16 (t, $^3J_{HH}$ = 7.3 Hz, 12H, m-H, Ph)	–	19.7 (s, $^1J_{Pt\text{-}P}$ = 2985 Hz)
$[Pt(SC_6H_4COOH\text{-}3)_2(dppm)]$[a#]	–	7.83 (s, 2H, 2-H), 7.57 (m, 8H, o-H, Ph), 7.42 (t, $^3J_{HH}$ = 7.2 Hz, 4H, p-H, Ph), 7.33 (t, $^3J_{HH}$ = 7.4 Hz, 8H, m-H, Ph), 7.25 (d, $^3J_{HH}$ = 7.6 Hz, 2H, 6-H), 7.18 (d, $^3J_{HH}$ = 8.0 Hz, 2H, 4-H), 6.52 (t, $^3J_{HH}$ = 7.6 Hz, 2H, 5-H), 3.27 (m, 2H, PCH_2)	–	–48.85 (s, $^1J_{Pt\text{-}P}$ = 2522 Hz)

$[Pt(SC_6H_4COOH\text{-}4)_2(dppm)]$[b]	–	8.14 (m, 8H, Ph), 7.85-7.75 (m, 8H, o-H, Ph), 7.57-7.50 (m, 4H, p-H, Ph), 7.48-7.39 (m, 8H, m-H, Ph), the peak for PCH_2 is merged in the base of the peak due to H_2O present in the solvent.	–	–50.04 (s, $^1J_{Pt\text{-}P}$ = 2465 Hz)

[a] Recorded in methanol-d_4; $^{195}Pt\{^1H\}$ NMR data in (δ ppm) = –4697 (d, $^1J(Pt\text{-}P)$ = 2510 Hz)

#$^{195}Pt\{^1H\}$ NMR data in (δ ppm) =–4090 (t, $^1J(Pt\text{-}P)$ = 2530 Hz)

[b] Recorded in acetone-d_6.

[c] When the spectrum is recorded in 400 MHz instrument, a small peak (~ 5%) is resolved at δ 14.0 ppm in $^{31}P\{^1H\}$ NMR spectra.

[d] A small peak (≈ 10 %) was observed in $^{31}P\{^1H\}$ NMR spectrum at δ 34.4 ppm due to dioxide of dppp.

The complex [Pt(SC_6H_4COOH-4)$_2$(PEt_3)$_2$] crystallizes with solvent molecules, either one molecule of water, [Pt(SC_6H_4COOH-4)$_2$(PEt_3)$_2$]·H_2O (Figure 16) or two molecules of methanol, [Pt(SC_6H_4COOH-4)$_2$(PEt_3)$_2$]·(MeOH)$_2$ (Figure 17). The structure of [Pt(SC_6H_4COOH-4)$_2$(PEt_3)$_2$] in both the solvated molecules is as expected with slightly distorted square-planar (<PPtS ~ 85.75-94.25°) platinum atom coordinated with two thiolate and two PEt_3 ligands which adopts a trans configuration. All the inter-atomic parameters are similar in both water and methanol solvated molecules except the C=O bond distances (Table 26). The crystal lattice of [Pt(SC_6H_4COOH-4)$_2$(PPh_3)$_2$] (Figure 18) has two independent molecules **a** and **b** each with *trans* configuration differing slightly in their inter-atomic parameters (Table 27). A number of mononuclear Pt(II) complexes having *trans*-"PtE_2P_2" moiety (E = S [195-197], Se [91, 173, 174], Te [198]) with arylchalcogenolate and monodentate phosphine ligands have been reported. The centrosymmetric molecule [Pt(SC_6H_4COOH-4)$_2$(PEt_3)$_2$] has two equal Pt–S and Pt–P distances which are in close agreement with the similar distances reported in *trans*-[Pt($SC_6H_3Me_2$-2,6)$_2$(PR_3)$_2$] (R = Me, Et) [195] having two dissimilar Pt–S and Pt–P bond lengths. The Pt–S bond lengths in molecule **a** of [Pt(SC_6H_4COOH-4)$_2$(PPh_3)$_2$] (2.372(2), 2.384(2) Å) are longer than in molecule **b** (2.359(2), 2.339(2) Å), which are slightly higher than the Pt–S bond lengths in similar reported complex *trans*-[Pt(PPh_3)$_2$(SC_6H_4-2-$SiCH_3Ph_2$)$_2$] (2.3402(16), 2.3275(16) Å) [197]. In both the structures of complexes [Pt(SC_6H_4COOH-4)$_2$(PEt_3)$_2$] and [Pt(SC_6H_4COOH-$_4$)$_2$(PPh_3)$_2$] , the benzoic acid substituents of two thiolate ligands are in *anti* position, as noted in *trans*-[Pt($SC_6H_3Me_2$-2,6)$_2$(PEt_3)$_2$] [195]. A *syn* configuration has however, been reported in *trans*-[Pt($SC_6H_3Me_2$-2,6)$_2$(PMe_3)$_2$] [195] and *trans*-[Pt(2-SC_6H_4Cl)$_2$(PPh_3)$_2$] [196, 199].

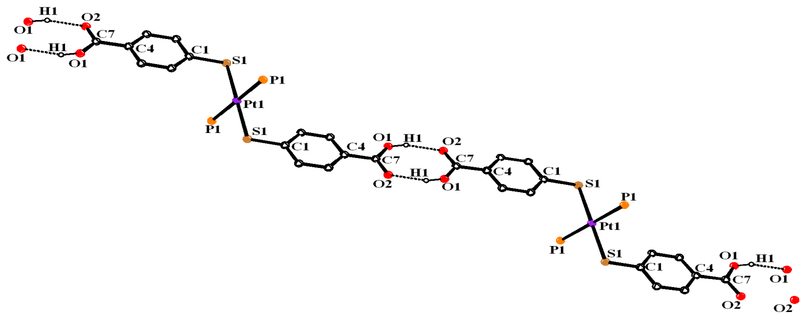

Figure 16. Dimeric unit of 1 aggregated via H-bonding in $[Pt(SC_6H_4COOH\text{-}4)_2(PEt_3)_2]\cdot H_2O$ ($1\cdot H_2O$). The PEt_3 ethyl groups, hydrogen atoms in benzene ring and solvent molecules have been omitted for clarity.

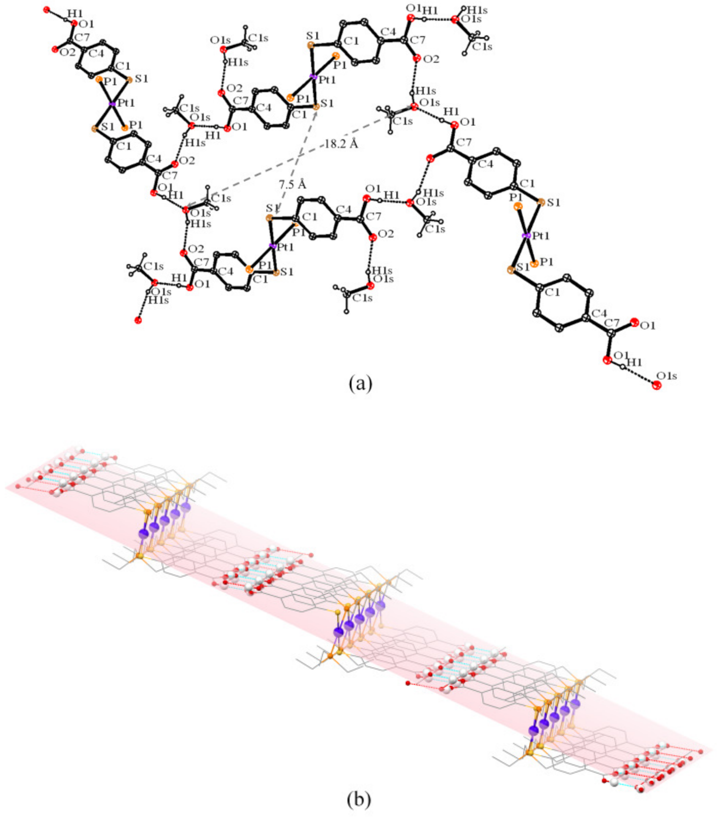

(a)

(b)

Figure 17. (a) Molecular structure of $[Pt(SC_6H_4COOH\text{-}4)_2(PEt_3)_2]\cdot(MeOH)_2$ ($1\cdot(MeOH)_2$) and highlighting their mode of association via H-bonding. The PEt_3 ethyl groups and hydrogen atoms in benzene ring have been omitted for clarity. (b) Two dimensional stair like network of the molecules in $1\cdot(MeOH)_2$ via H-bonding

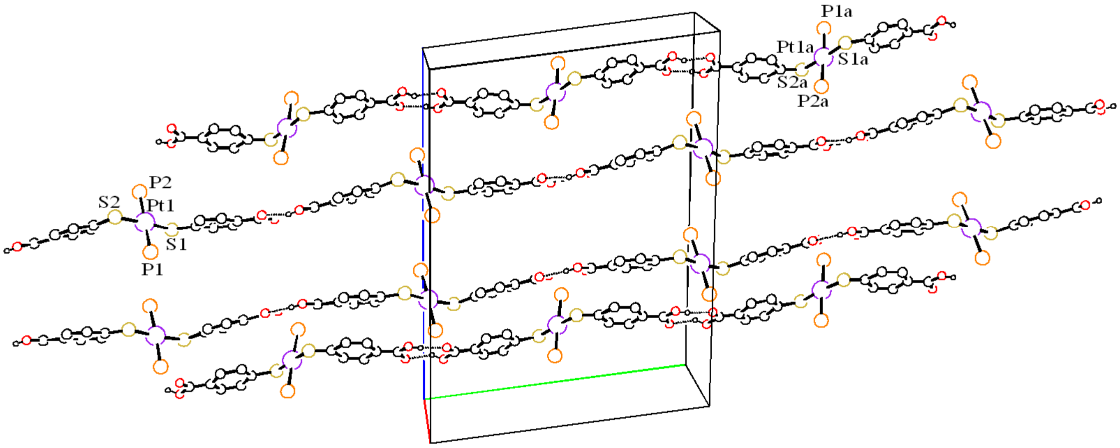

Figure 18. Two layers of molecules **a** and **b** forming ribbons in the crystals of $[Pt(SC_6H_4COOH\text{-}4)_2(PPh_3)_2]$.

Table 26. Selected interatomic distances [Å] and angles [°] of mononuclear neutral complexes *trans*-$[Pt(SC_6H_4COOH\text{-}4)_2(PEt_3)_2]\cdot$solvent (1·solvent)

	$[Pt(SC_6H_4COOH\text{-}4)_2(PEt_3)_2]\cdot H_2O$	$[Pt(SC_6H_4COOH\text{-}4)_2(PEt_3)_2]\cdot(MeOH)_2$
Pt1-S1	2.349(4)	2.358(3)
Pt1-P1	2.319(5)	2.318(3)
S1-C1	1.757(14)	1.737(9)
C4-C7	1.50(2)	1.485(13)
C7-O1	1.27(2)	1.310(11)
C7-O2	1.25(2)	1.228(11)
P1···S1	3.177	3.207
P1···S1#	3.421	3.405
P1-Pt1-S1	85.76(16)	86.54(10)
P1-Pt1-S1#	94.24(16)	93.46(10)
P1-Pt1-P1#	180.000(1)	180.0
Pt1-S1-C1	108.8(5)	108.1(3)
S1-Pt1-S1#	180.000(1)	180.00(10)
Angle Pt sq. plane and Ph ring	75.10	82.49

Table 27. Selected interatomic distances [Å] and angles [°] of mononuclear neutral complexes *trans*-$[Pt(SC_6H_4COOH\text{-}4)_2(PPh_3)_2]$

	molecule **a**	molecule **b**
Pt1-S1	2.372(2)	2.359(2)
Pt1-S2	2.384(2)	2.339(2)
Pt1-P1	2.309(2)	2.321(2)
Pt1-P2	2.311(2)	2.325(2)
S1-C1	1.693(9)	1.758(8)
S2-C8	1.649(10)	1.539(9)
O1-C7	1.248(12)	1.234(12)
O2-C7	1.294(12)	1.320(13)
S1-Pt1-S2	174.75(7)	177.64(8)
P1-Pt1-S1	94.21(7)	93.02(7)
P1-Pt1-S2	85.00(7)	85.19(7)
P1-Pt1-P2	177.47(8)	177.16(7)
P2-Pt1-S1	86.71(7)	89.12(7)
P2-Pt1-S2	94.30(7)	92.62(7)
C1-S1-Pt1	111.1(3)	108.6(3)
C8-S2-Pt1	107.4(3)	109.0(2)

The complexes $[Pt(SC_6H_4COOH\text{-}3)(PEt_3)_2]_2(OTf)_2$ (Figure 19), $[Pt(SC_6H_4COOH\text{-}4)(PEt_3)_2]_2\cdot(OTf)_2$ (Figure 20), $[Pd(SC_6H_4COOH\text{-}3)(dppe)]_2(OTf)_2$ (Figure 21) are centrosymmetric binuclear molecules in which two metal atoms are held together by two bridging thiolato ligands with benzoic acid substituents adopting an *anti* configuration. Except $[Pt(SC_6H_4COOH\text{-}3)(PEt_3)_2]_2(OTf)_2$, crystals of other complexes are solvated. In a similar binuclear complex of d_8 metal, $[Rh(SC_6H_4COOH\text{-}4)(PPh_3)_2]_2$, the *syn-exo* conformer exists in the crystal structure [200]. The R groups on thiolate ligands in complexes of composition $[M_2(\mu\text{-}SR')_2(PR_3)_4]^{2+}$ can adopt either *syn* or *anti* configuration [52]. The complex $[Pt(SC_6H_4COOH\text{-}4)(PEt_3)_2]_2(OTf)_2$ crystallizes with two independent molecules **c** and **d** in an asymmetric unit, which are very similar in their dimensions (Table 28). The two triethylphosphine ligands are *cis*-coordinated to the platinum atom in $[Pt(SC_6H_4COOH\text{-}3)(PEt_3)_2]_2(OTf)_2$ and $[Pt(SC_6H_4COOH\text{-}4)(PEt_3)_2]_2.(OTf)_2$, whereas in $[Pd(SC_6H_4COOH\text{-}3)(dppe)]_2(OTf)_2$ the two *cis* positions are chelated by one dppe ligand to the palladium atom. Although a handful binuclear platinum complexes with "$P_2Pt(\mu\text{-}SAr)PtP_2$" motif are known [201-205], the structures close to $[Pt(SC_6H_4COOH\text{-}3)(PEt_3)_2]_2(OTf)_2$ and $[Pt(SC_6H_4COOH\text{-}4)(PEt_3)_2]_2.(OTf)_2$ are $[Pt(\mu\text{-}SAr)(PEt_3)_2]_2^{2+}$ (Ar = C_6H_5 [202], $C_6H_4C_6H_5$ [201]). The palladium complexes with pyridyl carboxylate ligand and *cis*-blocked phosphine co-ligands generate self-assembled macrocyclic squares, triangles and rectangles [206-208]. Due to the two cis-positioned PEt_3 groups, the P1-Pt1-P2 angle is widened (~ 96.6 – 98.3°) and the S1-Pt1-S1# angle is contracted (~ 81.5°), thus forming a rhombohedral planar Pt_2S_2 ring. The Pt···Pt separation (> 3.61 Å) is more than the sum of van der Waals distances of two platinum atoms reflecting absence of any metal metal intramolecular interaction. The structure of palladium complex ($[Pd(SC_6H_4COOH\text{-}3)(dppe)]_2(OTf)_2 \cdot (H_2O)_2$) is similar to the one reported for $[M_2(\mu\text{-}SC_6F_5)_2(dppe)_2](OTf)_2 \cdot$acetone (M = Pd, Pt) [205].

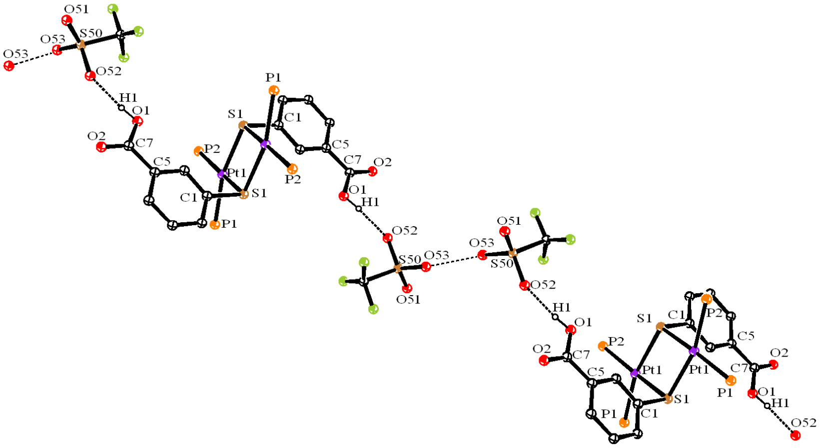

Figure 19. Molecular structure of $[Pt(SC_6H_4COOH\text{-}3)(PEt_3)_2]_2(OTf)_2$ and intermolecular interactions. The PEt_3 ethyl groups and hydrogen atoms in benzene ring have been omitted for clarity.

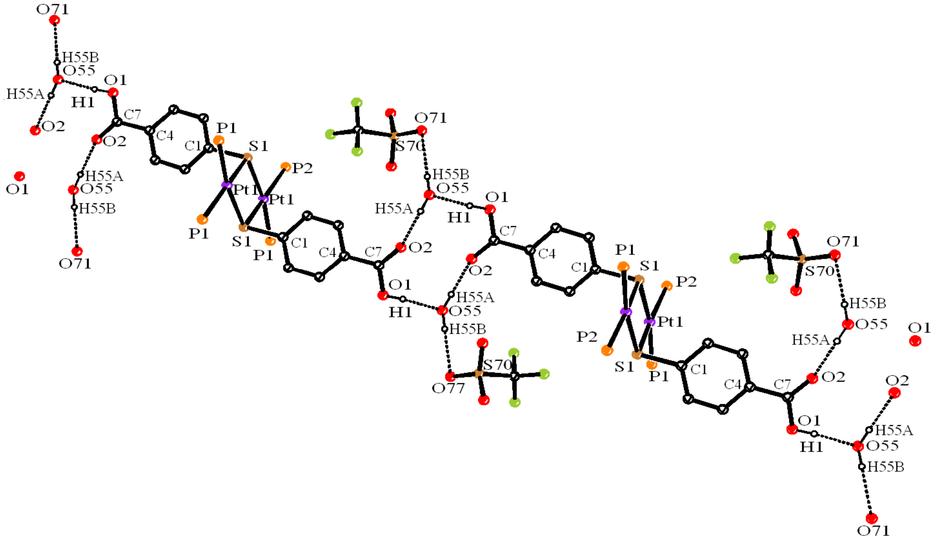

Figure 20. Molecular structure of $[Pt(SC_6H_4COOH\text{-}4)(PEt_3)_2]_2(OTf)_2{\cdot}(H_2O)_2$ and intermolecular H-bonding. The PEt_3 ethyl groups and hydrogen atoms in benzene ring have been omitted for clarity.

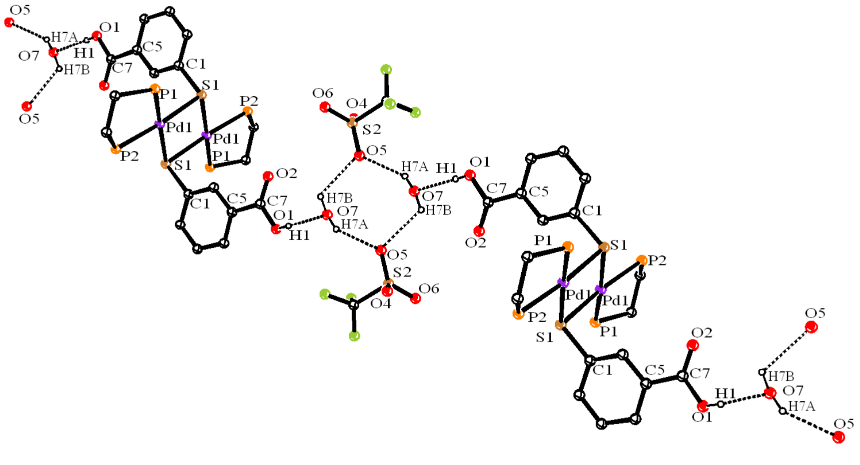

Figure 21. Molecular structure and intermolecular interactions of $[Pd(SC_6H_4COOH\text{-}3)(dppe)]_2(OTf)_2{\cdot}2(H_2O)$. The dppe phenyl groups, hydrogen atoms in benzene ring and dppe have been omitted for clarity.

Table 28. Selected interatomic distances [Å] and angles [°] of dinuclear cationic complexes

	2 (M = Pt)	**3**·$(H_2O)_2$ (M = Pt)		**4**·$(H_2O)_2$ (M = Pd)
		molecule **c**	molecule **d**	
M1-S1	2.3878(18)	2.3764(10)	2.3890(11)	2.408(2)
M1-S1#1	2.3904(18)	2.3845(10)	2.3872(10)	2.403(2)
M1-P1	2.294(2)	2.2907(10)	2.2864(12)	2.277(2)
M1-P2	2.293(2)	2.2979(12)	2.2957(11)	2.268(3)
S1-C1	1.808(7)	1.794(3)	1.796(3)	1.798(9)
C7-C4/C5	1.493(10)	1.491(6)	1.485(5)	1.477(15)
C7-O1	1.320(8)	1.323(7)	1.321(4)	1.324(13)
C7-O2	1.212(8)	1.206(7)	1.214(4)	1.205(14)
M1···M1 intramolecular	3.612	3.615	3.628	3.462
P1-M1-P2	98.26(7)	96.97(4)	96.62(4)	84.94(9)
P1-M1-S1	165.32(6)	170.48(3)	169.49(3)	172.92(9)
P2-M1-S1	93.23(7)	90.15(4)	90.57(4)	91.96(9)
P1-M1-S1#	87.96(7)	92.53(4)	92.99(4)	95.81(9)
P2-M1-S1#	170.87(6)	168.39(3)	167.08(3)	173.90(9)
S1-M1-S1#	81.79(7)	81.20(4)	81.15(4)	87.95(8)
M1-S1-M1#	98.21(7)	98.80(4)	98.85(4)	92.05(8)
M1-S1-C1	98.3(2)	101.92(12)	99.27(10)	100.9(3)
Angle between "M_2S_2" plane and Ph ring	89.60	83.96	83.79	88.31

General trend of hydrogen bonding

All the complexes with two free carboxylic acid groups are involved in intermolecular H-bonding with various patterns (Schemes 14 and 15) which are described by graph sets[209, 210]. The donor and acceptor groups and the geometrical features such as donor-acceptor separation (D···A), D-H-A angles, etc. were calculated by Mercury [211] program and are summarized in Table 29. In the present examples, the carboxyl dimer synthon [212] is formed in $[Pt(SC_6H_4COOH\text{-}4)_2(PEt_3)_2].H_2O$ (Scheme 14) and $[Pt(SC_6H_4COOH\text{-}4)_2(PPh_3)_2]$, whereas in the solid state structures of $[Pt(SC_6H_4COOH\text{-}4)(PEt_3)_2]_2.(OTf)_2.2(H_2O)$ (Scheme 15) and $[Pd(SC_6H_4COOH\text{-}3)(dppe)]_2(OTf)_2.2(H_2O)$ (Scheme 15), water and counter-anion are involved in hydrogen bonding and consequently interrupting the carboxyl dimer synthons. The dimer formation is also prevented by MeOH in $[Pt(SC_6H_4COOH\text{-}4)_2(PEt_3)_2].2(MeOH)$ instead a large network resulted (Scheme 14). Similarly, the triflate ion in $[Pt(SC_6H_4COOH\text{-}3)(PEt_3)_2]_2(OTf)_2$ prevents dimerization leading to an open chain structure (Figure 19, Scheme 15). The zig-zag coordination polymer of palladium complexes of *cis*-blocked phosphines are reported with pyridyl carboxylate ligand without any H-bonding [207]. This is due to the presence of strong H-bond donor hydroxyl group in H_2O and MeOH, and strong H-bond acceptor SO group in triflate ion [213].

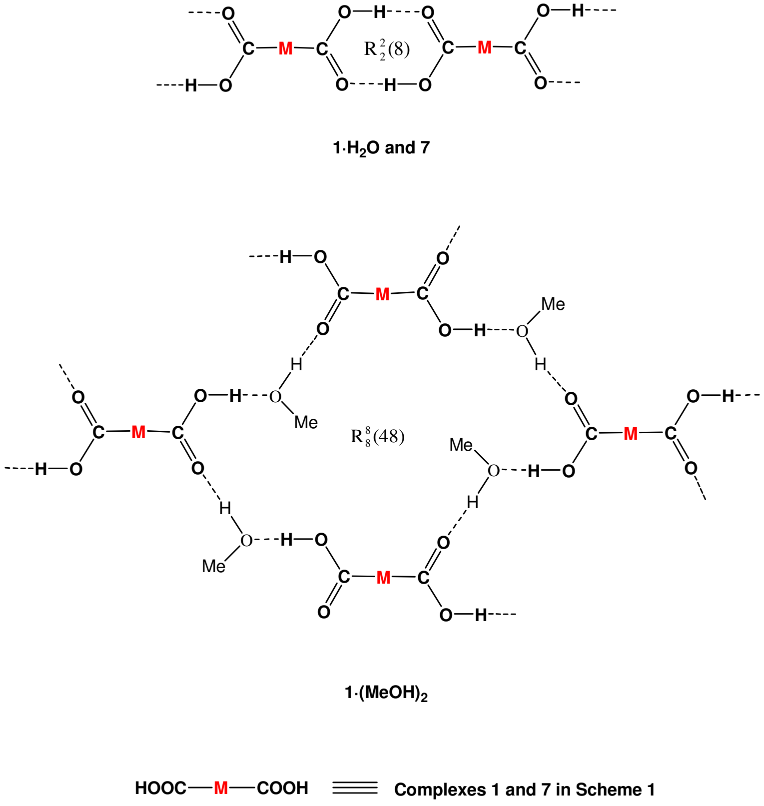

Scheme 14. H-bonding pattern in the crystals of mononuclear complexes

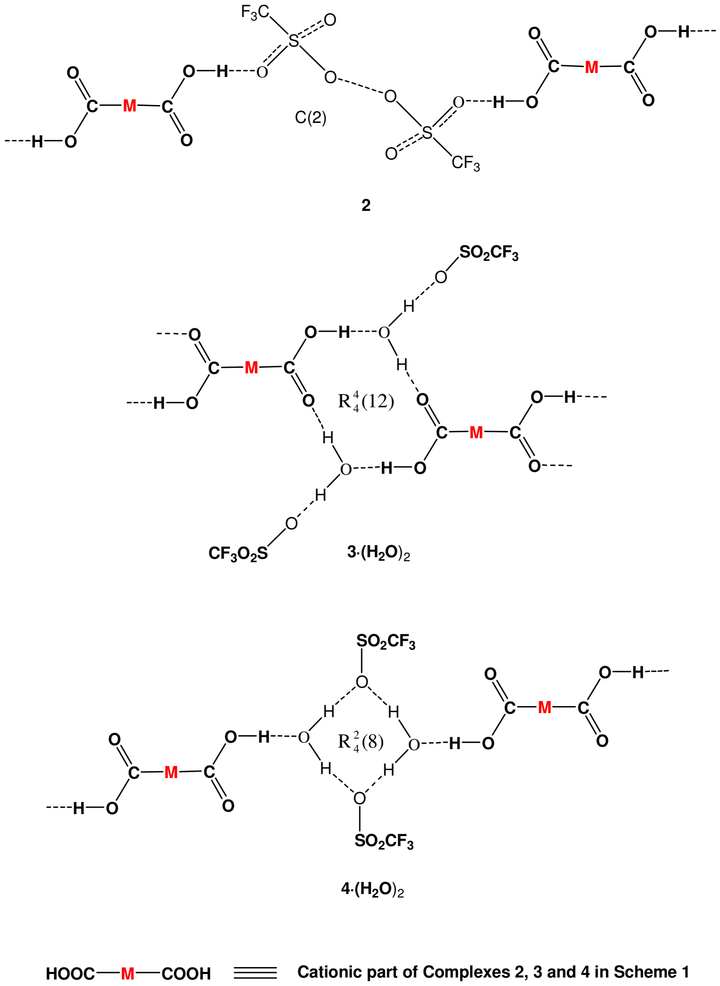

Scheme 15. H-bonding pattern in the crystals of dinuclear complexes

Hydrogen bonding in mononuclear complexes

In $[Pt(SC_6H_4COOH\text{-}4)_2(PEt_3)_2].H_2O$ and $[Pt(SC_6H_4COOH\text{-}4)_2(PPh_3)_2]$ crystallographically equivalent monomers are linked through hydrogen bonding typical for familiar carboxylic acids. The system is formed by the dimerization of two free carboxylic acid groups. The infinite repeating dimer pattern of one dimensional zigzag chain is formed through hydrogen bonding, as observed in dicarboxylic acid, such as terephthalic acid. In $[Pt(SC_6H_4COOH\text{-}4)_2(PEt_3)_2].H_2O$ the water molecule is situated in the lattice and do not take part in the cyclic ring formation of dimer. The average plane of 8-membered ring formed by the two carboxylic acid groups is almost coplanar (~7.85°) with the phenyl ring in $[Pt(SC_6H_4COOH\text{-}4)_2(PEt_3)_2] \cdot H_2O$. Whereas the same 8-membered ring deviates from planarity in $[Pt(SC_6H_4COOH\text{-}4)_2(PPh_3)_2]$ and forms puckered structure due to the deviation of donor–H–acceptor angles (D–H…A) from the linearity such as O4–H4···O1 (159.67°, Table 29). Both crystals contain “ribbons” of molecules inter linked via hydrogen bonding. In the crystal of $[Pt(SC_6H_4COOH\text{-}4)_2(PPh_3)_2]$ two types of ribbons and the corrugated sheets are formed by two independent molecules **a** and **b** stacking up along the *c*-axis (Figure 18). The overall structural feature have similarity with the reported complexes *trans*-$[PdCl_2(NC_5H_4COOH\text{-}4)_2]$ [214].

In the structure of $[Pt(SC_6H_4COOH\text{-}4)_2(PEt_3)_2].2(MeOH)$, methanol takes part in intermolecular H-bonding between two –COOH of two adjacent molecules and forms a large ring of the type (Scheme 14). The carboxylic acid groups in each molecule act as donor and acceptor. The –COOH groups of the neighbouring molecules are connected in head to tail fashion via one MeOH molecule, thus forming a stair like 2D network (Figure 17) of macrocyclic ring systems linked by two independent O–H···O interactions (Table 29). The macrocycle possesses a large cavity of dimension (18.2 × 7.5 Å) (Figure 17, O1S···O1S, S1···S1 distances, respectively) having potential for inclusion of guest molecules.

Hydrogen bonding in cationic binuclear complexes

The $[Pt(SC_6H_4COOH\text{-}4)(PEt_3)_2]_2.(OTf)_2$ and $[Pd(SC_6H_4COOH\text{-}3)(dppe)]_2(OTf)_2$ crystallize with two molecules of water; accordingly hydrogen bonding pattern is different from $[Pt(SC_6H_4COOH\text{-}3)(PEt_3)_2]_2(OTf)_2$. The two oxygen atoms of triflate anions in $[Pt(SC_6H_4COOH\text{-}3)(PEt_3)_2]_2(OTf)_2$ take part in two distinct non-covalent interactions, one is H-bonding (S-O: 1.446 (7) Å) with the proton of the carboxylic acid group and the other is van der Waals interactions (S-O: 1.597 (10) Å) of similar oxygen atom (O···O: 2.832 Å) of another triflate anion leading to the formation of an infinite linear chain (Figure 19). The third oxygen with shorter S-O bond (S-O: 1.380 (9) Å) is not involved in any interaction.

The supra-molecular synthons of carboxyl dimers with rings of graph set $R_4^4(12)$ and $R_4^2(8)$ are formed in $[Pt(SC_6H_4COOH\text{-}4)(PEt_3)_2]_2\cdot(OTf)_2\cdot 2(H_2O)$ and $[Pd(SC_6H_4COOH\text{-}3)(dppe)]_2(OTf)_2.2(H_2O)$, with the help of H_2O and triflate anion, respectively. In $[Pt(SC_6H_4COOH\text{-}4)(PEt_3)_2]_2.(OTf)_2.(H_2O)$ both C=O and O-H groups make the 12-membered ring and OTf remain outside of this ring (Figure 20, Scheme 14) whereas in the case of $[Pd(SC_6H_4COOH\text{-}3)(dppe)]_2(OTf)_2\cdot 2(H_2O)$ one of the O atom of triflate anion participates in hydrogen bonding with water to give $R_4^2(8)$. The oxygen atoms of the water molecules of this ring make contact with carboxylic groups leading to the formation of infinite one-dimensional chain. One of the H-bonding interactions O7-H7A···O5 in $[Pd(SC_6H_4COOH\text{-}3)(dppe)]_2(OTf)_2\cdot 2(H_2O)$ is bent (125°) and longer one (H7A···O5: 2.239 Å) falls in the category of weak hydrogen bond [215].

Table 29. Intermolecular Hydrogen bonding interactions and associated distances (distances in Å, angles in deg) in crystalline complexes.

Crystal	D-H···A	D-H	H···A	D···A	D-H···A	$\mathrm{CF_3SO_3}$ anion	
$\mathrm{[Pt(SC_6H_4COOH\text{-}4)_2(PEt_3)_2]\cdot H_2O}$	O1-H1···O2	1.3(2)	1.294	2.602	178.39		
$\mathrm{[Pt(SC_6H_4COOH\text{-}4)_2(PEt_3)_2]\cdot (MeOH)_2}$	O1-H1···O1S	0.8200	1.796	2.612	173.12		
	O1S-H1S···O2	0.8200	1.872	2.670	163.75		
$\mathrm{[Pt(SC_6H_4COOH\text{-}3)(PEt_3)_2]_2(OTf)_2}$	O1-H1···O52	0.84	1.8	2.636	174.27	S50-O51	1.380(9)
						S50-O52	1.446(7)
						S50-O53	1.597(10)
						O53···O53	2.832
$\mathrm{[Pt(SC_6H_4COOH\text{-}4)(PEt_3)_2]_2\cdot (OTf)_2\cdot (H_2O)_2}$	O1-H1···O55	0.8399	1.712	2.55	175.72	S70-O71	1.451(4)
	O55-H55A···O2	0.8501	1.909	2.759	179.71	S70-O73	1.426(3)
	O55-H55B···O71	0.85	2.155	3.005	179.25	S70-O72	1.420(4)
$\mathrm{[Pd(SC_6H_4COOH\text{-}3)(dppe)]_2(OTf)_2\cdot (H_2O)_2}$	O1-H1···O7	0.8200	1.845	2.638	162.13	S2-O4	1.381(11)
	O7-H7A···O5	0.8500	2.239	2.813	124.84	S2-O5	1.378(11)
	O7-H7B···O5	0.8501	2.103	2.832	143.62	S2-O6	1.458(14)
	O2-H2···O3	0.8400	1.830	2.665	171.30		
$\mathrm{[Pt(SC_6H_4COOH\text{-}4)_2(PPh_3)_2]}$	O4-H4···O1	0.8400	1.773	2.578	159.67		

A comparison of all hydrogen bonds (Table 29) shows that the donor-acceptor distances are comparatively shortened in structures, $[Pt(SC_6H_4COOH\text{-}4)_2(PEt_3)_2]\cdot H_2O$ (2.602 Å), $[Pt(SC_6H_4COOH\text{-}4)(PEt_3)_2]_2\cdot(OTf)_2\cdot(H_2O)_2$ (2.550 Å) and $[Pt(SC_6H_4COOH\text{-}4)_2(PPh_3)_2]$ (2.578 Å) than those found in other structures, possibly due to stronger H-bond interactions. In the case of Fe(II) and Co(III) complexes containing ligands with free COOH groups it has been observed that the O···O i.e., donor-acceptor separations, does not depend on the neutral or ionic nature of the complexes [184]. Among the five structures having H-bonded rings, the nearly equal C=O distances (1.25(2), 1.27(2) Å) which are intermediate between single and double bond distances of C=O bond in –COOH group indicates the equal sharing of H atom between the two oxygen atoms of carboxylic acid [191]. Nearly equal CO distances reported in $[PdCl_2(NC_5H_4COOH\text{-}3)_2]$ has been attributed to crystallographic disorder arising from strong H-bonding [214].

3.3 Chemistry of aryldithiolate complexes of palladium and platinum

Among the transition series, d^8 metal ions such as Rh(I), Pd(II) and Pt(II), have been extensively used to construct the supra-molecular structures due to their well-defined square planar geometry. A library of closed and discrete two- (square, triangle, rectangle, etc.) and three-dimensional (tetrahedra, cubes, octahedra, pyramids, etc.) architectures have been constructed by capping two *cis*-positions with phosphines/amines of the metal square plane, making use of several pyridyl based ligands [95, 215-219]. Thiolate ligands have hardly been employed to design supra-molecular coordination complexes (SCCs) due to their high propensity to act as a bridging ligand thus leading to oligomerization of resulting metal complexes which are either insoluble or sparingly soluble in organic solvents, limiting their utility as functional material.

Ligand structures are equally critical to determine the overall architecture besides metal ion stereochemistry. A bridging ligand capable to coordinate multiple metal ions together in a well-defined configuration must be conformationally rigid or at least restricted [220]. Accordingly, the S atom linked to the rigid aromatic back bone (e.g., phenyl, biphenyl) in combination with other donor atoms at *para*- or *meta*-position is a good choice in the formation of supra-molecular structures. The ligands containing two S donor atoms symmetrically separated by a rigid aromatic core have not been explored as building blocks to prepare functional SCCs of Pd and Pt, whereas the flexible and hemilabile hetero-ligands containing phosphine and chalcogen (S, Se) groups are used for the synthesis of palladium and platinum macrocyclic structures *via* weak-link approach [221]. These dithiolate ligands (**IV – VI**) are versatile to act in bridging mode as well as the same S donor atom can bridge two different metal centers. Thus aryl dithiolate ligands IV-VI were chosen to design palladium and platinum supra-molecular coordination complexes.

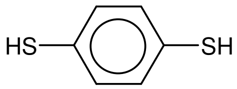

IV

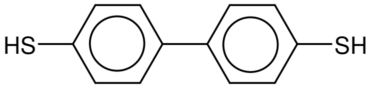

V

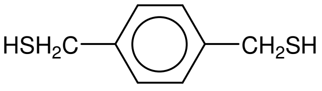

VI

Treatment of metal *cis*-triflate complexes ($[Pd(dppe)(OTf)_2]$ and $[Pt(PEt_3)_2(OTf)_2]$) with aryldithiols in 2:1 stoichiometry at room temperature afforded corresponding palladium ($[Pd_2(SC_6H_4S)(dppe)_2]_2(OTf)_4$, $[Pd_2(SC_{12}H_8S)(dppe)_2]_2(OTf)_4$, $[Pd_2(SCH_2C_6H_4CH_2S)(dppe)_2]_4(OTf)_8$) and platinum ($[Pt_2(SC_6H_4S)(PEt_3)_4]_2(OTf)_4$, $[Pt_2(SC_{12}H_8S)(PEt_3)_4]_2(OTf)_4$, $[Pt_2(SCH_2C_6H_4CH_2S)(PEt_3)_4]_4(OTf)_8$) complexes in nearly quantitative yields (Scheme 16). The resulting complexes were characterized by analytical and spectroscopic data and also by X-ray structural analyses. Although the complexes are of high molecular weights ($[Pd_2(SCH_2C_6H_4CH_2S)(dppe)_2]_4(OTf)_8$: 5904 Da; $[Pt_2(SCH_2C_6H_4CH_2S)(PEt_3)_4]_4(OTf)_8$: 5317 Da) and possesses 4 or 8 charges, they are highly soluble in acetone, methanol and dichloromethane. A sharp singlet in the ^{31}P NMR spectra with associated Pt satellites in the case of the Pt complexes (Figure 22) is consistent with the highly symmetric macrocyclic structures [216, 222]. The singlet at about –78 ppm in ^{19}F NMR spectra is indicative of triflate anion. The microanalysis and integration of the ^{1}H NMR signals (Figure 23) suggest the metal to ligand ratio is 2:1 with the general formula $[M_2\{SX(C_6H_4)_nXS\}]_m(OTf)_{2m}$ ($m = 2$ or 4) of the complexes. The chemical shift for the phenylene protons of the coordinated dithiolate ligands are shielded in the range from $\Delta\delta = 0.9–1.2$ ppm for Pd complexes whereas it is deshielded upto $\Delta\delta \sim 0.6$ ppm for analogous Pt complexes.

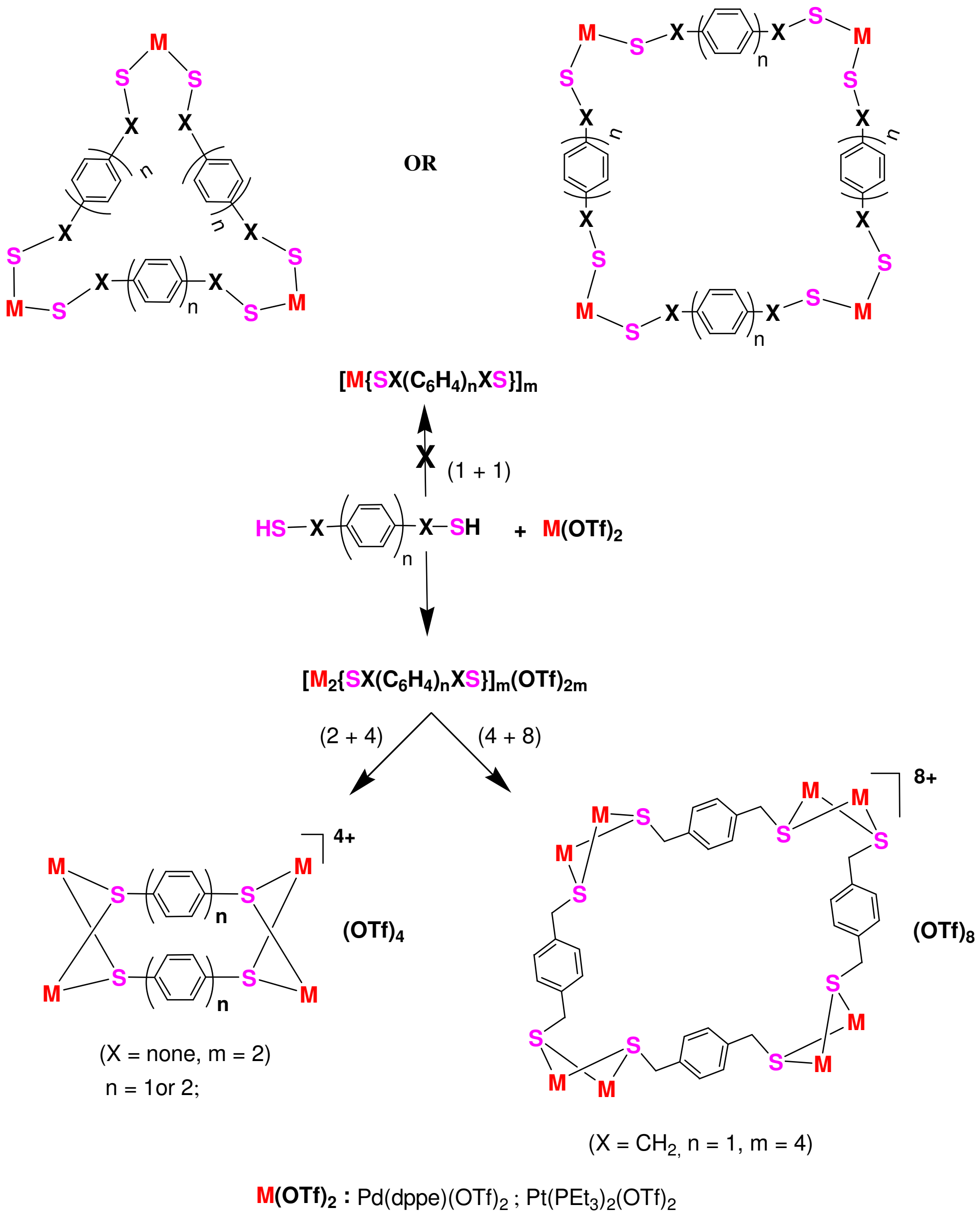

Scheme 16. Syntheses of palladium and platinum SCCs

The sharp singlet for benzylic and benzene ring protons of aryldithiolate ligand for $[Pd_2(SC_6H_4S)(dppe)_2]_2(OTf)_4$, $[Pd_2(SCH_2C_6H_4CH_2S)(dppe)_2]_4(OTf)_8$, $[Pt_2(SC_6H_4S)(PEt_3)_4]_2(OTf)_4$ and $[Pt_2(SCH_2C_6H_4CH_2S)(PEt_3)_4]_4(OTf)_8$ indicates that the rotation about the H_2C–C (phenylene) bond is rapid on the NMR time scale at room temperature. In the case of $[Pd_2(SC_{12}H_8S)(dppe)_2]_2(OTf)_4$ and $[Pt_2(SC_{12}H_8S)(PEt_3)_4]_2(OTf)_4$, appearance of two doublets suggests that α and β biphenylene protons are equivalent and also the rotation of biphenylene rings is rapid. This rules out, the possibility of existence of inner and outer environment, unusually observed in other macrocyclic rigid structures [219, 223].

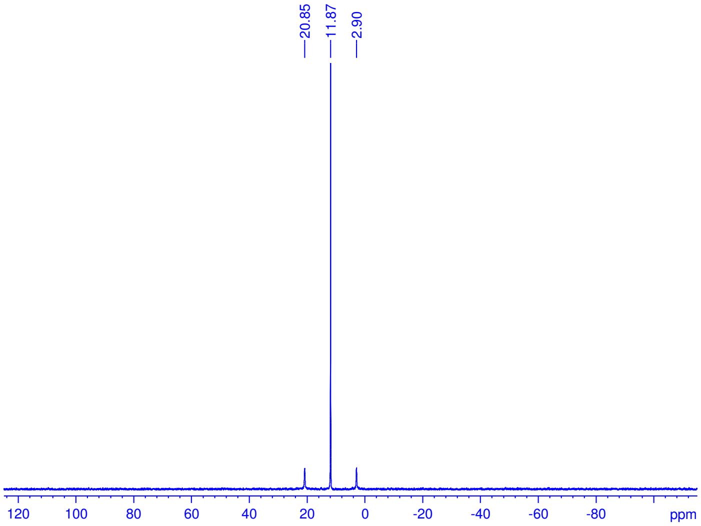

Figure 22. $^{31}P\{^1H\}$ NMR spectrum of $[Pt_2(SC_{12}H_8S)(PEt_3)_4]_2(OTf)_4$ in CD_3OD

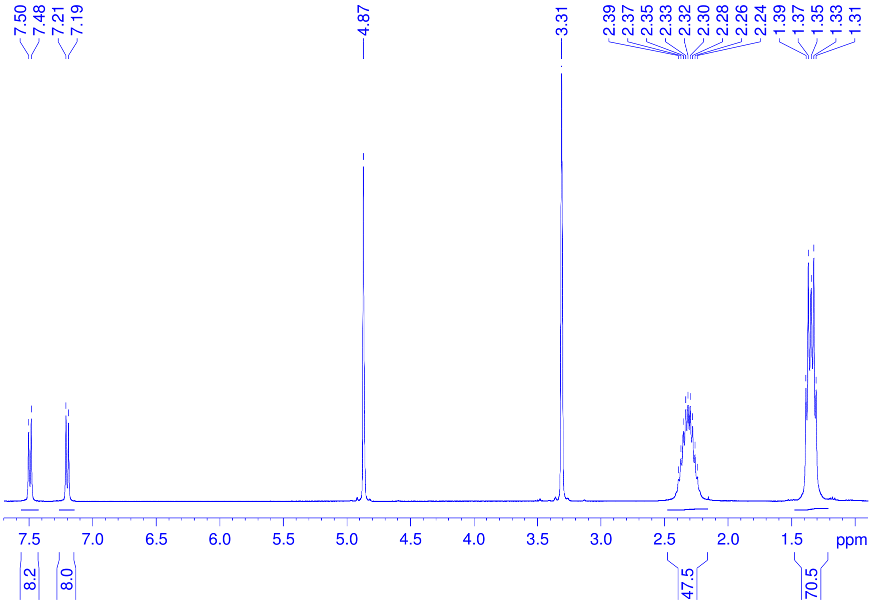

Figure 23. ^1H NMR spectrum of $[Pt_2(SC_{12}H_8S)(PEt_3)_4]_2(OTf)_4$ in CD_3OD

The $^1J(Pt-P)$) values of platinum complexes (2833-2912 Hz) (Table 30) are significantly reduced as compared to sub unit [$Pt(PEt_3)_2(OTf)_2$] (~ 3704 Hz) due to two strong trans influencing thiolate groups. All the Pt nuclei are magnetically equivalent as a triplet in ^{195}Pt NMR spectra for [$Pt_2(SC_6H_4S)(PEt_3)_4]_2(OTf)_4$ and [$Pt_2(SC_{12}H_8S)(PEt_3)_4]_2(OTf)_4$ (Figure 24) is observed due to coupling with two equivalent ^{31}P nuclei. The ESI-MS measurement gave convincing evidence for the formation of [$Pt_2(SC_{12}H_8S)(PEt_3)_4]_2(OTf)_4$ (Figure 25) and [$Pt_2(SCH_2C_6H_4CH_2S)(PEt_3)_4]_4(OTf)_8$. The prominent peaks were observed for [$Pt_2(SC_{12}H_8S)(PEt_3)_4]_2(OTf)_4$ corresponding to the intact structure minus triflate anions at *m/z*: 1227 ([M-2OTf]$^+$), 769 ([M-3OTf]$^{3+}$) and 651 ([M-OTf]$^{4+}$) strongly supports the formation of proposed structure. In the case of [$Pt_2(SCH_2C_6H_4CH_2S)(PEt_3)_4]_4(OTf)_8$, peaks at *m/z*: 1216 ([M-3OTf]$^{4+}$), 1063 ([M]$^{5+}$), 811 ([M-3OTf]$^{6+}$), 687 ([M-8OTf]$^{6+}$) and ([M-4OTf]$^{8+}$) indicate the formation of octanuclear structure.

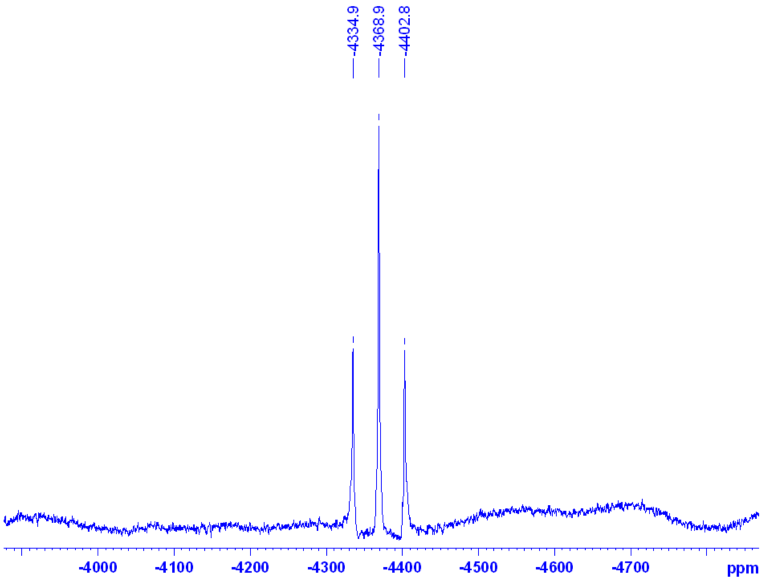

Figure 24. $^{195}Pt\{^1H\}$ NMR spectrum of [$Pt_2(SC_{12}H_8S)(PEt_3)_4]_2(OTf)_4$ in CD_3OD

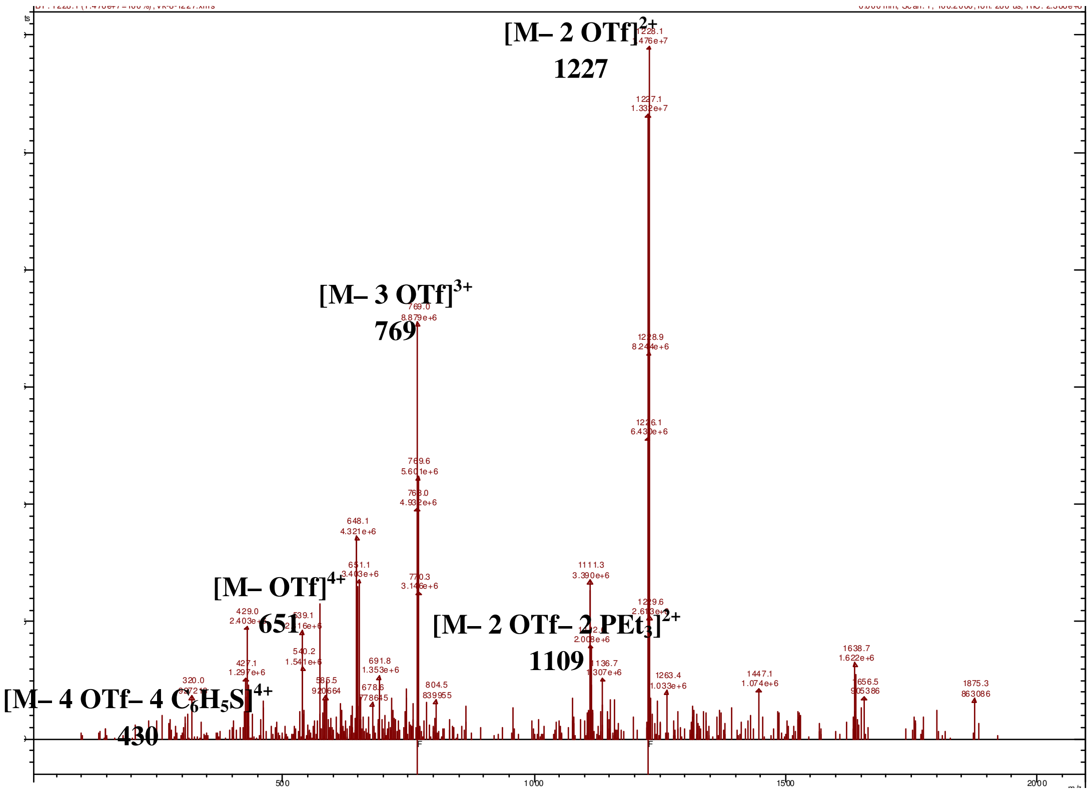

Figure 25. ESI-mass spectrum of $[Pt_2(SC_{12}H_8S)(PEt_3)_4]_2(OTf)_4$. The prominent peaks derived from the parent complex are indicated.

The above complexes were also crystallized out from the reactions of 1,4-benezenedithiol, 4,4′-biphenyldithiol to $M(OTf)_2$ and 1,4-benezenedimethanethiol with $[Pd(dppe)(OTf)_2]$ and $[Pt(PEt_3)_2(OTf)_2]$ when carried out in 1:1 ratio showing the formation of identical products. This is confirmed by the experiments involving stepwise addition of ligand to metal (Figure 26) and metal to ligand employing $[Pd(dppe)(OTf)_2]$ and $HSCH_2C_6H_4CH_2SH$. The formation of $[Pd_2(SCH_2C_6H_4CH_2S)(dppe)_2]_4(OTf)_8$ was monitored by ^{31}P NMR spectroscopy. The Figure 26 reveals the existence of at least two products or intermediates at δ 63.4 and 63.8 ppm along with the expected complex $[Pd_2(SCH_2C_6H_4CH_2S)(dppe)_2]_4(OTf)_8$ at δ 62.9 when ligand concentration was less than 1 equivalent. When it was above 1 equivalent the yield of $[Pd_2(SCH_2C_6H_4CH_2S)(dppe)_2]_4(OTf)_8$ became quantitative (> 90%).

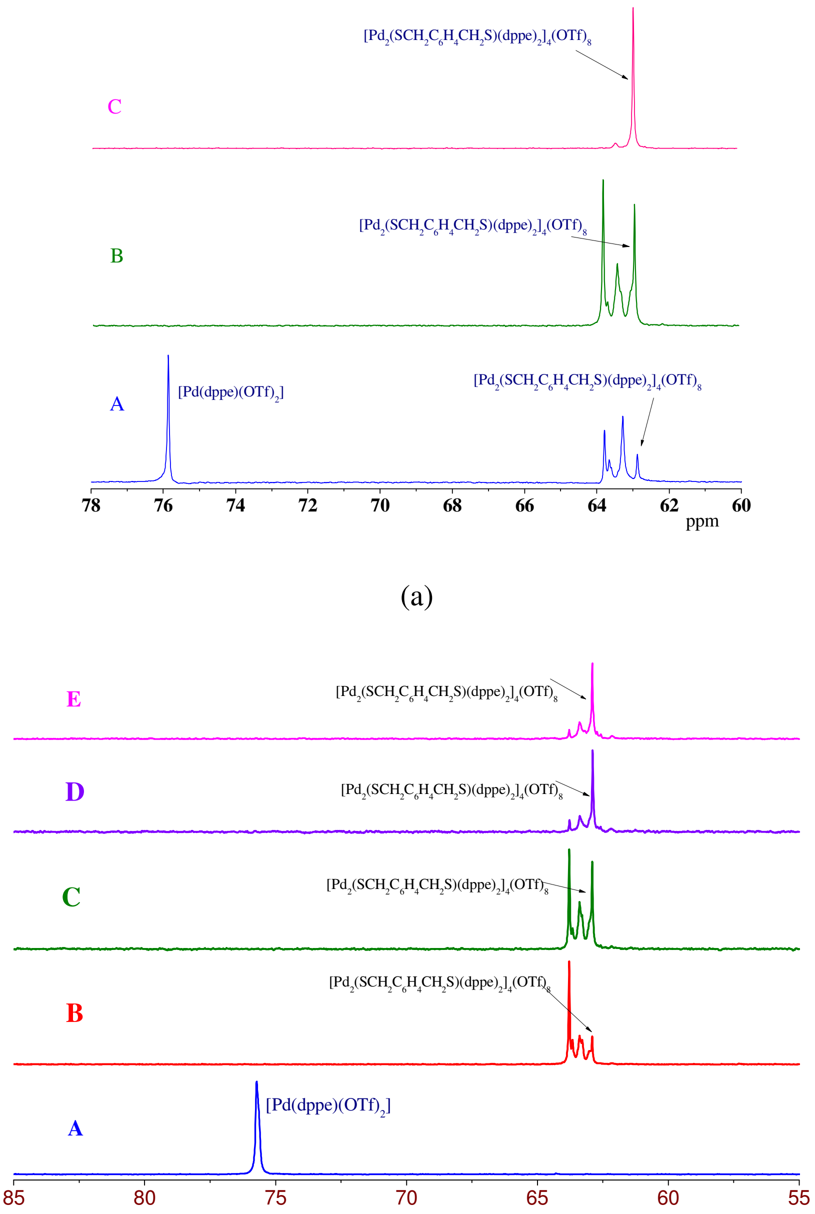

(a)

(b)

Figure 26. a) $^{31}P\{^{1}H\}$ NMR spectra (162 MHz, CD_3OD) obtained from the mixture of $[Pd(dppe)(OTf)_2]$ upon stepwise addition of ($HSCH_2C_6H_4CH_2SH$) in an NMR tube (ligand variation) (**A**) $[Pd(dppe)(OTf)_2$**:** ($HSCH_2C_6H_4CH_2SH$) = 2:0·25; (**B**) $[Pd(dppe)(OTf)_2$**:** ($HSCH_2C_6H_4CH_2SH$) = 2:0·75; (**C**) $[Pd(dppe)(OTf)_2$**:** ($HSCH_2C_6H_4CH_2SH$) = 2:1·25; b) ^{31}P NMR spectra (162 MHz, CD_3OD) obtained from the mixture of $[Pd(dppe)(OTf)_2$ and ($HSCH_2C_6H_4CH_2SH$) in 2:1 ratio in NMR tube. (**A**) no addition of ($HSCH_2C_6H_4CH_2SH$); (**B**) immediately after addition; (**C**) after 3 hrs; (**D**) after 25 hrs; (**E**) after 3 days.

Similar experiments keeping fixed ratio of metal ([Pd(dppe)(OTf)$_2$]) to ligand (HSCH$_2$C$_6$H$_4$CH$_2$SH), ^{31}P NMR spectra were monitored versus time. In case of low ratio 2:0·5, an equilibrium existed between [Pd(dppe)(OTf)$_2$] and [Pd$_2$(SCH$_2$C$_6$H$_4$CH$_2$S)(dppe)$_2$]$_4$(OTf)$_8$ with the intermediates whereas the higher ratios 2:1 and 2:1.5 yielded [Pd$_2$(SCH$_2$C$_6$H$_4$CH$_2$S)(dppe)$_2$]$_4$(OTf)$_8$ as major product with the same spectral features as observed in the case of metal to ligand variation experiments. These studies support the formation of thermodynamically favored rigid and cyclic products which are sufficiently stable in solid as well as in solution for several months without any dissociation as observed by NMR spectra in methanol and acetone. Surprisingly the complex *trans*-Pd(PEt$_3$)$_2$(OTf)$_2$ upon reaction with 1,4-benezenedithiol and HSCH$_2$C$_6$H$_4$CH$_2$SH resulted only insoluble oligomeric products of the general formula [Pd$_2$(SXC$_6$H$_4$XS)(PEt$_3$)$_4$]$_m$(OTf)$_{2m}$ as indicated by microanalysis.

The absorption spectra of the complexes, orange [Pd$_2$(SC$_6$H$_4$S)(dppe)$_2$]$_2$(OTf)$_4$ and [Pd$_2$(SC$_{12}$H$_8$S)(dppe)$_2$]$_2$(OTf)$_4$, yellow [Pd$_2$(SCH$_2$C$_6$H$_4$CH$_2$S)(dppe)$_2$]$_4$(OTf)$_8$ and pale yellow [Pt$_2$(SC$_6$H$_4$S)(PEt$_3$)$_4$]$_2$(OTf)$_4$ and [Pt$_2$(SC$_{12}$H$_8$S)(PEt$_3$)$_4$]$_2$(OTf)$_4$ were recorded in acetone (Table 31). The UV/vis spectra of [Pd$_2$(SC$_6$H$_4$S)(dppe)$_2$]$_2$(OTf)$_4$ and [Pd$_2$(SC$_{12}$H$_8$S)(dppe)$_2$]$_2$(OTf)$_4$ were characterized by a long wavelength, strong and relatively broad band at about 449 nm (2.76 ev) in the visible region responsible for the distinct orange colour of the complexes (Figure 27). While the absorption of the [Pd$_2$(SCH$_2$C$_6$H$_4$CH$_2$S)(dppe)$_2$]$_4$(OTf)$_8$ and platinum complexes are blue shifted in the near UV region. Such long wavelength absorption were confirmed as transitions from the E orbital to the mixed orbital contributed from phosphine and metal in our mixed ligand complexes [MCl(ECH$_2$CH$_2$NMe$_2$)(PR$_3$)] (E = S, Se, Te) [54, 55]. The hypsochromic shift of the absorption band on replacement of Pd by Pt keeping common combination of donor atoms of

Table 30. NMR spectroscopic data of aryldithiolate complexes of palladium and platinum

Complex	^{1}H NMR data in (δ ppm)	^{31}P{^{1}H} NMR data in (δ ppm)	^{195}Pt {^{1}H} NMR data in (δ ppm)	^{19}F{^{1}H} NMR data in (δ ppm)
$[Pd_2(S(C_6H_4)S)(dppe)_2]_2(OTf)_4$	2.60–2.85 (m, 8H, PCH_2), 3.25–3.45 (m, 8H, PCH_2), 5.98 (s, 8H, C_6H_4), 7.26–7.33 (m, 8H, *p*-H, C_6H_5), 7.45–7.69 (m, 32H, *o*/*m*-H, C_6H_5)	60.9 (s)	–	–77.9 (s)
$[Pd_2(S(C_{12}H_8)S)(dppe)_2]_2(OTf)_4$[a]	2.58–3.15 (m, 8H, PCH_2) (another multiplet for PCH_2 merged with the base of the peak for H_2O present in the solvent), 6.45 (d, $^3J_{HH}$ = 8.4 Hz, 8H, *o*-H, $C_{12}H_8$), 6.56 (d, $^3J_{HH}$ = 8.4 Hz, 8H, *m*-H, $C_{12}H_8$), 7.53 (t, $^3J_{HH}$ = 7.2 Hz, 16H, *m*-H, Ph), 7.65 (br s, 24H, *m*/*p*-H, Ph), 7.71 (t, $^3J_{HH}$ = 7.6 Hz, 8H, *p*-H, Ph), 7.75–7.85 (m, 16H, *o*-H, Ph), 7.85–7.96 (m, 16H, *o*-H, Ph)	62.7 (s)	–	–78.7 (s)
$[Pd_2(SCH_2C_6H_4CH_2S)(dppe)_2]_4(OTf)_8$[a]	2.65–3.10 (m, 32H, PCH_2), 3.28 (s, 16H, SCH_2), 6.33 (s, 16H, C_6H_4), 7.30–7.90 (m, 160H, PPh)	63.5 (s)	–	–77.1 (s)
$[Pt_2(SC_6H_4S)(PEt_3)_4]_2(OTf)_4$[b]	1.30 (dt, $^3J_{P,H}$ (d) = 17.2 Hz, $^3J_{H,H}$ (t) = 7.6 Hz, 72 H, PCH_2CH_3), 2.29 (m, 48H, PCH_2), 7.49 (s, 8H, C_6H_4)	13.3 (s, $^1J_{Pt\text{-}P}$ = 2911 Hz)	–4359 (t, $^1J_{Pt\text{-}P}$ = 2951 Hz)	–80.0 (s)

$[Pt_2(SC_{12}H_8S)(PEt_3)_4]_2(OTf)_4$[c]	1.35 (dt, $^3J_{P,H}$ (d) = 17.2 Hz, $^3J_{H,H}$ (t) = 7.6 Hz, 72H, PCH_2CH_3), 2.32 (m, 48H, PCH_2), 7.20 (d, $^3J_{HH}$ = 8.4 Hz, 8H, *m*-H, $C_{12}H_8$), 7.49 (d, $^3J_{HH}$ = 8.4 Hz, 8H, *o*-H, $C_{12}H_8$)	11.9 (s, $^1J_{Pt-P}$ = 2907 Hz)	–4369 (t, $^1J_{Pt-P}$ = 2917 Hz)	–79.9 (s)
$[Pt_2(SCH_2C_6H_4CH_2S)(PEt_3)_4]_4(OTf)_8$[d]	0.90–1.40 (m, 144 H, PCH_2CH_3, peak for PCH_2 group merged with the solvent peak at δ 2.05), 4.97 (s, 16 H, SCH_2), 7.90 (s, 16 H, C_6H_4)	12.9 (s, $^1J_{Pt-P}$ = 2833 Hz)	–	–

[a] Recorded in acetone-d_6.

[b] Recorded in methanol-d_4.

[c] Mass in *m/z* : 1638 ($[M - (Pt(PEt_3)_2 + 2PEt_3 + 3OTf)]^{+1}$, 11%), 1227 ($[M - 2OTf]^{2+}$, 100%), 1109 ($[M - (2OTf + 2PEt_3)]^{2+}$, 23%), 769 ($[M - 3OTf]^{3+}$, 60%), 651 ($[M - OTf]^{4+}$, 29%), 539 ($[M - 4OTf]^{4+}$, 16%), 430 ($[M - (4OTf + 4C_6H_5S)]^{4+}$, 16%)

[d] Mass in *m/z* : 1216 ($[M - 3OTf]^{4+}$, 17%), 1062 ($[M]^{5+}$, 69%), 1047 ($[M - (OTf + 8SCH_2C_6H_4)]^{4+}$, 100%), 927 ($[M - (3OTf + 5CH_2S)]^{5+}$, 28%), 811 ($[M - 3OTf]^{6+}$, 27%), 778 ($[M - (8OTf + 5CH_2S)]^{5+}$, 29%), 746 ($[M - (5OTf + 2CH_2S)]^{6+}$, 17%), 687 ($[M - 8OTf]^{6+}$, 59%), 463 ($[M - (2OTf + 8PEt_3 + 8CH_2S)]^{8+}$, 20%)

the ligands also supports the above assignment. The high molar extinction coefficient of about 31800 M^{-1} cm^{-1} indicates symmetry allowed transition with a good orbital overlap.

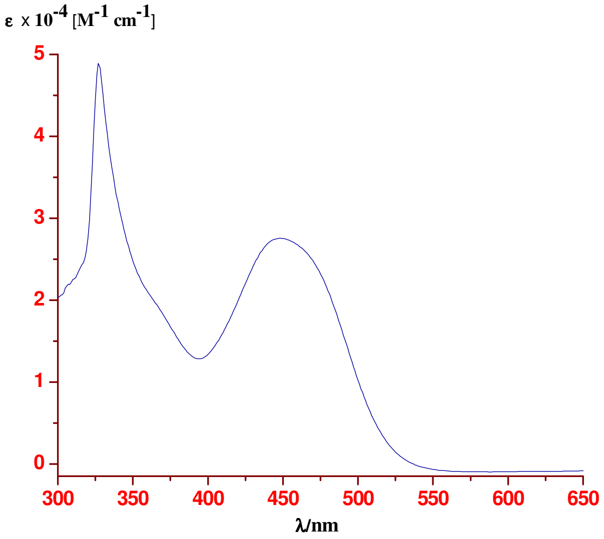

Figure 27. UV/vis spectrum of $[Pd_2(S(C_6H_4)S)(dppe)_2]_2(OTf)_4$ in acetone solution.

Table 31: UV-vis absorption[a] and electrochemical data[b,c] of complexes

Complex	**λ_{max} (ε)**	**Ox**	**Red 1**	**Red 2**	**Red 3**
$[Pd_2(SC_6H_4S)(dppe)_2]_2(OTf)_4$	327 (48800), 369 (sh, 18400), 447 (27500)	*d*	–1.07	–1.68	–1.95
$[Pd_2(SC_{12}H_8S)(dppe)_2]_2(OTf)_4$	327 (60400), 388 (28000), 449 (31800)	0.98	–1.18	–1.59	–1.93
$[Pd_2(SCH_2C_6H_4CH_2S)(dppe)_2]_4(OTf)_8$	327 (110500), 346 (sh, 78100)	*d*	–1.25	–2.15	–2.42
$[Pt_2(SC_6H_4S)(PEt_3)_4]_2(OTf)_4$	328 (19600), 364 (18700)	*d*	–1.45	–1.69	–2.19
$[Pt_2(SC_{12}H_8S)(PEt_3)_4]_2(OTf)_4$	339 (44500), 382 (sh, 20400)	*d*	–1.29	–1.59	–2.26

[a] Wavelengths λ_{max} at the absorption maxima in nm in acetone, molar extinction coefficients in $M^{-1}cm^{-1}$.

[b] From cyclic voltammetry at 50 mV s^{-1} scan rate, peak potentials in V vs. $FeCp_2/FeCp_2^+$.

[c] Measurement in CH_3CN/ Me_4NPF_6.

[d] Not observed.

Electrochemistry

Cyclic voltammetry of the complexes were measured by using three electrode cell in CH_3CN/0.05 M Me_4NPF_6, cycling between –2.5 and 1.5 V (Table 31). The CV measurements on one representative Pd and Pt complexes in acetone and dichloromethane did not show detectable peaks. The electrochemical peak potentials of all the palladium complexes in general exhibited three irreversible reduction steps while complex $[Pd_2(SC_6H_4S)(dppe)_2]_2(OTf)_4$ showed one irreversible oxidation step. As the overall charge of the complexes i.e., +4 for tetranuclear and +8 for octanuclear is considered to be spread over the whole molecules as a result the localized charge on all the metal centers should be similar in all the complexes. So the oxidation at M(II) centers or the reduction at S center which is in its most reduced form, are chemically less acceptable. It is assigned that the peak potential at 0.98 V is due to the oxidation taking place primarily at the thiolate site whereas the most negative peak potential at –1.93 V is due to the irreversible reduction at the phosphine ligand in $[Pd_2(SC_{12}H_8S)(dppe)_2]_2(OTf)_4$ (Figure 28) [54, 55]. Although the processes involved corresponding to the other two negative peak potentials (–1.18 and –1.59 V), are not clearly understood, they could possibly be originating from two reduction processes involving metal centers where Pd(II) is reduced to Pd(0), as one of the peak potentials is quasi-reversible in nature. It is reported that the dithiolate complexes $[M(Ph_2C_2S_2)_2]$ (M = Ni, Pd, Pt) exhibited two quasi-reversible reduction processes at the metal center and one oxidation at the thiolate center whereas the selenide clusters $[Pd_5(\mu_3\text{–}Se)_4(dppe)_4]^{+2}$ showed three reduction steps [224]. Although the oxidation peak potential was not observed in $[Pd_2(SC_6H_4S)(dppe)_2]_2(OTf)_4$, the little variation in three negative peak potentials indicate similar positioning of the frontier orbitals involved both in $[Pd_2(SC_6H_4S)(dppe)_2]_2(OTf)_4$ and $[Pd_2(SC_{12}H_8S)(dppe)_2]_2(OTf)_4$, as observed in absorption spectra. However by changing the ligand backbone from "phenylene" to "benzenedimethylene" moiety in , $[Pd_2(SCH_2C_6H_4CH_2S)(dppe)_2]_4(OTf)_8$ a significant negative shift of the peak potentials particularly of the most negative peak potential (~ 0.49 V) was observed. This result supports the observed blue shift of the long wavelength band in absorption spectra while comparing $[Pd_2(SC_6H_4S)(dppe)_2]_2(OTf)_4$ / $[Pd_2(SC_{12}H_8S)(dppe)_2]_2(OTf)_4$ vs $[Pd_2(SCH_2C_6H_4CH_2S)(dppe)_2]_4(OTf)_8$. The platinum complexes $[Pt_2(SC_6H_4S)(PEt_3)_4]_2(OTf)_4$ and $[Pt_2(SC_{12}H_8S)(PEt_3)_4]_2(OTf)_4$ also showed three irreversible reduction steps at the more negative side in comparison to Pd analogues and no oxidation step was observed. The most negative potential shift of about 0.24 V in platinum complex $[Pt_2(SC_6H_4S)(PEt_3)_4]_2(OTf)_4$ was observed relative to the Pd analogue $[Pd_2(SC_6H_4S)(dppe)_2]_2(OTf)_4$. The other two negative potentials (–1.45, 1.69 V) in $[Pt_2(SC_6H_4S)(PEt_3)_4]_2(OTf)_4$ may be attributed to the reduction at Pt^{II} center as above.

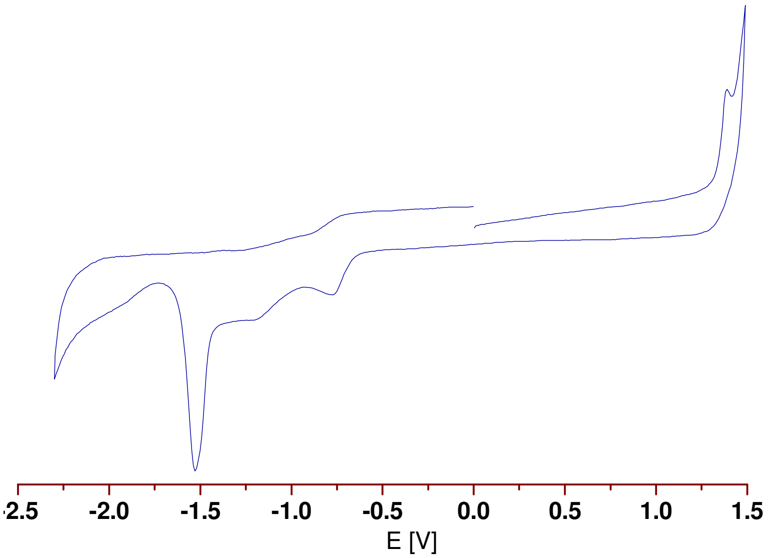

Figure 28. Cyclic voltammogram of $[Pd_2(S(C_{12}H_8)S)(dppe)_2]_2(OTf)_4$ in 0.05 M CH_3CN/TMAF solution.

Crystal Structures

The structures of macrocycles $[Pd_2(SC_6H_4S)(dppe)_2]_2(OTf)_4$, $[Pd_2(SC_{12}H_8S)(dppe)_2]_2(OTf)_4$, $[Pd_2(SCH_2C_6H_4CH_2S)(dppe)_2]_4(OTf)_8$ and $[Pt_2(SC_6H_4S)(PEt_3)_4]_2(OTf)_4$ were unambiguously determined by X-ray crystallography. The

ORTEP drawings with crystallographic numbering schemes are shown in Figures 29-32 while selected interatomic parameters are given in Tables 32-34.

The crystal lattices of $[Pd_2(SC_6H_4S)(dppe)_2]_2(OTf)_4$, $[Pd_2(SC_{12}H_8S)(dppe)_2]_2(OTf)_4$, $[Pd_2(SCH_2C_6H_4CH_2S)(dppe)_2]_4(OTf)_8$ consist of rectangular or square cations with well-separated, but electro-statically interacting anions. The asymmetric unit cell of $[Pd_2(SC_6H_4S)(dppe)_2]_2(OTf)_4$ and $[Pd_2(SC_{12}H_8S)(dppe)_2]_2(OTf)_4$ comprise of half rectangle and two triflate anions, in the case of $[Pd_2(SC_6H_4S)(dppe)_2]_2(OTf)_4$ partially occupied dichloromethane ($[Pd_2(SC_6H_4S)(dppe)_2]_2(OTf)_4{\cdot}0{\cdot}36CH_2Cl_2$) is also associated with the crystal lattice. Similarly the asymmetric unit cell of $[Pd_2(SCH_2C_6H_4CH_2S)(dppe)_2]_4(OTf)_8$ contains only a half square, two triflate anions and one acetone molecule as solvent. In case of $[Pd_2(SCH_2C_6H_4CH_2S)(dppe)_2]_4(OTf)_8$, the Z is 1 for the unit cell and Z' is 0.5, as the asymmetric unit doubles there will be 8 triflate and 2 acetone in the unit cell. Some of the solvent was also squeezed out. The entire rectangle or square is generated via an inversion center that is located at the mid-point between the two diagonal S atoms.

The molecules $[Pd_2(SC_6H_4S)(dppe)_2]_2(OTf)_4$, $[Pd_2(SC_{12}H_8S)(dppe)_2]_2(OTf)_4$, consist of two dithiolate ligands and four Pd atoms ($m = 2$) forming a rectangular shaped macrocycles, the four dppe chelating ligands attached to four Pd atoms form two boats of “$Pd_2(dppe)_2S_2$” unit at head and tail position. Interestingly the molecule $[Pd_2(SCH_2C_6H_4CH_2S)(dppe)_2]_4(OTf)_8$ is a square shaped octanuclear ($m = 4$) and comprises of four similar boats at four corners. All the three structures $[Pd_2(SC_6H_4S)(dppe)_2]_2(OTf)_4$, $[Pd_2(SC_{12}H_8S)(dppe)_2]_2(OTf)_4$ and $[Pd_2(SCH_2C_6H_4CH_2S)(dppe)_2]_4(OTf)_8$ have common feature i.e., hinged four-membered “Pd_2S_2”ring, capped with dppe ligand which are bridged via phenylene, biphenylene and benzenedimethylene groups, respectively. Although half of the phenyl groups of the dppe ligand lie inside the macrocycle and close to the phenylene rings, the metal–S–C angle and S–C bond help in bending and lengthening of the bridge, thus successfully self-assemble into macrocycles. It may be noted that the self-assembly of $Pd(dppp)(OTf)_2$ and pyrazine is prevented due to the steric crowding of phenyl groups of the phosphine ligand, whereas molecular squares are formed with 1,4-dicyanobenzene [222]. The hinging of Pd_2S_2 rings is reflected in the dihedral angles (~ 127 - 144°) deviated from the flat conformation ($\theta = 180°$), which has been established due to the attractive donor-acceptor interactions between the d_z^2 and p_z orbitals of the metal atoms [225, 226]. The Pd···Pd distances in $[Pd_2(SC_6H_4S)(dppe)_2]_2(OTf)_4$ (3.190 Å), $[Pd_2(SC_{12}H_8S)(dppe)_2]_2(OTf)_4$ (3.254 Å) and $[Pd_2(SCH_2C_6H_4CH_2S)(dppe)_2]_4(OTf)_8$ (3.258, 3.306 Å) within the same "Pd_2S_2" core falls in the expected range of binuclear thiolato bridged palladium complexes [52, 227, 228]. Although numerous sulfido and thiolato-bridged palladium and platinum complexes of diverse nuclearity are reported [52, 227, 228], the present macrocyclic structures are the first examples of supra-molecular coordination complexes with thiolate ligands.

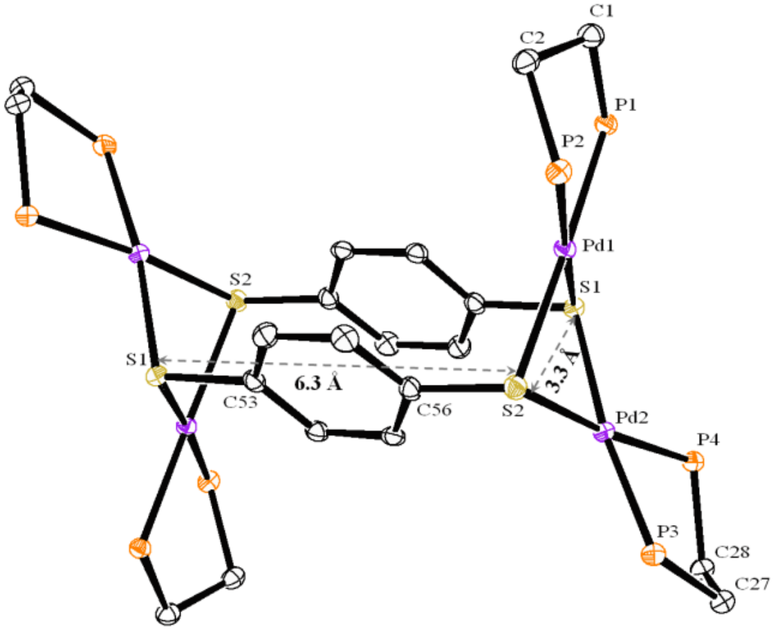

\

Figure 29. Molecular structure of $[Pd_2(SC_6H_4S)(dppe)_2]_2(OTf)_4$; ellipsoids drawn at 50% probability. The dppe phenyl groups, hydrogen atoms and triflate ions are omitted for clarity.

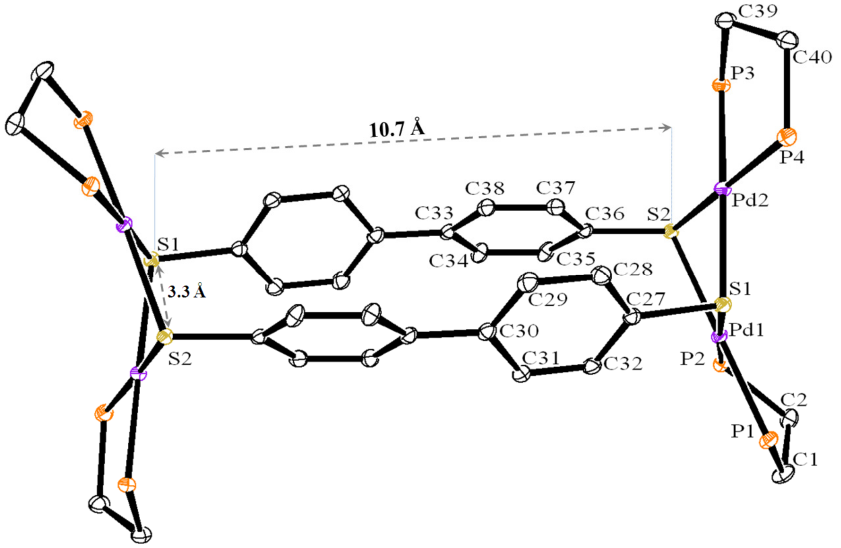

Figure 30. Molecular structure of $[Pd_2(SC_{12}H_8S)(dppe)_2]_2(OTf)_4$ ellipsoids drawn at 50% probability. The dppe phenyl groups, hydrogen atoms and triflate ions are omitted for clarity.

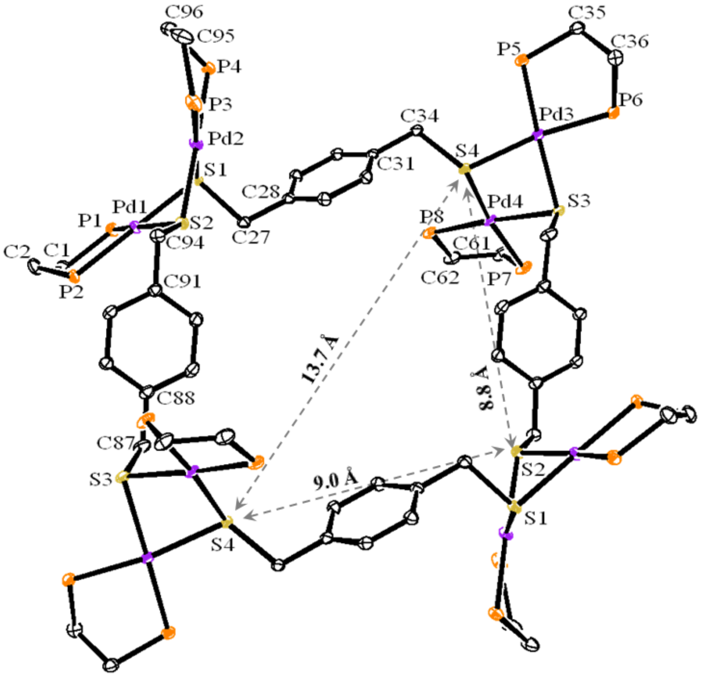

Figure 31. Molecular structure of $[Pd_2(SCH_2C_6H_4CH_2S)(dppe)_2]_4(OTf)_8$ ellipsoids drawn at 50% probability. The dppe phenyl groups, hydrogen atoms and triflate ions are omitted for clarity.

The rectangular shape of $[Pd_2(SC_6H_4S)(dppe)_2]_2(OTf)_4$ and $[Pd_2(SC_{12}H_8S)(dppe)_2]_2(OTf)_4$ is given by four sulfur atoms of the bridging ligands at the four corners. The length of the smaller rectangle $[Pd_2(SC_6H_4S)(dppe)_2]_2(OTf)_4$ as defined by edge-to-edge S···S distance is 6.3 Å and the height as defined by S1···S2 distance in a same Pd_2S_2 unit is 3.3 Å, while the distance between the two centroids of benzene rings of dithiolate ligand i.e., π···π stacking is 3.4 Å (Figure 29). Similar way the length and height of the larger rectangle, $[Pd_2(SC_{12}H_8S)(dppe)_2]_2(OTf)_4$ is 10.7 and 3.3 Å, respectively and the π···π stacking is 3.8 Å. The comparison between the two rectangular shaped rigid structures of $[Pd_2(SC_6H_4S)(dppe)_2]_2(OTf)_4$ and $[Pd_2(SC_{12}H_8S)(dppe)_2]_2(OTf)_4$ reflects the increased π-π stacking of the phenyl group of the thiolate ligand and metal…metal interaction in $[Pd_2(SC_6H_4S)(dppe)_2]_2(OTf)_4$. The two phenyl groups in $[Pd_2(SC_6H_4S)(dppe)_2]_2(OTf)_4$ are tightly packed and aligned parallel to each other within the cavity. Whereas in $[Pd_2(SC_{12}H_8S)(dppe)_2]_2(OTf)_4$, the C–C single bond between two phenyl groups helps in bending of the biphenyl group thus creating slight space to allow the twisting of the adjacent phenyl rings by 26.47°.

The square shaped highly symmetric structure of octanuclear complex $[Pd_2(SCH_2C_6H_4CH_2S)(dppe)_2]_4(OTf)_8$ is different from that of rectangular shaped tetranuclear complexes $[Pd_2(SC_6H_4S)(dppe)_2]_2(OTf)_4$ and $[Pd_2(SC_{12}H_8S)(dppe)_2]_2(OTf)_4$. The structure of $[Pd_2(SCH_2C_6H_4CH_2S)(dppe)_2]_4(OTf)_8$ consists of four "Pd_2S_2" units capped by dppe ligands, which occupy the corners of a square, held together by bridging dimethylene phenyl dithiolate groups. Since both the Pd atoms of the "Pd_2S_2" unit lie outside the macrocycle, two S2 and two S4 sulfur atoms residing inside define the corners of a square. Though the molecular shape looks like square, its lengths are not perfectly equal possibly due to two linkers, benzylic C atom and S atom of tetrahedral geometry. The dimensions of the cavity as defined by the edge-to-edge S···S distances are 8.8 and 9.0 Å, whereas the diagonal

S···S distance is 13.7 Å. Macrocyclic structure of analogous platinum complexes may show interesting features. Thus attempts have been made to elucidate structures of such complexes, after several attempts crystals of $[Pt_2(SC_6H_4S)(PEt_3)_4]_2(OTf)_4$ (Figure 32) could be obtained. Partial data collection (~ 40%) on a crystal sealed in a capillary with mother liquor at room temperature showed approximate structure similar to its palladium analogue $[Pd_2(SC_6H_4S)(dppe)_2]_2(OTf)_4$ and the structural features are undeniable. Thus by introducing one flexible methylene group in the ligand backbone, the same reaction condition easily yield lower-order (m = 2) tetranuclear to higher order (m = 4) octanuclear supra-molecular coordination complexes. The effect of ligand rigidity on structural changes has been observed in the case of catecholamide forming supra-molecular structures of Fe(III) and Ga(III) by addition of methylene group in the ligand [229].

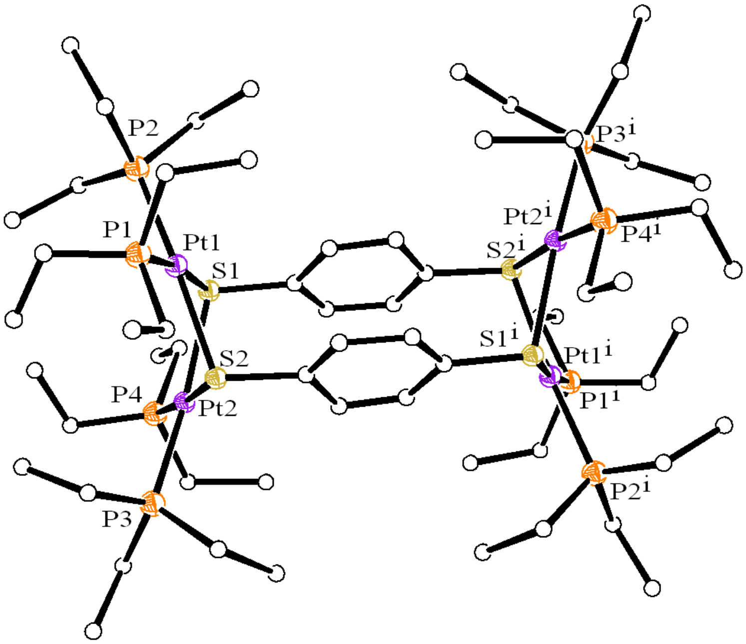

Figure 32. Molecular structure of $[Pt_2(SC_6H_4S)(PEt_3)_4]_2(OTf)_4.2CH_2Cl_2$. The hydrogen atoms in benzene ring, solvent molecules and triflate ions have been omitted for clarity.

Table 32. Selected interatomic distances [Å] and angles [°] of complexes $[Pd_2(SC_6H_4S)(dppe)_2]_2(OTf)_4.0.36CH_2Cl_2$ and $[Pd_2(SC_{12}H_8S)(dppe)_2]_2(OTf)_4$

	$[Pd_2(SC_6H_4S)(dppe)_2]_2(OTf)_4.$ $0.36CH_2Cl_2$	$Pd_2(SC_{12}H_8S)(dppe)_2]_2(OTf)_4$
Pd1–S1	2.3691(6)	2.4020(9)
Pd1–S21	2.4209(6)	2.3992(9)
Pd2–S21	2.4049(6)	2.3761(9)
Pd2–S1	2.3723(6)	2.4239(9)
Pd1–P1	2.2796(6)	2.2907(9)
Pd1–P2	2.2737(6)	2.2641(10)
Pd2–P3	2.2881(6)	2.2616(9)
Pd2–P4	2.2675(6)	2.2840(10)
Pd1···Pd2[a]	3.190	3.254
Pd1···Pd2[b]	7.647	11.717
S1···S2[c]	3.311	3.369
π···π stacking	3.386	3.830
θ[d]	135.1	144.1
S1–C53/C27	1.783(2)	1.793(3)
S2–C56/C36	1.783(2)	1.783(3)
S1–Pd1–S21	87.454(18)	89.12(3)
P1–Pd1–P2	83.62(2)	83.98(3)
P1–Pd1–S1	90.522(19)	94.34(3)
P2–Pd1–S21	98.39(2)	92.54(3)
S1–Pd2–S21	87.75(2)	89.12(3)
P4–Pd2–S21	91.26(2)	95.82(3)
S2–Pd2–P4	172.89(2)	172.85(3)
P3–Pd2–P4	83.27(2)	84.67(4)

[a] distance between Pd1 and Pd2 atoms within the same “Pd2S2” core.

[b] distance between Pd1 and Pd2 atoms separated by dithiolate ligand.

[c] distance between S1 and S2 atoms within the same “Pd2S2” core.

[d] dihedral angle between S1-Pd1-S2 and S1-Pd2-S2 planes.

Table 33. Selected interatomic distances [Å] and angles [°] of complex $[Pd_2(SCH_2C_6H_4CH_2S)(dppe)_2]_4(OTf)_8{\cdot}(CH_3COCH_3)_2$

Pd1–S1	2.3584(10)	Pd3–S3	2.3541(11)
Pd1–S2	2.3890(11)	Pd3–S4	2.3493(11)
Pd2–S1	2.3679(10)	Pd4–S3	2.3545(12)
Pd2–S2	2.3458(11)	Pd4–S4	2.3642(10)
Pd1–P1	2.2603(12)	Pd4–P7	2.2605(12)
Pd1–P2	2.2855(11)	Pd4–P8	2.3048(13)
S1–C27	1.847(4)		
Pd1…Pd2[a]	3.258	Pd3…Pd4[a]	3.306
S1…S2	3.024	S3…S4	3.032
θ^b	127.12		
θ^c	132.94		
S1–Pd1–S2	79.11(4)	S1–C27–C28	110.1(3)
P1–Pd1–P2	84.40(4)	S4–C34–C31	110.1(3)
Pd1–S1–Pd2	87.15(3)	S2–C94–C91	109.3(3)
Pd1–S1–C27	99.78(13)		

[a] distance between two Pd atoms within the same “Pd2S2” core.

[b] dihedral angle between S1-Pd1-S2 and S1-Pd2-S2 planes.

[c]dihedral angle between S3-Pd3-S4 and S3-Pd4-S4 planes.

Table 34. Selected interatomic parameters (Å/°) of $Pt_2(SC_6H_4S)(PEt_3)_4]_2(OTf)_4.2CH_2Cl_2$

Pt1–S1	2.396(7)	Pt2–S1	2.392(7)
Pt1–S2	2.399(8)	Pt2–S2	2.390(8)
Pt1–P1	2.296(9)	Pt2–P3	2.306 (9)
Pt1–P2	2.271(10)	Pt2–P4	2.297(9)
S1-Pt1-S2	82.0(3)	S1-Pt2-S2	82.3(3)
P1-Pt1-S1	173.3(3)	P3-Pt2-S1	165.4(3)
P1-Pt1-S2	92.1(3)	P3-Pt2-S2	85.2(3)
P2-Pt1-S1	87.5(3)	P4-Pt2-S1	93.2(3)
P2-Pt1-S2	168.8(3)	P4-Pt2-S2	175.2(3)
P1-Pt1-P2	98.2(3)	P3-Pt2-P4	99.1(3)

Catalysis

The potential of sulfur based metal complexes as homogenous catalysts has been neglected for the long time due to the belief that sulfur acts as catalyst poison [230]. Recently Vanjari et.al. have demonstrated the role of sulfur as a promoter rather than catalyst poison in C–C bond formation reactions [231]. Ananikov et. al. have employed 1-dimensional nanoparticles of *in-situ* prepared $[Pd(SCy)_2]_n$ as catalyst for the addition of cyclohexanethiol to alkynes leading to the formation of Markovnikov–type product [232]. Although supra-molecular dendritic palladium complexes [232, 234] and self-assembled palladium complexes with amphiphilic phosphine ligands [235] have been used as catalysts in Suzuki and Heck reactions, the catalytic activity of multinuclear chalcogenolate complexes is hardly explored. Catalytic activity of mono- and bi-nuclear palladium chalcogenolate complexes in C–C bond formation has been reported recently [155, 236, 237].

To assess the suitability of macrocyclic palladium complexes as homogenous catalyst in C–C coupling reaction, the activity of these complexes is examined in Suzuki coupling reactions. Based on our recent experiments on optimization study of reaction conditions in Suzuki coupling reactions using palladium chalcogenolate/chalcogeno ether complex as catalysts, the solvent dioxane, base K_2CO_3 and temperature 100 °C were used as reaction conditions [237, 238]. It is evident from Table 35 that the complexes $[Pd_2(SC_6H_4S)(dppe)_2]_2(OTf)_4$, $[Pd_2(SC_{12}H_8S)(dppe)_2]_2(OTf)_4$ and $[Pd_2(SCH_2C_6H_4CH_2S)(dppe)_2]_4(OTf)_8$ efficiently catalyzed the coupling reaction of both electron-rich and -poor aryl bromides with phenylboronic acids more than 90% isolated yield. To start the investigation the deactivated 4-bromotoluene was used as a substrate, since its coupling reaction can be conveniently monitored. The reactions proceeded smoothly with 0.04 mol% of "Pd" (entries 1, 3). The palladium complexes were active at loading as low as 10^{-4} mol% leading to slightly lower yield but higher TON upto 97500 (entries 4, 5, 8) under the same reaction condition and time.

The palladium supra-molecular complexes also promote the coupling of bulky or sterically demanding substrates. The reaction of 2,6-dimethylbromobenzene and 2-bromomesitylene with phenylboronic acid gave moderate to good yields of biaryls (entries 9-13). Under the same conditions cross-coupling of electron-poor aryl bromides gave quantitative yields of the corresponding biaryls (entries 14-16). After lowering the catalyst concentration gradually to 10^{-6} mol% of Pd, the complex was highly active to yield 85% product with a very high TON of twenty million in case of bromoacetophenone as substrate (entries 17-19).

Table 35. Suzuki-Miyaura cross-coupling of aryl halide with phenylboronic acid[a]

Entry	R	X	Complex	mol% of 'Pd'	Time (hrs)	Yield (%)[b]	TON
1.	4–CH_3	Br	$[Pd_2(SC_6H_4S)(dppe)_2]_2(OTf)_4$	0.04	10	90	2250
2.	4–CH_3	Br	$[Pd_2(SC_{12}H_8S)(dppe)_2]_2(OTf)_4$	0.4	10	96	240
3.	4–CH_3	Br	$[Pd_2(SC_{12}H_8S)(dppe)_2]_2(OTf)_4$	0.04	10	90	2250
4.	4–CH_3	Br	$[Pd_2(SC_{12}H_8S)(dppe)_2]_2(OTf)_4$	0.004	10	67	16750
5.	4–CH_3	Br	$[Pd_2(SC_{12}H_8S)(dppe)_2]_2(OTf)_4$	0.0004	10	39	97500
6.	4–CH_3	Br	$[Pd_2(SCH_2C_6H_4CH_2S)(dppe)_2]_4(OTf)_8$	0.8	10	97	121
7.	4–CH_3	Br	$[Pd_2(SCH_2C_6H_4CH_2S)(dppe)_2]_4(OTf)_8$	0.08	10	82	1025
8.	4–CH_3	Br	$[Pd_2(SCH_2C_6H_4CH_2S)(dppe)_2]_4(OTf)_8$	0.008	10	62	7750
9.	2,6–CH_3	Br	$[Pd_2(SCH_2C_6H_4CH_2S)(dppe)_2]_4(OTf)_8$	0.8	10	58	73
10.	2,6–CH_3	Br	$[Pd_2(SC_6H_4S)(dppe)_2]_2(OTf)_4$	0.8	10	70	88
11.	2,4,6–CH_3	Br	$[Pd_2(SC_6H_4S)(dppe)_2]_2(OTf)_4$	0.4	10	48	120
12.	2,4,6–CH_3	Br	$[Pd_2(SC_6H_4S)(dppe)_2]_2(OTf)_4$	0.8	10	82	103
13.	2,4,6–CH_3	Br	$[Pd_2(SCH_2C_6H_4CH_2S)(dppe)_2]_4(OTf)_8$	0.8	10	83	104
14.	2–CHO	Br	$[Pd_2(SCH_2C_6H_4CH_2S)(dppe)_2]_4(OTf)_8$	0.08	10	95	1188
15.	4–CHO	Br	$[Pd_2(SC_6H_4S)(dppe)_2]_2(OTf)_4$	0.04	10	94	2350
16.	4–$COCH_3$	Br	$[Pd_2(SC_6H_4S)(dppe)_2]_2(OTf)_4$	0.04	10	99	2475
17.	4–$COCH_3$	Br	$[Pd_2(SC_6H_4S)(dppe)_2]_2(OTf)_4$	0.0004	10	95	237500
18.	4–$COCH_3$	Br	$[Pd_2(SC_6H_4S)(dppe)_2]_2(OTf)_4$	0.00004	10	93	2325000
19.	4–$COCH_3$	Br	$[Pd_2(SC_6H_4S)(dppe)_2]_2(OTf)_4$	0.000004	8	85	21250000
20.	3–$COCH_3$	Cl	$[Pd_2(SC_6H_4S)(dppe)_2]_2(OTf)_4$[c]	4	16	43	11
21.	4–CHO	Cl	$[Pd_2(SC_6H_4S)(dppe)_2]_2(OTf)_4$[c]	2	16	57	29

[a]Reaction conditions: Aryl halide (1.0 mmol), aryl boronic acid (1.3 mmol), K_2CO_3 as base (2 mmol), dioxane (2 mL), H_2O (1 mL). [b]Isolated yield, [c]TBAB (5 mmol) used.

These results are better than the carbene-thiolato Pd(II) complexes [155] but comparable with respect to the catalytic activity of phosphino-thiolato Pd(II) complexes [236]. The present Pd complexes are superior precatalysts than the supra-molecular cationic Pd complexes with flexible coordination cage [239]. Encouraged by these results, the more challenging coupling reactions of aryl chloride were attempted. The coupling of less reactive chlorobenzene exhibited very low yield. Nevertheless moderate yields were achieved for the electron-deficient aryl chloride in the presence of TBAB as a promoter (entries 20-21).

A general comparative study on the relative activities of the three macrocyclic complexes showed the comparable results (entries 1vs 3; 12 vs 13; 14 vs 15) under the same reaction conditions. However the critical comparison revealed that the activities of $[Pd_2(SC_6H_4S)(dppe)_2]_2(OTf)_4$ and $[Pd_2(SC_{12}H_8S)(dppe)_2]_2(OTf)_4$, are slightly higher than $[Pd_2(SCH_2C_6H_4CH_2S)(dppe)_2]_4(OTf)_8$ (entries 9 vs 10). The similar trend was observed after careful consideration of the amount of catalyst used, e.g., 0.04 mol% of Pd of $[Pd_2(SC_6H_4S)(dppe)_2]_2(OTf)_4$ and $[Pd_2(SC_{12}H_8S)(dppe)_2]_2(OTf)_4$ resulted 90% yield (entries 1,3) whereas twice the concentration i.e., 0.08 mol% of Pd of $[Pd_2(SCH_2C_6H_4CH_2S)(dppe)_2]_4(OTf)_8$ reached a corresponding yield of 82% (entry 7), this is reflected in the difference of their TONs. These results indicate that the complexes $[Pd_2(SC_6H_4S)(dppe)_2]_2(OTf)_4$ and $[Pd_2(SC_{12}H_8S)(dppe)_2]_2(OTf)_4$ produce more catalytically active species after relieving the strain associated with the rigid macrocyclic structures in comparison to the more flexible and easily accessible larger macrocyclic complex $[Pd_2(SCH_2C_6H_4CH_2S)(dppe)_2]_4(OTf)_8$. The tetranuclear complexes $[Pd_2(SC_6H_4S)(dppe)_2]_2(OTf)_4$ and $[Pd_2(SC_{12}H_8S)(dppe)_2]_2(OTf)_4$ are less stable relative to the octanuclear complex $[Pd_2(SCH_2C_6H_4CH_2S)(dppe)_2]_4(OTf)_8$. Although the actual nature of the active species is not clearly known, the high activity upon lowering of Pd loading [180, 240] could possibly be due to the formation of Pd-nanoparticles (PdNPs). The excellent activity of the previously reported palladacycles in Suzuki and Heck C–C coupling reaction is now attributed to the formation of PdNPs [241-243]. In the present case the thiolate ligands may stabilize the PdNPs which can act as catalysts or precatalyst.

Chemistry of palladium and platinum complexes of hybrid nitrogen and organoselenium/tellurium donor ligands

Metal directed self-assemblies possessing cavities that can accommodate various guest molecules has received considerable attention. Self-assembly of large discrete supra-molecules from simple precursors has been extensively studied [244, 245] particularly derived from pyridyl based ligands. 4,4′-Dithiodipyridine has been successfully employed as nucleophilic tecton in self-assembly reactions with metal centres of varying lability [165]. Thus it was considered worthwhile to explore heavier congeners as ligands for constructing large self assemblies. First example of conformationally defined palladium and platinum molecular rhombhoids making use of 4,4′-dipyridyldichalcogenide as ligand *via* self-assembly is described.

The reaction of inert electrophilic bis(triflate) complex $[Pt(PEt_3)_2(OTf)_2]$ with an equimolecular 4,4'-py_2E_2 (E = Se, Te) at room temperature resulted in the formation of $[Pt(py_2E_2)(PEt_3)_2]_2(OTf)_2$ (E = Se, Te) in high yield. A similar reaction with more reactive $[Pd(dppe)(OTf)_2]$ with 4,4'-py_2Se_2 also gave an analogous product $[Pd(py_2Se_2)(dppe)]_2(OTf)_2$ in nearly quantitative yield (Scheme 17). All the complexes are highly soluble in methanol and acetone, moderately soluble in dichloromethane and acetonitrile, sparingly soluble in chloroform and insoluble in hexane, diethylether and toluene.

The ^{1}H NMR chemical shift of pyridyl protons of $[Pt(4,4'\text{-}py_2Se_2)(PEt_3)_2]_2(OTf)_4$ and $[Pt(4,4'\text{-}py_2Te_2)(PEt_3)_2]_2(OTf)_4$ are significantly deshielded with respect to the free ligand, whereas there is hardly any change in the case of $[Pd(4,4'\text{-}py_2Se_2)(dppe)]_2(OTf)_4$. In the latter the phenyl groups of the dppe ligand might have provided shielding over the pyridyl group [222]. The ^{1}H NMR spectra exhibited two doublets due to each of α and β protons which may be due to slow rotation of the pyridyl group which experience two different environment inside and outside of the macrocycle of $[Pt(4,4'\text{-}py_2Se_2)(PEt_3)_2]_2(OTf)_4$ and [Pt(4,4'-

$py_2Te_2)(PEt_3)_2]_2(OTf)_4$. However a broad singlet and doublet are observed due to the α and β protons in the case of $[Pd(4,4'\text{-}py_2Se_2)(dppe)]_2(OTf)_4$. A similar pattern has been reported in case of palladium and platinum macrocycles with phenanthroline [219] and dipyridyl bridging ligands [223]. The single peak at about −80 ppm in $^{19}F\{^1H\}$ NMR spectra is characteristic of triflate ions.

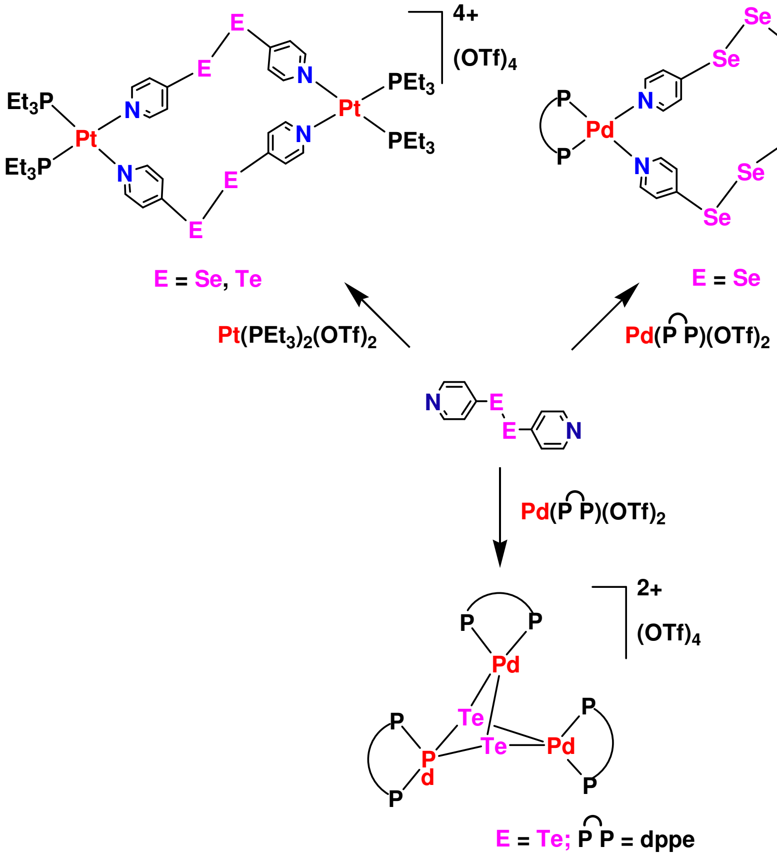

Scheme 17

The single sharp $^{31}P\{^1H\}$ NMR resonance (Figure 33) with platinum satellites for platinum complexes is the signature of the four equivalent phosphorus nuclei and symmetric macrocyclic structures of $[Pt(4,4'\text{-}py_2Se_2)(PEt_3)_2]_2(OTf)_4$, $[Pt(4,4'\text{-}py_2Te_2)(PEt_3)_2]_2(OTf)_4$ and $[Pd(4,4'\text{-}py_2Se_2)(dppe)]_2(OTf)_4$. The $^1J(^{195}Pt\text{-}^{31}P)$ values of $[Pt(4,4'\text{-}py_2Se_2)(PEt_3)_2]_2(OTf)_4$ and $[Pt(4,4'\text{-}py_2Te_2)(PEt_3)_2]_2(OTf)_4$ (Table 36) are well in agreement with the $^1J(^{195}Pt\text{-}^{31}P)$ values for other Pt-N bonded pyridyl complexes containing *trans* to Et_3P group [222]. In

$^{77}Se\{^1H\}$ NMR spectra sharp peaks at δ 427 ppm and 421 ppm for [Pt(4,4'-py_2Se_2)(PEt_3)$_2$]$_2$(OTf)$_4$ (Figure 34) and [Pd(4,4'-py_2Se_2)(dppe)]$_2$(OTf)$_4$, respectively with little shift from the free ligand (δ 409 ppm) is indicative of non-coordinating Se atom in the metal complex. The $^{125}Te\{^1H\}$ NMR spectrum of [Pt(4,4'-py_2Te_2)(PEt_3)$_2$]$_2$(OTf)$_4$ displayed a peak at δ 428 ppm (Figure 35). In addition to these major peaks, other small resonances were observed in approximately 1.6:10 ratio at δ 445 and 435 ppm, for [Pt(4,4'-py_2Se_2)(PEt_3)$_2$]$_2$(OTf)$_4$ and [Pd(4,4'-py_2Se_2)(dppe)]$_2$(OTf)$_4$, respectively in $^{77}Se\{^1H\}$ NMR spectra and at δ 478 ppm for [Pt(4,4'-py_2Te_2)(PEt_3)$_2$]$_2$(OTf)$_4$ in $^{125}Te\{^1H\}$ NMR spectrum. The $^{195}Pt\{^1H\}$ NMR spectrum (Figure 36) of [Pt(4,4'-py_2Se_2)(PEt_3)$_2$]$_2$(OTf)$_4$ also displayed two close triplets at δ −4385 and −4395 ppm in 1.5:10 ratio with same $^1J(^{195}Pt\text{-}^{31}P)$ coupling constant of 3102 Hz. The $^{31}P\{^1H\}$ NMR could be reproduced after measuring the other hetero-nuclear NMR experiments indicating retention of the same molecular species in solution even after prolonged acquisition time. The appearance of the small peak in all the three macrocyclic complexes could be due to the existence of two isomeric species resulting from the orientation of the E-E linkage.

The mass spectral data for [Pt(4,4'-py_2Se_2)(PEt_3)$_2$]$_2$(OTf)$_4$ and [Pd(4,4'-py_2Se_2)(dppe)]$_2$(OTf)$_4$ gave convincing evidence for the formation of the complex. The MALDI TOF-MS measurements showed the molecular ion peaks minus the counter ions. For [Pt(4,4'-py_2Se_2)(PEt_3)$_2$]$_2$(OTf)$_4$, the peaks were observed at m/z (Figure 37): 1494 ([M − 4OTf)]$^+$), 1169 ([M − (3OTf + 3SeC_5H_4N)]$^+$), 1020 ([M − (4OTf + 3SeC_5H_4N)]$^+$), 668 ([M − (4OTf + SeC_5H_4N)]$^{2+}$), 585 ([M − (3OTf + 3SeC_5H_4N)]$^{2+}$) due to the formation of [Pt(4,4'-py_2Se_2)(PEt_3)$_2$]$_2$(OTf)$_4$. In the case of [Pd(4,4'-py_2Se_2)(dppe)]$_2$(OTf)$_4$, the peaks at *m/z*: 1482 ([M − (4OTf + SeC_5H_4N)]$^+$), 1409 ([M − (4OTf + 3C_6H_5)]$^+$), 1011 ([M − (4OTf + dppe + 3C_6H_5)]$^+$) and 582 ([M − (4OTf + 2SeC_5H_4N + 2C_5H_4N)]$^{2+}$) indicate the analogous structure of [Pd(4,4'-py_2Se_2)(dppe)]$_2$(OTf)$_4$.

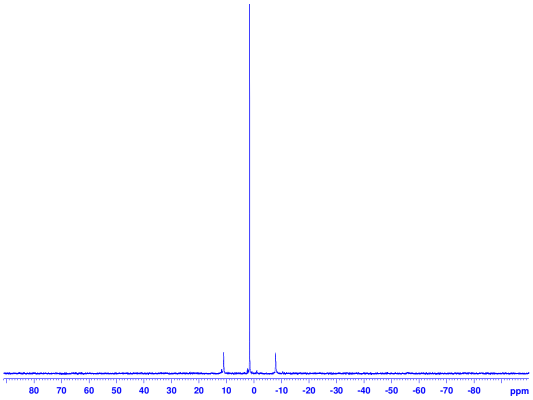

Figure 33 $^{31}P\{^1H\}$ NMR spectrum of $[Pt(4,4'\text{-}py_2Te_2)(PEt_3)_2]_2(OTf)$ in acetone-d_6

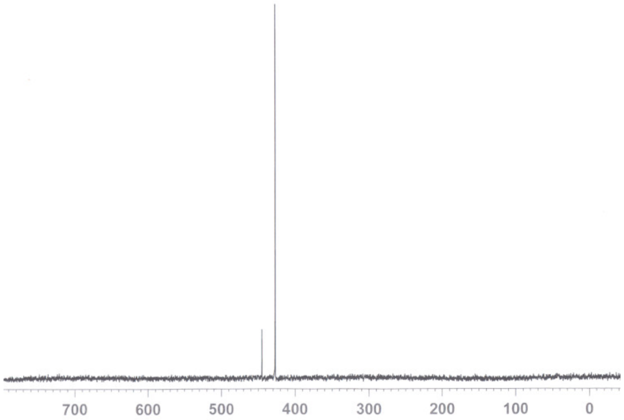

Figure 34. $^{77}Se\{^1H\}$ NMR spectrum of $[Pt(4,4'\text{-}py_2Se_2)(PEt_3)_2]_2(OTf)_4$ in acetone-d_6

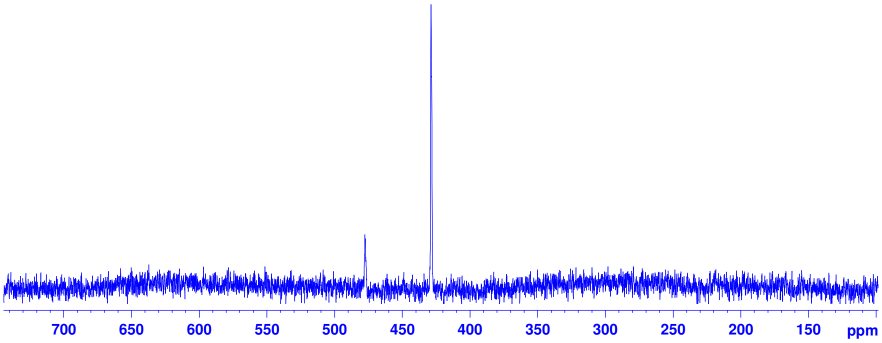

Figure 35. $^{125}Te\{^1H\}$ NMR spectrum of $[Pt(4,4'\text{-}py_2Te_2)(PEt_3)_2]_2(OTf)_4$ in acetone-d_6

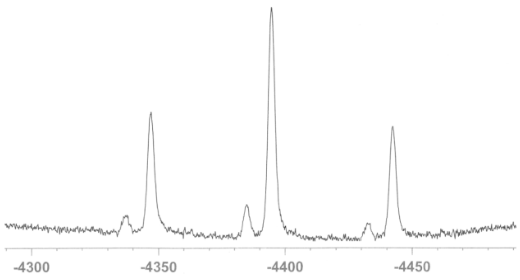

Figure 36. $^{195}Pt\{^1H\}$ NMR spectrum of $[Pt(4,4'\text{-}py_2Se_2)(PEt_3)_2]_2(OTf)_4$ in acetone-d_6

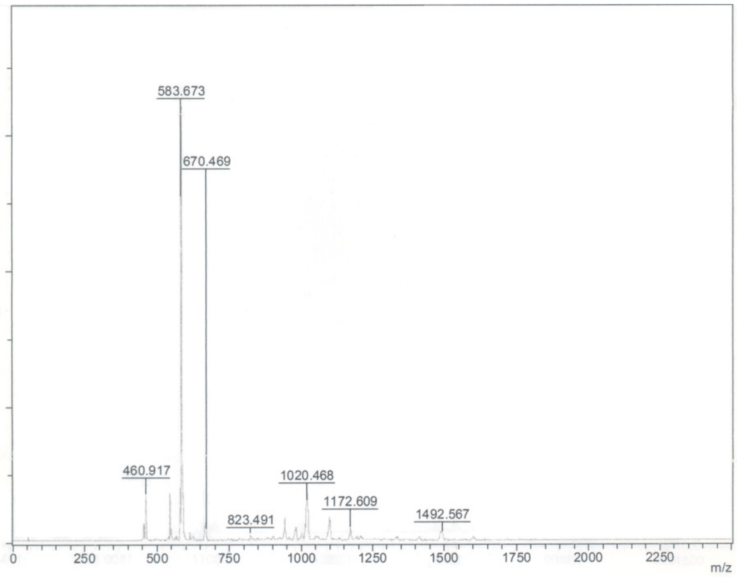

Figure 37. MALDI-TOF spectrum of $[Pt(4,4'\text{-}py_2Se_2)(PEt_3)_2]_2(OTf)_4$ in DHB matrix

The reaction of $[Pd(dppe)(OTf)_2]$ with 4,4'-py_2Te_2 surprisingly afforded $[Pd_3(\mu\text{-}Te)_2(dppe)_3)](OTf)_2$ in 84% yield rather than the expected complex $[Pd(py_2Te_2)(dppe)]_2(OTf)_4$. The preliminary characterization by ^1H NMR of the product showed the absence of pyridyl group while elemental analysis was in conformity with a composition of $[Pd_3(\mu\text{-}Te)_2(dppe)_3)](OTf)_2$. A sharp singlet at δ 46.6 ppm in the ^{31}P NMR spectrum is shielded with respect to the resonance for the parent complex $[Pd(dppe)(OTf)_2]$ (δ 75.7 ppm). The $^{125}Te\{^1H\}$ NMR resonance at δ −432 ppm (Figure 38) is significantly shielded as compared to the free ligand (δ 370 ppm). The formula of the complex $[Pd_3(\mu\text{-}$

Te)$_2$(dppe)$_3$)](OTf)$_2$ clearly indicates that the reduction takes place at the Te center from −1 in free ligand to −2 in [Pd$_3$(μ-Te)$_2$(dppe)$_3$)](OTf)$_2$. The same and similar ionic clusters of the type [M$_3$E$_2$(dppe)$_3$]$^{2+}$ (M = Ni, Pd, Pt; E = S, Se, Te) have been isolated from the reaction of [M^{II}(dppe)(solvent)]$^{2+}$ with NaEH [246]. The oxidative addition reaction of dipyridylditelluride with [M^0(PPh$_3$)$_4$] or [M^0(P$^\frown$P)$_2$] (P$^\frown$P = dppe, dppp) also yield similar trinuclear clusters [63, 64].

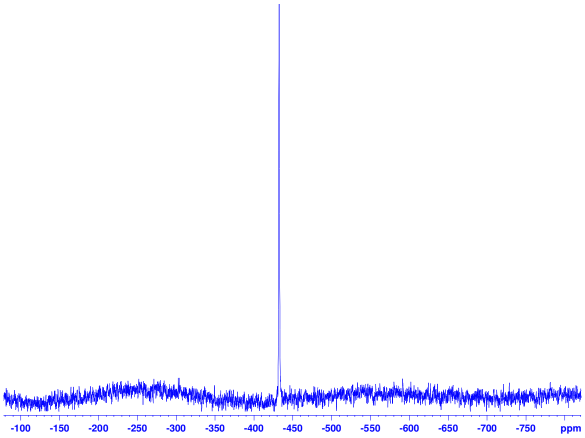

Figure 38. ^{125}Te{^{1}H} NMR spectrum of [Pd$_3$(μ-Te)$_2$(dppe)$_3$)](OTf)$_2$ in acetone-d$_6$

The molecular structures of [Pt(4,4'-py$_2$Te$_2$)(PEt$_3$)$_2$]$_2$(OTf)$_4$ and [Pd$_3$(μ-Te)$_2$(dppe)$_3$)](OTf)$_2$ have been unambiguously determined by single crystal X-ray diffraction analyses. The ORTEP diagrams are given in Figures 39, 40 and selected inter-atomic parameters are summarized in Tables 37, 38. As indicated by spectral and analytical data, the structural analysis of [Pt(4,4'-py$_2$Te$_2$)(PEt$_3$)$_2$]$_2$(OTf)$_4$ confirms the Pt–N bonded binuclear molecular unit comprising of 22-membered macrocylcle. The complex crystallizes with four molecules of water, two of which were disordered and one of them partially occupied. The latter disorder was modelled successfully. The hydrogen atoms could not be located on the water molecules. They were placed geometrically only to satisfy the stoichiometry. Absence of additional symmetry or voids was verified using PLATON. All the four triflate anions show larger thermal ellipsoids indicating possible disorder.

Table 36. NMR data for nitrogen bonded hemilabile organoselenium/ tellurium complexes of palladium and platinum

Complex	^{1}H NMR data in (δ ppm)	^{19}F{^{1}H} NMR data in (δ ppm)	^{31}P{^{1}H} NMR data in (δ ppm)	^{77}Se{^{1}H}/ ^{125}Te{^{1}H} NMR data in (δ ppm)	^{195}Pt {^{1}H} NMR data in (δ ppm)
$[Pt(4,4'\text{-}py_2Se_2)(PEt_3)_2]_2(OTf)_4$ [a]	1.24 (m, 36H), 1.89 (m, 24H), 8.11-8.03 (m, 8H), 8.93 (br, 8H)	-	-1.1(s, $^1J(^{195}Pt\text{-}^{31}P)$ = 3085 Hz)	445.1 (s), 427.1 (s)	–4395 (t, $^1J(^{195}Pt\text{-}^{31}P)$ = 3106 Hz), δ –4385 (t, $^1J(^{195}Pt\text{-}^{31}P)$ = 3116 Hz) (~ 5%)
$[Pt(4,4'\text{-}py_2Te_2)(PEt_3)_2]_2(OTf)_4$ [b]	1.23 (m, PCH_2CH_3), 1.92 (m, PCH_2), 8.07 (d, 5Hz, 2H), 8.31 (d, 5 Hz, 2H), 8.80 (d, 5 Hz, 4 H)	-81.4 (s)	-2.4(s, $^1J(^{195}Pt\text{-}^{31}P)$ = 3066 Hz)	428.8 (major), 477.7 (minor)	-4401 (t, $^1J(^{195}Pt\text{-}^{31}P)$ = 3154 Hz).
$[Pd(4,4'\text{-}py_2Se_2)(dppe)]_2(OTf)_4$ [c]	3.0-3.12 (dd, 8H, PCH_2), 7.47 (d, 8H, Ph); 7.54-7.72 (m, 40H, Ph), 8.23 (s, 8H, py)	-79.8 (s)	66.7 (s)	421.4 (major); 435.7 (minor)	-
$[Pd_3(\mu\text{-}Te)_2(dppe)_3)](OTf)_2$ [a]	2.66-2.72 (m, PCH_2), 7.31-7.35 (m), 7.49-7.56 (m, Ph)	-78.8 (s)	46.6 (s)	–432.5 (s)	-

[a] Recorded in acetone-d_6; [b] Recorded in methanol-d_1; [c] Recorded in methanol-d_4.

The macrocycle formed by the two *cis*-Pt(PEt_3)$_2$ units and two enantiomers of the 4,4'-py$_2$Te$_2$ which are typically called as *P*- and *M*-form having axial chirality with 90° bent structure [247]. The rhomboid shape and chair-like configuration of the molecular unit of [Pt(4,4'-py$_2$Te$_2$)(PEt$_3$)$_2$]$_2$(OTf)$_4$ closely resemble with the analogous structure of [Pt(PEt$_3$)$_2$(4pds)]$_2$(OTf)$_4$ (4pds = 4,4'-dipyridyldisulfide) reported earlier [165]. The square planar geometries around the Pt centres are as usually observed in other pyridyl N coordinated platinum complexes [248-250]. The similar metallamacrocycles are formed in the complexes of Co, Ni [247], Cu [165], Ru [251] and Pd [252] metals with 4pds. The sizes of the macrocyclic cavities in the present case are 11.0 Å (Pt1…Pt2) and 9.7 Å (Te1−Te2…Te3−Te4). The key factor for this macrocyclic structure, is the dihedral angle or C−Te−Te−C torsion angle which is of about 87° in [Pt(4,4'-py$_2$Te$_2$)(PEt$_3$)$_2$]$_2$(OTf)$_4$ indicating the approximate rigid nature of the ligand. However similar macrocycles comprising of C−S−S−C torsion angle close to 90° [247, 248] and large deviation to 78° are reported [247].

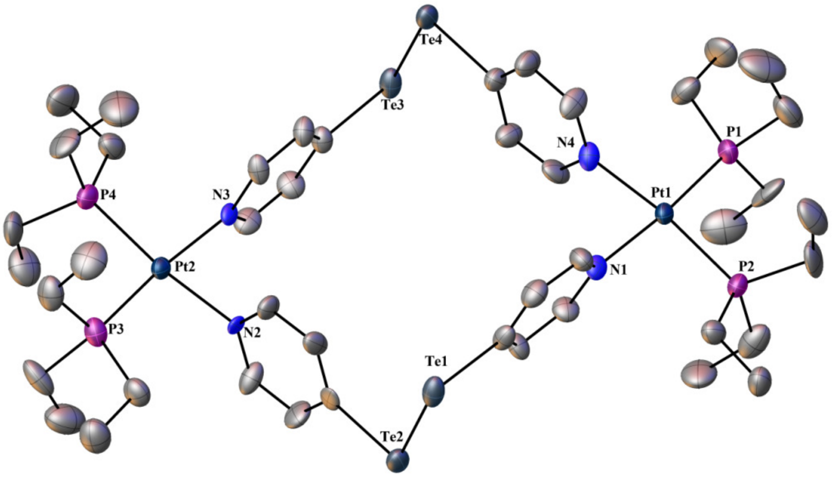

Figure 39. Molecular structure of [Pt(PEt$_3$)$_2$(4,4'-py$_2$Te$_2$)]$_2$(OTf)$_4$·3.75H$_2$O (**2**·3.75H$_2$O) ellipsoids drawn at 50% probability. The hydrogen atoms and triflate ions are omitted for clarity.

Table 37. Selected interatomic parameters [Å / °] of $[Pt(4,4'\text{-}py_2Te_2)(PEt_3)_2]_2(OTf)_4 \cdot 3.75H_2O$

Pt1–P1	2.283(3)	Pt2–P3	2.283(4)
Pt1–P2	2.271(3)	Pt2–P4	2.279(3)
Pt1–N1	2.113(11)	Pt2–N2	2.099(8)
Pt1–N4	2.094(10)	Pt2–N3	2.089(10)
Te1–Te2	2.6913(15)	Te3–Te4	2.6919(15)
Te1–C3	2.145(12)	Te2–C6	2.127(12)
P1–Pt1–P2	96.23(13)	P3–Pt2–P4	96.34(13)
P1–Pt1–N1	173.0(3)	P3–Pt2–N2	89.4(3)
P1–Pt1–N4	89.3(3)	P3–Pt2–N3	173.2(3)
P2–Pt1–N1	89.7(3)	P4–Pt2–N2	173.2(3)
P2–Pt1–N4	173.0(3)	P4–Pt2–N3	89.9(3)
N1–Pt1–N4	84.5(4)	N2–Pt2–N3	84.2(4)
C3–Te1–Te2	98.3(4)	C13–Te3–Te4	98.9(3)
C6–Te2–Te1	98.7(4)	C16–Te4–Te3	98.3(4)

Table 38. Selected inter-atomic parameters [Å / °] of $[Pd_3(\mu\text{-}Te)_2(dppe)_3)](OTf)_2$

Pd1–Te1	2.6068(5)	Pd2–Te1	2.6059(5)	Pd3–Te1	2.6131(5)
Pd1–Te2	2.6101(5)	Pd2–Te2	2.6071(5)	Pd3–Te2	2.6143(5)
Pd1–P1	2.2697(16)	Pd2–P3	2.2740(16)	Pd3–P5	2.2767(15)
Pd1–P2	2.2764(16)	Pd2–P4	2.2783(16)	Pd3–P6	2.2712(15)
Pd1–Pd2	3.356	Pd2–Pd3	3.357	Pd3–Pd1	3.306
P1–Pd1–P2	86.99(6)	P3–Pd2–P4	86.27(6)	P5–Pd3–P6	86.20(6)
P1–Pd1–Te1	175.47(4)	P3–Pd2–Te1	174.85(5)	P5–Pd3–Te1	172.67(4)
P1–Pd1–Te2	93.68(4)	P3–Pd2–Te2	93.11(4)	P5–Pd3–Te2	97.03(4)
P2–Pd1–Te1	94.79(4)	P4–Pd2–Te1	96.02(4)	P6–Pd3–Te1	93.12(4)
P2–Pd1–Te2	177.09(4)	P4–Pd2–Te2	177.05(5)	P6–Pd3–Te2	172.39(4)
Te1–Pd1–Te2	84.755(17)	Te1–Pd2–Te2	84.832(17)	Te1–Pd3–Te2	84.545(17)

The structure of trinuclear complex $[Pd_3(\mu\text{-}Te)_2(dppe)_3)](OTf)_2$ (Figure 40) is similar to other ionic clusters of the type $[M_3(\mu\text{-}E_2)(P^\frown P)_3]^{2+}$ (M = Pd, Pt; E = S, Se, Te; $P^\frown P$ = dppp [64, 253], dppe [246, 254], dppm [255]) with respect to bonding and shape. The structure of the complex can be compared with $[Pd_3(\mu\text{-}Te)_2(dppp)_3)]Cl_2$ [64]. The crystal lattice of $[Pd_3(\mu\text{-}Te)_2(dppe)_3)](OTf)_2$ consists of well-separated but electrostatically interacting complex cations and triflate counter anions. The structure comprises of three square planar *cis*-"Pd(dppe)" units bridged by two μ_3-Te^{2-} ligands, thus forming a trigonal bipyramidal Pd_3Te_2 core. All the six Pd–Te bond distances are almost equal (2.61 Å) and are comparable with the reported structures. Two of the Pd…Pd distances are same (3.36 Å) as observed in analogous complex $[Pd_3(\mu\text{-}Te)_2(dppp)_3)]Cl_2$ [64] but the other distance (Pd1…Pd3: 3.31 Å) is slightly shortened. An elongation of the Te…Te separation (3.52 Å) is observed than the one reported in $[Pd_3(\mu\text{-}Te)_2(dppp)_3)]Cl_2$ (3.32 Å) and $[Pd_2(\mu\text{-}Te)_2(dppe)_2]$ (3.319(1) Å) [256]. The observed elongation may be due to the shorter Pd–P bond distance (2.27 Å), smaller P–Pd–P angle (~ 86°) and less acute Te–Pd–Te angle (~ 84°) as compared to the Pd–P bond distance (2.29 Å), P–Pd–P angle (~ 92°, 96°) and Te–Pd–Te angle (~ 79°) in $[Pd_3(\mu\text{-}Te)_2(dppp)_3)]Cl_2$.

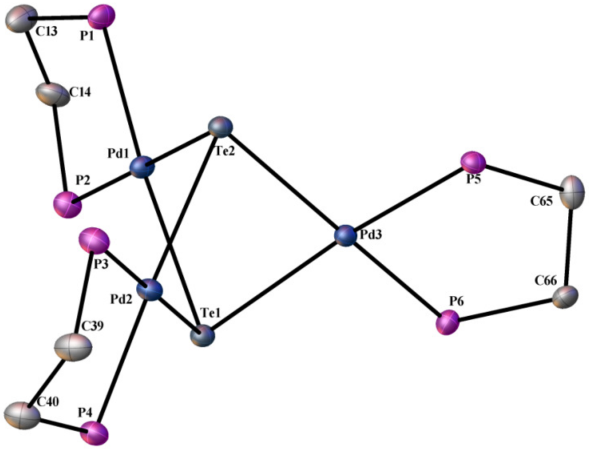

Figure 40. Molecular structure of $[Pd_3(\mu\text{-}Te)_2(dppe)_3)](OTf)_2$ (**4**) ellipsoids drawn at 50% probability. The dppe phenyl groups, hydrogen atoms and triflate ions are omitted for clarity.

Chemistry of pyridyltellurolate complexes of palladium and platinum

The chemistry of organotellurium ligands has attracted considerable attention during the last 15 years so. The ligantion and reactivity of these ligands are quite often distinctly different from those of the corresponding sulfur and selenium analogs [50, 51]. In this regard the N-hetrocyclic (e.g., pyridyl and pyrimidyl) tellurium ligands have shown markedly different reactivity resulting in the formation of numerous serendipitous products such as $[Pt(Te)(TeC_5H_4N)_2(PPh_3)]$ containing a Te(0) as ligand [62]. Thus far metal complexes of 2-pyridyl and 2-pyrimidyl tellurium ligands have been investigated, whereas the 4-pyridyl analog remains almost unexplored [51]. The 4-pyridyl analog not only offers several bonding possibilities but also provides an opportunity to study its reactivity pattern. Thus it was considered worthwhile to investigate reactivity of 4-pyridyltellurolate group.

The reactions of $MCl_2(dppe)$ (M = Pd, Pt) with two equivalents of $NaTeC_5H_4N$-4, prepared by the reductive cleavage of the Te-Te bond in 4,4′-$(C_5H_4N)_2Te_2$ with sodium borohydride in methanol, gave *cis*-$[M(TeC_5H_4N\text{-}4)_2(dppe)]$ in more than 76% yield (Scheme 18). It is worth noting that the reaction of $PdCl_2(dppe)$ with 2-pyridyltellurolate yields a trinuclear cluster $[Pd_3(\mu\text{-}Te)_2(dppe)_3)]Cl_2$, but the desired complex $[Pd(TeC_5H_4N\text{-}2)_2(dppe)]$ could be isolated from the reaction of $PdCl_2(dppe)$ with $Pb(TeC_5H_4N\text{-}2)_2$ [64].

The ^{1}H NMR spectra of these complexes showed the expected integration and peak multiplicities. The $^{31}P\{^{1}H\}$ and $^{125}Te\{^{1}H\}$ NMR peaks of palladium complex (δ 51.3 and 238 ppm) are deshielded with respect to the platinum analogue (δ 47.3 and 142 ppm). In the $^{31}P\{^{1}H\}$ NMR spectrum of $[Pt(TeC_5H_4N\text{-}4)_2(dppe)]$, in addition of $^{1}J(^{195}Pt\text{-}^{31}P)$ coupling (2928 Hz), both *trans* and *cis* $^{2}J(^{125}Te\text{-}^{31}P)$ couplings are also observed (Figure 41). The $^{195}Pt\{^{1}H\}$ NMR resonance showed a triplet at δ −5349 ppm with $^{1}J(^{195}Pt\text{-}^{31}P)$ coupling of

2928 Hz. The ${}^{1}J({}^{195}Pt-{}^{125}Te)$ coupling ~ 263 Hz is observed in both the ${}^{125}Te\{{}^{1}H\}$ and ${}^{195}Pt\{{}^{1}H\}$ NMR spectra of $[Pt(TeC_5H_4N-4)_2(dppe)]$.

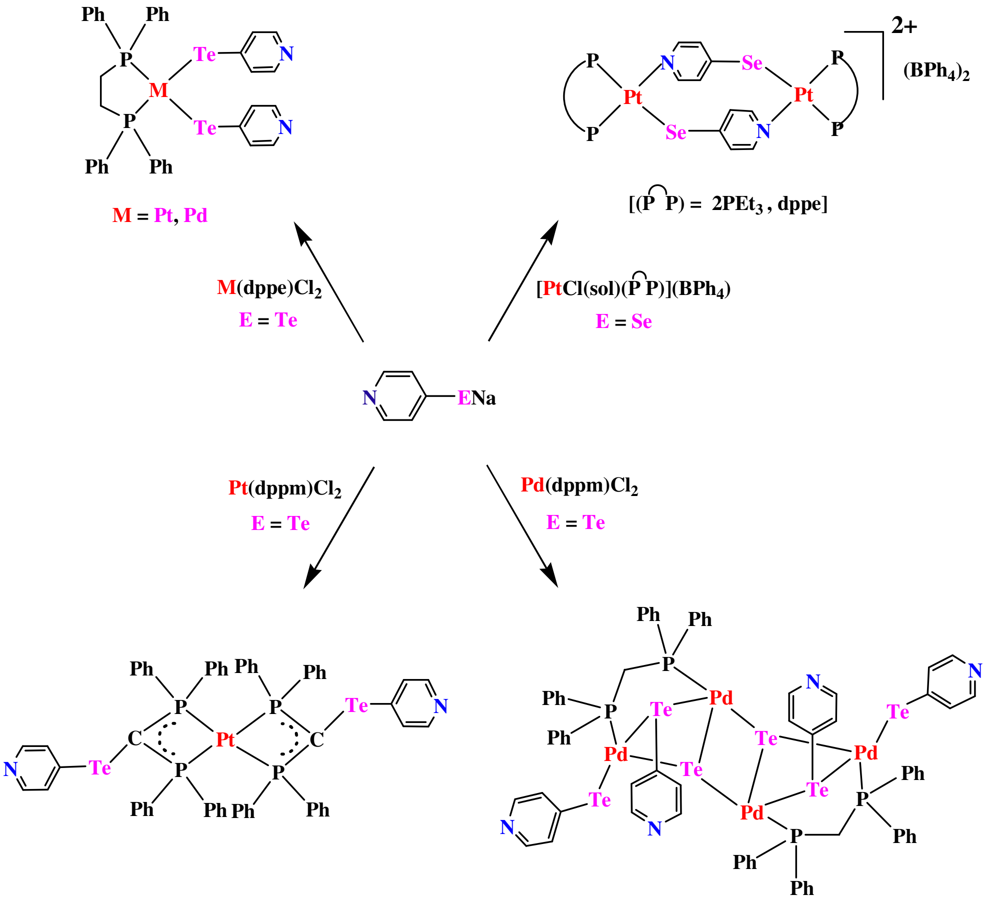

Scheme 18

Unlike $MCl_2(dppe)$, $MCl_2(dppm)$ showed different reactivity. The reaction of $PdCl_2(dppm)$ with two equivalents of $NaTeC_5H_4N-4$ resulted in an unexpected product of composition $[Pd_2(\mu-Te)(\mu-TeC_5H_4N-4)(TeC_5H_4N-4)(dppm)]_2$ as confirmed by X-ray structural anlysis. The presence of ligand Te^{2-} in the palladium complex shows reduction at the Te center, as well as the Te–C bond cleavage in the ligand. The dppm ligand is also unusually changed from *cis*-chelating to bridging mode. The analogous reaction with $PtCl_2(dppm)$ gave only $[Pt\{PPh_2C(TeC_5H_4N-4)PPh_2\}_2]$ (Scheme 18) in 57% yield which is also characterized by X-ray structure. In contrast, the reaction of 2-pyridyltellurolate gives a mixture of [Pt{$PPh_2C(TeC_5H_4N$-2)PPh_2}$_2$] and [Pt(2-$TeC_5H_4N)_2$(dppm)] in 45% and 25% yield, respectively [63]. The ^{1}H NMR showed the absence of the methylene group of the phosphine ligand. The ^{31}P NMR spectrum displayed a single sharp resonance indicating equivalence of all the phosphorus nuclei. The $^1J(^{195}Pt-^{31}P)$ coupling of about 1909 Hz is significantly reduced and can be compared with [Pt{$PPh_2C(TeC_5H_4N$-2)PPh_2}$_2$] [63]. The formation of these complexes is rather supervising and appears to take place by the attack of tellurolate ligand on methylene carbon as well as its deprotonation. Deprotonation (both single and double) of methylene proton in dppm and related ligands, Ph_2PCH_2L (L = SMe, NHR, PR_2) is well documented in literature [257-261]. Double deprotonation of dppm ligands in the present case seems to be elicited by strong nucleophilicity of pyridyltellurolate ligand. During substitution reaction the tellurolate ion attacks the chelating dppm to give $Ph_2PCH(TeC_5H_4N)PPh_2PtCl_2$ which in the presence of a base generates [Pt{$PPh_2C(TeC_5H_4N$-4)PPh_2}$_2$]

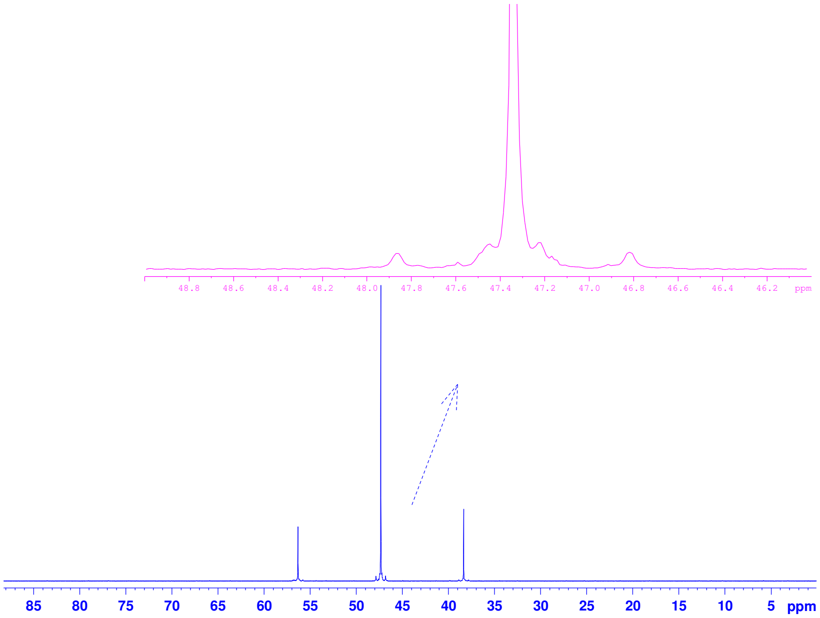

Figure 41. $^{31}P\{^1H\}$ NMR spectrum of [Pt(TeC_5H_4N-4)$_2$(dppe)] in acetone-d_6

The reaction of $NaTeC_5H_4N$-4 with $MCl_2(PR_3)_2$ and $[M_2Cl_2(\mu\text{-}Cl)_2(PR_3)_2]$ (PR_3 = PEt_3, PPh_3) did not yield products with satisfaction, instead excessive decomposition was observed with black suspension in the reaction mixtures which were not further followed up. Thus a different route was conceived to synthesize such complexes. The reaction of Na_2PdCl_4 with 4,4'-$(C_5H_4N)_2Te_2$ yielded a brown colored insoluble product of composition $[PdCl_2(4,4'\text{-}(C_5H_4N)_2Te_2)]_n$ (Scheme 19), as previously isolated an analogous product $[PdCl_2(4,4'\text{-}(C_5H_4N)_2Se_2)]_n$ from the similar reaction with 4,4'-$(C_5H_4N)_2Se_2$. Generally such reactions give complexes of composition $[PdCl(EAr)]_n$ (E = S, Se, Te; Ar = aryl) [167]. Treatment of $[PdCl_2(4,4'\text{-}(C_5H_4N)_2Te_2)]_n$ with one and two equivalents of PPh_3 was monitored in NMR tube by $^{31}P\{^1H\}$ NMR spectroscopy in acetone-d_6. Initially two peaks were observed at δ 23.4 and 26.6 ppm, but after 3 days a major peak (> 90%) at δ 23.4 ppm existed. The resonance showed a coupling of 103 Hz which could be due to $^2J(^{125}Te\text{-}^{31}P)$. This solution after recystallization gave crystals of *cis*-$[PdCl(TeC_5H_4N\text{-}4)(PPh_3)]_2$ which was structurally characterized. It is noteworthy that the complex $[PdCl(SeC_5H_4N\text{-}4)(PPh_3)]_n$ exist as a mixture of dimer/trimer in solution.

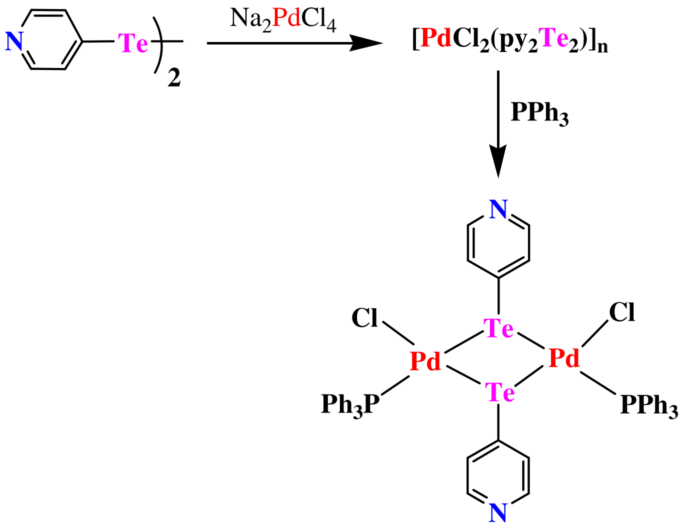

Scheme 19

The reaction of $PtCl_2(P^\frown P)$ ($P^\frown P$ = $2PEt_3$, dppe) with one equivalent of $NaSeC_5H_4N$-4 in the presence of $NaBPh_4$ afforded cationic binuclear complexes $[Pt(SeC_5H_4N\text{-}4)(P^\frown P)]_2(BPh_4)_2$. The $^{31}P\{^1H\}$ NMR spectra of $[Pt(SeC_5H_4N\text{-}4)(P^\frown P)]_2(BPh_4)_2$ showed two doublets, a pattern indicative of non-equivalence of the two phosphorus nuclei of two PEt_3 or dppe ligands. The $^{31}P\{^1H\}$ NMR spectrum of $[Pt(SeC_5H_4N\text{-}4)(dppe)]_2(BPh_4)_2$ (Figure 42) showed two doublets at δ 37.5 ($^1J(^{195}Pt\text{-}^{31}P)$ = 3194 Hz) and 47.8 ($^1J(^{195}Pt\text{-}^{31}P)$ = 2885 Hz) ppm (Table 39) due to the P *trans* to N and P *trans* to Se, respectively. Each signal appeared as a doublet due to the $^{31}P\text{-}^{31}P$ coupling of 3.9 Hz. The $^{195}Pt\{^1H\}$ (Figure 43) resonance showed doublet of doublet due to coupling with two different phosphorus nuclei. Two doublets in $^{31}P\{^1H\}$ spectrum of $[Pt(SeC_5H_4N\text{-}4)(PEt_3)_2]_2(BPh_4)_2$ are shielded at δ 0.1 ($^1J(^{195}Pt\text{-}^{31}P)$ = 3013 Hz) and 11.6 ($^1J(^{195}Pt\text{-}^{31}P)$ = 2885 Hz) ppm with respect to the dppe analogue. The crystal structures of $[Pt(SeC_5H_4N\text{-}4)(P^\frown P)]_2(BPh_4)_2$ show that both N and Se atoms coordinate to the platinum centers. However based on NMR spectra, it was assigned that the Se atoms bridged between the two platinum atoms whereas the N atoms are free in other reported complexes $[Pt_2(SeCH_2CH_2NMe_2)_2(P^\frown P)_2][BPh_4]_2$ [55].

Table 39. NMR data for pyridyltellurolate complexes of palladium and platinum

Complex	^{1}H NMR data in (δ ppm)	^{31}P{^{1}H} NMR data in (δ ppm)	^{77}Se{^{1}H}/ ^{125}Te{^{1}H} NMR data in (δ ppm)	^{195}Pt {^{1}H} NMR data in (δ ppm)
$[Pd(TeC_5H_4N\text{-}4)_2(dppe)]$	2.38 (d, 4H, PCH_2); 7.22 (d, 6 Hz, 4H, py); 7.41-7.46 (td, 8H, *m*-H, Ph), 7.50-7.54 (m, 4H, *p*-H, Ph), 7.63 (d, 6 Hz, 4H, py), 7.66-7.71 (m, 8H, *o*-H, Ph)	51.3 (s)	237.7 (d, $^{2}J_{(Te\text{-}P)}$ = 197 Hz).	-
$[Pt(TeC_5H_4N\text{-}4)_2(dppe)]$	2.28 (t, 4H, PCH_2); 7.22 (d, 5.6 Hz, 4H, py); 7.43 (td, 8.2 Hz, 8H, m-H, Ph), 7.51 (td, 8.2 Hz, 4H, *p*-H, Ph), 7.62 (d, 5.6 Hz, 4H, py), 7.71-7.76 (m, 8H, *o*-H, Ph)	47.3 (s, $^{1}J(^{195}Pt\text{-}^{31}P)$ = 2912 Hz, $^{2}J(^{125}Te\text{-}^{31}P)$ = 168 (trans), 37 (cis) Hz)	142 (d, $^{2}J(^{125}Te\text{-}^{31}P)$ = 162 Hz; $^{1}J(^{195}Pt\text{-}^{125}Te)$ = 768 Hz)	-5349 (t, $^{1}J(^{195}Pt\text{-}^{31}P)$ = 2928 Hz; $^{1}J(^{195}Pt\text{-}^{125}Te)$ = 763 Hz).
$[Pt\{PPh_2C(TeC_5H_4N\text{-}4)PPh_2\}_2]$	6.17 (d, 5.7 Hz, 4H, py), 7.03 (t, 16H, m-H, Ph), 7.19 (t, 8H, *p*-H, Ph), 7.31 (d, 5.7 Hz, 4H, py), 7.40 (br, 16H, *o*-H, Ph)	-27.5 (s, $^{1}J(^{195}Pt\text{-}^{31}P)$ = 1909 Hz)	486 (s)	-
$[Pd_2(\mu\text{-}Te)(\mu\text{-}TeC_5H_4N\text{-}4)(TeC_5H_4N\text{-}4)(dppm)]_2$	-	-	-	-

[Pt(SeC$_5$H$_4$N-4)(dppe)]$_2$(BPh$_4$)$_2$.4CH$_2$Cl$_2$	2.32 (m, PCH$_2$); 6.80-7.02 (m), 7.29 (br), 7.38-7.43 (m), 7.53-7.75 (m) (Ph, C$_5$H$_4$)	37.5 (d, 1.6 Hz, ^{2}J(^{77}Se-^{31}P)$_{cis}$ = 37 Hz; ^{1}J(^{195}Pt-P) = 3194 Hz) (P trans to N); 47.8 (d, 3 Hz; ^{2}J(^{77}Se-^{31}P) = 65 Hz; ^{1}J(^{195} Pt-^{31}P) = 2885 Hz (P trans to Se)	-	–4592 (dd, ^{1}J(^{195}Pt-^{31}P) = 3200, 2903 Hz).
[Pt(SeC$_5$H$_4$N-4)(PEt$_3$)$_2$]$_2$(BPh$_4$)$_2$	1.08-1.26 (m, PCH$_2$CH$_3$); 1.74-1.81, 2.07-2.13 (m, PCH$_2$), 6.77 (t), 6.91 (t), 7.16 (br, Ph); 7.32 (d), 7.44 (d), 7.94 (d), 8.13 (d)	0.1 (d, J = 123 Hz, ^{1}J(^{195}Pt-P) = 2855Hz); 11.6 (d, ^{1}J(^{195}Pt-P) = 2855 Hz)	-	-
[PdCl(TeC$_5$H$_4$N-4)(PPh$_3$)]$_2$				

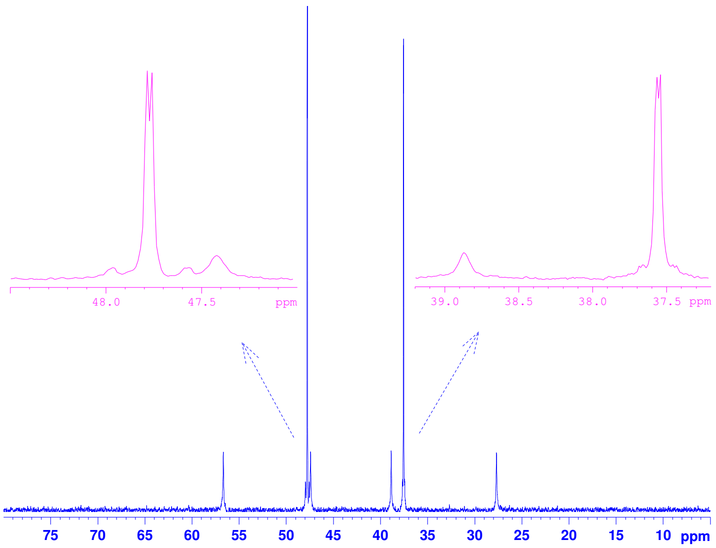

Figure 42. $^{31}P\{^{1}H\}$ NMR spectrum of $[Pt(SeC_5H_4N\text{-}4)(dppe)]_2(BPh_4)_2.4CH_2Cl_2$ in CD_2Cl_2

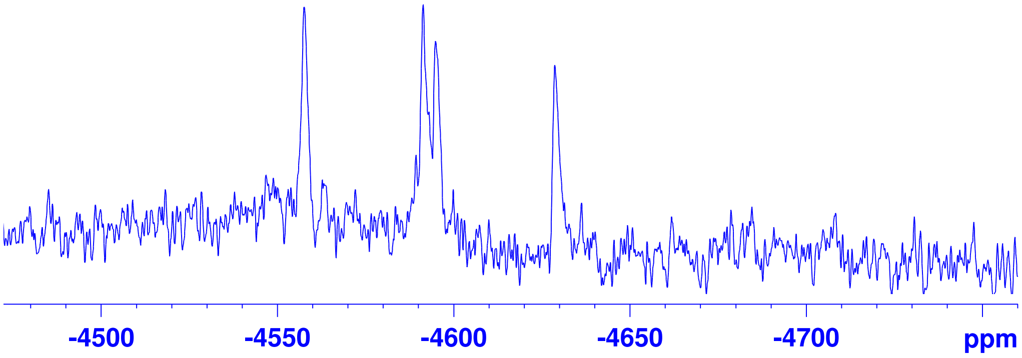

Figure 43. $^{195}Pt\{^{1}H\}$ NMR spectrum of $[Pt(SeC_5H_4N\text{-}4)(dppe)]_2(BPh_4)_2.4CH_2Cl_2$ in CD_2Cl_2

The structures of *cis*-$[M(TeC_5H_4N\text{-}4)_2(dppe)]$ (M = Pd or Pt) are isomorphous (Figures 44, 45). Various bond lengths and angles in the two structures are comparable (Table 40). The geometry around the metal centers are essentially square planar. Both Pd and Pt atoms are slightly above (0.04 Å) the average coordination plane made by the four donor atoms, two P and two Te atoms. One of the Te–C bond is almost coplanar (8°) with coordination plane whereas the other Te–C bond is tilted at 72° above the coordination plane in both the structures. This might have affected in lengthening one of the M–Te bond by about 0.04 Å possibly due to the repulsion exerted by one of the lone pair of Te atom to the opposite M–Te bond.

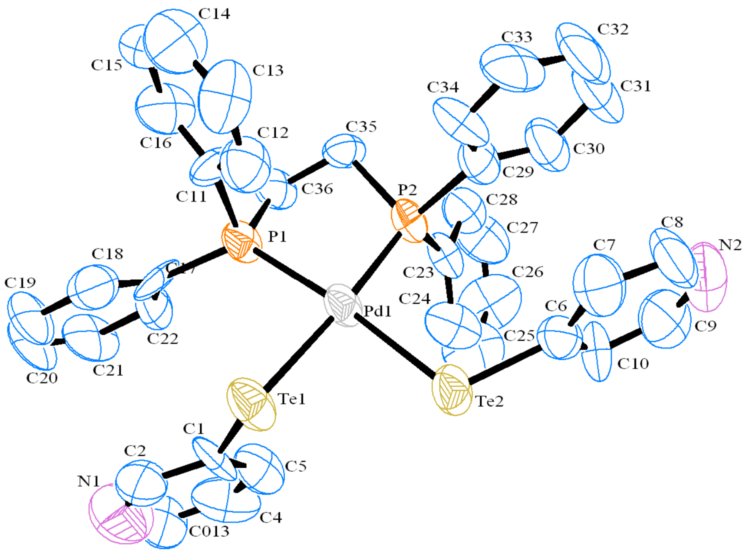

Figure 44. Structure of [Pd(TeC$_5$H$_4$N-4)$_2$(dppe)]. The hydrogen atoms are omitted for clarity.

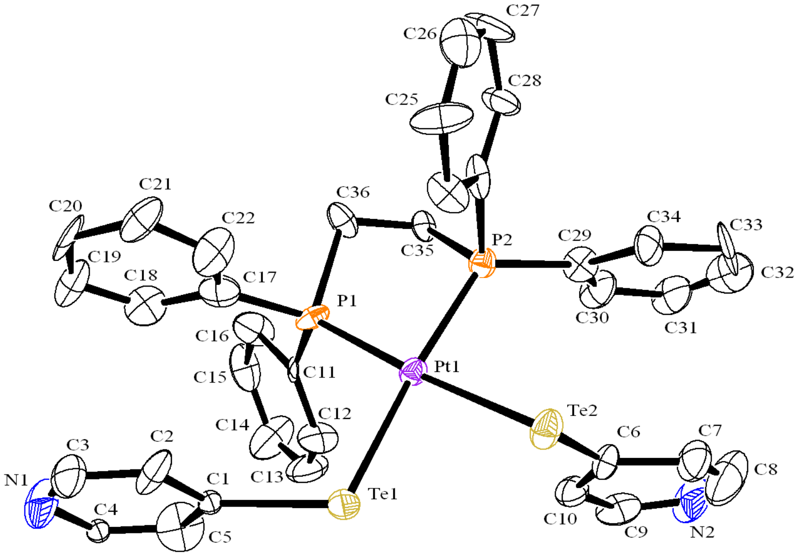

Figure 45. Structure of [Pt(TeC$_5$H$_4$N-4)$_2$(dppe)]. The hydrogen atoms are omitted for clarity.

Table 40. Selected inter-atomic parameters [Å / °] of [M(TeC_5H_4N-4)$_2$(dppe)] (M = Pd, Pt)

	M = Pd	M = Pt
M1–P1	2.267(5)	2.263(7)
M1–P2	2.267(5)	2.264(7)
M1–Te1	2.638(2)	2.603(2)
M1–Te2	2.5953(18)	2.643(2)
C1–Te1	2.127(19)	2.18(2)
C6–Te2	2.12(2)	2.10(3)
P1–M1–P2	86.32(19)	85.1(3)
P1–M1–Te2	171.60(16)	175.7(2)
P2–M1–Te1	175.75(15)	172.0(2)
Te1–M1–Te2	82.70(6)	82.34(7)
M1–Te1–C1	97.0(5)	110.3(7)
M1–Te2–C6	110.2(5)	96.4(8)

The mononuclear structure of [Pt{$PPh_2C(TeC_5H_4N$-4)PPh_2}$_2$] (Figure 46, Table 41) is very similar to the recently reported complex [Pt{$PPh_2C(TeC_5H_4N$-2)PPh_2}$_2$] [63]. A distorted square planar Pt(II) is coordinated by four phosphorus atoms of the ligand in chelating mode. The angles around the coordination center (69 and 111°) are largely deviated from the ideal right angle. All other structural features closely match with the reported complexes except the two Pt–P distances in the present complex are dissimilar (2.40 and 2.27 Å). Two chelating units "PtPCP" and coordination plane are coplanar and the two pyridyl groups adopt an *anti* conformation. The sum of the angles of three coplanar bonds around C6 atom is 359.5°, indicating a sp^2 hybridization of the carbon atom.

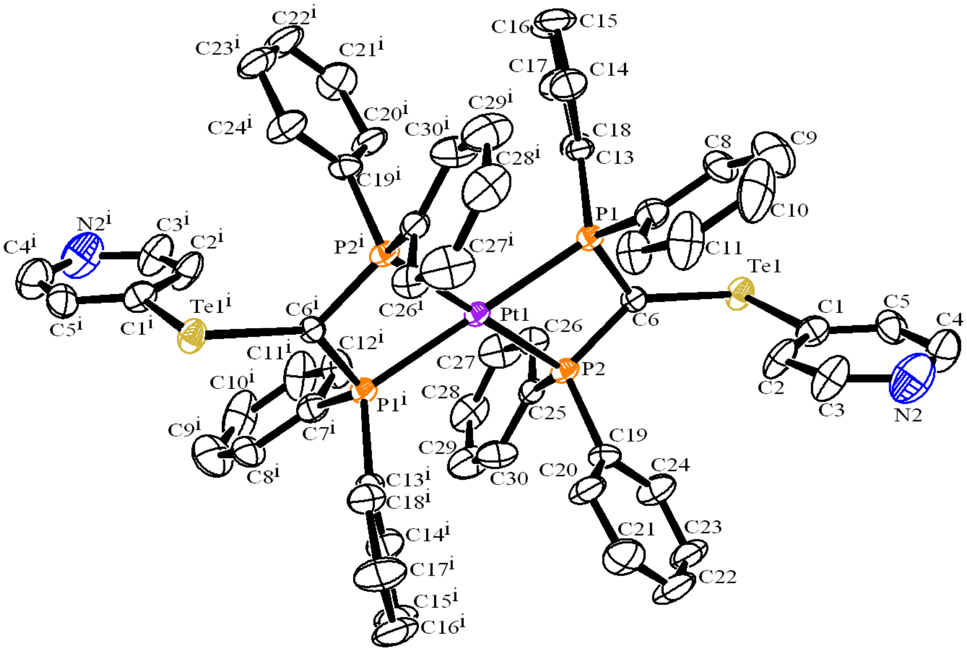

Figure 46. Molecular structure of [Pt{$PPh_2C(TeC_5H_4N\text{-}4)PPh_2$}$_2$]. The hydrogen atoms are omitted for clarity.

Table 2. Selected inter-atomic parameters [Å / °] of [Pt{$PPh_2C(TeC_5H_4N\text{-}4)PPh_2$}$_2$]

Pt1–P1	2.401(3)	Pt1–P2	2.265(3)
P1–C6	1.695(10)	P2–C6	1.793(10)
Te1–C1	2.194(7)	Te1–C6	2.086(10)
P1–Pt1–P2	68.96(10)	P1–Pt1–P2^{i}	111.04(10)
P1–Pt1–P1^{i}	180.0	P1–C6–P2	98.5(5)
P1–C6–Te1	128.9(6)	P2–C6–Te1	132.1(5)
Pt1–P1–C6	95.2(4)	Pt1–P1–C13	117.5(3)
C6–Te1–C1	101.3(4)		

The tetranuclear molecular unit of $[Pd_2(\mu\text{-Te})(\mu\text{-TeC}_5H_4N\text{-4})(TeC_5H_4N\text{-4})(dppm)]_2$ (Figure 47) reveals a number of interesting structural features. The structure comprises of two units of $[Pd_2(\mu\text{-Te})(\mu\text{-TeC}_5H_4N\text{-4})(TeC_5H_4N\text{-4})(dppm)]$ which are bridged by one Te^{2-} and one 4-TeC_5H_4N ligands. In this unit, one of the Pd atom (Pd1) is surrounded by two Te^{2-}, one P and one bridging Tepy ligands, whereas the other Pd atom (Pd2) is coordinated by one Te^{2-}, one P, one bridging Tepy and one terminal Tepy (Te5) ligands. The dppm ligand unusually bridges two Pd centers rather than in chelating mode, as a result the three Pd–Te distances are different (Table 42). The shortest bond length found with Te^{2-} ligand, for example Pd1–Te1, Pd3–Te2 distances are of 2.57 Å. The longest distance observed with the terminal Tepy ligand (Pd2–Te5, Pd4–Te6: 2.65 Å). All the Pd–P bond lengths are almost equal and match with the reported values. The Te1…Te2 and the shortest Pd…Pd (Pd2…Pd3) separation are 3.34 and 3.22 Å, respectively. The pyridyl group with Te6 is highly disordered.

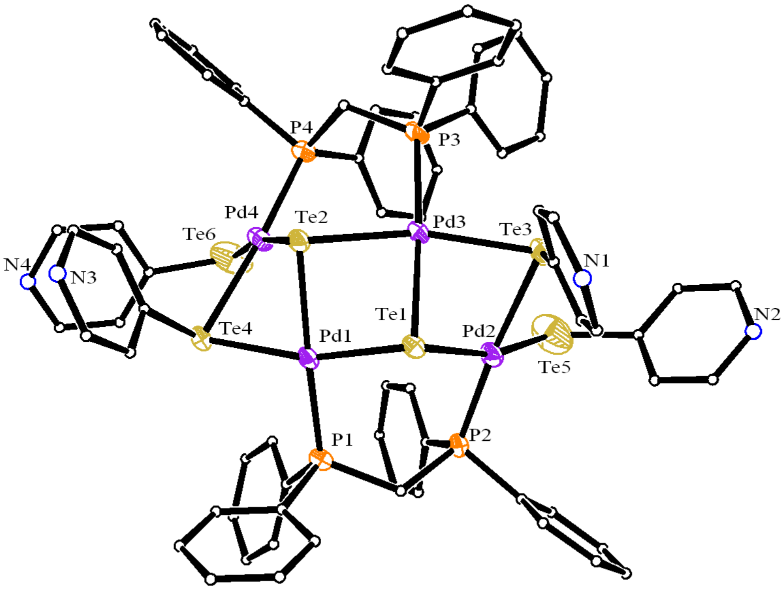

Figure 47. Molecular structure of $[Pd_4(\mu_3\text{-Te})_2(\mu_2\text{-Tepy})_2(Tepy)_2(dppm)_2]$. The hydrogen atoms are omitted for clarity.

Table 42. Selected inter-atomic parameters [Å / °] of $[Pd_4(\mu_3\text{-}Te)_2(\mu_2\text{-}Tepy)_2(Tepy)_2(dppm)_2]$

Pd1–Te1	2.569(2)	Pd3–Te1	2.605(2)
Pd1–Te2	2.592(2)	Pd3–Te2	2.5707(19)
Pd1–Te4	2.619(2)	Pd3–Te3	2.637(2)
Pd2–Te1	2.578(2)	Pd4–Te2	2.578(2)
Pd2–Te3	2.617(2)	Pd4–Te4	2.617(2)
Pd2–Te5	2.648(3)	Pd4–Te6	2.653(3)
P1–Pd1	2.274(6)	P3–Pd3	2.282(5)
P2–Pd2	2.271(5)	P4–Pd4	2.272(5)
Pd2···Pd3	3.224(2)		
P1–Pd1–Te1	96.14(16)	P3–Pd3–Pd2	133.59(17)
P1–Pd1–Te2	176.71(17)	Te1–Pd3–Pd2	51.14(5)
Te1–Pd1–Te2	80.63(6)	Te2–Pd3–Pd2	118.35(6)
P1–Pd1–Te4	99.59(16)	Te3–Pd3–Pd2	51.86(5)
Te1–Pd1–Te4	164.24(8)	P3–Pd3–Te1	175.26(17)
Te2–Pd1–Te4	83.63(7)	Te2–Pd3–Te1	80.34(6)
P2–Pd2–Pd3	132.32(14)	P3–Pd3–Te2	96.25(15)
Te1–Pd2–Pd3	51.92(5)	P3–Pd3–Te3	99.45(15)
Te3–Pd2–Pd3	52.42(5)	Te1–Pd3–Te3	83.69(6)
Te5–Pd2–Pd3	112.89(9)	Te2–Pd3–Te3	163.56(8)
P2–Pd2–Te1	97.22(14)	P4–Pd4–Te2	96.74(17)
P2–Pd2–Te3	174.77(16)	P4–Pd4–Te4	175.96(17)
Te1–Pd2–Te3	84.64(7)	Te2–Pd4–Te4	83.94(7)
P2–Pd2–Te5	91.52(16)	P4–Pd4–Te6	90.36(17)
Te1–Pd2–Te5	164.27(10)	Te2–Pd4–Te6	169.02(10)
Te3–Pd2–Te5	87.81(8)	Te4–Pd4–Te6	89.55(8)
Pd1–Te1–Pd2	102.49(7)	C51–Te3–Pd2	107.2(5)
Pd1–Te1–Pd3	87.61(7)	C51–Te3–Pd3	94.8(5)
Pd2–Te1–Pd3	76.94(6)	Pd2–Te3–Pd3	75.72(6)
Pd3–Te2–Pd1	87.88(6)	C56–Te4–Pd1	101.1(5)
Pd4–Te2–Pd1	79.82(7)	Pd4–Te4–Pd1	78.60(6)
Pd3–Te2–Pd4	101.96(7)	C56–Te4–Pd4	101.5(5)
C61–Te5–Pd2	104.0(17)	C66–Te6–Pd4	86.37
C61A–Te5–Pd2	108(2)	C66A–Te6–Pd4	99.8(12)
C13–P1–C1	105.6(8)	C38–P3–C26	104.6(9)
C13–P1–C7	102.5(8)	C38–P3–C32	104.5(9)
C1–P1–Pd1	118.2(6)	C26–P3–Pd3	121.2(6)
C13–P1–Pd1	117.8(6)	C32–P3–Pd3	104.3(6)
C7–P1–Pd1	107.2(6)	C38–P3–Pd3	116.6(7)
C13–P2–C14	102.4(8)	C38–P4–C39	102.7(9)
C13–P2–C20	99.4(8)	C45–P4–C39	109.3(9)
C13–P2–Pd2	118.8(6)	C38–P4–Pd4	118.0(7)
C14–P2–Pd2	116.5(6)	C39–P4–Pd4	107.5(6)
C20–P2–Pd2	108.3(6)	C45–P4–Pd4	115.7(6)

The dinuclear complex [PdCl(μ-TeC_5H_4N-4)(PPh_3)]$_2$ (Figure 48) adopts a *sym-cis* configuration stabilized by two bridging tellurolate ligands. Interestingly the analogous selenolate complex [PdCl(μ-SeC_5H_4N-4)(PPh_3)]$_2$ exist in a *sym-trans* configuration (Section 1) whereas complexes [PdCl(SC_5H_4N-4)(PPh_3)]$_n$ [160] and [MCl(SeC_5H_4N-4)(PEt_3)]$_n$ (Section 1) acquire a trinuclear macrocyclic structure in which the N-atoms are coordinated to the Pd centers. The four-membered Pd_2Te_2 ring in the present case is almost coplanar with the Pd coordination plane and the two pyridyl groups of bridging selenolate adopt an *anti* conformation. A large number of thiolate bridged binuclear complexes are found mostly with hinged M_2S_2 ring [228], although a few complexes with planar ring have also been reported [52]. The Pd–P (2.34 Å) and Pd–Cl (2.37 Å) distances (Table 43) are slightly longer than in [PdCl(μ-SeC_5H_4N-4)(PPh_3)]$_2$ due to the stronger *trans* influence of tellurolate than selenolate ligand.

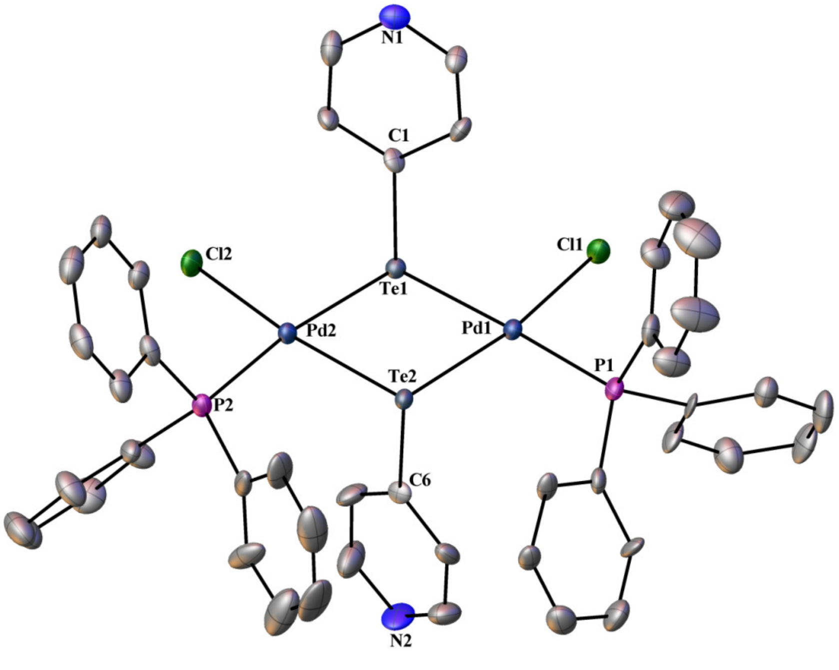

Figure 48. Molecular structure of [PdCl(TeC_5H_4N-4)(PPh_3)]$_2$. Hydrogen atoms are omitted for clarity.

Table 43. Selected inter-atomic parameters [Å / °] of $[PdCl(TeC_5H_4N\text{-}4)(PPh_3)]_2$

Pd1–P1	2.338(3)	Pd2–P2	2.333(3)
Pd1–Te1	2.6118(11)	Pd2–Te1	2.6115(11)
Pd1–Te2	2.5572(11)	Pd2–Te2	2.5590(11)
Pd1–Cl1	2.368(3)	Pd2–Cl2	2.377(3)
Te1–C1	2.140(12)	Te2–C6	2.143(12)
Te1–Pd1–Te2	78.88(3)	Pd1–Te1–Pd2	99.53(4)
Te1–Pd1–Cl1	92.34(8)	Pd1–Te2–Pd2	102.41(4)
Te1–Pd1–P1	177.64(9)	Pd1–Te2–C6	96.5(3)
Te2–Pd1–P1	99.03(9)	Pd1–Te1–C1	100.4(3)

The structures of $[Pt(SeC_5H_4N\text{-}4)(dppe)]_2(BPh_4)_2$ (Figure 49) and $[Pt(SeC_5H_4N\text{-}4)(PEt_3)_2]_2(BPh_4)_2$ (Figure 50) comprise of a rectangular shaped macrocyclic unit of "$Pt_2(4\text{-}SeC_5H_4N\text{-}4)_2$" with Pt…Pt separation of 7.51 Å and 7.81 Å, respectively. The smaller and longer arms of the rectangles are considered as Pt–Se bond (2.48 Å, 2.50 Å) and non-bonded Pt…Se separation of 6.74 Å, 6.90 Å, respectively. The π…π stacking between two pyridyl rings are 3.24 Å and 3.12 Å, respectively for the two structures. In $[Pt(SeC_5H_4N\text{-}4)(dppe)]_2(BPh_4)_2$, the Pt1–P2 bond is slightly longer in length (2.28 Å) (Table 44) as compared to Pt1–P1 distance (2.24 Å) due to the stronger *trans* imfluence of the selenolate ligand.

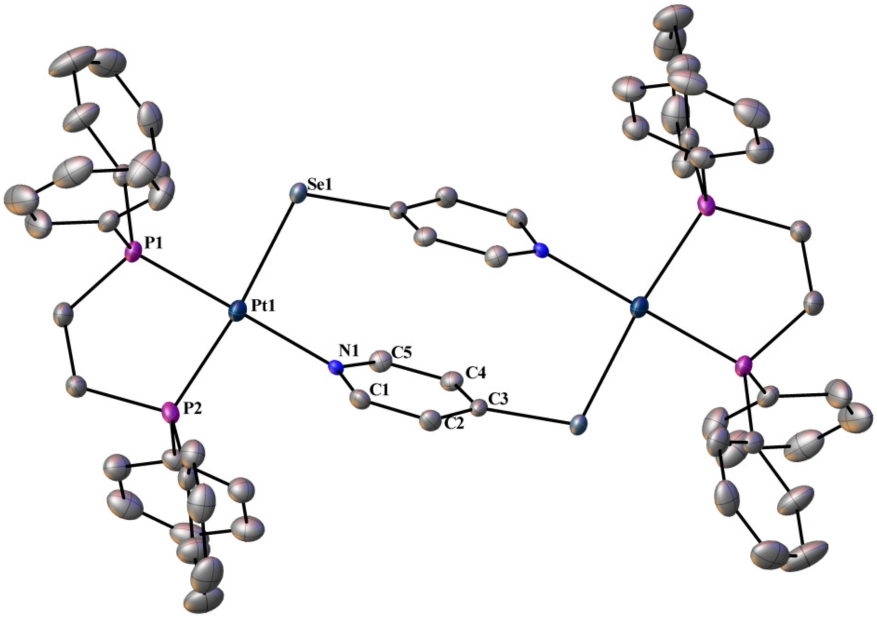

Figure 49. Molecular structure of $[Pt(SeC_5H_4N\text{-}4)(dppe)]_2(BPh_4)_2.4CH_2Cl_2.$ Hydrogen atoms are omitted for clarity.

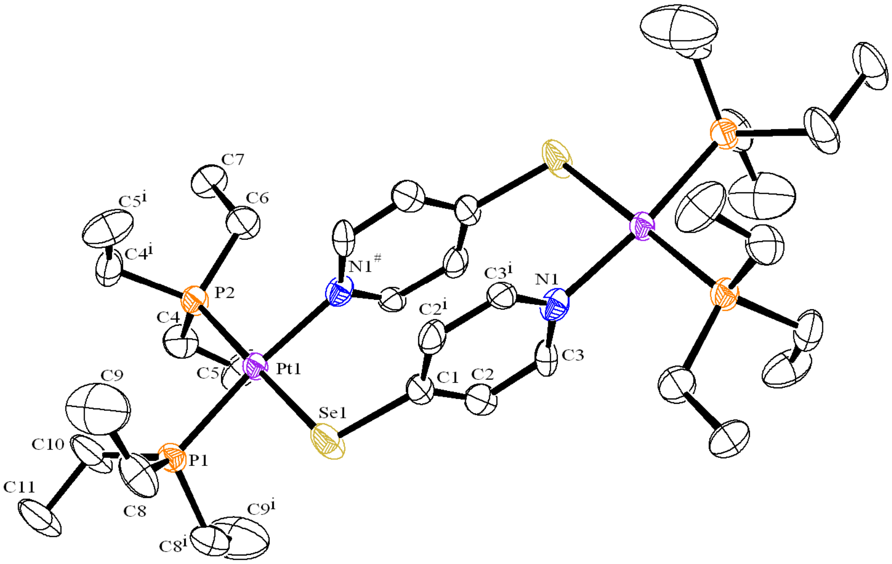

Figure 50. Molecular structure of $[Pt(SeC_5H_4N\text{-}4)(PEt_3)_2]_2(BPh_4)_2.$ Hydrogen atoms are omitted for clarity.

Table 44. Selected inter-atomic parameters [Å / °] of $[Pt(SeC_5H_4N\text{-}4)(P^{\cap}P)]_2(BPh_4)_2$ ($P^{\cap}P$ = dppe or $2PEt_3$)

	$[Pt(SeC_5H_4N\text{-}4)(dppe)]_2(BPh_4)_2$ $.4CH_2Cl_2$	$[Pt(SeC_5H_4N\text{-}4)(PEt_3)_2]_2(BPh_4)_2$
Pt1–P1	2.2382(10)	2.306(6)
Pt1–P2	2.2796(11)	2.296(5)
Pt1–Se1#/Se1	2.4837(5)	2.498(2)
Pt1–N1/N1#	2.120(3)	2.135(17)
Se1–C3/C1	1.916(4)	1.94(2)
Pt···Pt	7.509	7.806
P1–Pt1–P2	86.11(4)	96.4(2)
P1–Pt1–Se1#/Se1	87.94(3)	84.56(14)
P2–Pt1–Se1#/Se1	171.61(3)	179.01(16)
P1–Pt1–N1/N1#	178.29(9)	172.3(4)
N1–Pt1–Se1#/Se1	92.71(80	87.7(4)
N1–Pt1–P2	93.41(8)	91.3(4)
Pt1–Se1–C3/C1	106.37(11)	108.2(5)

Chapter 4

Summary and Conclusions

Summary and Conclusions

The present thesis consists of four chapters, *viz* Introduction, Experimental, Results and Discussion and Summary and Conclusion followed by references.

Chapter 1 deals with the general introduction to the chemistry of palladium and platinum complexes with organochalcogenolate ligands with an emphasis on the formation of supra-molecular assemblies followed by their applications in catalysis, biology and materials science. A brief coverage on various types of organometallic reactions along with the complex chemistry of chalcogen ligands (S, Se, Te) are described. Scope of the present work is discussed at the end of the chapter 1.

Chapter 2, "Experimental", describes the details of materials and methods followed by analysis of compounds by various experimental techniques employed during the course of present work. Details of synthesis and characterization of various ligands, metal precursors, metal chalcogenolates, are included. The complexes were well characterized by elemental analyses, IR, NMR, UV/Vis spectroscopy and single crystal X-ray analysis. The structure refinement details of the complexes characterized by crystallography are included in this chapter.

Chapter 3 deals with the results obtained during the present investigation and discussion on the present work. This chapter is further divided into five sections.

Section **3.1** deals with the chemistry of palladium and platinum complexes of non-chelating bidentate ligand, 4-pyridylslenolate. The oxidative addition of bis(4-pyridyl)diselenide to $Pt(PPh_3)_4$ yielded exclusively *trans*-$[Pt(SeC_5H_4N\text{-}4)_2(PPh_3)_2]$. Treatment of two eqv. of $Na(SeC_5H_4N\text{-}4)$, prepared by reductive cleavage of Se–Se bond of 4,4'-py_2Se_2 by $NaBH_4$ in methanol, with *cis*-$[PtCl_2(PR_3)_2]$ ($PR_3 = PPh_3$, PEt_3) afforded similar products, *trans*-$[Pt(SeC_5H_4N\text{-}4)_2(PPh_3)_2]$ and *trans*-$[Pt(SeC_5H_4N\text{-}4)_2(PEt_3)_2]$. The reactions of *cis*-[$MCl_2(P^\frown P)$] and [$M_2Cl_2(\mu\text{-}Cl)_2(PR_3)_2$] with two eqv. of Na($SeC_5H_4N$-4) yielded *cis*-[M($SeC_5H_4N$-4)$_2$($P^\frown P$)] (M/$P^\frown P$ = Pd/dppe, Pt/dppm and Pt/dppp) and [MCl(SeC_5H_4N-4)(PR_3)]$_n$, respectively. The complex *trans*-[PtCl(SeC_5H_4N-4)(PEt_3)$_2$] can be prepared by redistribution reaction between *trans*-[Pt(SeC_5H_4N-4)$_2$(PEt_3)$_2$] and *cis*-[$PtCl_2(PEt_3)_2$]. Molecular structures of a number of complexes were established by single crystal X-ray diffraction analyses. The catalytic activity of *trans*-[PdCl(SeC_5H_4N-4)(PPh_3)$_2$] and [PdCl(SeC_5H_4N-4)(PPh_3)]$_n$ in Suzuki C–C cross coupling reaction was investigated.

Section **3.2** deals with the preparation and characterization of Pd(II)/Pt(II) complexes with 3-/4-mercaptobenzoic acids. Addition of 3-/4-mercaptobenzoic acid to *cis*-[$Pt(PEt_3)_2(OTf)_2$] and *cis*-[$M(P^\frown P)_2(OTf)_2$] gave self-assembled complexes *cis*-[Pt(μ-SC_6H_4COOH-n)(PEt_3)$_2$]$_2$(OTf)$_2$ (n = 3, 4) and [M(μ-SC_6H_4COOH-n)($P^\frown P$)$_2$]$_2$(OTf)$_2$ (M /n /$P^\frown P$ = Pd/ 3/ dppe, Pd/ 4/ dppe, Pt/ 4/ dppp) respectively. Treatment of *cis*-[$PtCl_2(P^\frown P)$] with 3-/4-mercaptobenzoic acids in the presence of triethylamine yielded mononuclear complexes [Pt{SC_6H_4COOH-n}$_2$($P^\frown P$)] {$P^\frown P$ = dppm, (PR_3)$_2$; R = Et, Ph; n = 3, 4}. One of the above mentioned mononuclear complexes can also be obtained from the reaction of *cis*-[$Pt(PEt_3)_2(OTf)_2$] with 4-mercaptobenzoic acid in the presence of sodium methoxide.

Section **3.3** describes the synthesis of rigid Pd(II) and Pt(II)-based macrocyclic tetranuclear rectangles and octanuclear squares derived from 1,4-aryl dithiolates. Addition of 1,4-benezenedithiol and 4,4′-biphenyldithiol to M(OTf)$_2$ (M = *cis*-[$Pt(PEt_3)_2$]$^{2+}$ or *cis*-[Pd(dppe)]$^{2+}$) gave self-assembled tetranuclear complexes [M_2\{S(C_6H_4)$_n$S\}]$_2$(OTf)$_4$ (n = 1, 2). The same reaction of 1,4-benezenedimethanethiol yielded octanuclear supra-molecular coordination complexes (SCC) [M_2\{$SCH_2C_6H_4CH_2S$\}]$_4$(OTf)$_8$. The palladium complexes showed excellent catalytic activity in Suzuki C–C cross coupling reactions with high turnover numbers (2×10^7), even with low catalyst loading.

Section **3.4** covers the synthesis of coordination directed self-assembled Pd(II)/Pt(II) metallacycles. The reactions of M(P$^\cap$P)(OTf)$_2$ (P$^\cap$P = (PEt$_3$)$_2$, dppe) with 4,4'-py$_2$Se$_2$ in 1:1 ratio gave highly symmetrical self-assembled binuclear complexes of composition [M(P$^\cap$P)(py$_2$Se$_2$)]$_2$(OTf)$_4$. When 4,4'–py$_2$Te$_2$ was employed as nucleophilic tecton in the reaction with *cis*-Pt(PEt$_3$)$_2$(OTf)$_2$, [Pt(PEt$_3$)$_2$(py$_2$Te$_2$)]$_2$(OTf)$_4$ was isolated whereas the reaction with Pd(dppe)(OTf)$_2$ under similar conditions gave a trinuclear tellurido-bridged Pd(II) complex, [Pd$_3$(μ-Te)$_2$(dppp)$_3$]$^{2+}$. The molecular structures of the complexes have been established by single crystal X-ray diffraction analyses.

Section **3.5** describes the reactions of 4-telluropyridine with Pt(II)/Pd(II) precursors. Substitution reactions between [MCl$_2$(dppe)] (M = Pd, Pt) and NaTepy, prepared by reductive cleavage of Te–Te bond in 4,4'–py$_2$Te$_2$ by NaBH$_4$ in methanol gave expected mononuclear complexes, [M((Tepy)$_2$(dppe)] whereas in the case of MCl$_2$(dppm) (M = Pt, Pd) serendipitous products such as [Pt{PPh$_2$C(TeC$_5$H$_4$N)PPh$_2$}$_2$], [Pd$_4$(μ$_3$-Te)$_2$(μ$_2$-Tepy)$_2$(Tepy)$_2$(dppm)$_2$] have been isolated, respectively in good yields. On the other hand, hemilabile ambidentate ligand moiety 4-pyridyl selenolate was employed *in situ* reaction with M(P$^\cap$P)Cl$_2$ and NaBPh$_4$, in order to make use of both hard nitrogen atom and soft selenium atom in bonding. In this case self-recognition and self-selection lead to the formation of essentially a single product [Pt$_2$(dppe)$_2$(Se$^\cap$N)(N$^\cap$Se)](BPh$_4$)$_2$ in high yield (84 %). Reaction of [PdCl$_2$(py$_2$Te$_2$)]$_n$ with one equivalent of PPh$_3$ was monitored by NMR spectroscopy which indicated the formation of telluride-bridged binuclear complex *cis*-[Pd$_2$Cl$_2$(PPh$_3$)$_2$(TeC$_5$H$_4$N)$_2$] together with an unidentified product in solution.

From the forgoing results the following conclusions can be drawn:

- Diverse binding modes of 4-pyridylselenolate ligand has a promising potential in constructing multinuclear complexes which may exhibit dynamic behavior in solution depending on the nature of metal atom and also other auxiliary ligands. The palladium complexes have been shown to serve as good catalysts in Suzuki C–C coupling reactions.

- Directional intermolecular hydrogen bonding has been exploited to form a supra-molecular assembly of square-planar building blocks containing two carboxylic acid groups in the case of 3-/4-mercaptobenzoic acid as ligand by varying the phosphine as co-ligands and reaction conditions. The triflate counter-anions takes part in hydrogen bonding which led to the formation of molecular chains and rings, whereas solvent methanol interrupts the formation of carboxy dimer synthons, resulting in a stair like 2D network.
- Aryldithiol ligands while holding the Pt/Pd metals through bridging mode, facilitate stabilizing rigid unique supra-molecular coordination complexes. The rigid donor S atom, coupled with flexible CH_2 group, control the sizes, shapes and cavities of the Pd and Pt macrocycles. The excellent catalytic application of palladium complexes with both 4-pyridylselenolate and aryldithiol ligands have been demonstrated in Suzuki C–C cross coupling reactions.
- Depending on the nature of phosphine and the chalcogen atom, variety of complexes has been isolated by the reactions of 4,4′-dipyridyldichalcogenides with phosphine precursors. The tellurium ligands also undergo Te–C bond cleavage leading to the formation of tellurido-bridged derivatives trinuclear product $[M_3(\mu\text{-Te})_2(P^\frown P)_3]^{2+}$.
- The reactivity of tellurium ligands is markedly different from those of sulfur/ selenium ligands yielding unexpected and interesting products. The tellurolate complexes are highly susceptible to halogenated solvents and undergo facile Te-C bond cleavage.

References

References

1. F. R. Hartley, *“The Chemistry of Platinum and Palladium”*, John Wiley & Sons, New York, (1973); F. J. Berry, in: G. Wilkinson, R. D. Gillard and J. A. McCleverty (Eds.), *“Comprehensive Coordination Chemistry”*, Pergamon, Oxford, (1987) 668; M. L. Tobe, *Comprehensive Coordination Chemistry*: Wilkinson, Geoffrey, Sir, 1 (1987) 281.
2. T. Murahashi and H. Kurosawa, *Coord. Chem. Rev.*, 231 (2002) 207.
3. V. K. Jain, *Rev. Inorg. Chem.*, 9 (1988) 299.
4. O. Rivada-Wheelaghan, M. A. Ortuno, J. Diez, S. E. Garcia-Garrido, C. Maya, A. Lledos and S. Conejero, *J. Am. Chem. Soc.*, 134 (2012) 15261.
5. O. Rivada-Wheelaghan, M. A. Ortuno, S. E. Garcia-Garrido, J. Diez, P. J. Alonso, A. Lledos and S. Conejero*, Chem. Commun.*, 50 (2014) 1299.
6. V. Sicilia, P. Borja and A. Martin, *Inorganics*, 2 (2014), 508.
7. D. C. Powers and T. Ritter, *Nature Chemistry*, 1 (2009) 302.
8. J. R. Khusnutdinova, N. P. Rath and L. M. Mirica, *J. Am. Chem. Soc.*, 132 (2010) 7303.
9. L. M. Mirica and J. R. Khusnutdinova, *Coord. Chem. Rev.*, 257 (2013) 299.
10. R. Uson, J. Fornies, M. Thomas, B. Menjon, R. Bau, K. Suenkel and E. Kuwabara, *Organometallics*, 5 (1986) 1576.
11. V. K. Jain, G. S. Rao and L. Jain, *Adv. Organomet. Chem.*, 27 (1987) 113.
12. A. J. Canty, *Acc. Chem. Res.*, 25 (1992) 83.
13. S. R. Whitfield and M. S. Sanford, *J. Am. Chem. Soc.*, 129 (2007) 15142.
14. P. M. Maitlis, *The Organic Chemistry of Palladium, Academic Press*, (1971); U. Belluco, *Organometallic and coordination chemistry of Platinum*, Academic, New York, 1974; D. M. Roundhill, *Comprehensive Coordination Chemistry*, Ed. G. Willkinson, Pergamon Press, 5 (1987) 353.
15. St. Ahrland, J. Chatt and N. R. Davies, *Quart. Rev.*, 12 (1958) 265.
16. R. G. Pearson, *J. Am. Chem. Soc.*, 85 (1963) 3533.

17. F. Basolo, and R. G. Pearson, *Mechanisms of Inorganic Reactions, 2nd ed.; Wiley: New York*, (1967).

18. F. Basolo and R. *G.* Pearson*, Progress in Inorganic Chemistry* (F. *A. Cotton, ed.), Wiley-Interscience, New York*, 4 (1962).

19. F. Basolo, *Adv. Chem. Ser*., 49 (1965) 81.

20. J. M. Gonzales, D. G. Musaev and K. Morokuma, *organometallics.*, 24 (2005) 4908.

21. C. A. Tolman, *J. Am. Chem. Soc.*, 92 (1970) 2953.

22. P. W. N. M. van Leeuwen, Paul C. J. Kamer, Joost N. H. Reek and Peter Dierkes, *Chem. Rev.*, 100 (2000) 2741.

23. C. A. Tolman, *Chem. Rev.*, 77 (1977) 3123.

24. P. Dierkes and P. W. N. M. van Leeuwen, *J. Chem. Soc. Dalton Trans.*, (1999) 1519.

25. A. Immirzi, A. Musco and B. E. Mann, *Inorg. Chim. Acta*, 21 (1977) L37.

26. A. Immirzi and A. Musco, *Inorg. Chim. Acta*, 25 (1977) L41.

27. I. M. Al-Najjar, *Inorg. Chim. Acta*, 128 (1987) 93.

28. E. C. Alyea, A. Costin, G. T. Fey, G. Ferguson, R. G. Goel and R. J. Restivo, *J. Chem. Soc. Dalton Trans.*, (1975) 1294.

29. R. Mason, M. Textor, N. Al-Salem and B. L. Shaw, *J. Chem. Soc. Chem. Commun.*, (1976) 292.

30. Z. Freixa and P. W. N. M. van Leeuwen, *J. Chem. Soc. Dalton trans.,* (2003) 1890.

31. P. W. N. M. van Leeuwen, M. A. Zuideveld, B. H. G. Swennenhuis, Z. Freixa, P. C. J. Kamer, K. Goubitz, J. Fraanje, M. Lutz and A. L. Spek, *J. Am. Chem. Soc*., 125 (2003) 5523.

32. I. G. Dance, *Polyhedron,* 5 (1986) 1037.

33. P. J. Blower and J. R. Dilworth, *Coord. Chem. Rev*., 76 (1987) 121.

34. J. R. Dilworth and N. Wheatley, *Coord. Chem. Rev*., 199 (2000) 89.

35. A. Kumar, G. K. Rao, F. Saleem and A. K. Singh, *Dalton Trans.*, 41 (2012) 11949.

36. G. K. Rao, A. Kumar, S. Kumar, U. B. Dupare and A. K. Singh, *Organometallics*, 32 (2013) 2452.

37. A. Singhal, V. K. Jain, R. Misra and B. Varghese, *J. Mat. Chem*., (2000) 1121.

38. S. Dey, V. K. Jain, S. Chaudhury, A. Knoedler, F. Lissner and W. Kaim, *J. Chem. Soc.*, *Dalton Trans*., (2001) 723.

39. B. Radha and G. U. Kulkarni, *Adv. Funct. Mater.*, 20 (2010) 879.
40. P. D. Akrivos, *Coord. Chem. Rev.*, 213 (2001) 181.
41. L. C. Roof and J. W. Kolis, *Chem. Rev.*, 93 (1993) 1037.
42. S. Kuwata and M. Hidai, *Coord. Chem. Rev.,* 213 (2001) 211.
43. M. Peruzzini, I. de los Rios and A. Romerosa, *Prog. Inorg. Chem.*, 49 (2001) 169.
44. S. Narayan and V. K. Jain, *Trans. Met. Chem.*, 25 (2000) 400.
45. V. W. W. Yam, K. L. Yu, E. C. C. Cheng, P. K. Y. Yeung, K. K. Chenung and N. Zhu, *Chem. Eur. J.,* 8 (2002) 4122.
46. J. S. L. Yeo, J. J. Vittal, W. Henderson and T. S. A. Hor, *Inorg. Chem.*, 41 (2002) 1194.
47. J. G. Brennan, T. Siegrist, S. M. Stuczynski and M. L. Steigerwald, *J. Am. Chem. Soc.*, 112 (1990) 9233.
48. H. Wolkers, K. Dehnike, D. Finske, A. Kassanov and S. S. Hafner, *Acta Cryst. C,* 47 (1991) 1627.
49. A. L. Ma, J. B. Thoden and L. F. Dahl, *J. Chem. Soc. Chem. Commun.*, (1992) 1516.
50. G. Kedarnath and V. K. Jain, *Coord. Chem. Rev.*, 257 (2013) 1409.
51. V. K. Jain and R. S. Chauhan, *Coord. Chem. Rev.*, 306 (2015) 270.
52. V. K. Jain and L. Jain, *Coord. Chem. Rev.*, 249 (2005) 3075.
53. V. K. Jain and L. Jain, *Coord. Chem. Rev.*, 254 (2010) 2848.
54. S. Dey, V. K. Jain, A. Knoedler, A. Klein, W. Kaim and S. Zalis, *Inorg. Chem.*, 41 (2002) 2864.
55. S. Dey, V. K. Jain, A. Knoedler, W. Kaim and S. Zalis, *Eur. J. Inorg. Chem.*, (2001) 2965.
56. S. Dey, V. K. Jain, A. Knoedler and W. Kaim, *Inorg. Chim. Acta.*, 349 (2003) 104.
57. S. Dey, V. K. Jain, A. Klein and W. Kaim, *Inorg. Chem. Commun.*, 7 (2004) 601.
58. S. Dey, L. B. Kumbhare, V. K. Jain, T. Schurr, W. Kaim, A. Klein and F. Belaj, *Eur. J. Inorg. Chem.*, (2004) 4510.
59. S. Dey, V. K. Jain, B. Varghese, T. Schurr, M. Niemeyer, W. Kaim and R. J. Butcher, *Inorg. Chim. Acta*, 359 (2006) 1449.
60. S. Dey, V. K. Jain and R. J. Butcher, *Inorg. Chem. Commun.*, 10 (2007) 1385.

61. S. Dey, V. K. Jain, J. Singh, V. Trehan, K. K. Bhasin and B. Varghese, *Eur. J. Inorg. Chem.*, (2003) 744.

62. R. S. Chauhan, G. Kedarnath, A. Wadawale, A. M. Castro, R. A. Perez, V. K. Jain and W. Kaim, *Inorg. Chem.*, 49 (2010) 4179.

63. R. S. Chauhan, G. Kedarnath, A. Wadawale, A. L. Rheingold, A. M. Castro, R. A. Perez and V. K. Jain, *Organometallics*, 31 (2012) 1743.

64. R. S. Chauhan, G. Kedarnath, A. Wadawale, A. M. Z. Slawin and V. K. Jain, *Dalton Trans.*, 42 (2013) 259.

65. E. S. Raper, *Coord. Chem. Rev.*, 165 (1997) 475.

66. V. K. Jain and G. S. Rao, *Inorg. Chim. Acta*, 127 (1987) 161.

67. R. Uson, J. Fornies, M. A. Uson and S. Herrero, *J. Organomet. Chem.*, 447 (1993) 137.

68. R. Zanella, R. Ros and M. Grazian, *Inorg. Chem.*, 12 (1973) 2736.

69. R. Oilunkaniemi, R. S. Laitinen and M. Ahlgren, *J. Organomet. Chem.*, 623 (2001) 168.

70. J. G. Brennan, T. Siegrist, S. M. Stuczynski, and M. L. Steigerwald, *J. Am. Chem. Soc.,* 111 (1989) 9240.

71. S. G. Murray and F. R. Hartley, *Chem. Rev.*, 81 (1981) 365.

72. H. J. Gysling, *The Chemistry of Organoselenium and Organotellurium Compounds*, S. Patai (ed), 1(18), Wiley, N. -Y., (1986), 679.

73. W. Levason, S. D. Orchard and G. Reid, *Coord. Chem. Rev.*, 225 (2002) 159.

74. W. Levason and G. Reid, *J. Chem. Soc., Dalton Trans.*, (2001) 2953.

75. A. M. Masdeu-Bulto, M. Diegez, E. Martin and M. Gomez, *Coord. Chem. Rev.*, 242 (2003) 159.

76. K. G. Orrell, *Coord. Chem. Rev.*, 96 (1989) 1.

77. J. Chatt, and L. M. Venanzi*, J. Chem. Soc.*, (1957) 2351.

78. J. Chatt, and L. M. Venanzi, *J. Chem. Soc.*, (1955) 2787.

79. K. Ofele, and E. Dotzauer, *J. Organomet. Chem.*, 42 (1972) C87.

80. J. Chatt, L.A. Duncanson and L.M. Venanzi, *J. Chem. Soc.*, (1958) 3203.

81. R. Uson, J. Fornies, R. Navaro, P. Espinet and C. Mendivic, *J. Organomet. Chem.*, 290 (1985) 125.

82. P. K. Byers and A. J. Canty, *Organometallics*, 9 (1990) 210.

83. V. G. Albano, C. Castellari, M. E. Cucciolito, A. Panunzi and A. Vitagliano, *Organometallics,* 9 (1990) 1269.

84. H. Jin, K. J. Cavell, B. W. Skelton and A. H. White, *J. Chem. Soc. Dalton Trans*., (1995) 2159.

85. J. D. Scott and R. J. Puddephatt, *Organometallics*, 5 (1986) 1253.

86. G. Alibrandi, D. Minniti, L. Scolaro and R. Romeo, *Inorg. Chem*., 28 (1989) 1939.

87. D. Liotta, *Acc. Chem. Res*., 17 (1984) 28.

88. V. P. Ananikov, I. P. Beletskaya, G. G. Aleksandrov and I. L. Eremenko, *J. Organomet. Chem*., 22 (2003) 1414.

89. V. K. Jain, S. Kannan and E. R. T. Tiekink, *J. Chem. Res*.(S), (1994) 85.

90. R. Oilunkaniemi, R. S. Laitinen and M. J. Ahlgren, *J. Organomet. Chem*., 587 (1999) 200.

91. C. P. Morley, C. A. Webster, M. Divaira, *J. Organomet. Chem*., 691 (2006) 4244.

92. R. S. Chauhan, R. K. Sharma, G. Kedarnath, D. B. Cordes, A. M. Z. Slawin and V. K. Jain, *J. Organomet. Chem*., 717 (2012) 180.

93. J. -M. Lehn, *Angew. Chem., Int. Ed. Engl*., 27 (1988) 89.

94. J. M. Lehn, *Science,* 260 (1993) 1762.

95. R. Chakrabarty, P. S. Mukherjee and P. J. Stang, *Chem. Rev*., 111 (2011) 6810.

96. S. Sculfort and P. Braunstein, *Chem. Soc. Rev*., 40 (2011) 2741.

97. S. Leininger, B. Olenyuk and P. Stang, *Chem. Rev*., 100 (2000) 853.

98. M. Fujita, J. Yazaki and K. Ogura, *J. Am. Chem. Soc.*, 112 (1990) 5645.

99. S. Y. Yu, T. Kusukawa, K. Biradha and M. Fujita, *J. Am. Chem. Soc.*, 122 (2000) 2665; K. Ono, M. Yoshizawa, T. Kato, K. Watanabe and M. Fujita, *Angew. Chem. Int. Ed.*, 46 (2007) 1803.

100. B. J. Holliday and C. A. Mirkin, *Angew. Chem., Int. Ed. Engl*., 40 (2001) 2022.

101. C. S. Slone, D. A. Weinberger and C. A. Mirkin, *Progress in Inorganic Chemistry,* 48 (1999) 233.

102. N. C. Gianneschi, M. S. Masar and C. A. Mirkin, *Acc. Chem. Res*., 38 (2005) 825.

103. R. Breslow and L. E. Overmann, *J. Am. Chem. Soc*., 92 (1970) 1075.

104. J. Kang and J. Rebek, Jr., *Nature,* 385 (1997) 50.

105. J. Kang, J. Santamaría, G. Hilmersson, and J. Rebek, Jr., *J. Am. Chem. Soc.,* 120 (1998) 7389.

106. K. Suzuki, S. Sato and M. Fujita, *Nat. Chem*., 2 (2010) 25.

107. M. Fujita and M. Yashizawa, *Modern Supramolecular Chemistry*, (2008) 277.

108. "Metal Catalysed Cross-Coupling Reactions", 2nd Edn., eds. A. De. Meijere and F. Diederich, Wiley-VCH, Weinheim, Germany, 2004.

109. J. Tsuji, *Palladium Reagents and Catalysts, John Wiley & Sons, Inc.,* New York, 2004.

110. K. Tamao, K. Sumitani and M. Kumada, *J. Am. Chem. Soc*., 94 (1972) 4374.

111. R. J. P. Corriu and J. P. Masse, *J. Chem. Soc., Chem. Commun*., (1972), 144.

112. N. Miyaura and A. Suzuki, *J. Chem. Soc., Chem. Commun*., (1979) 866.

113. N. Miyaura, K. Yamada and A. Suzuki, *Tetrahedron Lett.,* 20 (1979) 3437.

114. E. Negishi and S. Baba, *J. Chem. Soc., Chem. Commun*., (1976) 596.

115. S. Baba and E. Negishi, *J. Am. Chem. Soc*., 98 (1976) 6729.

116. Y. Hatanaka and T. Hiyama, *J. Org. Chem*., 53 (1988) 918.

117. D. Milstein and J. K. Stille, *J. Am. Chem. Soc*., 100 (1978) 3636.

118. A. S. Guram, R. A. Rennels and S. L. Buchwald, *Angew. Chem.,Int. Ed. Engl*., 34 (1995) 1348.

119. M. Palucki, J. P. Wolfe and S. L. Buchwald, *J. Am. Chem. Soc*., 118 (1996) 10333.

120. M. A. Fernandez-Rodriguez, Q. L. Shen and J. F. Hartwig, *J. Am. Chem. Soc*., 128 (2006) 2180.

121. J. C. Hierso, C. Satto, R. Feurer and P. Kalck, *Chem. Mater.*, 8 (1996) 2481.

122. J. C. Hierso, R. Feurer and P. Kalck, Coord. *Chem. Rev.*, 178-180 (1998) 1811.

123. A. Niklewski, T. Strunskus, G. Gregor and C. Woll, *Chem. Mater.*, 17 (2005) 861.

124. L. B. Kumbhare, V. K. Jain, P. P. Phadnis and M. Nethaji, *J. Organomet. Chem.*, 692 (2007) 1546.

125. L. B. Kumbhare, V. K. Jain and B. Varghese, *Inorg. Chim. Acta*, 359 (2006) 409.

126. V. K. Jain, L. B. Kumbhare, S. Dey and N. D. Ghavale, *Phosphoros, sulfur, silicon*., 183 (2008) 1003.

127. H. Joshi, K. N. Sharma, A. K. Sharma, O. Prakash and A. K. Singh, *Chemical Commun*., 49 (2013) 7483.

128. B. Rosenberg, L. Vancamp and T. Crigas, *Nature*, 205 (1965) 698.

129. T. W. Hambley, *Coord. Chem. Rev.*, 166 (1997) 181.

130. J. A. G. Williams, S. Develay, D. L. Rochester and L. Murphy, *Coord. Chem., Rev.*, 252 (2008) 2596.

131. V. W. -W. Yam, K. M. -C. Wong and N. Zhu, *J. Am. Chem. Soc.*, 124 (2002) 6506.

132. X. Zhang, B. Cao, E. J. Valente and T. K. Hollis, *Organometallics*, 32 (2013) 752.

133. Y. Tanaka, K. M. -C. Wong and V. W. -W. Yam, *Chem. Sci.*, 3 (2012) 1185.

134. L. -Y. Zhang, L. -J. Xu, X. Zhang, J. -Y. Wang, J. Li and Z. N. Chen, *Inorg. Chem.*, 52 (2013) 5167.

135. Y. Sun, K. Ye, H. Zhang, J. Zhang, L. Zhao, B. Li, G. Yang, B. Yang, Y. Wang, S.-W. Lai and C.-M. Che, *Angew. Chem.*, 118 (2006) 5738.

136. W. Zhang, W. Jin, T. Fukushima, N. Ishii and T. Aida, *Angew. Chem., Int. Ed.*, 48 (2009) 4747.

137. V. N. Kozhevnikov, B. Donnio and D. W. Bruce, *Angew. Chem., Int. Ed.*, 47 (2008) 6286.

138. V. W. W. Yam, P. K. Y. Yeung and K. K. Cheung, *Angew. Chem. Int. Ed.*, 35 (1996) 739.

139. E. Vogel, *Textbook of Practical Organic Chemistry*, 4th Ed. English Language Book Society, Longmann, London (1987).

140. APEX2 “*Program for Data Collection on Area Detectors*” BRUKER AXS Inc., 5465 East Cheryl Parkway, Madison, WI 53711–5373 USA.

141. SADABS, G. M. Sheldrick, “*Program for Absorption Correction of Area Detector Frames*”, BRUKER AXS Inc., 5465 East Cheryl Parkway, Madison, WI 53711–5373 USA.

142. G. M. Sheldrick, *ActaCryst.*, A64 (2008) 112–122. XS, BRUKER AXS Inc., 5465 East Cheryl Parkway, Madison, WI 53711-5373 USA.

143. O. V. Dolomanov, L. J. Bourhis, R. J. Gildea, J. A. K. Howard, H. Puschmann, “OLEX2: *A Complete Structure Solution, Refinement and Analysis Program*”, *J. Appl. Cryst.* 42 (2009) 339.

144. A. L. Spek, "PLATON - A Multipurpose Crystallographic Tool" *J. Appl. Cryst.*, 36 (2003) 7; b) A. L. Spek, Utrecht University, Utrecht, The Netherlands 2008.

145. PSISCANS- A. C. T. North, D. C. Phillips, F. S. Mathews, *Acta Crystallogr.*, A24 (1968) 351.

146. C. K. Johnson, ORTEP-II, Report ORNL-5136, Oak ridge National Laboratory, Oak Ridge, TN (1976).

147. L. J. Farrugia, *J. Appl. Crystallogr.*, 30 (1997) 565. *APEX2 "Program for Data Collection on Area Detectors*" BRUKER AXS Inc., 5465 East Cheryl Parkway, Madison, WI 53711–5373 USA.

148. B. Boduszek and R. Gancarz, *J. Prakt. Chem.*, 338 (1996) 186.

149. S. J. Dunne, L. A. Summers and E. I. Von Nagy Felsobuki, *J. Heterocyclic Chem.*, 30 (1993) 409.

150. H. L. Grube, "Handbook of preparative Inorganic chemistry", Ed., G. Brauer, Academic Press, London 2 (1965)1584

151. G. B. Kaufmann and D. O. Cowan, *Inorg. Synth.*, 7 (1963) 240.

152. A. R. Sanger, *J. Chem. Soc. Dalton Trans.*, (1977) 1971.

153. A. Sen and J. Halpern, *Inorg. Chem.*, 19 (1980) 1073.

154. P. Espinet and K. Soulantica, *Coord. Chem. Rev.*, 193–195 (1999) 499.

155. D. Yuan and H. V. Huynh, *Organometallics,* 29 (2010) 6020.

156. D. K. Paluru, S. Dey, A. Wadawale and V. K. Jain, *J. Organomet. Chem.*, 728 (2013) 52.

157. T. Chakraborty, K. Srivastava, H. B. Singh and R. J. Butcher, *J. Organomet. Chem.*, 696 (2011) 2559.

158. G. K. Rao, A. Kumar, B. Kumar, D. Kumar and A. K. Singh, *Dalton Trans.*, 41 (2012) 1931.

159. R. K. Sharma, G. Kedarnath, A. Wadawale, C. A. Betty, B. Vishwanadh and V. K. Jain, *Dalton Trans.*, 41 (2012) 12129.

160. H. Wang, R. Zhong, X. -Q. Guo, X. -Y. Feng and X. -F. Hou, *Eur. J. Inorg. Chem.*, (2010) 174.

161. Y. –F. Han, Y. –J. Lin, W. –G. Jia and G. –X. Jin, *Dalton Trans.*, (2009) 2077.

162. B. –C. Tzeng, C. –S. Ding, T. –Y. Chang, C. –C. Hu and G. –H. Lee, *Cryst. Eng. Comm.*, 14 (2012) 8228.

163. K. Nunokawa, S. Onaka, Y. Mizuno, K. Okazaki, T. Sunahara, M. Ito, M. Yaguchi, H. Imai, K. Inoue, T. Ozeki, H. Chiba and T. Yosida, *J. Organomet. Chem.*, 690 (2005) 48.

164. K. E. Neo, H. V. Huynh, L. L. Koh, W. Henderson and T. S. A. Hor, *Dalton Trans.*, (2007) 5701.

165. F. M. Tabellion, S. Seidel, A. M. Arif and P. J. Stang, *J. Am. Chem. Soc.*, 123 (2001) 7740.

166. S. Narayan, V. K. Jain and B. Varghese, *J. Chem. Soc. Dalton Trans.*, (1998) 2359.

167. N. Ghavale, A. Wadawale, S. Dey and V. K. Jain, *Indian J. Chem.*, 48A (2009) 1510.

168. L. B. Kumbhare, A. P. Wadawale, V. K. Jain, S. Kolay and M. Nethaji, *J. Organomet. Chem.*, 694 (2009) 3892.

169. M. K. Pal, V. K. Jain, A. P. Wadawale, S. A. Glazum, Z. A. Starikova and V. I. Bregadze, *J. Organomet. Chem.*, 696 (2012) 4257.

170. M. S. Hannu-Kuure, R. Oilunkaniemi, R. S. Laitinen and M. Ahlgre´n, *Z. Kristallogr.-New Cryst. Struct.*, 219 (2004) 23.

171. E. C. Alyea, G. Fergusan and S. Kannan, *Polyhedron*, 17 (1998) 2231.

172. M. D. Rudd and S. V. Lindeman, *J. Chem. Cryst.*, 37 (2007) 375.

173. M. S. Hannu-Kuure, R. Oilunkaniemi, R. S. Laitinen and M. Ahlgre´n, *J. Organomet. Chem.*, 666 (2003) 111.

174. D. G. Musaev, K. Morokuma and J. M. Gonzales, *Organometallics*, 24 (2005) 4908.

175. R. S. Chauhan, G. Kedarnath, A. Wadawale, D. K. Maity, J. A. Golen, A. L. Rheingold and V. K. Jain, *J. Organomet. Chem.*, 737 (2013) 40.

176. A. Singhal, V. K. Jain, B. Varghese and E. R. T. Tiekink, *Inorg. Chim. Acta.*, 285 (1999) 190.

177. N. K. Lokanath, H. C. Devarajegowda, S. M. Anandalwar, J. S. Prasad, S. Narayan and V. K. Jain, *Anal. Sci.*, 17 (2001) 565.

178. M. S. Hannu-Kuure, R. Oilunkaniemi, R. S. Laitinen and M. Ahlgre´n, *Acta Cryst.*, E60 (2004) m214.

179. M. Schweiger, S. R. Seidel, A. M. Arif and P. J. Stang, *Angew. Chem. Int. Ed.*, 40 (2001) 3467.

180. T. Rosner, J. L. Bars, A. Pfaltz and D. G. Blackmond, *J. Am. Chem. Soc.*, 123 (2001) 1848.

181. J. M. Lehn, ‘*Supramolecular chemistry: Concepts and Prospects’*, VCH, Verlagesellschaft, Weinhein, Germany (1995).

182. M. Fujita, *Acc. Chem. Res.*, 32 (1999) 53.

183. C. G. Oliveri, P. A. Ulmann, M. J. Wiester and C. A. Mirkin, *Acc. Chem. Res.*, 41 (2008) 1618.

184. D. Braga and F. Grepioni, *Acc. Chem. Res.*, 33 (2000) 601.

185. C. Ma, Q. Zhang, R. Zhang and D. Wang, *Chem. Eur. J.*, 12 (2006) 420.

186. D. Braga, S. d’Agostino and F. Grepioni, *Organometallics*, 31 (2012) 1688.

187. D. E. T. James, W. Ely, A. Schier, N. W. Mitzel and H. J. Schmidbaur, *Chem. Soc., Dalton Trans.*, (2001) 1058.

188. U. Helmstedt, S. Lebedkin, T. Hocher, S. Blaurock and E. Hey-Hawkins, *Inorg. Chem.*, 47 (2008) 5815.

189. W. Schneider, A. Bauer and H. Schmidbaur, *Organometallics*, 15 (1996) 5445.

190. D. R. Smyth, J. Hester, V. G. Jr. Young and E. R.T. Tiekink, *CrystEngComm.*, 4 (2002) 517.

191. D. R. Smyth, B. R. Vincent and E. R. T. Tiekink, *Crystal Growth & Design*, 1 (2001)113.

192. C. Ma, Q. Zhang, R. Zhang and L. Qiu, *J. Organomet. Chem.*, 690 (2005) 3033.

193. T. G. Appleton, H. C. Clark and L. E. Manzer, *Coord. Chem. Rev.*, 10 (1973) 335.

194. H. Kuniyasu, K. Sugoh, M. –S. Su and H. Kurosawa, *J. Am. Chem. Soc.*, 119 (1997) 4669.

195. M. Hirano, S. Tatesawa, M. Yabukami, Y. Ishihara, Y. Hara, N. Komine and S. Komiya, *Organometallics*, 30 (2011) 5110.

196. H. Kuniyasu, F. Yamashita, J. Terao and N. Kambe, *Angew. Chem. Int. Ed.*, 46 (2007) 5929.

197. V. Cordero-Pensado, V. Gómez-Benítez, S. Hernández-Ortega, R. A. Toscano and D. Morales-Morales, *Inorg. Chim. Acta.*, 359 (2006) 4007.

198. S. Kato, O. Niyomura, Y. Kawahara and T. Kanda, *J. Chem. Soc., Dalton Trans.*, (1999) 1677.

199. H. Kuniyasu, F. Yamashita, J. Terao and N. Kambe, *Angew. Chem. Int. Ed.*, 119 (2007) 6033.

200. U. Helmstedt, P. Lo1nnecke and E. Hey-Hawkins, *Inorg. Chem.*, 45 (2006) 10300.

201. J. J. Garcia, A. Arevalo, V. Montiel, F. D. Rio, B. Quiroz, H. Adams and P. M. Maitlis, *Organometallics*, 16 (1997) 3216.

202. C. Bruhn, S. Becke and D. Steinborn, *Acta Cryst.,* C54 (1998) 1102.

203. G. Rivera, S. Bernes and H. Torrens, *Polyhedron*, 26 (2007) 4276.

204. B. J. Deadman, W. Henderson, B. K. Nicholson, L. E. Petchell, S. L. Rose and T. S. A. Hor, *Inorg. Chim. Acta*., *362 (2009) 5122*.

205. G. Rivera, S. Bernes, C. R. D. Barbarin and H. Torrens, *Inorg. Chim. Acta*., 367 *(2009*) 5122.

206. P. Teo, L. L. Koh and T. S. A. Hor, *Inorg. Chem*., 42 (2003) 7290.

207. P. Teo, L. L. Koh and T. S. A. Hor, *Inorg. Chem*., 47 (2008) 6464.

208. S. Ghosh and P. S. Mukherjee, *Inorg. Chem*., 48 (2009) 2605.

209. M. C. Etter, *Acc. Chem. Res*., 23 (1990) 120.

210. F. H. Allen, W. D. S. Motherwell, P. R. Raithby, G. P. Shields and R. Taylor, *New J. Chem*., 23 (1999) 25.

211. *Mercury, Crystal Structure Visualization, Exploration and Analysis Program, CCDC, Cambridge, UK.*

212. G. R. Desiraju, *J. Am. Chem. Soc*., 135 (2013) 9952.

213. G. R. Desiraju, J. J. Vittal and A. Ramanan, *Crystal Engineering: A Text Book, World Scientific*, (2011) p 65.

214. Z. Qin, M. C. Jennings, R. J. Puddephatt and K. W. Muir, *Inorg. Chem*., 41 (2002) 5174.

215. T. R. Cook, Y. R. Zheng and P. J. Stang, *Chem. Rev*., 113 (2013) 734.

216. M. Fujita, J. Yazaki and K. Ogura, *J. Am. Chem. Soc*., 112 (1990) 5645.

217. I. Mutikainen, C. J. L. Lock, L. Randaccio, E. Zangrando, E. Chiarparin, B. Lippert, H. Rauter, P. Amo-Ochoa, E. Freisinger and M. Blomberg, *Angew. Chem. Int. Ed. Engl*., 36 (1997) 1296.

218. G. S. Hanan, C. R. Arana, J. -M. Lehn, G. Baum and D. Fenske, *Chem. Eur. J*., 2 (1996) 1292.

219. J. R. Hall, S. J. Loeb, G. K. H. Shimizu and G. P. A. Yap, *Angew. Chem. Int. Ed. Engl.*, 37 (1998) 121.

220. R. M. Yeh, A. V. Davis and K. N. Raymond, *Supramolecular Systems: Self-assembly. In: "Comprehensive Coordination Chemistry II*"; vol *7*; Eds. J. A. McClevety, T. J. Meyer, Elsevier; Oxford, (2004) 327.

221. R. D. Kennedy, C. W. Machan, C. M. McGuirk, M. S. Rosen, C. L. Stern, A. A. Sarjeant and C. A. Mirkin, *Inorg. Chem.*, 52 (2013) 5876.

222. P. J. Stang, D. H. Cao, S. Sait and A. M. Arif, *J. Am. Chem. Soc.*, 117 (1995) 6273.

223. C. J. Kuehl, S. D. Huang and P. J. Stang, *J. Am. Chem. Soc.*, 123 (2001) 9634.

224. G. A. Bowmaker, P. D. W. Boyd and G. K. Campbell, *Inorg. Chem.*, 22 (1983) 1208.

225. M. Capdevila, W. Clegg, P. G. Duarte, A. Jarid and A. Lledos, *Inorg. Chem.*, 35 (1996) 490.

226. G. Aullon, G. Ujaque, A. Lledos, S. Alvarez and P. Alemany, *Inorg. Chem.*, 37 (1998) 804.

227. J. Chatt and D. M. P. Mingos, *J. Chem. Soc. A.*, (1970) 1243.

228. S. –W. A. Fong and T. S. A. Hor, *J. Chem. Soc., Dalton Trans.*, (1999) 639.

229. D. L. Caulder, C. Bruckner, R. E. Powers, S. Konig, T. N. Parac, J. A. Leary and K. N. Raymond, *J. Am. Chem. Soc.*, 123 (2001) 8923.

230. J. K. Dunleavy, *Platinum Met. Rev.*, 50 (2006) 110.

231. R. Vanjari, T. Guntreddi, S. Kumar and K. N. Singh, *Chem. Commun.*, 51 (2015) 366.

232. V. P. Ananikov, N. V. Orlov, L. P. Beletskaya, V. N. Khrustalev, M. Yu. Antipin and T. V. Timofeeva, *J. Am. Chem. Soc.*, 129 (2007) 7252.

233. A. Garcia-Bernabe, C. C. Tzschucke, W. Bannwarth and R. Haag, *Adv. Synth. Catal.*, 347 (2005) 1389.

234. M. Ooe, M. Murata, T. Mizugaki, K. Ebitani and K. Kaneda, *J. Am. Chem. Soc.*, 126 (2004) 1604.

235. Y. M. A. Yamada, K. Takeda, H. Takahashi and S. Ikegami, *Tetrahedron Lett.*, 44 (2003) 2379.

236. A. Dervisi, D. Koursarou, L. –L. Ooi, P. N. Horton and M. B. Hursthouse, *Dalton Trans.*, (2006) 5717.

237. D. K. Paluru, S. Dey, K. R. Chaudhari, M. V. Khedkar, B. M. Bhanage and V. K. Jain, *Tetrahedron Lett.,* 55 (2014) 2953.

238. D. K. Paluru, S. Dey, A. Wadawale, D. K. Maity, N. Bhuvanesh and V. K. Jain, *Eur. J. Inorg. Chem*., (2015) 397.

239. T. H. Noh, E. Heo, K. H. Park and O. -S. Jung, *J. Am. Chem. Soc*., 133 (2011) 1236.

240. C. Deraedt and D. Astruc, *Acc. Chem. Res*., 47 (2014) 494.

241. D. Astruc, *Inorg. Chem*., 46 (2007) 1884.

242. J. Louie and J. F. Hartwig, *Angew Chem., Int. Ed. Engl*., 35 (1996) 2359.

243. N. T. S. Phan, M. van der Sluys and C. J. Jones, *Adv. Synth. Catal*., 348 (2006) 609.

244. S. R. Seidel and P. J. Stang, *Acc. Chem. Res.*, 35 (2002) 972.

245. F. A. Cotton, C. Lin and C. A. Murillo, *Acc. Chem. Res.*, 34 (2001) 759.

246. K. Matsumoto, M. Ikuzawa, M. Kamikubo and S. Ooi, *Inorg. Chim. Acta*., 217 (1994) 129.

247. R. Horikoshi, T. Mochida, M. Kurihara and M. Mikuriya, *Cryst. Growth Des*., 5 (2005) 243

248. R. W. Seidel, C. Dietz and I. M. Oppel, Z. *Anorg. Allg. Chem*., 637 (2011) 94.

249. Y. –F Han, H. Li, Y. Fei, Y. –J. Lin, W. –Z. Zhang and G. –X. Jin, *Dalton Trans.*, 39 (2010) 7119.

250. X. –Q. Xiao, A. –Q. Jia, Y. –J. Lin and G. –X. Jin, *Organometallics*, 29 (2010) 4842.

251. A. K. Chantzea, N. Karakostas, C. P. Raptopoulou, V. Psycharis, E. Saridakis, J. Griebel, R. Hermann and G. Pistolis, *J. Am. Chem. Soc.,* 132 (2010) 16327.

252. B. Chatterjee, J. C. Noveron, M. J. E. Resendiz, J. Liu, T. Yamamoto, D. Parker, M. Cinke, C. V. Nguyen, A. M. Arif and P. J. Stang, *J. Am. Chem. Soc*., 126 (2004) 10645.

253. R. M. Balleste, G. Aullon, P. A. Champkin, W. Clegg, C. Megret, P. Gonzalez-Duarte and A. Lledos, *Chem. Eur. J.*, 9 (2003) 5023.

254. M. J. Pilkington, A. M. Z. Slawin, D. J. Williams, J. D. Woollins, *J. Chem. Soc., Dalton Trans.*, (1992) 2425.

255. B. –C. Tzeng, S. –C. Chan, M. C. W. Chan, C. –M. Che, K. K. Cheung and S. –M. Peng, *Inorg. Chem.*, 40 (2001) 6699.

256. C. Nishitani, T. Shizuka, K. Matsumoto, S. Okeya and H. Kimoto, *Inorg. Chem. Commun.*, 1 (1998) 325.

257. (a) R. J. Puddephatt, *Chem. Soc. Rev.* 12 (1983) 99; (b) A. P. Katritzky, O. Meth-Cohn and C. W. Rees (Eds.) "*Comprehensive Organic Functional Group Transformation*", 1st ed., Pergamon, Oxford, 2 (1995) 425.

258. J. R. Torkelson, O. Oke, J. Muritu, R. McDonand and M. Cowie, *Organometallics,* 1*9* (2000) 854.

259. J. J. Li and P. R. Sharp, *Inorg. Chem.,* 33 (1994) 183; J. J. Li and P. R. Sharp, *Inorg. Chem.,* 35 (1996) 604.

260. J. J. Li, W. Li, A. J. James, T. Holbert, T. P. Sharp, P. R. Sharp, *Inorg. Chem.,* 38 (1999) 1563.

261. (a) E. J. Fernandez, M. C. Gimeno, P. G. Jones, A. Laguna, M. Laguna and J. M. Lobez-de-Luzuriaga, *Organometallics,* 14 (1995) 2918 (b) J. Ruiz, M. E. G. Mosquera, V. Riera, M. Vivanco and C. Bois, *Organometallics,* 16 (1997) 3388.